



Sergeev, Eugenia (2018) Investigating the molecular pharmacology of the short chain fatty acid receptor FFA2. PhD thesis.

<http://theses.gla.ac.uk/8963/>

Copyright and moral rights for this work are retained by the author

A copy can be downloaded for personal non-commercial research or study, without prior permission or charge

This work cannot be reproduced or quoted extensively from without first obtaining permission in writing from the author

The content must not be changed in any way or sold commercially in any format or medium without the formal permission of the author

When referring to this work, full bibliographic details including the author, title, awarding institution and date of the thesis must be given

Enlighten:Theses
<http://theses.gla.ac.uk/>
theses@gla.ac.uk

Investigating the Molecular Pharmacology of the Short Chain Fatty Acid Receptor FFA2

Eugenia Sergeev

MSc, BSc (Hons), BSc

Submitted in fulfilment of the requirements for the Degree of
Doctor of Philosophy

Institute of Molecular, Cell and Systems Biology
College of Medical, Veterinary & Life Sciences
University of Glasgow

September 2017



**University
of Glasgow**

Abstract

The G protein-coupled receptor FFA2 is a key mediator of short chain fatty acid signalling, which are produced in the gut via fermentation of poorly digested carbohydrates by the gut microbiota. Therefore, FFA2 has attracted interest as a potential therapeutic target for metabolic and inflammatory diseases. However, several limitations have hindered validation of FFA2 as a drug target, including the limited understanding of the molecular determinants of ligand binding and species-specific differences in pharmacology. Herein, novel tool compounds and assay systems were developed for FFA2 and utilised to address some of these limitations. Following the characterisation of functional assays for detection of FFA2 signalling, these were employed to examine the structure-activity relationship and pharmacology of FFA2 agonists versus antagonists. To assess how the pharmacology of FFA2 ligands is defined by their mode of binding, a radioligand binding assay was developed using a tritiated form of FFA2 antagonist GLPG0974 that was utilised in combination with site-directed mutagenesis and homology modelling to explore FFA2 ligand binding sites. These studies showed that FFA2 agonist binding was defined by an essential interaction between the ligand carboxylate and an orthosteric Arg-His-Arg triad. In contrast, FFA2 antagonists only required one orthosteric arginine for high-affinity binding and could tolerate modifications of the carboxylate moiety. This knowledge was applied to develop an antagonist-based fluorescent tracer for FFA2 that was utilised in BRET binding assays but displayed complex pharmacological behaviour that was shown to be based on the bitopic nature of FFA2 antagonists. The secondary binding site of FFA2 antagonists was also related to their lack of action at rodent orthologues of FFA2, whose molecular basis was explored using homology models of human and murine FFA2. This facilitated the identification of a single lysine to arginine variation at position 2.60 that might provide a basis for antagonist selectivity. Extending these studies to agonist function demonstrated that removal of the positive charge at this position produced a signalling-biased form of FFA2, in which only coupling to G_i G proteins was fully maintained. In summary, these findings contribute to understanding the complex pharmacology of FFA2 ligands and the underlying mechanisms that define their function, and conclusions drawn from these studies may help advance future efforts to validate the therapeutic potential of targeting FFA2.

Table of Contents

Abstract	ii
List of Tables	viii
List of Figures	x
List of Publications	xiii
Acknowledgements	xv
Author's Declaration	xvi
Abbreviations	xvii
1 Introduction	1
1.1 Drug discovery and development.....	1
1.1.1 Different approaches to drug discovery	1
1.1.2 Principles of rational target-based drug discovery	3
1.1.3 Significance of G protein-coupled receptors as drug targets	6
1.2 G protein-coupled receptors.....	7
1.2.1 Overview of GPCRs and their subfamilies.....	7
1.2.2 Canonical GPCR signalling pathways.....	10
1.2.3 Structural investigations of GPCR activation	12
1.2.4 Pharmacology of GPCR ligands	16
1.2.5 Impact of diverse ligand binding sites on GPCR signalling.....	18
1.3 Identification of the free fatty acid receptor family.....	21
1.3.1 Relevance of metabolites as signalling molecules	21
1.3.2 Deorphanisation of FFA receptors.....	22
1.4 Short chain fatty acid receptors as novel drug targets	24
1.4.1 SCFAs as endogenous GPCR ligands	24
1.4.2 Therapeutic implications of SCFA receptors.....	28
1.5 Drug development for SCFA receptors.....	33
1.5.1 Homology modelling as a tool to predict structural features	33
1.5.2 Overview of FFA2 and FFA3 drug development efforts	37
1.5.3 Orthosteric FFA2 agonists	39
1.5.4 Orthosteric FFA2 antagonists	41
1.5.5 Allosteric FFA2 regulators	43
1.6 Aims	45
2 Materials and methods	47
2.1 Pharmacological reagents	47
2.2 Molecular Biology	49
2.2.1 DNA constructs.....	49

2.2.2	Preparation of competent bacteria	49
2.2.3	Bacterial transformation	50
2.2.4	Plasmid DNA purification	50
2.2.5	Sequencing	52
2.2.6	Cloning strategy	52
2.2.7	Generation of hemagglutinin (HA)-tagged FFA2 constructs	55
2.2.8	Generation of NanoLuciferase (NLuc)-tagged FFA2 constructs	56
2.2.9	Site-directed mutagenesis.....	57
2.2.10	Generation of FFA2 point mutant constructs.....	58
2.3	Mammalian cell culture.....	59
2.3.1	Cell line maintenance.....	59
2.3.2	Transient transfection	60
2.3.3	Generation of stably transfected Flp-In™ T-REx™ 293 cell lines....	60
2.4	Biochemical assays	62
2.4.1	Preparation of cellular membranes.....	62
2.4.2	Determination of membrane protein concentration	62
2.4.3	[³⁵ S]-GTPγS binding assay	63
2.4.4	Radioligand binding assay	63
2.4.5	Bioluminescence resonance energy transfer (BRET)-based binding assay	66
2.5	Cell-based assays	68
2.5.1	Inositol monophosphate (IP1) accumulation assay.....	68
2.5.2	Cyclic adenosine monophosphate (cAMP) inhibition assay	69
2.5.3	ERK phosphorylation assay	70
2.5.4	BRET-based β-arrestin recruitment assay.....	71
2.5.5	TGFα shedding assay	72
2.6	Structural studies.....	73
2.6.1	Homology modelling.....	73
2.6.2	Ligand docking	74
2.7	Data analysis	74
2.7.1	Analysis of functional agonist and antagonist assays	75
2.7.2	Global Gaddum/Schild analysis.....	75
2.7.3	Analysis of binding parameters	76
2.7.4	Calculation of signalling bias	78
2.7.5	Statistical analysis.....	79
3	Exploring the structure-activity relationships of FFA2 agonists and antagonists	81
3.1	Introduction	81

3.2	Results	84
3.2.1	Selection of assay systems to screen FFA2 ligands	84
3.2.2	Screening of a structurally unexplored FFA2 agonist series	90
3.2.3	Comparing the pharmacology of FFA2 antagonists GLPG0974 and CATPB	98
3.2.4	Effect of carboxylate moiety modifications on FFA2 antagonists ..	101
3.3	Discussion	102
3.3.1	Use of multiple screening assays is important for promiscuous receptors	102
3.3.2	Hemi-equilibrium conditions can affect investigations of antagonist pharmacology	107
3.3.3	Carboxylate moiety contributes to binding of FFA2 antagonists, but is not essential	108
3.3.4	Conclusions	109
4	Defining molecular and kinetic determinants of FFA2 ligand binding using [³ H]-GLPG0974	112
4.1	Introduction	112
4.2	Results	115
4.2.1	Binding of [³ H]-GLPG0974 to hFFA2 does not require both orthosteric arginine residues	115
4.2.2	FFA2 agonists and antagonists have different binding determinants	117
4.2.3	Carboxylate moiety present in FFA2 antagonists is not necessary for high-affinity binding	120
4.2.4	FFA2 homology model and ligand docking supports diverse binding poses of FFA2 agonists and antagonists.....	122
4.2.5	Orthosteric arginine pair may regulate antagonist release from the FFA2 binding pocket	125
4.2.6	Competitive kinetic binding experiments indicate distinct kinetics of GLPG0974 and CATPB despite similar affinity	126
4.2.7	Binding of FFA2 agonists appears to have a cooperative effect on [³ H]-GLPG0974 kinetics.....	128
4.3	Discussion	130
4.3.1	FFA2 agonists are defined by their interaction with the Arg180-His242-Arg255 triad.....	130
4.3.2	Key orthosteric binding site residues play limited role in hFFA2 antagonist binding	132
4.3.3	Relationship between FFA2 antagonist interaction with orthosteric arginine residues and binding kinetics	133
4.3.4	Cooperative effect of hFFA2 agonists on [³ H]-GLPG0974 kinetics may be rooted in co-binding or cross-dimer cooperativity	135

4.4	Conclusions	138
5	Development and characterisation of a fluorescent probe for FFA2	139
5.1	Introduction	139
5.2	Results	142
5.2.1	Development of a FFA2 fluorescent ligand for BRET binding assays	142
5.2.2	Real-time tracking of F-1 association and dissociation	146
5.2.3	Assessment of hFFA2 antagonist binding and kinetics using fluorescent ligand F-1	147
5.2.4	FFA2 agonists and allosteric ligands cannot outcompete fluorescent ligand F-1 binding	150
5.2.5	Fluorescent ligand F-1 can be used to assess binding to R180A-R255A hFFA2	151
5.3	Discussion	154
5.3.1	GLPG0974 analogue GLPG-3 provides a good backbone for NBD fluorophore attachment.....	154
5.3.2	BRET binding assay utilising fluorescent ligand F-1 can be employed to screen hFFA2 antagonists.....	156
5.3.3	Fluorescent tracer F-1 does not behave as an orthosteric FFA2 ligand	157
5.3.4	Certain hFFA2 antagonists retain the ability to bind to R180A-R255A hFFA2	159
5.4	Conclusions	160
6	Investigating the role of Lys65 in FFA2 signalling and ligand binding	162
6.1	Introduction	162
6.2	Results	165
6.2.1	Assessment of the structural basis for the selectivity of FFA2 antagonists for the human versus mouse orthologue	165
6.2.2	Identity of residue 65 in human versus mouse FFA2 defines species selectivity of antagonists	167
6.2.3	Charge-altering Lys65 mutations in hFFA2 affect $G_{q/11}$ - but not $G_{i/o}$ - mediated responses to agonists.....	173
6.2.4	Alterations of Lys65 do not affect response of hFFA2 to $G_{i/o}$ -biased allosteric ligand AZ1729.....	176
6.2.5	A TGF α shedding assay can be employed to assess impact of Lys65 mutations on signalling of hFFA2 via $G_{q/11}$ and $G_{12/13}$	177
6.2.6	Use of chimeric G proteins to examine the diverse effect of charge- altering Lys65 mutations on hFFA2 signalling.....	182
6.2.7	Allosteric modulation of hFFA2 response to C3 by AZ1729 may differ between $G_{q/11}$ - and $G_{12/13}$ -mediated signals.....	185

- 6.3 Discussion189
 - 6.3.1 Lys65 defines a secondary binding site that is unique to the human orthologue of FFA2.....189
 - 6.3.2 Generation of a biased form of hFFA2 by modifying the positive charge of the residue in position 2.60193
 - 6.3.3 Complex allostereism of biased FFA2 ligand AZ1729197
- 6.4 Conclusions198
- 7 Final discussion.....201
- References.....208

List of Tables

Table 3.1 Affinity and potency of hFFA2 reference ligands	87
Table 3.2 Screening of compound 2 analogues with eastern part variations	91
Table 3.3 Screening of compound 2 analogues with northern part variations ...	92
Table 3.4 Screening of compound 2 analogues with isoxazole and eastern part variations	93
Table 3.5 Affinity of compound 2 and representative analogues for hFFA2	95
Table 3.6 Comparing potency of compound 2 analogues at human and murine FFA2	98
Table 3.7 Impact of carboxylate moiety modifications on hFFA2 antagonist function	101
Table 4.1 Affinity of [³ H]-GLPG0974 for orthosteric binding site mutants of hFFA2	117
Table 4.2 Affinity of hFFA2 antagonist analogues for wild type and orthosteric binding site mutants of hFFA2	119
Table 4.3 Kinetic parameters of [³ H]-GLPG0974 binding to wild type and orthosteric arginine mutants of hFFA2	126
Table 4.4 Kinetic parameters of antagonist binding to wild type hFFA2	127
Table 4.5 Effect of different ligands on the [³ H]-GLPG0974 dissociation rate ..	130
Table 5.1 Affinity and potency of potential fluorescent tracers for hFFA2	144
Table 5.2 Affinities of hFFA2 antagonists determined in F-1 competition binding assay	148
Table 5.3 Kinetics of FFA2 antagonists determined in F-1 competitive kinetic binding assay	149
Table 5.4 Affinities of hFFA2 antagonists for wild type versus R180A-R255A hFFA2	153
Table 6.1 Alterations of Lys65 in hFFA2 affect both agonist potency to generate IP1 and the ability of antagonists to inhibit this response	169
Table 6.2 Effect of Lys65 alterations in hFFA2 on the binding affinity of radioligand [³ H]-GLPG0974 and fluorescent tracer F-1	171
Table 6.3 Alterations of Lys65 in hFFA2 have modest effects on agonist potency in G _{i/o} -coupled assays	175
Table 6.4 Effect of Lys65 mutations on FFA2 agonist potency in the TGF α shedding assay	179
Table 6.5 Agonist bias factor calculation for Lys65 mutants of hFFA2	182
Table 6.6 FFA2 agonists display increased potency at charge-altering mutations of Lys65 when G α_{q-i} versus G α_q or G α_{q-o} is reintroduced into cells with a $\Delta G_{q/11/12/13}$ background	184
Table 6.7 Effect of AZ1729 on the potency of C3 in the TGF α shedding assay in different cell backgrounds	187

Table 6.8 Effect of Lys65 mutations on FFA2 agonist potency in the BRET-based β -arrestin recruitment assay.....	188
--	-----

List of Figures

Figure 1.1 The pipeline of target-based drug discovery	3
Figure 1.2 Structural features of the GPCR families	8
Figure 1.3 Signalling cascades induced by GPCR activation.....	11
Figure 1.4 Structural changes induced by GPCR activation	14
Figure 1.5 Pharmacology of GPCR ligands	17
Figure 1.6 Unusual mechanisms of GPCR ligand binding.....	19
Figure 1.7 Biased signalling by GPCR ligands.....	20
Figure 1.8 SCFA receptor signalling.....	27
Figure 1.9 Potential physiological role of SCFA receptors.....	32
Figure 1.10 Crystal structure of the FFA1 receptor	34
Figure 1.11 FFA receptor amino acid sequences and important residues.....	35
Figure 1.12 Chemical structures of SCFA receptor ligands	38
Figure 3.1 FFA2 reference compounds	84
Figure 3.2 Characteristics of [³ H]-GLPG0974 binding to wild type hFFA2.....	85
Figure 3.3 Assay systems for assessment of hFFA2 agonist signalling.....	88
Figure 3.4 Assay systems for assessment of hFFA2 antagonists.....	89
Figure 3.5 Assessment of an hFFA2 agonist series based on compound 2 in functional assays	94
Figure 3.6 Screening of an hFFA2 agonist series based on compound 2 in competition binding assays	95
Figure 3.7 Correlation between hFFA2 agonist potencies and affinities	96
Figure 3.8 Effect of hFFA2 antagonists on agonist responses in a β -arrestin 2 recruitment assay	99
Figure 3.9 Effect of hFFA2 antagonists on agonist response in an ERK1/2 phosphorylation assay	100
Figure 3.10 Importance of carboxylate moiety for hFFA2 antagonist action	102
Figure 4.1 Binding characteristics of [³ H]-GLPG0974 to orthosteric binding site mutants of hFFA2.....	116
Figure 4.2 Agonists but not antagonists of hFFA2 show reduced ability to compete with [³ H]-GLPG0974 at receptor binding site mutants	118
Figure 4.3 Modification of the carboxylate moiety of hFFA2 antagonists results in loss of binding affinity	120
Figure 4.4 Methyl ester analogues of hFFA2 antagonists display higher affinity at orthosteric binding site mutants of hFFA2.....	121
Figure 4.5 Modelling of orthosteric FFA2 agonist binding poses	123
Figure 4.6 Modelling of orthosteric hFFA2 antagonist binding poses	124

Figure 4.7 Alanine replacement of orthosteric arginines increases the speed of [³ H]-GLPG0974 binding kinetics	125
Figure 4.8 Effects of hFFA2 antagonists on [³ H]-GLPG0974 association demonstrate different kinetic parameters for the antagonist series	127
Figure 4.9 FFA2 agonists increase the dissociation rate of [³ H]-GLPG0974	129
Figure 5.1 Principle of a BRET binding assay	141
Figure 5.2 Assessment of function and binding of potential fluorescent tracers for hFFA2	143
Figure 5.3 Fluorescent tracer F-1 shows highest affinity for hFFA2 in the BRET binding assay	145
Figure 5.4 BRET binding assay can be employed to monitor F-1 binding kinetics in real-time	147
Figure 5.5 F-1 competition binding assay can be employed to determine unlabelled hFFA2 antagonist affinity	148
Figure 5.6 Use of F-1 competitive kinetic binding assay to determine kinetic parameters of hFFA2 antagonists	149
Figure 5.7 FFA2 agonists are unable to fully outcompete F-1	150
Figure 5.8 Binding characteristics of F-1 to orthosteric binding site mutants of hFFA2	151
Figure 5.9 Selected hFFA2 antagonists are able to compete with F-1 for binding to R180A-R255A hFFA2	152
Figure 5.10 Potential F-1 binding site in relation to FFA2 agonists and antagonists	159
Figure 6.1 FFA2 antagonists display species selectivity for the human versus mouse orthologue	166
Figure 6.2 Lys65 plays a role in anchoring antagonists in the hFFA2 binding pocket	167
Figure 6.3 Species selectivity of antagonists for human FFA2 is defined by the identity of residue 65 in FFA2	168
Figure 6.4 Binding of [³ H]-GLPG0974 to various forms of human and mouse FFA2 confirms the importance of residue 65 for antagonist binding affinity	170
Figure 6.5 Binding of fluorescent tracer F-1 to hFFA2 is dependent on Lys65 ..	172
Figure 6.6 Predicted binding poses of antagonists in R65K mFFA2	173
Figure 6.7 FFA2 agonists are able to bind to K65A hFFA2 with modest loss in affinity	173
Figure 6.8 Activation of G _{i/o} G proteins by FFA2 agonists is only modestly affected by charge-altering mutations of Lys65	175
Figure 6.9 Signalling of the allosteric ligand AZ1729 is unaffected by mutation of Lys65 in hFFA2	176
Figure 6.10 FFA2 agonists C3 and compound 1 induce a TGF α shedding response through G _{q/11} and G _{12/13}	178

Figure 6.11 Charge-modifying mutations of Lys65 have a detrimental effect on hFFA2 response to agonists in $G_{q/11}$ - and $G_{12/13}$ -coupled TGF α shedding assays. 181

Figure 6.12 Introduction of chimeric $G_{\alpha_{q-i}}$ and $G_{\alpha_{q-o}}$ allows detection of hFFA2-mediated $G_{i/o}$ signalling in TGF α shedding assay 183

Figure 6.13 Charge-modifying Lys65 mutants of hFFA2 show enhanced TGF α shedding response to agonists upon introduction of chimeric $G_{\alpha_{q-i}}$ but not $G_{\alpha_{q-o}}$ 185

Figure 6.14 Differences in AZ1729 allosteric modulation of $G_{q/11}$ - and $G_{12/13}$ -mediated hFFA2 response to C3 in TGF α shedding assay 186

Figure 6.15 Recruitment of β -arrestin in response to FFA2 agonists is affected by charge-altering mutations of Lys65 188

Figure 6.15 Sequence alignment of FFA2 orthologues with focus on residue 65 190

List of Publications

Manuscripts

Sergeev, E., Hansen, A. H., Bolognini, D., Kawakami, K., Kishi, T., Aoki, J., Ulven, T., Inoue, A., Hudson, B. D., Milligan, G. (2017) 'A Single Extracellular Amino Acid in Free Fatty Acid Receptor 2 Defines Both Species Ortholog Selectivity for Antagonists and G Protein Selection Bias for Agonists', *Sci Rep*, 7(1), pp. 13741.

Sergeev, E., Hansen A. H., Pandey S. K., Hudson, B. D., Christiansen, E., Milligan, G., Ulven, T. (2017) 'Development and Characterization of a Fluorescent Tracer for the Free Fatty Acid Receptor 2 (FFA2/GPR43)', *J Med Chem*, 60(13), pp. 5638-45.

Milligan, G., Bolognini, D., Sergeev, E. (2017) 'Ligands at the Free Fatty Acid Receptors 2/3 (GPR43/GPR41)', *Handb Exp Pharmacol*, 236, pp. 17-32.

Bolognini, D., Moss, C. E., Nilsson, K., Petersson, A. U., Donnelly, I., Sergeev, E., König, G. M., Kostenis, E., Kurowska-Stolarska, M., Miller, A., Dekker, N., Tobin, A. B., Milligan, G. (2016) 'A Novel Allosteric Activator of Free Fatty Acid 2 Receptor Displays Unique Gi-functional Bias', *J Biol Chem*, 291(36), pp. 18915-31.

Sergeev, E., Hansen, A. H., Pandey, S. K., Mackenzie, A. E., Hudson, B. D., Ulven, T. and Milligan, G. (2016) 'Non-equivalence of Key Positively Charged Residues of the Free Fatty Acid 2 Receptor in the Recognition and Function of Agonist Versus Antagonist Ligands', *J Biol Chem*, 291(1), pp. 303-17.

Poster Presentations

Sergeev, E., Hansen, A. H., Hudson, B. D., Ulven, T., Milligan, G. 'Molecular Determinants of Ligand Binding to the Short-Chain Fatty Acid Receptor FFA2'

British Pharmacological Society 6th Focused Meeting on Cell Signalling

18-19 April 2016, University of Leicester, Leicester, UK

Sergeev, E., Hansen, A. H., Hudson, B. D., Ulven, T., Milligan, G. 'Molecular Determinants of Ligand Binding to the Short-Chain Fatty Acid Receptor FFA2'

G Protein-Coupled Receptors: Structure, Signaling and Drug Discovery

21-25 February 2016, Keystone Resort, Keystone, Colorado, USA

Sergeev, E., Hudson, B. D., Milligan, G. 'Mapping the ligand binding pocket of the short-chain fatty acid receptor FFA2'

British Pharmacological Society Focused Meeting on Exploiting the New Pharmacology and Application to Drug Discovery

20-21 April 2015, Royal College of Physicians, Edinburgh, UK

Acknowledgements

I would firstly like to thank my supervisors Graeme Milligan and Brian Hudson for all of their support over the last four years. They contributed immensely to my personal and professional development by providing guidance throughout the course of my PhD project, while also encouraging me to work independently and to pursue my own ideas. I am grateful for the opportunity to learn from such outstanding scientists. I would especially like to thank Graeme Milligan for proposing my visit to Tohoku University in Japan, which has been an incredible experience from a scientific and personal point of view.

Thanks to all members of the Milligan lab, past and present, for always having an open ear for my questions. In particular, I wish to thank Laura Jenkins for supervising my technical training, Daniele Bolognini for the lengthy discussions on the complexities of FFA2 receptor pharmacology, and my office mates Sara Marsango, Daniele Bolognini and Richard Ward for their general support and creative input during my thesis writing process. Thank you to Anders Hansen at the University of Southern Denmark for his homology modelling expertise and the continuous supply of test compounds for my project. I would also like to thank Asuka Inoue for welcoming me in his laboratory group at Tohoku University and supervising my short-term project, Kouki Kawakami for sharing his technical knowledge, and all members of the Molecular Pharmaceutics Department who supported me during my visit.

I am also grateful to the friends that I have met through this PhD, which have contributed to making this time an enjoyable experience. A big thank you to Nina, Frederike, Sara, Daniele, Laura, Kenneth and Elisa for your friendship, humour and continuous encouragement. I wish to thank my family for always believing in me and never doubting that I will be able to achieve my goals. My final thanks goes to Charles for your endless emotional support and keeping me sane throughout this journey. I simply would not have made it without you.

Author's Declaration

“I declare that, except where explicit reference is made to the contribution of others, this dissertation is the result of my own work and has not been submitted for any other degree at the University of Glasgow or any other institution.”

Signature: _____

Printed name: _____

Abbreviations

ANOVA	Analysis of variance
AP	Alkaline phosphatase
β₂AR	Beta-2 adrenergic receptor
BCA	Bicinchoninic acid
BRET	Bioluminescence resonance energy transfer
BSA	Bovine serum albumin
cAMP	Cyclic adenosine monophosphate
CPM	Counts per minute
dATP	Deoxyadenosine triphosphate
dCTP	Deoxycytidine triphosphate
dGTP	Deoxyguanosine triphosphate
DMEM	Dulbecco's Modified Eagle's Medium
DMSO	Dimethyl sulfoxide
DNA	Deoxyribonucleic acid
dNTP	Deoxyribonucleotide
DPM	Disintegrations per minute
dTTP	Deoxythymidine triphosphate
ECL	Extracellular loop
eYFP	Enhanced yellow fluorescent protein
FCS	Foetal calf serum
FFA	Free fatty acid
FRET	Fluorescence resonance energy transfer
FRT	Flippase recognition target
GABA	γ-Aminobutyric acid
GCGR	Glucagon receptor
GDP	Guanosine diphosphate
GF	Germ-free
GI	Gastrointestinal
GLP-1	Glucagon-like peptide 1
GPCR	G protein-coupled receptor
GRK	G protein-coupled receptor kinase

GTP	Guanosine triphosphate
HA	Hemagglutinin
HBSS	Hank's Balanced Salt Solution
HDAC	Histone deacetylase
HFD	High-fat diet
HTRF	Homogeneous time-resolved fluorescence
ICL	Intracellular loop
IP1	Inositol monophosphate
K_d	Dissociation constant
KO	Knock-out
K_{off}	Dissociation rate
K_{on}	Association rate
LCFA	Long chain fatty acid
MAPK	Mitogen-activated protein kinase
MCFA	Medium chain fatty acid
M₂R	Muscarinic M ₂ receptor
μOR	Mu-opioid receptor
NAM	Negative allosteric modulator
NBD	Nitrobenzoxadiazole
NLuc	Nanoluciferase
NMR	Nuclear magnetic resonance
PAM	Positive allosteric modulator
PAR2	Protease-activated receptor 2
PBS	Phosphate-buffered saline
PCR	Polymerase chain reaction
PE	Polyethylene
PEI	Polyethylenimine
PPAR	Peroxisome proliferator-activated receptor
PTX	Pertussis toxin
PYY	Peptide YY
RLuc	<i>Renilla reniformis</i> luciferase
RNA	Ribonucleic acid
RT	Room-temperature

TGFα	Transforming growth factor alpha
TM	Transmembrane domain
T_m	Melting temperature
TNFα	Tumour necrosis factor alpha
SAR	Structure-activity relationship
SCFA	Short chain fatty acid
SDS	Sodium dodecyl sulfate

1 Introduction

1.1 Drug discovery and development

1.1.1 Different approaches to drug discovery

One of the defining features of human nature is the drive to expand our knowledge and exploit discoveries to guide the progress of society and enhance our quality of life. This has led to impressive scientific and technological advances that have transformed the way we live our lives including, possibly most importantly, drastically improved medical treatments and a revolutionised approach to the development of medicines. Some therapeutics that are still widely in use today were discovered centuries ago by pure serendipity. A prominent example is paracetamol, whose complex mechanism of action remains to be fully understood and recent studies have highlighted novel safety concerns regarding its overuse (Aminoshariae and Khan, 2015). In addition to serendipitous discoveries, a phenotypic drug discovery approach has long dominated the pharmaceutical industry (Swinney, 2013). In phenotypic assays crude extracts or compound libraries are tested for their activity in cellular and/or animal models relevant to the respective disease background to identify new drug candidates. Only after compound efficacy in disease-relevant assay systems has been demonstrated, is effort invested into identifying its target and mechanism of action. The quality and translational value of the selected assay systems are absolutely imperative, as they need to reflect the condition to be treated as closely as possible and allow measurement of an appropriate biomarker to track treatment progress. Although the respective target does not necessarily need to be identified for regulatory bodies to allow progression into clinical trials, an extensive body of evidence is required to demonstrate the therapeutic benefit of the candidate drug and moving forward without a defined mechanism of action can be very challenging. Furthermore, with structure-based investigations playing an important role in the compound optimisation progress, the lack of a known target can also hinder progress.

In contrast, a more recent approach to drug development follows a reverse methodology by starting with the search for an appropriate protein target that has a clear implication in the disease mechanism (Eder et al., 2014). Target

identification and validation follows on to development of compounds with the desired pharmacological action. Disease-relevant model systems to confirm compound efficacy are then employed during the optimisation process of identified candidate drugs. The concept of target-based (or rational) drug discovery is deeply rooted in our significantly improved understanding of the underlying molecular mechanisms of disease origin and progression. By utilising rational drug development important therapeutic needs have been addressed, including the identification of tyrosine kinase inhibitors as novel cancer treatments (Arora and Scholar, 2005) and antivirals to treat HIV infection (Pommier et al., 2005). However, despite our increased knowledge base, some conditions are governed by complex interlinked processes that are not fully understood and targeting only one component may not be sufficient to exert a therapeutically beneficial effect. Therefore, it is important to ensure that sufficient evidence is present to demonstrate the therapeutic potential of the selected target, with studies in disease-relevant animal models that employ tool compounds being particularly important.

The informed nature of target-based drug development was initially thought to be superior to phenotypic screening, but recently phenotypic approaches have once more attracted industrial attention. Pharmaceutical companies including Novartis AG and GlaxoSmithKline plc are investing in the development of novel phenotypic screening methodologies (Kotz, 2012). This may in part be due to the results of an analysis of new molecular entities approved between 1999 and 2008, which revealed that the majority (37%) of first-in-class drugs were identified by phenotypic screening rather than rational development (23%) (Swinney, 2013). The report suggested that target-based screening is likely to play a more important role in the development of follower drugs, of which half were identified following such an approach, while only a fifth were identified by phenotypic screening. However, a more recent study encompassing data up to 2013 came to a different conclusion with 70% of first-in-class drugs resulting from target-based development and phenotypic screening contributing to only 30% (Eder et al., 2014). In 2011 and 2012 alone, 22 new approved first-in-class drugs were developed in a target-based fashion, while only 4 were initially identified by phenotypic screening. The relevance of rational drug discovery has potentially only become apparent recently due to the long time-frame between

target selection and drug approval. However, scientific advances have not only affected rational drug discovery in a positive fashion (Kotz, 2012). Most recent phenotypic screening efforts employ elaborate assay systems, such as the use of organotypic multicellular cultures that aim to mimic the responses of organs *in vivo*, and the means of drug target identification have also drastically improved with chemical proteomics being particularly successful. These use a mass spectrometry-based affinity chromatography approach to identify small molecule-protein interactions. With these developments in mind, the choice of drug discovery approach will perhaps become dependent on the available knowledge base and screening methodologies in the respective disease context.

1.1.2 Principles of rational target-based drug discovery

While phenotypic screening is commonly executed by pharmaceutical companies with large compound libraries and high-throughput equipment, the initial stages in rational drug discovery are often performed in an academic setting or in collaborations between academia and industry (Vallance, 2016). In the rational drug discovery pipeline such preclinical studies can progress from target identification all the way to selection of a candidate lead compound to proceed into clinical trials and regulatory approval (Figure 1.1).

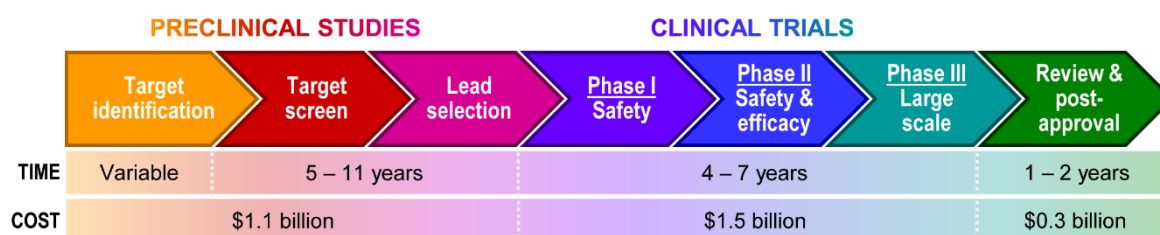


Figure 1.1 The pipeline of target-based drug discovery Development of novel therapeutics is a long and cost-intensive process. The initial identification of an appropriate target is often based on work generated by academia, as it requires a substantial amount of basic science research. Once a target has been selected, a high-throughput screening system must be developed in which large libraries of potential ligands can be tested. Any compounds that are identified in this fashion likely require further optimisation, which includes extensive medicinal chemistry to develop a lead compound appropriate for clinical testing. At this stage the ligands are commonly also employed in animal models to validate the chosen target and define properties such as bioavailability, toxicity and potential metabolism. Clinical trials initially evaluate the safety of the lead drug in healthy subjects (Phase I) and then assess both safety and efficacy in a small cohort of patients with the condition to be treated (Phase II). If sufficient efficacy is observed, the trial is performed in a larger group with a focus on avoidable adverse effects that may only become apparent in a larger test population (Phase III). The last hurdle that needs to be overcome is the approval process, which may have to be repeated for different regions of the world depending on the target market. Figure modified from (Roses, 2008) and cost estimations obtained from (DiMasi et al., 2016).

The key features of a good drug target are its ability to be modulated by a drug molecule to exert a therapeutic benefit without causing side effects (Hughes et al., 2011). The term drug target itself is relatively broad and includes classical protein targets, but also genes and non-coding RNAs. A range of different methodologies and sources can be employed to identify such targets, but essentially these all come down to data mining of published information such as gene expression, proteomics and transgenic phenotyping (Yang et al., 2012). Correlating such data with risk of disease and its incidence can highlight genes and proteins that may be involved in the mechanism of disease, for example by identifying relevant genetic polymorphisms, as in case of the amyloid precursor protein in Alzheimer's Disease (Bertram and Tanzi, 2008). Any potential target identified in this fashion is subjected to a detailed validation process in which multiple techniques are combined to confirm its therapeutic potential (Hughes et al., 2011). Common methods include manipulation of target expression by use of RNA-based antisense technology to block protein synthesis and transgenic knock-out animals, or studies employing available tool compounds in cell-based and *in vivo* disease models. The more evidence is available on the role of the identified target in the disease of interest and the exact mechanism by which it modulates disease progression, the higher is the likelihood of a successful drug discovery project.

Once the drug target has been selected and thoroughly validated, the screening process begins. Selection of an appropriate assay format is a deciding factor in the drug discovery process. In the case of signalling proteins that alter the concentration of secondary messengers, such as calcium ions, in the cell or affect expression of downstream reporter genes, this can be relatively straightforward. Important considerations, in particular for high-throughput screens commonly employed by the pharmaceutical industry, include reproducibility and quality of the assay, but also the associated costs (Hughes et al., 2011). A good example for G protein-coupled receptors (GPCRs) (see section 1.2) is the aequorin-based assay (Stables et al., 2000). Some active GPCRs signal by coupling to the $G_{q/11}$ subfamily of G proteins, which results in an increase of intracellular levels of calcium ions. This can be quantified in presence of aequorin, which is a natural calcium-sensitive protein that produces bioluminescence by oxidising its substrate coelenterazine in presence of calcium

ions. Alternative approaches to high-throughput screening include informed focussed screening, in which a smaller number of compounds to be screened is selected based on known ligands or molecular modelling (Valler and Green, 2000), or fragment screening, which aims to identify small molecules with a low molecular weight to be used as building blocks for larger compounds (Erlanson et al., 2016). If sufficient structural information of good quality is available, virtual screening can also be employed, in which putative ligands are docked computationally into potential binding sites (Congreve et al., 2011).

When developing a clinical candidate from compounds identified in initial screens, medicinal chemistry projects run in parallel with screening efforts to generate the best possible compound. In addition to the ability of the compound to modulate the desired target, other factors are also assessed that are crucial for clinical testing. Studies need to be performed to define *in vivo* properties such as compound absorption, distribution, metabolism and excretion; and pharmacokinetics. In some cases, compound activity needs to be sacrificed for optimisation of such *in vivo* parameters to reduce the likelihood of side effects. At earlier stages it can be beneficial to confirm whether the compound can be classified as drug-like according to the Lipinski Rule of Five (Lipinski et al., 2001), which includes assessment of the molecular weight (<400 kDa) and lipophilicity in terms of clogP (<4). Furthermore, initial toxicity tests in hepatocytes and other cell lines can provide an indication of the likelihood of *in vivo* toxicity (Gomez-Lechon et al., 2010). Failure of a potential drug can occur at any of the stages described above, from the inability to develop an appropriate assay system to lack of compound efficacy in disease-relevant tests or off-target toxicity. Only approximately 10% of industrial drug discovery projects result in a clinical candidate, of which again only 10% reach the market (Hughes et al., 2011). The further along the pipeline the failure takes place, the costlier the drug discovery project becomes, hence careful target selection and validation are one of the most important factors in the drug discovery process. Therefore, academic research also plays an important role in rational drug development with exploratory drug discovery projects contributing significantly to validation of drug targets and their therapeutic potential.

1.1.3 Significance of G protein-coupled receptors as drug targets

Looking back at the past to analyse successfully targeted protein families can provide us with valuable information for informed drug target selection. Perhaps it is to be expected that the class including the most successfully utilised drug targets are GPCRs, followed by ion channels, nuclear receptors and kinases (Santos et al., 2017). These protein families all act in response to a stimulus provided directly (GPCRs and ion channels) or indirectly (nuclear receptors and kinases) by the cellular surroundings; they are a component of the cellular machinery that senses the extracellular environment and induces a corresponding response by activating a specific intracellular signalling cascade. GPCRs seem to play a particularly important role, with roughly a third of all small-molecule drugs exerting their effects by acting on these receptors (Santos et al., 2017). Interestingly, the contribution of GPCRs to the pool of drug targets has not changed significantly over the last six years as a similar analysis in 2011 came to the same conclusion (Rask-Andersen et al., 2011). Although the bulk of drugs targeting GPCRs has been approved before 1990, innovation in drug development has been ongoing with 4-5 new drugs, including small molecules and biologics, being approved per year (Santos et al., 2017).

But what are GPCRs and what makes them such superior drug targets? GPCRs are the largest family of transmembrane receptors in the human genome with approximately 800 members (Fredriksson et al., 2003) and they are complemented by a strikingly diverse selection of ligands, ranging from small organic compounds and lipid-like molecules to peptides and even proteins. In response to their respective stimulus GPCRs can induce signalling cascades by coupling to different G protein subtypes and arrestins, which can exert a variety of downstream effects. From a drug discovery perspective, being involved in virtually every physiological process and having a readily druggable binding site makes GPCRs very suitable target candidates. By designing synthetic molecules with different pharmacological properties, one could conceptually be able to manipulate any disease-relevant cellular process in the desired fashion by inducing, blocking or modulating the response of different GPCRs. Indeed, drugs that target GPCRs are in use in the majority of officially classified therapeutic areas, highlighting their universal drug target potential (Santos et al., 2017).

1.2 G protein-coupled receptors

1.2.1 Overview of GPCRs and their subfamilies

The number of GPCRs in the human genome and the variety of their ligands highlight the functional diversity of this superfamily, however certain properties that designate them as GPCRs are shared by all members. In addition to the common nature of their signalling, the most notable defining characteristics are their structural features. All GPCRs are composed of seven transmembrane domain helices (termed TM1-7), linked by three intracellular (ICL1-3) and three extracellular (ECL1-3) loops with the N terminus facing the extracellular environment and the C terminus being intracellular. The N terminus and, in some cases the ECLs, show high structural diversity as they often play a key role in receptor functionality and ligand binding, especially as for some GPCR classes it is the main point of ligand-receptor interaction.

The structural variation among GPCRs is reflected in their phylogenetic relationship and led to the first classification of the receptor family into class A-F (also referred to as class 1-6) (Kolakowski, 1994). This nomenclature system has been modified over the years and was also adapted by the International Union of Pharmacology (Foord et al., 2005). The sequencing of the human genome in 2001 allowed for a more comprehensive investigation of the GPCR repertoire and resulted in the now commonly accepted classification system (Fredriksson et al., 2003), which retains most of the characteristics of the initially defined classes. GPCRs cluster into five main groups referred to as *Rhodopsin* (class A), *Secretin* (class B), *Adhesion* (class B), *Glutamate* (class C) and *Frizzled/Taste2* families (**Figure 1.2**).

The *Rhodopsin* family is the largest subfamily of GPCRs with approximately 670 members and is also the most diverse in its ligands (Fredriksson et al., 2003), which undoubtedly contributes to the fact that it also contains the largest number of therapeutic targets. Examples include muscarinic receptors that bind the neurotransmitter acetylcholine (Wess, 1993); receptors activated by chemokines, which are small signalling proteins (Gershengorn et al., 1998); protease-activated receptors that bind a peptide cleaved from their N terminus (Vu et al., 1991); and fatty acid receptors (Milligan et al., 2017). In contrast to

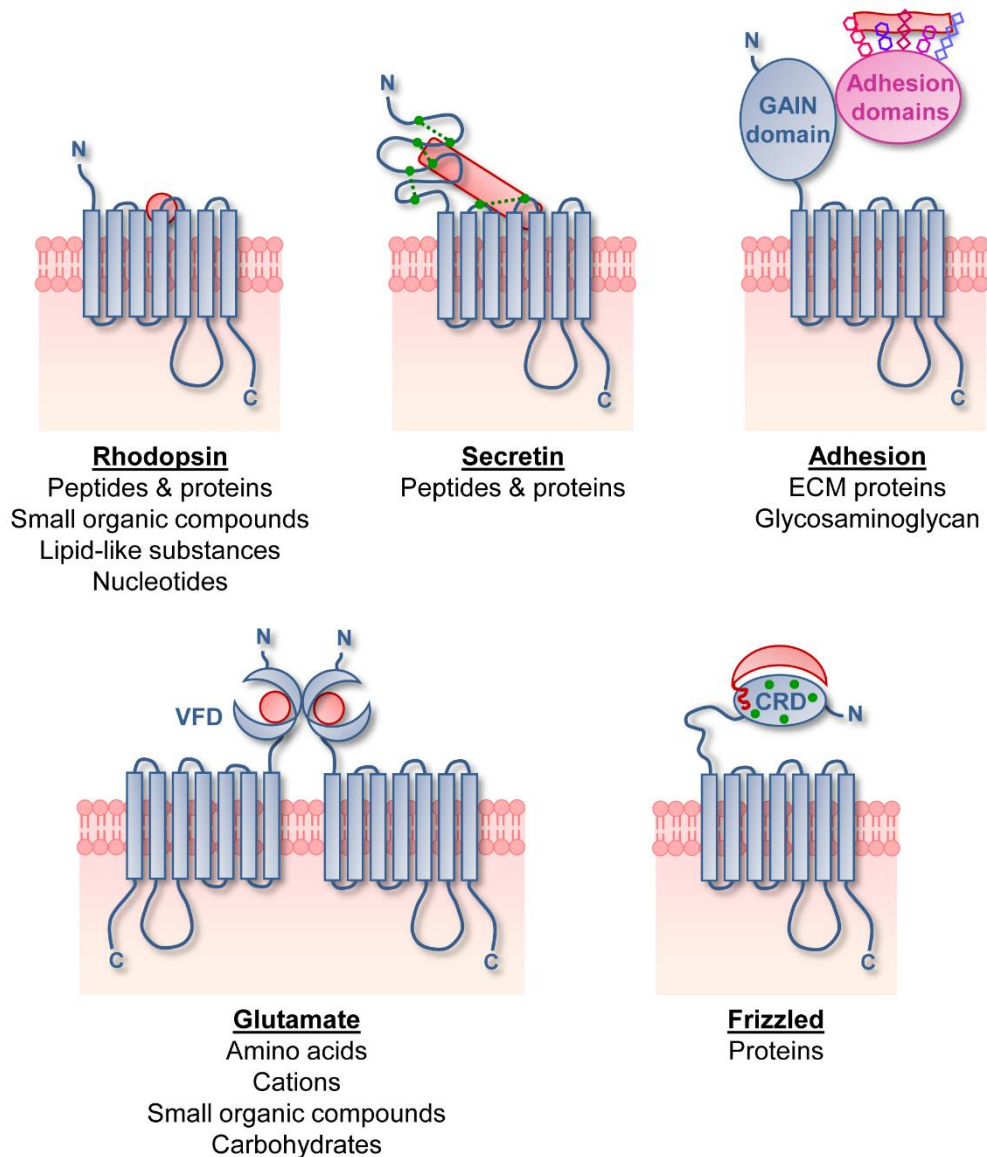


Figure 1.2 Structural features of the GPCR families All G protein-coupled receptors (GPCRs) share a 7-transmembrane helix arrangement with an extracellular N terminus and an intracellular C terminus. While the intracellular portions are relatively conserved between different families, the extracellular region is highly diverse. Red shapes represent the different modes of ligand interaction with respective GPCR families. Conserved cysteines that stabilise the N terminus to allow for ligand binding are shown in green. Properties of common GPCR subfamily ligands are listed below corresponding subclasses. The N terminus of the *Adhesion* family is composed of a GPCR autoproteolysis-inducing (GAIN) domain that catalyses the cleavage of the N terminus such that the adhesion domains, which contain a range of glycosylation sites, are non-covalently associated with the receptor. Most members of the *Glutamate* family exist in dimeric form and bind ligands by employing their venus fly trap domain (VFD). Protein ligands associate with the cysteine-rich domain (CRD) of *Frizzled* family receptors with help of their palmitoyl group (red line). The family of *Taste2* receptors is not shown as its structural features are less understood and they do not show distinctive N terminal modifications. Their transmembrane domains show highest similarity to the *Frizzled* family.

all other families, the majority of endogenous ligand binding sites lie within the TM region, which therefore varies more significantly between members of this family compared to others. Additionally, the TM region also contains the highly conserved DRY (Rovati et al., 2007) and NPxxY (Urizar et al., 2005) motifs that

are thought to stabilise different conformational states of the receptor. The *Secretin* family is relatively small with only 15 members and is characterised by an extracellular peptide hormone-binding domain that is also the most varied region within the family (Bazarsuren et al., 2002). However, as in case of the TM domains of the *Rhodopsin* family, this domain also contains conserved features, namely cysteine residues that are thought to stabilise the N terminus to allow for ligand binding. The *Adhesion* family and its 33 members were initially classed with the *Secretin* family due to the similarity of their TM domains, however their N termini have a long and rigid structure with extensive glycosylation sites allowing them to bind extracellular matrix proteins (Fredriksson et al., 2003). The most distinguishing feature of the *Glutamate* family is the dimeric quaternary structure adopted by most of its members that bind glutamate by employing a Venus flytrap mechanism using their large N terminal lobes (Kunishima et al., 2000). The GABA-binding members of the family use a similar mechanism to facilitate ligand binding. The *Frizzled* family is activated by Wnt glycoproteins that bind to a cysteine-rich region within their N terminus and may also engage the extracellular loops (Dann et al., 2001). The *Taste2* receptors are the most recently identified GPCR subfamily and are thought to translate the bitter taste of certain molecules that bind to the extracellular loops of the receptor (Pronin et al., 2004), however the ligands for most of their members remain to be identified (Chandrashekar et al., 2000). Furthermore, the family also shows a relatively high sequence diversity (Conte et al., 2002) with few conserved residues, which may be related to the fact that only 25 putative members are able to recognise more than a thousand different bitter compounds.

This overview of the different GPCR subfamilies exemplifies the link between the structural diversity and universal role that these receptors play in the functioning of the human body (Lagerstrom and Schioth, 2008). However, it also highlights that not all 800 members have equal therapeutic potential as sensory receptors are traditionally not thought to play a role in disease-related processes, leaving approximately 400 potential drug targets. Targeting different classes of GPCRs requires distinct approaches to ligand development, as the druggability of binding sites needs to be considered and the nature of the endogenous binding pocket plays a crucial role. For example, it is difficult to

design small-molecule ligands that bind with high affinity to the often shallow sites that are targeted by peptides, whose nature of binding to a receptor resembles interactions between proteins.

1.2.2 Canonical GPCR signalling pathways

The ability of GPCRs to transduce signals by activation of associated guanine nucleotide-binding proteins, or G proteins, is what gives the receptors their name and is the most studied component of the GPCR signalling cascade. G proteins are heterotrimeric proteins that are composed of three subunits: α , β and γ (Lambright et al., 1996). $G\alpha$ contains distinct structural features including a Ras-like GTPase domain, an α helical domain and an N-terminal α helix. $G\beta$ consists of β sheets that form a propeller-like structure and an α helix, while $G\gamma$ is largely unstructured with two α helices that form a multitude of interactions with the α helix and β sheets of $G\beta$. GPCR ligand binding and activation triggers the exchange of GDP for GTP in the cleft between the GTPase and α -helical domain of $G\alpha$ (Dror et al., 2015). This induces a conformational change in $G\alpha$ that facilitates its dissociation from the $G\beta\gamma$ heterodimer and allows for $G\alpha$ and $G\beta\gamma$ to independently interact with different downstream effectors. This signalling cascade is inactivated by the hydrolysis of GTP to GDP by the Ras-like GTPase domain of $G\alpha$, whose activity is augmented by the binding of regulators of G protein signalling, and promotes the reassociation of the heterotrimeric $G\alpha\beta\gamma$ complex (Mann et al., 2016). A single activated GPCR can turn over multiple G proteins and thereby constitutes the first amplifying step of the signalling cascade. Although the principle of G protein-dependent signalling is relatively straightforward, it is complicated significantly by the presence of 16 $G\alpha$, 5 $G\beta$ and 12 $G\gamma$ proteins in the human genome that all have the capacity to promote different signalling pathways (Hewavitharana and Wedegaertner, 2012). Association of a GPCR with differently composed heterotrimers can therefore induce highly diverse downstream effects, however traditionally the $G\alpha$ subunit was thought to be the deciding factor. $G\alpha$ proteins can be categorised into four families based on preferential downstream signalling and sequence similarity: $G\alpha_s$ (includes $G\alpha_{s(S)}$, $G\alpha_{s(L)}$ and $G\alpha_{s(olf)}$), $G\alpha_i$ (includes $G\alpha_{oA}$, $G\alpha_{oB}$, $G\alpha_{i1-3}$, $G\alpha_z$, $G\alpha_{t1-2}$ and $G\alpha_{gust}$), $G\alpha_q$ (includes $G\alpha_q$, $G\alpha_{11}$ and $G\alpha_{14-16}$) and $G\alpha_{12}$ (includes $G\alpha_{12}$ and $G\alpha_{13}$) (for detailed signalling pathways see **figure 1.3**). Additionally, different combinations of $G\beta\gamma$ heterodimers facilitate the activation of a variety of

downstream effectors. From a translational perspective it is therefore not only important to consider which G proteins are activated by a specific GPCR, but also the expression of the respective subunits in the disease-relevant tissue.

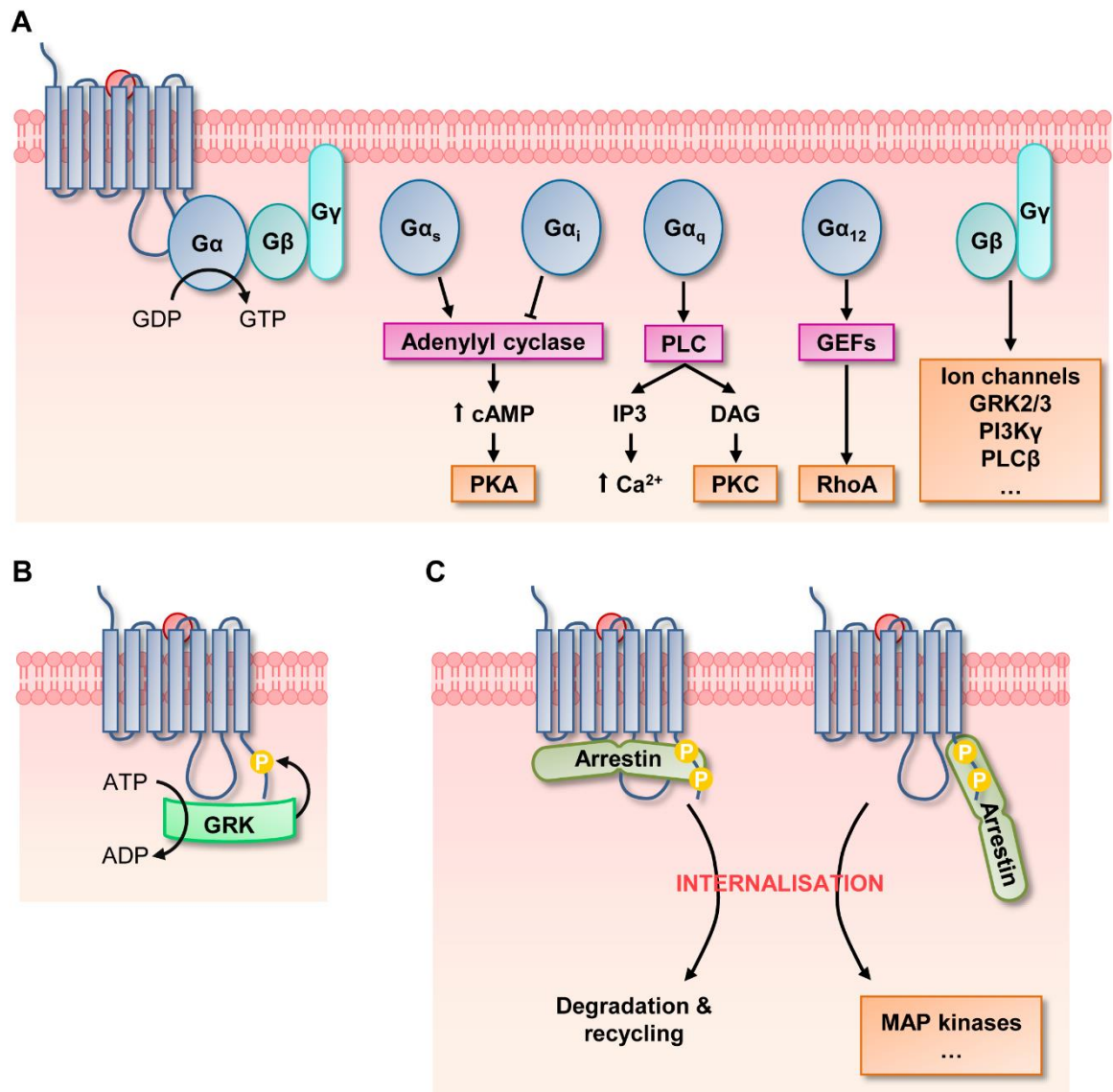


Figure 1.3 Signalling cascades induced by GPCR activation Association of a G protein-coupled receptor (GPCR) with its ligand promotes an active conformational state (**A**). This conformational rearrangement results in recruitment of a heterotrimeric G protein and facilitates guanosine nucleotide exchange in the $G\alpha$ subunit, which induces dissociation of $G\alpha$ from the $G\beta\gamma$ subunits. Depending on the $G\alpha$ subtype, different downstream signalling pathways are engaged with pink boxes showing direct protein targets and orange boxes representing proteins activated further downstream. The $G\beta\gamma$ subunits are also able to engage a range of different signalling cascades that depend on $G\beta\gamma$ subtypes and cell system. Actively signalling GPCRs are targeted by G protein-coupled receptor kinases (GRKs) that phosphorylate the C-terminal tail of GPCRs (**B**). Arrestins show high affinity for the phosphorylated C terminus of GPCRs and induce internalisation of the receptor upon association (**C**). Once internalised, the GPCR is either directly targeted for degradation or recycling pathways, or it induces arrestin-dependent signalling such as activation of mitogen-activated protein (MAP) kinases.

While actively signalling G proteins have an inherent inactivation mechanism, downregulation of activated GPCRs is a more complex process. G protein-coupled receptor kinases (GRKs) induce the first step in this cascade by phosphorylating multiple serine and threonine residues in the C terminal tail and/or intracellular loops (Tobin et al., 2008). These changes in the intracellular surface of the receptor increase the affinity of the receptor for binding of the arrestin adaptor proteins. The arrestin protein family includes only four members: arrestin 1 (or visual arrestin), arrestin 2 (or β -arrestin 1), arrestin 3 (or β -arrestin 2) and arrestin 4 (or cone arrestin). While arrestins 1 and 4 have a sensory function in photoreceptors, the β -arrestins were initially identified as regulators of the β_2 adrenergic receptor (β_2 AR), hence termed β -arrestins (Lohse et al., 1990), and are now known to be expressed ubiquitously to regulate non-photoreceptor GPCR desensitisation (DeWire et al., 2007). Upon association with a GPCR, β -arrestins facilitate clathrin-mediated endocytosis, which facilitates internalisation of the receptor and targeting of resulting intracellular vesicles for recycling to the cell membrane or degradation (Goodman et al., 1996). It is now universally accepted that β -arrestins are also able to induce specific signalling cascades by activating, among others, specific mitogen-activated protein kinases (MAPKs) (Daaka et al., 1998), making them an integral component of GPCR signalling (**Figure 1.3**). However, β -arrestin signalling does not seem to be triggered by activation of every GPCR, which may be regulated by the conformational changes induced in β -arrestins upon interaction with a GPCR, or the fashion in which it associates with the receptor (Cahill et al., 2017).

1.2.3 Structural investigations of GPCR activation

Deciphering how a GPCR translates the extracellular binding of a ligand into conformational rearrangements of its intracellular portion to facilitate the highly specific activation of interacting proteins is not only of fundamental research interest, but also has translational relevance due to its impact on future ligand development and rational targeting of specific GPCR signalling pathways. A key scientific advance that has undoubtedly played a critical role in understanding this process is the availability of high-resolution structures. The award of the Nobel Prize in Chemistry for solving the crystal structure of the β_2 AR in complex with its signalling partner, the G protein G_s , clearly highlights the impact of this work (Rasmussen et al., 2011). The flexible nature of GPCRs hinders the

formation of rigid crystals that are required for structure determination by X-ray diffraction, therefore recent approaches commonly induce artificial stabilisation of the GPCR. These include the fusion of easy-to-crystallise proteins such as T4 lysozyme to the receptor (Rosenbaum et al., 2007); conformational stabilisation by introduction of thermostabilising mutations (Magnani et al., 2016); and co-crystallisation with engineered interaction partners such as nanobodies (Pardon et al., 2014) or peptides of naturally interacting proteins such as G proteins (Carpenter and Tate, 2016) and arrestins (Szczeppek et al., 2014) to stabilise specific GPCR conformations. Availability of these and other methodologies has led to an explosion in the number of GPCR crystal structures. While 59 crystal structures were available in total in 2011, in 2016 alone 32 new crystal structures were published (Isberg et al., 2016). The GPCRdb database now lists a total of 203 crystal structures with the majority belonging to the *Rhodopsin* family. In addition to X-ray crystallography, other approaches to structure investigation have also become more advanced, including nuclear magnetic resonance (NMR), which has been used to visualise entire unmodified GPCRs in a lipid bilayer (Park et al., 2012) or to assess structural changes in localised areas by selectively labelling residues of interest (Manglik et al., 2015); and single-particle cryo-electron microscopy that enables visualisation of more flexible GPCR complexes (Liang et al., 2017). Finally, computational methods have also advanced substantially and simulation of the molecular dynamics of GPCR activation and ligand binding now play a crucial role in defining the link between structure and function (Latorraca et al., 2017).

Considering the invaluable information provided by crystal structures of receptors in different conformations, it is easy to overlook that the dynamic movement of GPCRs is what lies at the heart of the molecular basis of GPCR signalling (Latorraca et al., 2017). To truly appreciate this process, it is important to consider that common schematics that show signalling cascades as sequential mechanisms (**Figure 1.3**) do not reflect what occurs in cells. In reality GPCRs are highly flexible and molecular dynamics simulations indicate that GPCRs spontaneously adopt multiple conformations including inactive, active and intermediate states (Dror et al., 2011). Rather than switching all receptors into an active state, ligand binding seems to affect both the transition speed and resting time of a GPCR in certain conformations and thereby changes the

probability to detect the receptor in its active or inactive form. Association of G proteins and arrestins also plays a role in such conformational transitions and stabilisation of active-state structures, which may explain why many ligand-bound structures appear to be in an intermediate conformation between canonical inactive and active states (Lebon et al., 2012).

This complexity may suggest that GPCRs undergo different conformational changes upon activation, depending on the bound ligand and activated signalling pathways. However, structures of GPCRs in their active state appear to share certain structural rearrangements when compared to their inactive-state structures (**Figure 1.4**). In essentially all putative active-state crystal structures of *Rhodopsin* family GPCRs the TM6 is rotated and displaced by 6-14 Å away from the helical bundle (Rasmussen et al., 2011, Kruse et al., 2013, Huang et al., 2015). In some cases, this movement is also accompanied by an outward movement of TM5. This intracellular helix rearrangement is responsible for the formation of a crevice flanked by TM3, TM5 and TM7 that serves as the G protein (and likely also β -arrestin) binding site. Interestingly, this movement was also conserved in the cryo-EM structure of the *Secretin* family calcitonin receptor (Liang et al., 2017), suggesting that this may be conserved throughout the entire

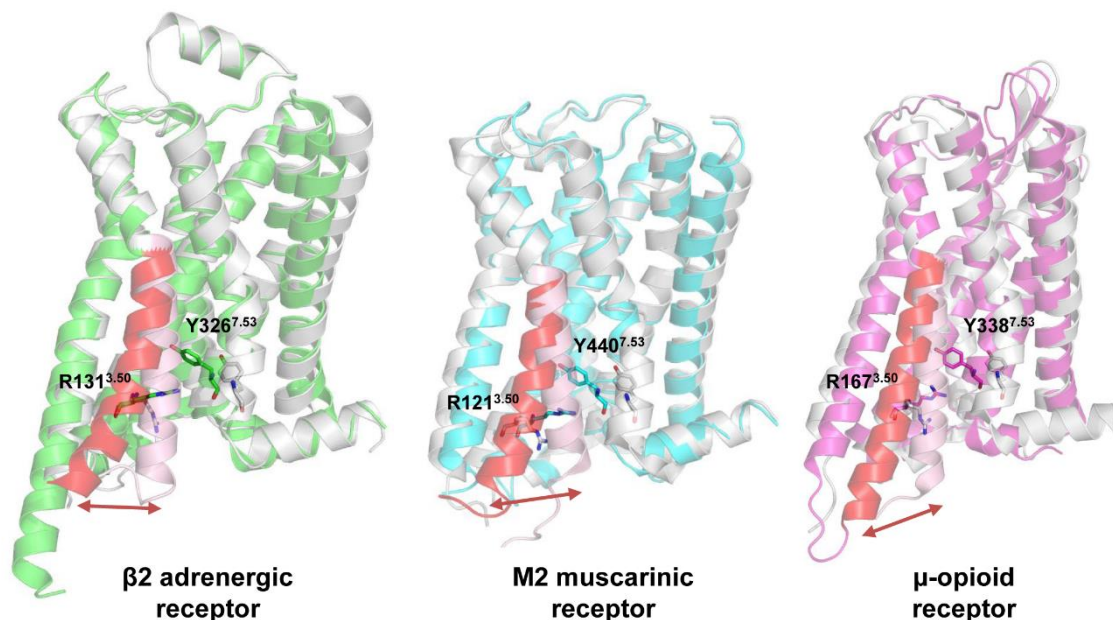


Figure 1.4 Structural changes induced by GPCR activation Inactive (grey) and active (coloured) state structures of three different receptors are aligned and the outward shift of the TM6 is illustrated in red. The rearrangement of arginine (R) and tyrosine (Y) residues within the conserved DRY and NPXXY motifs is highlighted. The PDB IDs of the respective structures are 2RH1 and 3SN6 (inactive and active β_2 AR); 3UON and 4MQS (inactive and active M₂R); 4DKL and 5C1M (inactive and active μ OR).

GPCR family. Other helices such as TM3 and TM7 undergo more subtle rotations. Defining the exact mechanism of G protein and β -arrestin association with GPCRs comprises a field of research that is continuously evolving due to new developments. In the case of G proteins, structures of rhodopsin with a G protein peptide (Choe et al., 2011) and the β_2 AR- G_s complex structure (Rasmussen et al., 2011) both suggested that the C terminal α_5 helix of the Ras-like domain inserts into the intracellular crevice, while the α -helical domain shows increased mobility and thereby potentially facilitates GDP release. Interaction of β -arrestin with the receptor is less understood, however the phosphorylated C terminal tail of GPCRs appears to act as the defining recruitment site. Some studies also suggest that a finger loop within one of the immunoglobulin-like domains of β -arrestin may occupy the same region as the α_5 helix of G proteins, thereby making association of G proteins and β -arrestins mutually exclusive (Szczeppek et al., 2014, Kang et al., 2015). The potential of β -arrestins to mediate either desensitisation or further downstream signalling seems to relate to different β -arrestin conformations that occupy either just the C terminal tail or engage with the transmembrane core of the receptor (Cahill et al., 2017, Shukla et al., 2014).

In some structures helical rearrangements also correlate with the role of conserved *Rhodopsin* family motifs, including the breaking of the ionic lock within the DRY motif upon ligand binding and the formation of interactions within the NPxxY motif once the receptor is in an active conformation (**Figure 1.4**) (Rasmussen et al., 2011, Kruse et al., 2013, Huang et al., 2015). But how does agonist binding facilitate these observations? This is a question that is more difficult to answer. While on the cytoplasmic side movements are relatively conserved between different GPCRs of one family, conformational rearrangements at the extracellular side differ substantially between receptors. The β_2 AR active-state structure and molecular dynamics simulations suggest that a central network of TM3, TM5, TM6 and TM7 residues located within the helical bundle may be responsible for transmitting the signal of ligand binding into the conserved intracellular rearrangements (Latorraca et al., 2017). It is likely that other receptors will also have such a “transmission network”, however residues and conformational changes induced may differ between receptors and depend on the pharmacology of employed ligands. It is also important to consider that it

is still challenging to obtain true active-state structures of GPCRs. Crystallisation-assisting techniques such as thermostabilising mutations induce an artificially stabilised conformational state of the receptor, in which agonist binding is often uncoupled from the structural rearrangement of the intracellular surface.

1.2.4 Pharmacology of GPCR ligands

The inherent pharmacological parameters that define the action of a ligand at a receptor are affinity and efficacy (or intrinsic activity). Affinity represents the strength of interaction between a compound and its binding site. To determine affinity values experimentally, a means of measuring ligand binding to the receptor is required, for example using a radioactively or fluorescently labelled probe. Should a suitable probe not be available, ligand potency in functional assays can be used as a surrogate measure of ligand affinity (Rosenkilde and Schwartz, 2000). However, functional potency may be dependent on both affinity and efficacy in assay systems with a significant receptor reserve present, and therefore care must be taken in selecting a suitable functional assay to use as a surrogate for agonist affinity (Kenakin, 2001). Defining efficacy can be more challenging; it essentially reflects the ability of a ligand to promote specific receptor conformations that change its basal behaviour by, for example, activating downstream effectors (Kenakin, 2002). Although the conformational changes in a receptor induced by a ligand are conceptually independent of the respective assay system, it is commonly assessed in a system-dependent fashion by measuring the maximum response achievable by a ligand in a functional assay. Efficacy measurements are also governed by the receptor reserve of the employed system, which is related to the number of receptors that need to be occupied by a specific ligand to induce a maximal response. Depending on the properties described above, ligands can be broadly separated into the following four classes: Full, partial or inverse agonists and neutral antagonists (for detailed description see **figure 1.5A**).

Although this classification is sufficient to describe orthosteric ligands that are defined by their interaction with the endogenous ligand binding site, advances in understanding GPCR ligand binding in the past decade have resulted in an emerging interest in allosteric ligands that can alter receptor activity by

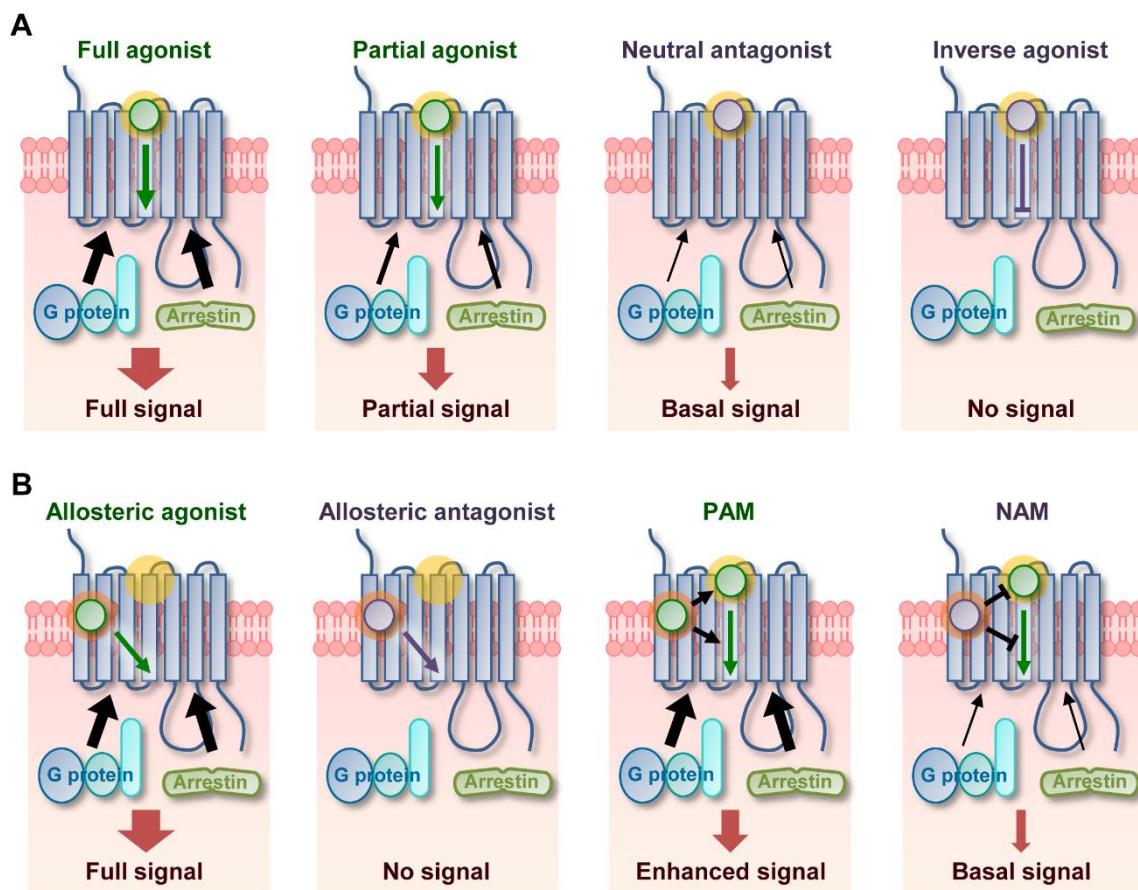


Figure 1.5 Pharmacology of GPCR ligands The pharmacology of orthosteric (**A**) and allosteric (**B**) ligands is illustrated. (**A**) Binding of an agonist (green) to the orthosteric binding site (yellow shading) can induce a full or partial recruitment of downstream signalling partners. Association of a neutral antagonist (purple) with the orthosteric site does not affect the basal activity level of receptor, while an inverse agonist is able to inhibit basal activity by promoting an inactive conformational state. (**B**) Allosteric ligands associate with a distinct binding site (orange shading) and can act as agonists (green) or antagonists (purple) independently of an orthosteric ligand. However, allosteric ligands often act as positive (PAM) or negative allosteric modulators (NAM) of agonist action by modulating agonist affinity (top arrow) and/or efficacy (bottom arrow). It is assumed that the ligands presented recruit G proteins and arrestins consecutively, but at equal measure.

associating with sites distinct from the orthosteric pocket (Wootten et al., 2013). Effects exerted by allosteric ligands add a significant level of diversity to GPCR ligand pharmacology (Figure 1.5B). Similarly to orthosteric ligands, they can show intrinsic agonism; ligands that act exclusively in this fashion are usually referred to as allosteric agonists. However, allosteric compounds often also have the ability to modulate the affinity and/or efficacy of ligands bound to the orthosteric site, making them positive or negative allosteric modulators (PAMs or NAMs) (Hudson et al., 2014). Such modulatory effects are highly dependent on the bound orthosteric ligand and the assessed pathway, and therefore they should always be considered in this context (Watson et al., 2005). Development of allosteric ligands for GPCRs has attracted much attention in recent years, in

particular due to potential therapeutic advantages. Compounds that are pure allosteric modulators and do not show intrinsic agonism have a saturable modulatory effect, which is restricted by the temporal and spatial properties of the respective endogenous ligand, thereby preventing possible side effects and overdose (Kenakin and Miller, 2010). Furthermore, when targeting highly conserved receptor subclasses allosteric sites can provide increased selectivity, for example to target muscarinic receptor subtypes in neurological disorders (Chan et al., 2008, Bradley et al., 2017), and for GPCRs with endogenous peptide ligands such as the chemokine (Dragic et al., 2000) or glucagon (Koole et al., 2010) receptor the targeting of allosteric sites may be the only feasible option for small-molecule drug development.

To complicate the matter even further, some molecules can simultaneously engage both orthosteric and allosteric sites and are therefore referred to as bitopic ligands (Valant et al., 2012). Therapeutically such compounds are attractive as they may show added affinity and selectivity over orthosteric ligands since they interact with additional sites. The majority of bitopic ligand examples were initially designated as orthosteric or allosteric ligands and only continuing pharmacological investigation revealed their bitopic mode of binding (Valant et al., 2008, Lane et al., 2014). Designing such ligands is theoretically straightforward as a combination of orthosteric and allosteric pharmacophores with a suitable linker should theoretically yield a ligand that occupies both sites. In practice this is more complicated and recent efforts often include in-depth medicinal chemistry efforts to define, for example, the contribution of primary and secondary compound pharmacophores and their linker to dopamine receptor subtype selectivity of bitopic ligands (Kumar et al., 2017). However, in the case of the M_2 muscarinic receptor the rational design of a bitopic agonist has been achieved by linking an orthosteric agonist compound to an allosteric fragment (Antony et al., 2009).

1.2.5 Impact of diverse ligand binding sites on GPCR signalling

The main determinant that defines GPCR ligand pharmacology is the mechanism by which the compound engages the receptor. Understanding how the mode of ligand binding translates into pharmacological action is one of the most important guides for rational drug design. Although a combination of receptor

mutagenesis and signalling studies has provided important information on ligand binding sites, GPCR structures in complex with different ligands are undoubtedly crucial. Recently solved crystal structures illustrate unexpected modes of ligand binding that, however, clearly correlate with ligand pharmacology (**Figure 1.6**). The structure of the glucagon receptor bound to the allosteric antagonist MK-0893 revealed that the ligand exerts its negative allosteric modulation by associating with an extra-helical binding site between TM6 and TM7 and may thereby restrict the outward movement of TM6 necessary for the glucagon receptor to adopt an active conformation (Jazayeri et al., 2016). A further example of an extra-helical binding site is the binding of protease-activated receptor 2 (PAR2) antagonist AZ3451, which is highly lipophilic and likely prohibits active-state conformational rearrangements by limiting movements of TM2-4 (Cheng et al., 2017). The recent structure of the CCR9 chemokine receptor in complex with the allosteric antagonist vercirnon demonstrated a further unexpected binding site: The intracellular side of the receptor (Oswald et al., 2016). In this way vercirnon locks the CCR9 receptor in a conformation that results in a steric clash with G protein or β -arrestin binding. These studies highlight that allosteric ligands can also exert their action through modulating receptor conformation independently of the orthosteric binding site by preventing helical movement or association of signalling partners. Such modes of action are difficult to identify without structural data and highlight that there may be much that we still do not know regarding GPCR ligand binding sites.

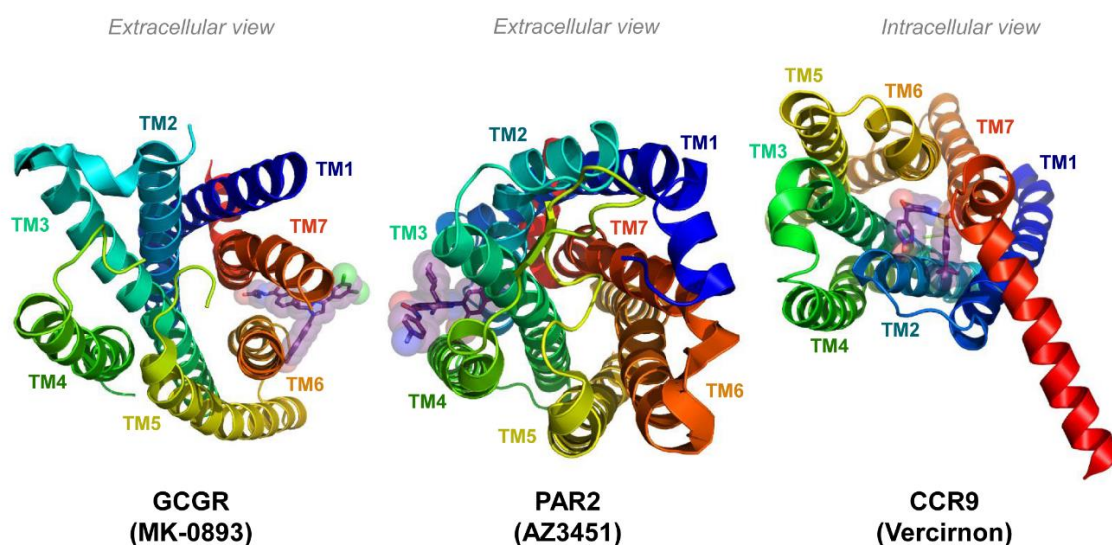


Figure 1.6 Unusual mechanisms of GPCR ligand binding Structures of the glucagon receptor (GCGR), protease-activated receptor 2 (PAR2) and C-C chemokine receptor type 9 (CCR9) are shown in complex with different allosteric ligands as indicated in brackets. The PDB IDs of the respective structures are 5EE7 (GCGR), 5NDZ (PAR2) and 5LWE (CCR9).

One pharmacological concept that lies on the interface between GPCR activation, signalling and ligand binding is that of biased ligands. These display functional selectivity and modulate the output of GPCR activation in a fashion that results in a different signalling profile compared to the receptor liganded with its endogenous agonist (**Figure 1.7**). Commonly such altered signalling behaviour refers to preferential ligand-induced activation of G protein or β -arrestin signalling by a receptor that can engage both pathways simultaneously. As in the case of the concept of bitopic binding modes, such pharmacological behaviour was first discovered retrospectively with a study suggesting that the well-established beta-blocker propranolol acts in a biased fashion by promoting MAPK activation via β -arrestin signalling, while suppressing G_s -coupled signalling (Baker et al., 2003). Considering recent advances in understanding the dynamic nature of GPCR conformations, it is not unexpected that distinct agonist ligands may promote different conformational states of the receptor that induce diverse downstream signalling.

Although allosterism and signalling bias are not directly connected, ligands that engage allosteric binding sites have a high potential to (a) induce distinct conformational changes and signalling compared to an orthosteric agonist if they show intrinsic agonism (Bolognini et al., 2016a) and/or (b) modulate the response of the receptor to the orthosteric ligand in a biased fashion (Goupil et al., 2010). Both of these studies also demonstrated that biased signalling does not only encompass the selection between G protein and β -arrestin signalling but can also include selective coupling to different G protein subtypes. In addition,

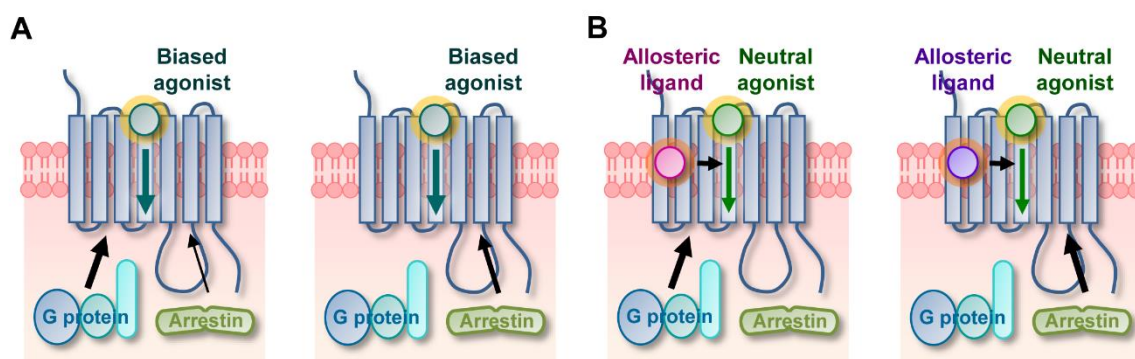


Figure 1.7 Biased signalling by GPCR ligands Both orthosteric (**A**) and allosteric (**B**) ligands can show biased signalling behaviour. Orthosteric ligand binding can preferentially induce recruitment of G proteins or arrestins (**A**). Some allosteric ligands have the capability to bias the signalling of a non-biased orthosteric ligand by promoting conformational states that preferentially associate with G proteins or arrestins (**B**).

it is also important to assess signalling bias by measuring the receptor response to the biased ligand at different levels of the signal transduction cascade, as two β -arrestin-biased ligands for the angiotensin II receptor induced distinct kinase substrate phosphorylation patterns (Santos et al., 2015). This may suggest that ligands inducing β -arrestin signalling have a means of promoting selective activation of downstream kinases, potentially in part by promoting differential phosphorylation patterns of the GPCR C terminus by GRKs (Nobles et al., 2011).

1.3 Identification of the free fatty acid receptor family

1.3.1 Relevance of metabolites as signalling molecules

The role of metabolites in regulating physiological processes is well established; they serve as crucial energy sources and intracellular signalling molecules that act on enzymes such as histone deacetylases (HDACs) (Shimazu et al., 2013) and nuclear hormone receptors including peroxisome proliferator-activated receptors (PPARs) (Ahmadian et al., 2013). However, recent research efforts revealed that metabolites also have the capability to act as extracellular signalling molecules by targeting a group of metabolite-sensing GPCRs on the cell surface of accessible tissues such as the gastrointestinal (GI) tract (Husted et al., 2017). One group of signalling metabolites that has recently attracted much attention as GPCR ligands are free fatty acids, which are composed of a carboxylic acid moiety linked to an aliphatic chain (Milligan et al., 2017). Fatty acids are typically grouped into classes defined by the length of their carbon chain including short chain fatty acids (SCFAs) with 6 or less carbons, medium chain fatty acids (MCFAs) with 7-12 carbons and long chain fatty acids (LCFAs) with more than 12 carbons. Furthermore, the number and position of unsaturations in the aliphatic chain is also highly relevant, in particular for LCFAs. With the global effort to educate the public on nutrition that promotes good health, use of polyunsaturated fats such as omega-3 fatty acids has been promoted due to their metabolic and inflammatory health benefits (Oh et al., 2010), while excessive consumption of specific saturated fats is thought to increase the risk of cardiovascular disease (Wang and Hu, 2017). A factor that further distinguishes SCFAs from MCFAs and LCFAs is their source. MCFAs and LCFAs are obtained primarily from dietary fats or synthesised *de novo* in the liver. In contrast, SCFAs are produced through fermentation of dietary fibre by the gut

microbiome and in response to alcohol consumption through ethanol metabolism in the liver. Therefore, their production is not only dependent on the level of fibre consumption, but also on the composition of the gut microbiota with some species preferentially producing different SCFAs that may exert distinct effects (den Besten et al., 2013). Targeting gut microbiome composition and signalling in general has been highlighted as a novel approach to treat metabolic and inflammatory disorders and using drugs to modulate SCFA effects presents a potential strategy (Jia et al., 2008).

1.3.2 Deorphanisation of FFA receptors

Understanding how free fatty acids (FFAs) exert their physiological effects is key to developing successful therapeutics targeting these processes. The deorphanisation of GPCRs activated by FFAs approximately 15 years ago revealed the role of FFAs as extracellular signalling molecules and has put the FFA receptor family on the map as potential drug targets. The family of FFA receptors is composed of four members: FFA1 (or GPR40), FFA2 (or GPR43), FFA3 (or GPR41) and FFA4 (or GPR120). FFA1-3 were the first FFA receptors to be deorphanised in 2003 in multiple independent studies with FFA1 responding to MCFAs and LCFAs, and FFA2-3 responding to SCFAs. These three receptors share a relatively high sequence identity of 30-40% and are encoded in tandem at chromosomal location 19q13.1 in humans (Sawzdargo et al., 1997). Interestingly, this genomic location also encodes GPR42, which shows six amino acid differences compared to FFA3 and whose function remains largely unexplored. Although it has long been considered simply a pseudogene, one study demonstrated that GPR42 could indeed be expressed in humans and might even show a different pharmacological profile in terms of SCFA potencies (Puhl et al., 2015). Therefore, GPR42 may play a physiological role, but due to lack of further investigations this remains to be confirmed.

The majority of deorphanisation studies employed a high-throughput screening approach to identify putative endogenous ligands. In particular pharmaceutical companies often have large compound libraries and the appropriate equipment to perform ligand screening on a large scale. In the case of FFA1 two independent groups found that MCFAs and LCFAs were able to induce a G_q -dependent calcium response in different immortalised cell line models

transiently expressing FFA1 (Briscoe et al., 2003, Itoh et al., 2003), while a further study took a more rational approach by testing FFAs on a range of orphan GPCRs based on the hypothesis that fatty acids could act as receptor ligands (Kotarsky et al., 2003). FFA2 was also deorphanised by three independent groups. Two studies performed high-throughput screening using either a yeast-based reporter assay with G protein chimeras (Brown et al., 2003) or a calcium-based approach (Le Poul et al., 2003). These screens yielded responses from a range of structurally unrelated compounds with the only common feature being their acetate (C2) counterion, leading to the unexpected conclusion that FFA2 was actually activated by SCFAs. As FFA3 shows relatively high sequence similarity to FFA2, its response to SCFAs was also assessed, thereby confirming the existence of two SCFA receptors. In contrast, the third study screened different FFAs at FFA2 based on the close phylogenetic relationship to FFA1, but came to the same conclusion (Nilsson et al., 2003).

Although FFA4 is clearly confirmed to be an LCFA receptor and thereby belongs to the FFA receptor family, it was deorphanised separately in 2005 and does not cluster with the other FFA receptors phylogenetically (Fredriksson et al., 2003). Its deorphanisation was also based on high-throughput screening, initially by assessing the internalisation response of the receptor tagged with enhanced green fluorescent protein (Hirasawa et al., 2005). Upon observation of its response to LCFAs, this was verified in a system detecting the calcium response of FFA4 fused to the promiscuous G_{16} $G\alpha$ protein. In particular polyunsaturated fatty acids tended to show the highest activity at FFA4 (Christiansen et al., 2015) and a later study established the therapeutic relevance of this observation, by demonstrating that FFA4 may be responsible for mediating the anti-inflammatory effects of omega-3 fatty acids through β -arrestin-dependent signalling (Oh et al., 2010).

In addition to the FFA receptor family, three other GPCRs have also been demonstrated to respond to fatty acids: GPR84, OR51E2 and GPR109A (Milligan et al., 2017). The endogenous ligand of GPR84 has not yet been officially identified, therefore it remains a so-called orphan GPCR. Studies aiming to deorphanise GPR84 demonstrated that it is able to respond to fatty acids with a carbon chain length of 9-14 with C10 and C11 being the most potent (Wang et

al., 2006). The expression profile of GPR84 in a range of immune cells such as neutrophils and eosinophils (Yousefi et al., 2001) and its suggested role as a pro-inflammatory receptor (Suzuki et al., 2013) has highlighted its potential as a drug target and future studies will likely explore this aspect further. Olfr78 is a murine olfactory receptor (OR51E2 in human) expressed in the kidney (Pluznick et al., 2009) and on peptide YY (PYY)-secreting enteroendocrine cells (Fleischer et al., 2015). Although olfactory receptors are traditionally not considered as drug targets, an increasing body of evidence suggests their involvement beyond sensory functions (Griffin et al., 2009, Busse et al., 2014) and Olfr78 has been shown to modulate physiological processes such as blood pressure in response to SCFAs (Pluznick et al., 2013). Although additional research is certainly required to dissect the function of this receptor, it is highly interesting that an olfactory receptor potentially regulates bodily functions in response to fatty acids. GPR109A has now been orphaned as a receptor for hydroxycarboxylic acids and is hence also referred to as HCA₂ receptor (Taggart et al., 2005). However, it also appears to respond to C4-C8 fatty acids, albeit with a lower potency than to endogenous agonist β -hydroxybutyrate. GPR109A modulates lipolysis in adipocytes (Offermanns et al., 2011) and appears to mediate anti-inflammatory effects in immune cells and the colon (Graff et al., 2016). Although the physiological function of this distinct set of receptors is far from being fully understood, their expression across tissues involved in metabolic regulation such as the GI system and immune cells makes them an attractive target for further studies.

1.4 Short chain fatty acid receptors as novel drug targets

1.4.1 SCFAs as endogenous GPCR ligands

Although all members of the FFA receptor family have received significant attention as potential drug targets, SCFA receptors are of particular interest due to their link to gut microbiome activity. To fully appreciate the therapeutic potential of FFA2 and FFA3 it is crucial to understand the unique properties of their ligands. Some physiological roles of SCFAs have already been demonstrated prior to identification of their receptors, particularly in context of the health benefits of fibre consumption that provides the basis for SCFA production by microbes in the gut (Cook and Sellin, 1998). The main SCFAs that are produced

during the fermentation process are acetate (C2), propionate (C3) and butyrate (C4). As the gut microbiota resides in the intestinal lumen, the concentration of SCFAs can reach up to 50-100 mM with C2 being the most prevalent (Cummings et al., 1987). SCFAs exert many of their actions on enterocytes and enteroendocrine cells, but also on resident immune cells such as macrophages and neutrophils after crossing the intestinal barrier into the lamina propria (Husted et al., 2017). Through the lamina propria SCFAs also have access to the liver via the portal vein and are further diluted, such that circulating plasma concentrations are reduced by approximately 1000-fold compared to the gut lumen (Akanji et al., 1989, Cummings et al., 1987). In target tissues several cell types such as pancreatic B cells, and likely also adipocytes, appear to have the capacity to produce C2 in an autocrine and paracrine manner from glucose metabolism, thereby increasing SCFA concentrations locally (Tang et al., 2015). In cases of obesity and diets rich in processed foods, not only the composition of the microbiome can be affected in a detrimental fashion (Sweeney and Morton, 2013), but also intestinal barrier function is often impaired, allowing for increased leakage of metabolites and bacterial by-products (Raybould, 2012), which can modulate circulating concentrations of SCFAs. The beneficial effects of SCFAs and their receptors is a carefully balanced process and drastic changes in circulating and tissue concentrations are likely to result in disruption of metabolic regulation, which will also become apparent the discussion of the therapeutic implications of SCFA receptors (see section 1.4.2).

To investigate the link between gut microbiome activity and SCFA receptors, mice with modified gut microbiota composition are often employed in combination with transgenic knock-out (KO) mice of SCFA receptors (Milligan et al., 2017). Animals that lack a gut microbiome, achieved by germ-free (GF) raising or treatment with antibiotics, can be treated with SCFAs to provide information on the function of SCFA receptors. The majority of studies on FFA2 have investigated its role in regulating inflammatory responses. Dysregulated immune responses were observed in GF mice with induced colitis, which was also the case in FFA2 KO mice, and C2 treatment was able to improve the condition of GF mice (Maslowski et al., 2009). Furthermore, it was shown that the population of regulatory T cells in the intestine was reduced in GF mice compared to regular animals and SCFA treatment was able to recover this

population in an FFA2-dependent fashion, while this effect was not observed in GF mice with FFA2 KO (Smith et al., 2013). In a mouse model of gout, gut microbiome-lacking and FFA2 KO mice both showed reduced production of pro-inflammatory IL1- β , and administration of SCFAs was able to restore IL1- β levels (Vieira et al., 2015). In addition, the role of SCFAs and FFA2 in adiposity was also explored by comparing the body weight of WT and FFA2 KO mice raised under conventional and GF conditions. Interestingly, FFA2 KO induced obesity in the animals, but was only observed in conventionally raised mice and not GF animals (Kimura et al., 2013). In contrast, when performing an equivalent experiment with FFA3 KO mice, decreased adiposity was found in FFA3 KO mice compared to wild type, which was not the case in GF animals (Samuel et al., 2008). Interestingly, FFA3 has also been demonstrated to play a protective role in allergic airway disease with mice on a diet with high fibre content, which led to a higher level of circulating SCFAs, showing reduced lung inflammation compared to chow-fed animals (Trompette et al., 2014). More detailed investigation of the effect of exogenous C3 administration revealed that this was, at least in part, due to impaired ability of dendritic cells in the lung to induce pro-inflammatory T helper type 2 cell function. These studies clearly demonstrate that there is a causative link between gut microbiome-mediated SCFA production and the function of SCFA receptors. Although information obtained from work in GF mice is already very informative, a closer investigation of the specific beneficial bacteria that contribute to SCFA production and how they depend on diet, in particular in humans, could be of interest to the probiotic industry.

Although SCFAs can act on both FFA2 and FFA3, they do so with different potencies depending on their carbon chain length. While FFA2 preferentially binds $C2 \approx C3 > C4 > C5 \approx C1$, FFA3 has a rank order of $C3 \approx C4 \approx C5 > C2 > C1$ (Hudson et al., 2011). In terms of signalling the SCFA receptors also differ substantially (**Figure 1.8**). FFA2 is a relatively promiscuous receptor and the deorphanisation study that employed a range of G protein subtype chimeras demonstrated that FFA2 was able to couple to multiple members of the $G_{q/11}$, $G_{i/o}$ and $G_{12/13}$ G protein families (Brown et al., 2003). Nowadays SCFA-mediated

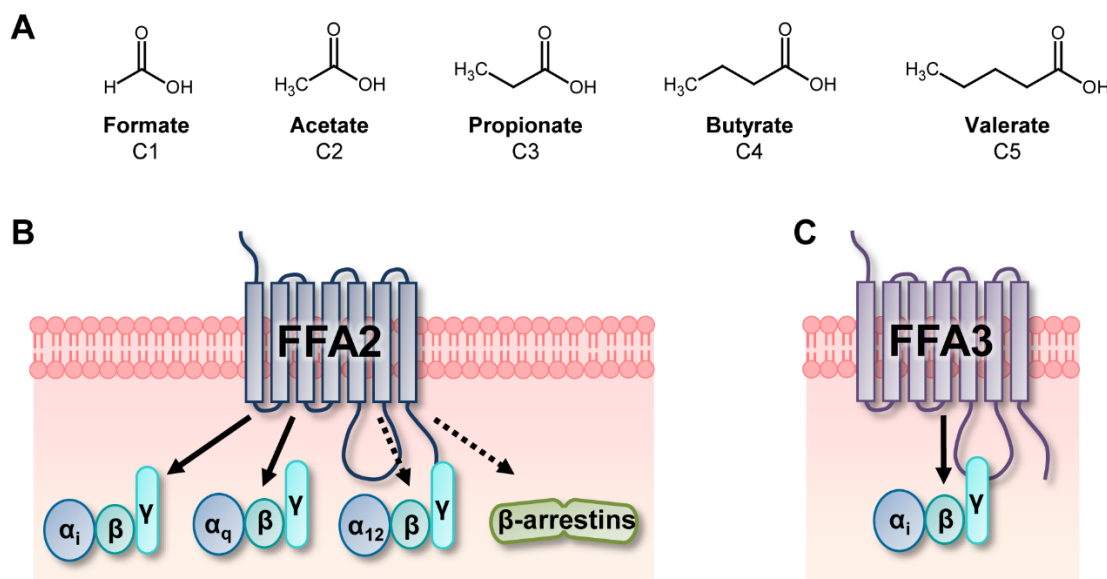


Figure 1.8 SCFA receptor signalling Fatty acids with a range of carbon chain length from 1 to 5 (**A**) can bind to FFA2 (**B**) and FFA3 (**C**) to induce GPCR signalling. Chemical structures of short chain fatty acids (SCFAs) are illustrated (**A**). Activation of FFA2 results in signalling through G_i and G_q G proteins (**B**). Only selected studies suggest that FFA2 can also stimulate G_{12} - and β -arrestin-dependent signalling, therefore dashed lines are shown. In contrast to FFA2, FFA3 only signals through G_i G proteins (**C**).

FFA2 coupling to both G_q and G_i is well established and functional assays measuring, for example, G_q -dependent Ca^{2+} release or G_i -coupled [^{35}S]-GTP γ S incorporation are routinely employed (Hudson et al., 2013a). Furthermore, FFA2 activation also induces β -arrestin 2 recruitment, albeit it is not fully confirmed whether this only leads to receptor desensitisation or if FFA2-bound β -arrestin 2 also activates G protein-independent signalling pathways. Activation of FFA2 also results in phosphorylation of ERK (Hudson et al., 2012a), which is likely an accumulated response from multiple signalling pathways and may also include β -arrestin-mediated signalling. In contrast, FFA3 shows a distinct signalling profile compared to FFA2, as the only reported G protein-mediated signalling is transduced by the $G_{i/o}$ subtype (Brown et al., 2003). Furthermore, it is not very likely that FFA3 signals through arrestins, as siRNA knock-down of β -arrestins in a mouse neuroblastoma cell line did not affect the FFA3 response to C3 (Kimura et al., 2011).

The marked difference in C2 potency at FFA2 and FFA3 led to its use as a selective ligand for FFA2 (Tolhurst et al., 2012, Zaibi et al., 2010), however the approximately 10-fold difference in C2 potency is likely not sufficient to achieve selective activation. Furthermore, when employing rodent models, it is

important to consider that not only will the inherent microbiome-dependent production of SCFAs likely differ, but the rank order of SCFA potencies at FFA2 and FFA3 is also altered at the rodent orthologues (Hudson et al., 2012b). Particularly relevant in mice is the loss of C2 selectivity between the two receptors and the increased potency of C3 for FFA3 over FFA2, which appears to be related to species-specific residue differences in ECL2. The factors outlined above have made it challenging to use SCFAs to dissect the specific physiological roles of FFA2 and FFA3, particularly in tissues where the receptors are co-expressed. Therefore, KO animals are commonly employed to confirm receptor-specific effects. However, such studies also have limitations. The pharmacology of the remaining SCFA receptor may be altered by the loss of the other receptor through functional redundancy in some tissues and at least one study has also reported altered expression of FFA2 in an FFA3 KO mouse line (Zaibi et al., 2010). Therefore, the development of selective synthetic ligands with a range of pharmacological profiles is crucial to fully understand the function of SCFA receptors.

1.4.2 Therapeutic implications of SCFA receptors

The relatively broad distribution of SCFAs in the human body upon entering the systemic circulation and their capacity to act in an autocrine and paracrine manner in tissues involved in metabolic regulation does not make it surprising that FFA2 and FFA3 are expressed in a variety of tissues. Both receptors are present in the gut epithelium with the highest level in enteroendocrine cells (Nohr et al., 2013, Karaki et al., 2006), which also express a range of other metabolite-sensing GPCRs and are responsible for secretion of gut hormones that affect processes such as satiety and gut motility. Furthermore, FFA2 and FFA3 are also co-expressed in pancreatic β cells (Priyadarshini et al., 2015) that regulate insulin secretion. Some studies also demonstrated expression of both receptors in adipose tissue (Xiong et al., 2004), however the consensus is that only FFA2 is likely to be expressed (Zaibi et al., 2010). Further cell types that primarily express FFA2 belong to the innate immune system and include monocytes and granulocytes (Le Poul et al., 2003), highlighting the link between metabolic regulation and immune response. In the case of FFA3 exclusive expression could only be shown in neurons such as ganglia of the sympathetic and enteric nervous system (Nohr et al., 2015). The following paragraphs will

highlight the proposed roles of SCFA receptors in these tissues and how they may be targeted therapeutically.

The GI tract shows both high local concentrations of SCFAs and prominent expression of FFA2 and FFA3, indicating the involvement of SCFA receptors in regulating GI processes. Indeed, SCFA treatment has initially been demonstrated to induce satietogenic PYY release in rodents (Darzi et al., 2011) and gut motility by promoting peristalsis through serotonin release (Karaki et al., 2006), which may be mediated by FFA2 due to its expression in enteroendocrine cells and mucosal mast cells (Fukumoto et al., 2003). The direct role of FFA2 in regulation of a different gut hormone that regulates blood glucose levels, glucagon-like peptide-1 (GLP-1), was demonstrated by the loss of C2- and C3-induced secretion of GLP-1 from colonic cultures from FFA2 KO mice (Tolhurst et al., 2012). In contrast, cultures from FFA3 KO animals retained the ability to release GLP-1 upon C2 and C3 treatment, indicating this to be an FFA2-dependent effect. This was further confirmed *in vivo* by C3 infusion stimulating increase of GLP-1 and PYY in plasma, which was not observed in FFA2 KO mice (Psichas et al., 2015). Dietary supplementation with the fermentable carbohydrate inulin augmented satiety in mice by expanding the population of PYY-producing cells and augmenting PYY release, which was not observed in FFA2 KO mice (Brooks et al., 2017). A further peptide involved in satiety regulation whose production appears to be in part regulated by FFA2 is appetite-increasing ghrelin, with one study demonstrating FFA2 expression in ghrelin-producing cells in the stomach and the ability of C2 and C3 to inhibit its release (Engelstoft et al., 2013). The ability to regulate the feeling of satiety would be of great value for treatment and prevention of obesity, in particular for individuals with genetic predisposition for obesity.

Developing new and improved treatment approaches for diabetes is a significant focus of current drug development programmes. Although obesity, GI health and insulin resistance are undoubtedly linked and may suggest a role for the SCFA receptors present on pancreatic β cells, the LCFA receptor FFA1 has been the main target of such efforts. This may be due to the contradicting results of several studies, with SCFA treatment shown to both activate (Priyadarshini et al., 2015) and inhibit (Tang et al., 2015) glucose-stimulated insulin secretion.

Hypotheses that attempt to explain these observations include the preferential activation of FFA2 or FFA3 by treatment with C2 or C3 (Bolognini et al., 2016b) and the diverse effect of G_q versus G_i G protein activation in islets enhancing or inhibiting insulin secretion, respectively (Milligan et al., 2017).

A variety of SCFA-mediated processes in adipocytes have also been investigated to understand the physiological role of SCFA receptors and while some effects are well established, such as the ability of SCFAs to inhibit lipolysis by activating FFA2 in immortalised and primary murine adipocytes (Ge et al., 2008), others, including influence on adipogenesis and secretion of satietogenic leptin, are less well understood. Multiple studies suggest an impact of FFA2 on adipogenesis, albeit with opposing effects. Expression of FFA2 was shown to be upregulated during differentiation of an adipocyte cell line (Hong et al., 2005) and an *in vivo* study found that FFA2 KO mice on a high fat diet (HFD) show reduced body fat compared to wild type animals (Bjursell et al., 2011). A contrasting study demonstrated the exact opposite with FFA2 KO resulting in obesity, while *in vivo* adipogenesis was not affected by FFA2 KO, suggesting that FFA2 actually plays no role in adipogenesis itself (Kimura et al., 2013). Perhaps most significantly, the only study employing human tissue was not able to demonstrate an FFA2-mediated effect of SCFAs on adipogenesis (Dewulf et al., 2013). The role of SCFA receptors in leptin secretion is similarly debated with both FFA2 (Zaibi et al., 2010) and FFA3 (Xiong et al., 2004) suggested as potential mediators, however it is likely that the net input of SCFAs on leptin secretion is positive. A further suggested function of SCFAs is their impact on insulin-stimulated glucose uptake. Although some studies in immortalised cell lines suggested a role of FFA3 in enhancing this process (Han et al., 2014), *in vivo* evidence demonstrated the ability of C2 to suppress insulin signalling in adipose tissue by acting through FFA2 (Kimura et al., 2013).

The best characterised role of SCFA receptors on immune cells is the ability of FFA2 activation to induce neutrophil chemotaxis (Maslowski et al., 2009). Conversely, SCFAs are traditionally thought to have anti-inflammatory effects with *in vivo* studies demonstrating that SCFAs can reduce production of tumour necrosis factor α (TNF α) by mononuclear cells in an FFA2-dependent fashion (Masui et al., 2013). However, SCFAs have also been shown to promote release

of inflammatory chemokines and cytokines through activation of both FFA2 and FFA3 in the colon (Kim et al., 2013). Interestingly, a recent study suggested that activation of FFA2 by SCFAs can differentially affect macrophage subtypes by inducing TNF α release in anti-inflammatory M2 macrophages, while leaving the pro-inflammatory M1 type unaffected (Nakajima et al., 2017). In the context of gut inflammation and potential targeting of FFA2 to treat inflammatory bowel disease, the best approach is also not clear as separate studies have shown both increased (Maslowski et al., 2009) and decreased (Sina et al., 2009) inflammation and mortality upon FFA2 KO in a murine model of colitis. Therefore, the role of SCFA receptors in inflammation is a further physiological process which requires additional investigation.

Although there is a large body of evidence that SCFA receptors do play a role in a variety of tissues that regulate metabolic processes, an overview of published studies makes clear that we are still far from a consensus regarding the underlying mechanisms (Ang and Ding, 2016). The only physiological impact whose investigation has not yielded contradictory results is the promotion of gut hormone release, therefore it is not clear whether SCFA receptors are indeed good therapeutic targets and if so, then which pharmacological targeting approach would be best. **Figure 1.9** summarises the diverse hypotheses for the physiological role of SCFA receptors and the signalling pathways that are thought to mediate the respective processes. As FFA2 and FFA3 have different downstream signalling profiles, treatment with pertussis toxin (PTX) that specifically inhibits G_i G proteins can provide some indication of which receptor is responsible for observed responses. However, PTX will also block G_i-mediated effects of FFA2 and therefore only allows differentiation between FFA3 effects and G_q-mediated FFA2 responses. Furthermore, PTX treatment can also have secondary effects including the induction of cytokine release and activation of tyrosine kinases (Mangmool and Kurose, 2011). This is important to consider, in particular for studies on immune cells. One additional factor that is easy to overlook when assessing studies of SCFA receptor physiology is the nature of the selected model animal. In rodents, the most commonly used animal for such studies, the gut microbiome can differ significantly between different strains and environmental conditions, which may have a drastic impact on SCFA receptor studies and potentially lead to contradictory results. Furthermore,

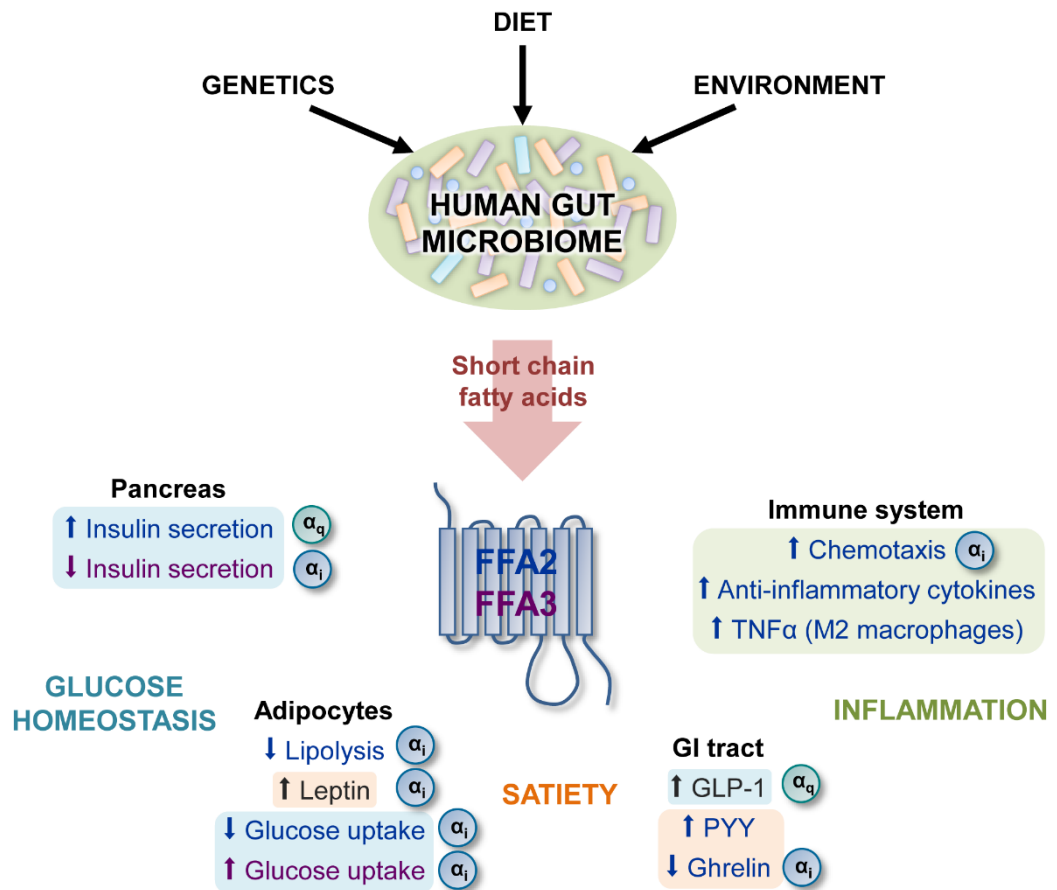


Figure 1.9 Potential physiological role of SCFA receptors The composition of the human gut microbiota is dependent on a range of different factors including genetics, diet and environment, which in turn influences the production of short chain fatty acids (SCFAs) that activate FFA2 and FFA3. The roles the receptors play can be broadly divided into glucose homeostasis (*blue*), satiety/gut health (*orange*) and inflammation (*green*). Known contribution of FFA2 and FFA3 to the observed physiological effects are written in blue and purple, respectively, and the G protein subtype that is thought to mediate respective effects is also shown.

dissecting the specific roles of FFA2 and FFA3 using SCFA treatments is challenging and highlights the need for specific high-potency ligands with good bioavailability. An alternative, chemogenetic approach is the generation of a transgenic animal expressing FFA2 modified to be a designer receptor exclusively activated by designer drugs (DREADD). As the name suggests, such a receptor has been modified, usually by introduction of amino acid sequence mutations, to lose responsiveness to intrinsic endogenous ligands and is instead activated solely by synthetic ligands that need to be administered externally (Lee et al., 2014). DREADD receptors play an increasingly important role in drug discovery, as they allow for dissection of specific signalling pathways and distinguishing between e.g. different receptor subtypes if selective ligands are not available. In the case of FFA2, by exploiting species differences between the human and bovine receptor, a FFA2 DREADD receptor that responds to the small molecule

sorbic acid, but not SCFAs, has been developed (Hudson et al., 2012a). Future studies that aim to employ a transgenic mouse line expressing FFA2 DREADD instead of wild type FFA2 are likely to provide a valuable insight into FFA2 and FFA3 physiology and may help to resolve some of the outstanding questions.

1.5 Drug development for SCFA receptors

1.5.1 Homology modelling as a tool to predict structural features

As highlighted in chapter 1.2, understanding receptor structure and function can provide an important contribution for successful drug discovery. However, FFA receptors were only orphanised relatively recently and compared to the β_2 AR or adenosine A_{2A} receptor there are limited high-affinity pharmacological tools available for them. Crystallising a receptor and solving its structure can be time-consuming and typically requires a high-affinity ligand to stabilise the receptor for crystallisation, therefore GPCR structural projects tend to focus on more established GPCRs with richly described pharmacology. For receptors without crystallographic information, homology modelling is commonly employed as a method to gain some structural insight (Costanzi, 2013). Homology modelling refers to the use of a known structure as a template to computationally predict that of a related receptor. In the case of GPCRs this is possible due to the high extent of evolutionary conservation of their three-dimensional structure. The predictability of homology models was tested in the community-wide GPCR Dock 2010 Assessment in which 35 groups submitted homology models of the dopamine D_3 and CXCR4 receptor without knowledge of the crystal structures about to be published (Kufareva et al., 2011). This study highlighted that homology models based on templates with 35-40% sequence identity can predict structural features and even ligand binding sites with high accuracy. However, a sequence identity of less than 30% is insufficient for complete structural predictions, making accurate docking of ligands and structure-based drug design close to impossible. Therefore, homology models need to be considered in the context of the GPCR providing the template structure and high-quality data on ligand binding and function is necessary to guide its construction. As high sequence identity is the deciding factor for selecting an appropriate template structure, it is convenient for the generation of a homology model for SCFA receptors that multiple crystal structures of FFA1 are available.

Although the close phylogenetic relationship between FFA1 and the SCFA receptors suggests that FFA1 is an appropriate template structure for FFA2 and FFA3, it is important to consider the state in which the receptor was crystallised and FFA1-specific structural features that may be erroneously translated into homology models. The understanding of the physiological role of FFA1 may be more advanced than that of SCFA receptors, but regarding ligand binding and pharmacology FFA1 comes with its own set of challenges. None of the available structures are crystallised in complex with an endogenous ligand, so the endogenous binding site of FFA1 remains to be fully defined and this makes it difficult to define orthosteric, allosteric or indeed bitopic binding sites with certainty (**Figure 1.10**). However, a pair of arginine residues conserved between FFA1, FFA2 and FFA3 is considered as a point of interaction for the fatty acid carboxylate (**Figure 1.11**). This has been confirmed in a range of functional studies in which mutation to alanine resulted in loss of agonist action (Stoddart et al., 2008, Sum et al., 2007). The first crystal structure of FFA1 was complexed with the partial agonist TAK-875, which is defined as an allosteric ligand, as it can modulate LCFA response in functional assays (Srivastava et al., 2014) and

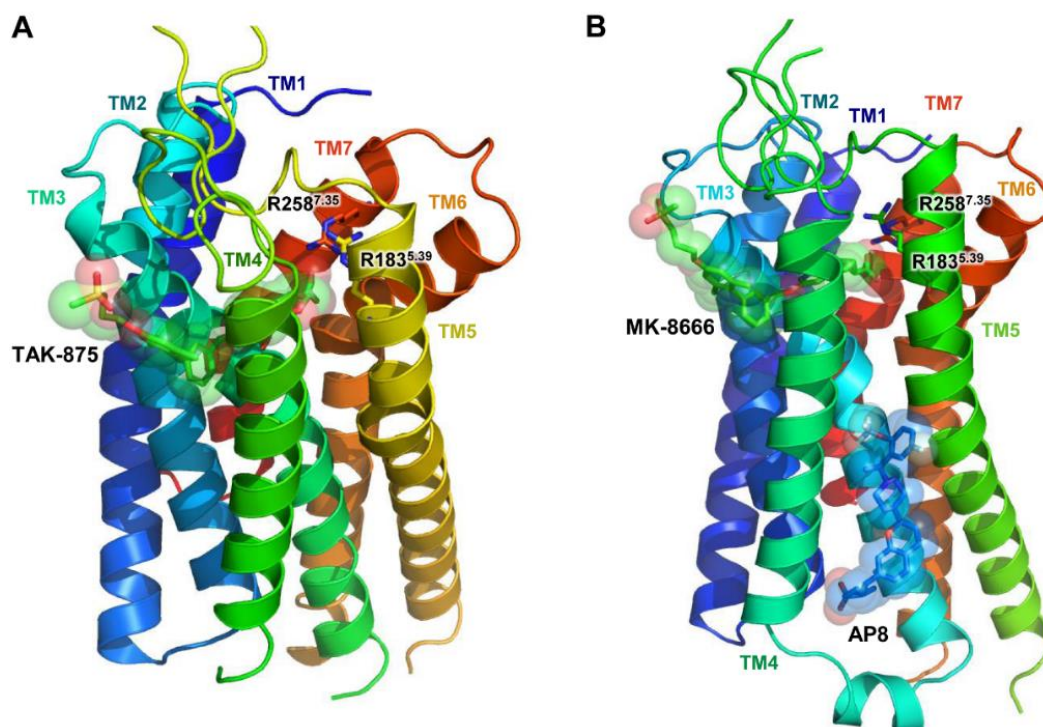


Figure 1.10 Crystal structure of the FFA1 receptor Published crystal structures of FFA1 in complex with TAK-875 (**A**) and MK-8666 and AP8 (**B**) are shown. Agonists are shown in green and allosteric modulators in blue. PDB IDs of respective structures are 4PHU for the structure in complex with TAK-875 (Srivastava et al., 2014) and 5TZY for MK-8666 and AP8 (Lu et al., 2017).

structures revealed the mechanism by which AP8 exerts its PAM effect on MK-8666 potency through facilitation of a ligand-induced fit that involved conformational changes in TM4, TM5 and ICL2. The TM architecture does seem to share some characteristics with published GPCR structures in their active-state, but the typical outward movement of TM6 cannot be observed, indicating that FFA1 is in an artificial or intermediate “inactive-like” state, which is likely due to the introduction of thermostabilising mutations to stabilise the receptor for crystallisation. Although these data are certainly of great interest to understand the structural basis for allosteric modulation and future development of FFA1 ligands, it is of limited use as a homology modelling template. In particular the gap between TM3 and TM4 may not be present in SCFA receptors, because they are unable to bind longer chain fatty acids. However, the conformation of the orthosteric binding site may be comparable between FFA1, FFA2 and FFA3 due to its conserved nature.

Much of the understanding of SCFA receptor structure and function was initially based on functional studies. In the effort to define the anchorage point of the negatively charged SCFA carboxylate an investigation of all ligand-accessible positively charged residues and the effect of their replacement with alanine on agonist action led to the identification of two arginine residues at positions 5.39 and 7.35 (Ballesteros and Weinstein, 1995), which were mentioned previously to be conserved between FFA1, FFA2 and FFA3 (Stoddart et al., 2008).

Furthermore, mutation of a histidine residue at position 6.55 was also detrimental for FFA2 and FFA3 activation by SCFAs. While FFA1 binds longer chain fatty acids that likely require further anchoring residues to allow for sufficient binding affinity, for binding of SCFAs to FFA2 and FFA3 this Arg-His-Arg triad may indeed represent the only point of interaction, thereby defining these residues as the orthosteric binding site. A more comprehensive analysis of homology models based on the FFA1 structure revealed that both SCFA receptors show a more interlinked network of residues around the orthosteric binding site, particularly in the case of FFA2 (Tikhonova and Poerio, 2015). This includes the presence of additional hydrogen bonds and hydrophobic interactions.

Furthermore, as expected by the smaller nature of their ligands, the accessible SCFA binding cavity is also significantly smaller. It would also be of value to be able to investigate the conformation of ECL2, which plays a significant role in

regulating constitutive activity and species differences, but the low similarity of the ECL2 of FFA1 makes it difficult to construct a precise model. Homology modelling of variable and flexible regions such as ECL2 are very challenging in general and even a sequence similarity as high as 40% between model and template receptor in the GPCR Dock 2010 Assessment did not result in accurate ECL2 predictions (Kufareva et al., 2011).

1.5.2 Overview of FFA2 and FFA3 drug development efforts

Developing novel treatment approaches for obesity-related disorders and inflammatory conditions of the gut is one of the key aims of the pharmaceutical industry due to an increasing demand for improved therapeutics in these areas. The apparent involvement of SCFA receptors in related processes has attracted attention of both academia and industry to target these receptors therapeutically. However, at this stage it is also important to consider that identification of novel FFA2- and FFA3-specific compounds does not only serve a therapeutic purpose, but it is also essential for understanding the pharmacology and physiological function of SCFA receptors. In particular considering the poor properties of endogenous SCFAs as ligands and their lack of selectivity between FFA2 and FFA3, specific synthetic ligands are required to answer the outstanding questions regarding SCFA receptor function.

As SCFAs are relatively small and defined by their carboxylic acid moiety, first efforts to develop orthosteric agonists were based on modifying the aliphatic tail of SCFAs (Schmidt et al., 2011). Although none of these analogues exceeded the potency of SCFAs, it revealed that the hybridisation state of the α carbon defines selectivity between SCFA receptors with FFA2 preferring sp - or sp^2 -hybridisation, such as in case of propionic and angelic acid, while substituted sp^3 -hybridised carbons, including 2-methylbutyric acid, show higher selectivity for FFA3. Despite their low potency, two selected FFA2-specific carboxylic acids were able to induce glucose-stimulated insulin secretion in isolated mouse islets, which was lost upon KO of FFA2 (Priyadarshini et al., 2015). Following on from this initial characterisation, a variety of patents for specific synthetic ligands have been filed that have likely been identified by high-throughput screening and served as the basis for tool compounds currently in use (**Figure 1.12**). In this context FFA2 has received significantly more attention than FFA3, although it is

unclear whether this is due to an increased therapeutic interest in FFA2 or if ligand development for FFA3 is inherently more difficult.

The only published FFA3 compound series is derived from a patent filed by Arena Pharmaceuticals (Leonard et al., 2016). Although the potential of compounds from this series for *ex vivo* use was demonstrated by the ability of representative ligand AR420626 to induce GLP-1 release from murine colonic crypt cultures (Nohr et al., 2013), the pharmacology of this series appears to be highly complicated (Hudson et al., 2014). Firstly, the ligands were able to activate FFA3 after alanine replacement of Arg185^{5,39} and Arg258^{7,35}, suggesting

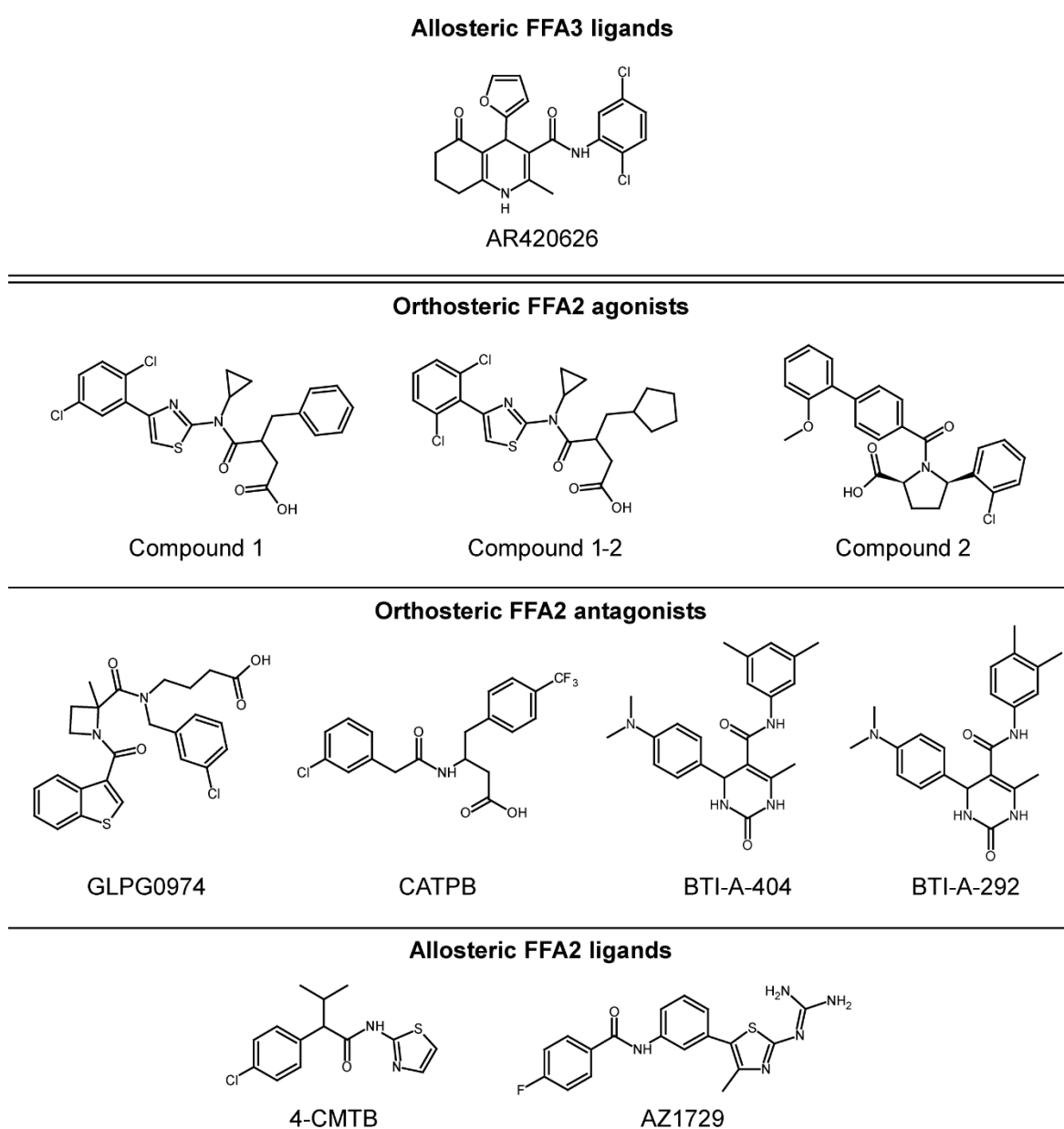


Figure 1.12 Chemical structures of SCFA receptor ligands The structures of different ligand classes for FFA3 and FFA2 are shown.

that they were binding to a different site than SCFAs and are therefore allosteric. Secondly, even minor modifications to the compound scaffold were able to switch compound pharmacology from agonism to antagonism and between PAM and NAM behaviour. One analogue even displayed divergent allosteric behaviour by having a NAM effect on C3 efficacy and a PAM effect on C3 potency. The complicated pharmacology of this compound series combined with a lack of binding site information and relatively low potency (low μM range) make compounds of this series sub-optimal tools, hence novel selective ligands are required to fully explore the function of FFA3.

Considering the complex pharmacology of available FFA3 tool compounds and the lack of a selection of ligands with distinct pharmacology, FFA2 presents a more attractive and accessible target for drug discovery. Furthermore, contributing to the development of selective FFA2 ligands will also provide information on the physiological role of FFA3, as it will allow dissection of their respective roles in tissues in which they are co-expressed. Therefore, the work presented in this thesis is focussed on FFA2 and an outline of available tool compounds and their proposed modes of binding is described in the following sections.

1.5.3 Orthosteric FFA2 agonists

The structure of the first synthetic agonist series for FFA2 was based on a backbone patented by the clinical-stage drug discovery company Euroscreen (now Ogeda) (Hoveyda et al., 2010). The pharmacology of two representative compounds, here referred to as compounds 1 and 1-2, has been characterised in detail (Hudson et al., 2013a). Both compounds were able to activate human and murine FFA2 (mFFA2) with potency in the high nM range, while inducing no response at other FFA receptors including FFA3. Their action was dependent on Arg180^{5.39}, Arg255^{7.35} and His242^{6.55} in a similar manner to SCFAs, indicating an orthosteric mode of binding. As the carboxylate moiety of SCFAs is crucial for their function, it was of interest to see that the patented compound 1 series also contained such a moiety. Indeed, replacement of the carboxylate with an ester moiety rendered compound 1-2 inactive, indicating that this structural feature is essential for orthosteric agonist function (Hudson et al., 2013a). Although compound 1 induced a similar signalling profile to C3, as may be anticipated for

an orthosteric agonist, further structural modifications yielded diverse responses in a variety of G_i -coupled assays (Brown et al., 2015). While all compounds retained the ability to activate FFA2 in [35 S]-GTP γ S assays, only selected analogues were able to inhibit cAMP production and when assessed in a yeast-based G_i coupling assay some compounds even acted as inverse agonists. As a synthetic ligand will likely interact with more residues than SCFAs to reach sufficient affinity, it is perhaps not surprising that some structural modifications yield ligands with diverse signalling profiles. However, all the assessed assay systems were employed to measure coupling through G_i , so it is not clear how far the observed bias was down to assay artifacts that may, for example, be caused by distinct binding kinetics of specific analogues. From a physiological perspective various FFA2-dependent effects could be demonstrated using this ligand series, including GLP-1 secretion, inhibition of lipolysis and the ability to induce a Ca^{2+} release in neutrophils (Hudson et al., 2013a, Brown et al., 2015). However, it is important to consider that the potency of compounds 1 and 1-2 was markedly species-specific and assay dependent. While compound 1 showed a potency reduction of up to 14-fold at murine compared to human FFA2 in Ca^{2+} release assays, compound 1-2 showed a significantly greater reduction of 420-fold (Hudson et al., 2013a). Therefore, compound 1 would likely be of most use for *in vivo* studies.

A further agonist series patented by Euroscreen that has only been investigated recently is based on the structure of compound 2 (Hoveyda et al., 2011). Although the study employing compound 2 was focussed on its physiological role, the presence of a carboxylate moiety and lack of allosteric modulation by C2 suggested an orthosteric mode of action (Forbes et al., 2015). Interestingly, compound 2 appeared to have diverse effects on metabolic regulation in FFA2 KO studies with a beneficial effect on gut transit and food intake, but no improvement of the impaired glucose tolerance displayed by FFA2 KO mice. Furthermore, the observed effects were mostly mediated through release of PYY rather than GLP-1, as *in vivo* release of GLP-1 was only observed when a dipeptidyl peptidase-4 inhibitor that prevents GLP-1 degradation was co-administered. This study provided further evidence of the role and therapeutic potential of FFA2 in obesity and satiety regulation, but more work is required to truly assess the therapeutic potential of this compound series.

1.5.4 Orthosteric FFA2 antagonists

Although the health benefits of SCFAs suggest that FFA2 agonists rather than antagonists would be of therapeutic value, the ability of FFA2 activation to promote immune cell recruitment indicates that treatment with antagonists may have an anti-inflammatory effect. The physiological function of FFA2 appears to be a delicately balanced process, therefore the desired pharmacological action of drugs targeting FFA2 likely depends on the condition to be treated. The first antagonist to be reported was based on a patent from Euroscreen (Brantis et al., 2011) and is commonly referred to as CATPB (Hudson et al., 2013a). Although structurally very distinct from FFA2 agonists, CATPB does contain a carboxylate moiety typical of orthosteric FFA2 ligands. It is able to inhibit the response of FFA2 to C3 and also reduces the constitutive activity of the receptor in [³⁵S]-GTPγS binding assays, indicating inverse agonist behaviour (Hudson et al., 2012b). However, it only acts as an antagonist at human FFA2 and does not inhibit SCFA responses at rodent forms of the receptor. When co-added with orthosteric agonists, CATPB induces a concentration-dependent, surmountable right-shift of their concentration-response curves, consistent with binding to the orthosteric site (Hudson et al., 2013a). Functionally CATPB has been employed to confirm FFA2 mediated inhibition of lipolysis in a human adipocyte cell line (Hudson et al., 2013a).

In addition to CATPB, a further FFA2 antagonist series was developed by Galapagos, a clinical-stage biotechnology company, with its lead compound referred to as GLPG0974 (Pizzonero et al., 2014). Although this ligand series has a different structure compared to CATPB, both antagonists share some features including the carboxylic acid and a chlorobenzene ring. The therapeutic potential of GLPG0974 was based on its ability to block both C2-induced migration of human neutrophils and expression of neutrophil activation marker CD11b in human blood, which served as an appropriate biomarker for target engagement (Pizzonero et al., 2014). As in the case of CATPB, GLPG0974 does not inhibit SCFA responses at rodent orthologues of FFA2. However, the convincing data of target engagement in human blood led to GLPG0974 being the first FFA2 ligand to enter clinical trials for treatment of ulcerative colitis, albeit no proof-of-principle studies in animal models were performed. Despite being well-tolerated and showing a good safety profile, treatment of patients showing

mild to moderate ulcerative colitis symptoms with GLPG0974 for four weeks did not yield a measurable health improvement compared to the placebo-treated control group (Vermeire et al., 2015). Nevertheless, it was demonstrated that GLPG0974 was indeed capable of reducing neutrophil activation and influx in patients, indicating that targeting only neutrophil migration in ulcerative colitis may not be sufficient to yield a measurable patient improvement within a short period of time. This highlights that a deeper understanding of the physiological functions of FFA2 is required to develop effective therapeutics. The characterisation of GLPG0974 binding and pharmacology will be the focus of the work discussed in chapter 4.

A more recent study has identified a third series of FFA2 antagonists, discovered through high-throughput screening (Park et al., 2016). Interestingly, although this compound series lacks a carboxylate, initial characterisation of two representative ligands, BTI-A-404 and BTI-A-292, indicates competitive behaviour with C2 and C3. Furthermore, this compound series also appears to be species-selective for the human receptor. Unexpectedly the compounds appeared to promote GLP-1 secretion in a human colorectal adenocarcinoma cell line, however due to the high concentrations employed this may be due to off-target effects. Therefore, although this compound series provides further information on possible structural features of FFA2 antagonists, their relatively low potency compared to other antagonists and potential to cause off-target effects, as potentially observed in the GLP-1 secretion assay, indicates limited potential for *in vivo* use.

The selectivity of FFA2 antagonists for the human receptor represents one of the key limitations for *in vivo* studies in rodents and has hindered progress in understanding the physiological roles of FFA2. The lack of active rodent FFA2 antagonists prohibits specific inhibition of the receptor, which is necessary to confirm that agonist-induced responses are mediated by FFA2 and would provide crucial information on the roles of FFA2 versus FFA3. Therefore, most *in vivo* studies have employed KO animals to overcome this limitation. These are also not an optimal system due to the potential for altered expression of FFA3. The molecular mechanism of the antagonist species selectivity is poorly understood to date but will be discussed in chapter 6.

1.5.5 Allosteric FFA2 regulators

The first selective FFA2 agonist was identified by the biopharmaceutical company Amgen in a high-throughput screen assessing G_i- and G_q-coupled signalling in cAMP inhibition and calcium release assays, respectively (Lee et al., 2008). The lead compound within the series, AMG7703 (here referred to as 4-CMTB), showed modest potency at human and rodent FFA2 with respective potencies of approximately 500 nM and 1 µM in a cAMP inhibition assay (Lee et al., 2008). However, it has been used in a range of studies that are described below, due to its commercial availability. The structure of 4-CMTB does not contain a carboxylate moiety and it retained the ability to activate FFA2 upon mutation of binding site residues Arg180^{5.39}, Arg255^{7.35} and His242^{6.55}, indicating that it binds to an allosteric site (Smith et al., 2011). Further investigation of the effect of 4-CMTB on SCFA concentration responses revealed that it acts as a PAM of SCFA potency. Interestingly, 4-CMTB does not have a modulatory effect on the response to synthetic agonist compound 1 (Hudson et al., 2013a), making it a typical example of the “probe dependence” that is common among allosteric ligands. Efforts to improve 4-CMTB potency using medicinal chemistry had limited success (Wang et al., 2010, Smith et al., 2011). None of the explored 4-CMTB analogues showed improved potency over the parent compound. However, in functional studies some of these analogues have been employed, potentially due to the poor pharmacokinetic profile of 4-CMTB (Wang et al., 2010). Other attempts to identify the binding site of 4-CMTB that did not initially yield any outcomes, were able to demonstrate that ECL2 appears to play a key role in the allosteric modulation of SCFA potency as its replacement with the ECL2 of FFA3 led to a loss of allosterism with C3 (Smith et al., 2011). A recent kinetic analysis of 4-CMTB binding, measuring both dynamic mass redistribution over time and inositol monophosphate (IP1) accumulation at different time points, suggested that 4-CMTB associates with the receptor in a distinct fashion by initially binding to the orthosteric site and activating the receptor, followed by a transition to the allosteric site through which its modulatory effects on SCFAs were mediated (Grundmann et al., 2016). Although more work is needed to confirm this mode of binding, it led to the identification of proposed allosteric residue Lys65^{2.60}, whose involvement in FFA2 ligand binding and signalling will be discussed in chapter 6. Functionally 4-CMTB has been shown to

mimic the effects of SCFAs at FFA2; it was able to inhibit lipolysis in a rat adipocyte cell line (Lee et al., 2008) and has been shown to mediate FFA2-dependent migration of neutrophils in conjunction with SCFAs (Vinolo et al., 2011). A close analogue of 4-CMTB has also been employed to demonstrate that SCFA treatment promoted GLP-1 release in mouse colonic crypts in an FFA2-dependent fashion (Nohr et al., 2013) and that FFA2 activation specifically had an inhibitory effect on ghrelin secretion in primary gastric mucosal cells (Engelstoft et al., 2013). 4-CMTB has certainly been a useful tool compound in functional studies, however its modest potency, allosteric nature and potentially complex mode of binding highlights that it is not equivalent to a high-affinity orthosteric agonist.

Much more recently the pharmacology of a novel allosteric ligand for FFA2, AZ1729, has been described (Bolognini et al., 2016a). As in the case of 4-CMTB, AZ1729 lacks a carboxylate moiety and was able to activate orthosteric binding site mutants of FFA2. Closer investigation of the signalling profile of AZ1729 revealed strongly biased behaviour as it was able to activate FFA2 in G_i -coupled cAMP inhibition and [35 S]-GTP γ S assays but was unable to promote G_q -dependent accumulation of IP1. Furthermore, AZ1729 was also able to allosterically modulate C3 and compound 1 concentration response curves, however also in a biased fashion. In G_i -coupled systems AZ1729 acted as a PAM of agonist potency, but when measuring G_q signalling in the same manner a NAM effect on agonist efficacy could be observed. Assessment of its direct effect on binding of C3 revealed that increasing concentrations of AZ1729 increase C3 affinity, which likely results in the PAM effect in G_i -coupled assays. However, more detailed investigations of AZ1729 pharmacology may be required to define the molecular basis for its NAM effect on responses through G_q . At the murine orthologue AZ1729 retains its biased agonist behaviour, however its negative allosterism in G_q -coupled assays at the human receptor appears to have switched to a PAM effect on C3 potency and efficacy. Despite its distinct allosterism at mFFA2, AZ1729 could still be employed to define the contribution of G_i and/or G_q pathways to different physiological outputs of FFA2 activation. AZ1729 was able to inhibit lipolysis in primary mouse adipocytes and induce human neutrophil migration, and potentiated the response to C3 in both assay systems, suggesting that these effects are primarily mediated through G_i . On the other hand, AZ1729

did not regulate release of GLP-1 from mouse colonic crypts, suggesting an underlying G_q -coupled mechanism. These observations confirm that the various physiological functions of FFA2 may be mediated by different signalling pathways and that it is possible to develop an FFA2 ligand that can induce downstream responses in a selective fashion. In particular for a receptor with a complex physiological role and promiscuous signalling behaviour as observed for FFA2, a biased tool compound could be of great translational value, especially considering that some biological outputs that are mediated by G_i versus G_q have been suggested to have contradictory effects (Priyadarshini et al., 2015, Tang et al., 2015). The species-specific pharmacology of AZ1729 limits its use in dissecting the physiological relevance of respective G proteins coupling to FFA2 in murine models, as AZ1729 will equally potentiate G_i and G_q responses of murine FFA2 to SCFAs. However, AZ1729 can still be employed in *ex vivo* or *in vivo* studies in absence of SCFAs to understand the contribution of G_i versus G_q signalling to individual physiological outputs, as it remains a biased agonist at mFFA2.

1.6 Aims

The SCFA receptor FFA2 is a fascinating GPCR that is deeply involved in the link between gut microbiome activity and metabolic regulation. Although FFA2 has been suggested as a potential therapeutic target in a range of conditions, a variety of factors have limited the progression of drug development. The work presented in this thesis aims to employ and develop pharmacological tool compounds and assay systems to provide a better understanding of FFA2 ligand binding and signal transduction. An initial characterisation of systems available to measure ligand action and binding will be followed by a detailed analysis of the structure-activity relationship of an agonist series recently investigated in a functional study (Forbes et al., 2015) at human and murine FFA2 (**Chapter 3**). The pharmacology and binding mode of FFA2 antagonists remains largely unexplored, therefore considerable effort has been invested herein to define the pharmacology of the GLPG0974 (Pizzonero et al., 2014) and CATPB (Hudson et al., 2012b) antagonist series. Although the use of signalling assays in combination with medicinal chemistry and mutagenesis can provide crucial information on ligand pharmacology and binding (**Chapter 3**), the lack of a means to directly assess binding to the receptor can limit investigation of

antagonists at FFA2 mutations that prohibit activation by agonists. Therefore, a radioligand based on GLPG0974 was employed to define the binding site and mechanism of FFA2 antagonists, particularly in the context of the known orthosteric binding pocket residues and in comparison to FFA2 agonists (**Chapter 4**). Fluorescence-based methodology has recently been proposed as an alternative to radioactive labelling, as it allows for real-time monitoring of ligand binding and is safe to use in live animals (Ma et al., 2014). To assess the feasibility and usefulness of fluorescence-based binding assays for FFA2, a novel binding assay based on bioluminescence resonance energy transfer between a fluorescently labelled ligand and nanoluciferase-tagged receptor was developed (**Chapter 5**). Another factor that has greatly hindered functional studies at FFA2 is the lack of antagonists active at rodent orthologues. Using a homology model based on direct binding studies at different FFA2 mutants the molecular basis of species selectivity was identified (**Chapter 6**). Finally, the mechanistic basis of the promiscuous signalling behaviour of FFA2 was explored to develop a biased receptor (**Chapter 6**). The findings discussed will shine some light on the complex pharmacology of synthetic FFA2 ligands and the mechanisms that produce their function. This will contribute to future drug development efforts.

2 Materials and methods

2.1 Pharmacological reagents

Sodium propionate: Sigma-Aldrich

AZ1729 (N-[3-(2-Carbamimidamido-4-methyl-1,3-thiazol-5-yl)phenyl]-4-fluorobenzamide): Synthesised in collaboration with AstraZeneca.

[³H]-GLPG0974 ([[³H]-4-[[1-(benzo[*b*]thiophene-3-carbonyl)-2-methylazetidine-2-carbonyl]-(3-chlorobenzyl)amino]butyric acid): Provided as a gift by AstraZeneca.

[³⁵S]-GTPγS ([³⁵S]-guanosine-5'-O-(3-thio)triphosphate): PerkinElmer

The following test compounds were all synthesised in collaboration with University of Southern Denmark. The identity and >95% purity of each compound was confirmed by nuclear magnetic resonance, mass spectrometry and liquid chromatography.

Compound 1 (3-benzyl-4-(cyclopropyl-(4-(2,5-dichlorophenyl)thiazol-2-yl)amino)-4-oxobutanoic acid)

Compound 2 ((2*S*,5*R*)-5-(2-chlorophenyl)-1-(2'-methoxy-[1,1'-biphenyl]-4-carbonyl)pyrrolidine-2-carboxylic acid)

Compound 2 analogues 1-28 (Chemical structures are related to compound 2 and will be described in chapter 3)

GLPG0974 (4-[[1-(benzo[*b*]thiophene-3-carbonyl)-2-methylazetidine-2-carbonyl]-(3-chlorobenzyl)amino]butyric acid)

GLPG-1 ((4-(1-(benzo[*b*]thiophene-3-carbonyl)-2-methyl-N-(4-trifluoromethylbenzyl)azetidine-2-carboxamido)butanoic acid)

MeGLPG-1 (methyl 4-(1-(benzo[*b*]thiophene-3-carbonyl)-2-methyl-N-(4-trifluoromethylbenzyl)azetidine-2-carboxamido)butanoate)

GLPG-2 (4-(1-(2-(benzo[*b*]thiophen-3-yl)acetyl)-N-(4-chlorobenzyl)-2-methylazetidine-2-carboxamido)butanoic acid)

MeGLPG-2 (methyl 4-(1-(2-(benzo[*b*]thiophen-3-yl)acetyl)-N-(4-chlorobenzyl)-2-methylazetidine-2-carboxamido)butanoate)

MoGLPG-2 (1-(2-(benzo[*b*]thiophen-3-yl)acetyl)-N-(4-chlorobenzyl)-2-methyl-N-(4-morpholino-4-oxobutyl)azetidine-2-carboxamide)

GLPG-3 (4-(1-(2-(benzo[*b*]thiophen-3-yl)acetyl)-2-methyl-N-(4-(trifluoromethyl)benzyl)azetidine-2-carboxamido)butanoic acid)

MeGLPG-3 (methyl 4-(1-(2-(benzo[*b*]thiophen-3-yl)acetyl)-2-methyl-N-(4-(trifluoromethyl)benzyl)azetidine-2-carboxamido)butanoate)

LinkGLPG-3 (tert-butyl (3-(4-(1-(2-(benzo[*b*]thiophen-3-yl)acetyl)-2-methyl-N-(4-(trifluoromethyl)benzyl)azetidine-2-carboxamido)butanamido)propyl)carbamate)

CATPB ((*S*)-3-(2-(3-chlorophenyl)acetamido)-4-(4-(trifluoromethyl)phenyl)butanoic acid)

MeCATPB (methyl (*S*)-3-(2-(3-chlorophenyl)-acetamido)-4-(4-trifluoromethylphenyl)butanoate)

LinkCATPB (tert-butyl (*S*)-3-(3-(2-(3-chlorophenyl)acetamido)-4-(4-(trifluoromethyl)phenyl)butanamido)propyl)carbamate)

F-1 (1-(2-(benzo[*b*]thiophen-3-yl)acetyl)-2-methyl-N-(4-((3-((7-nitrobenzo[*c*][1,2,5]oxadiazol-4-yl)amino)propyl)amino)-4-oxobutyl)-N-(4-(trifluoromethyl)benzyl)azetidine-2-carboxamide)

F-2 ((*S*)-3-(2-(3-chlorophenyl)acetamido)-N-(3-((7-nitrobenzo[*c*][1,2,5]oxadiazol-4-yl)amino)propyl)-4-(4-(trifluoromethyl)phenyl)butanamide)

F-3 ((2*R*,4*R*)-2-(2-chlorophenyl)-3-(4-(((7-nitrobenzo[*c*][1,2,5]oxadiazol-4-yl)amino)methyl)benzoyl)thiazolidine-4-carboxylic acid)

2.2 Molecular Biology

2.2.1 DNA constructs

For the work described in this thesis a range of different DNA constructs were employed to generate both transiently transfected and stably expressing cell lines. While most constructs were generated as part of this PhD project and will be described in later sections, several plasmids have been engineered previously. The vectors used to construct the plasmids include pcDNA3.1 (Thermo Fisher), pcDNA5/FRT/TO (Thermo Fisher) and pCAGGS (obtained in collaboration with Tohoku University), which all encode an ampicillin resistance gene for selection. Initially plasmids encoding human (h)FFA2, hFFA3 and murine (m)FFA2 were generated in the pcDNA3.1 vector with enhanced yellow fluorescent protein (eYFP) fused to the receptor C terminus (Stoddart et al., 2008), which was followed by a sub-cloning into the pcDNA5/FRT/TO vector (Hudson et al., 2012b). Orthosteric binding site mutations R180A, R255A and H242A were also introduced into pcDNA5/FRT/TO-hFFA2-eYFP previously (Hudson et al., 2012b). For the BRET-based β -arrestin recruitment assay, a pcDNA3 vector encoding Renilla luciferase (RLuc)-tagged β -arrestin 2 was generated in previous studies (Hudson et al., 2013a). For the transforming growth factor α (TGF α) shedding assay, pCAGGS vectors encoding alkaline phosphatase (AP)-tagged TGF α , FLAG epitope-tagged histamine H1 receptor, native G α proteins and G α chimeras were obtained in collaboration with Tohoku University (Inoue et al., 2012).

2.2.2 Preparation of competent bacteria

The chemically competent *Escherichia coli* strain XL1-Blue was utilised for chemical transformation of plasmid DNA. To prevent contamination with environmental bacteria, sterile technique was applied throughout and all culture media and reagents were autoclaved or filter-sterilised. A stock of XL-1 Blue cells stored at -80°C was defrosted on ice and streaked onto LB agar (10 g/L tryptone, 5 g/L yeast extract, 10 g/L NaCl and 15 g/L agar at pH 7). Streaked plates were incubated for 16 h at 37°C and a single colony was used to inoculate 5 mL of LB broth (10 g/L tryptone, 5 g/L yeast extract and 10 g/L NaCl at pH 7), which was grown for a further 16 h at 37°C in a shaking incubator. The bacterial

culture was then transferred into a conical flask with 100 mL LB broth and grown at 37°C in a shaking incubator until an optical density of 0.48 was reached at a wavelength of 600 nm. To halt bacterial growth the flask was incubated on ice for 5 min, then transferred into two 50 mL falcon tubes and centrifuged at 1,800 x g for 10 min at 4°C. The resulting pellet was resuspended in 20 mL of solution A (30 mM CH₃CO₂K, 10 mM RbCl₂, 10 mM CaCl₂, 50 mM MnCl₂ and 15% (v/v) glycerol at pH 5.8 with acetic acid), incubated on ice for 5 min and centrifuged as before. The pellet generated by this second centrifugation was resuspended in 2 mL of solution B (10 mM 3-morpholinopropane-1-sulfonic acid (MOPS), 10 mM RbCl₂, 75 mM CaCl₂ and 15% (v/v) glycerol at pH 6.5 with HCl) and incubated on ice for 15 min. The resulting competent XL1-Blue bacteria were aliquoted into pre-chilled microcentrifuge tubes and stored at -80°C.

2.2.3 Bacterial transformation

Chemically competent XL-1 Blue cells prepared as described above were defrosted on ice and 100-500 ng DNA was added to 50 µL bacteria in pre-chilled microcentrifuge tubes and incubated on ice for 15 min. Samples were then transformed at 42°C for 90 s, followed by immediate incubation on ice for 2 min. To allow for recovery and expression of the ampicillin resistance gene in successfully transformed bacteria, 450 µL LB broth were added and samples were placed in a shaking incubator for 1 h at 37°C. LB agar plates containing 50 µg/mL ampicillin were prepared in advance and were used to plate 100-250 µL of recovered bacterial culture. Resulting plates were incubated for 16 h at 37°C and cultures for preparation of plasmid DNA were inoculated with single colonies.

2.2.4 Plasmid DNA purification

Different kits were employed for purification of plasmid DNA, depending on the amount of DNA required for respective applications. A MiniPrep purification is commonly used when only small yield in the µg range is required, for example for initial screening of newly engineered plasmids. In contrast, MaxiPrep purification is appropriate when a larger yield in the mg range is necessary for downstream applications. Although the underlying mechanism of DNA isolation is

equivalent and manufacturer's instructions were followed, both procedures are briefly described below.

For MiniPrep purifications the Wizard® Plus SV Minipreps DNA Purification System (Promega) was employed. A 16 h bacterial culture of 5 mL was harvested by centrifugation at 9,300 x g for 5 min. The resulting bacterial pellet was resuspended in 250 µL resuspension solution and lysed by addition of 250 µL SDS-containing lysis solution. Additionally, 10 µL alkaline protease solution was added to inactivate endonucleases and other proteins. Lysates were incubated for 10 min at room temperature (RT) and 350 µL neutralisation buffer was added to induce precipitation of denatured proteins, cellular debris and chromosomal DNA, with plasmid DNA remaining in solution. The treated lysate was centrifuged at 16,000 x g for 10 min and the resulting supernatant was applied to a provided spin column, followed by a centrifugation at 16,000 x g for 1 min to allow the DNA to bind to the column. The flow-through was discarded and the column was washed two times with ethanol-containing buffer including centrifugations at 16,000 x g for 1 min each time. To remove remaining ethanol the column was centrifuged at 16,000 x g for a further 2 min and DNA was eluted in 100 µL nuclease-free water into a sterile microcentrifuge tube.

For MaxiPrep purifications the QIAGEN® Plasmid Maxi Kit (QIAGEN) was used. A 16 h bacterial culture of 100 mL was centrifuged at 3,200 x g for 30 min at 4 °C and the resulting pellet was resuspended in 10 mL RNase A-containing resuspension buffer at 4 °C. Bacteria were lysed by addition of 10 mL SDS-containing lysis buffer and incubation for 5 min at RT. To neutralise the solution, 10 mL of pre-chilled neutralisation buffer were added, followed by incubation for 20 min on ice and centrifugation at 3,200 x g for 20 min at 4 °C. A QIAGEN-tip 100 column was equilibrated with 10 mL equilibration buffer and the plasmid DNA-containing supernatant was carefully decanted into the column. After passing of the solution through the column by gravity flow, the column was washed twice with 30 mL of ethanol-containing wash buffer. Next, 15 mL elution buffer were applied to elute the DNA and by adding 10.5 mL isopropanol the DNA was precipitated, followed by a centrifugation at 3,200 x g for 30 min at 4 °C. The pellet was air-dried, desalted by washing with 2 mL of 70% (v/v) ethanol and transferred into a sterile microcentrifuge tube. The precipitated DNA was then

centrifuged at 20,000 x g for 10 min. The supernatant was aspirated and once the resulting pellet of purified DNA air-dried, it was dissolved in 600 μ L nuclease-free water.

Concentration and purity of purified plasmid DNA was assessed using a UV spectrophotometer to measure the absorbance of a sample diluted at 1:1000 at wavelengths of 260 and 280 nm. The absorbance at 260 nm (A_{260}) corresponds to the maximal absorbance wavelength of nucleic acids and therefore allows quantification of DNA concentration. In a cuvette with a path length of 1 cm the A_{260} value equals unity for a 50 μ g/mL solution of double-stranded DNA (Barbas et al., 2007). Proteins absorb at 280 nm and an absorbance ratio (A_{260}/A_{280}) between 1.8 and 2.0 is considered to be pure nucleic acid. After DNA quantification samples were stored at -20°C .

2.2.5 Sequencing

Completed cloning and mutagenesis products were sequenced to confirm that the desired DNA plasmid has indeed been produced and the sequence of plasmids obtained in collaboration was also confirmed in this fashion. DNA sequencing was performed by DNA Sequencing & Services (MRC I PPU, College of Life Sciences, University of Dundee, Scotland, www.dnaseq.co.uk) using Applied Biosystems Big-Dye Ver 3.1 chemistry on an Applied Biosystems model 3730 automated capillary DNA sequencer. DNA sequences were assessed for quality using SnapGene software, translated with the ExPASy Translate Tool (web.expasy.org/translate/) and analysed with the NCBI Basic Local Alignment Search Tool (www.blast.ncbi.nlm.nih.gov).

2.2.6 Cloning strategy

Polymerase chain reaction (PCR) is an essential tool for molecular biology to amplify specific fragments of DNA. By designing specific primers desired restriction sites and epitope tags can be introduced in the sequence. For amplification of DNA fragments, reactions were set up in nuclease-free water in sterile 500 μ L PCR tubes in a final volume of 50 μ L with the following final amounts of reagents:

- 1 x *Pfx* Amplification Buffer (Invitrogen)
- 1 mM MgSO₄ (Invitrogen)
- 250 μM deoxyribonucleotide (dNTP) mixture including deoxyadenosine triphosphate (dATP), deoxycytidine triphosphate (dCTP), deoxyguanosine triphosphate (dGTP) and deoxythymidine triphosphate (dTTP) (Promega)
- 2.5 units Platinum™ *Pfx* DNA Polymerase (Invitrogen)
- 400 nM each forward and reverse primers
- 50 ng template DNA

Reaction mixtures were then transferred into a thermal cycler and subjected to the following cycling programme:

1. Preheating	94 °C	3 min
2. Denaturing	94 °C	30 s
3. Annealing	55-60 °C	30 s
4. Extension	68 °C	1 min
5. Repeat steps 2-4 for 30 cycles		
6. Final extension	68 °C	5 min

The annealing temperature can be adjusted to optimise the PCR reaction and depends on the melting temperature (T_m) of respective primers with a temperature of approximately 5-10 °C lower than T_m being optimal. After the reaction samples are held at 4 °C and then transferred to -20 °C for long-term storage.

The QIAquick® PCR Purification Kit (QIAGEN) was used to purify PCR products after cycling and was employed as per manufacturer's instructions. Completed PCR reactions were diluted in five volumes of binding buffer, applied to a QIAquick spin column and centrifuged at 16,000 x g for 1 min. The flow-through was discarded and the column was washed with an ethanol-containing buffer, followed by a centrifugation as before. After the wash the column was centrifuged once more to remove residual ethanol and 50 μL of nuclease-free water were applied to the column for 1 min. DNA fragments were then eluted into a sterile microcentrifuge tube by centrifugation. Samples were either processed directly or stored at -20 °C.

Cloning of a novel DNA plasmid usually includes the insertion of a DNA fragment into an empty vector. To achieve this, both components need to be digested with restriction endonuclease enzymes to generate sticky-end DNA fragments optimal for ligation. Digestion reactions were performed in a volume of 50-100 μL and incubated for 16 h at 37°C with following reagents:

- 1 x CutSmart® Buffer (New England Biolabs)
- 10-50 μg vector DNA or 50 μL PCR product
- 1-10 units of High Fidelity (HF®) restriction endonucleases (New England Biolabs) with units used dependent on manufacturer's instructions

To purify digested DNA insert and vector fragments, they were first separated by agarose gel electrophoresis. Agarose gels were prepared by dissolving 1% (w/v) agarose in TAE buffer (40 mM Tris, 1 mM EDTA (at pH 8) and 20 mM acetic acid) and adding 1 x SYBR® Safe DNA Stain (Life Technologies) to allow visualisation of DNA. Samples were prepared by adding the respective volume of 6 x DNA loading buffer (0.4 mg/mL sucrose and 0.25% (w/v) bromophenol blue) and 5-50 μL were loaded per well onto the set gel immersed in TAE buffer. In addition to the samples, 5 μL Hyperladder™ 1kb (Bioline) was loaded into one well to allow quantification of DNA fragment size and concentration. The gel was then subjected to an electric current of 125 V for 20-30 min.

To extract the digested DNA fragments from the agarose gel the QIAquick Gel Extraction Kit (QIAGEN) was used as per manufacturer's instructions. The agarose gel bands that contain the DNA fragments of interest were visualised with a UV transilluminator and carefully excised with a razor blade. The gel pieces were weighed in sterile microcentrifuge tubes and three gel volumes of solubilisation buffer were added, followed by an incubation for 10 min at 50°C, vortexing every 2-3 min, to dissolve the gel pieces. One gel volume of isopropanol was added to the resulting solution and applied to a QIAquick spin column. The column was centrifuged at 16,000 x g for 1 min and after discarding the flow-through, the column was washed including a centrifugation as before. The wash was followed by a further centrifugation to remove residual ethanol and 30-50 μL nuclease-free water were added to the column, which was incubated for 1 min. DNA was then eluted into a sterile microcentrifuge tube by

means of a further centrifugation. When not processed immediately, samples were stored at -20°C.

To select appropriate concentrations of gel-extracted DNA vector and insert, a further agarose gel electrophoresis was performed, and the DNA concentration was estimated with the Hyperladder™ 1kb. After determination of vector and insert concentrations, the required amount of insert and vector DNA to reach molar ratios of 1:3 and 1:5 were calculated with the following formula:

$$Mass_{insert} (ng) = Molar\ Ratio \times Mass_{vector} (ng) \times \frac{Size_{insert} (kb)}{Size_{vector} (kb)}$$

Sticky-end ligation reactions were set up in a volume of 20 µL with the following reagents:

- 1 x T4 DNA Ligase Reaction Buffer (New England Biolabs)
- 75 ng vector DNA
- insert DNA (calculated in ng as above)
- 400 units T4 DNA Ligase (New England Biolabs)

Reactions were incubated for 2 h at RT and 5-10 µL of ligated product was transformed into XL1-Blue competent bacteria as described in section 2.2.3.

2.2.7 Generation of hemagglutinin (HA)-tagged FFA2 constructs

Plasmids encoding hFFA2 with a C-terminal HA tag (amino acid sequence YPYDVPDYA) were generated by using pcDNA5/FRT/TO-hFFA2-eYFP (see section 1.2.1) as a template. Forward primers were designed to add a *Hind*III restriction site followed by a Kozak sequence (*double line*), which facilitates initiation of translation, and the hFFA2 start codon (*grey*). Reverse primers were designed to fuse the HA tag (*broken line*) to the hFFA2 C terminus followed by a stop codon (*grey*) and an *Xho*I restriction site (*full line*).

*Hind*III hFFA2 Forward Primer

5' TTTTAAGCTTGCCACCATGCTGCCGGACTGGAAG 3'

hFFA2-HA *Xho*I Reverse Primer

5' TTTTCTCGAGCTAAGCGTAATCTGGAACATCGTATGGGTA
CTCTGTAGTGAAGTCCG
AACTTGG 3'

PCR products were cloned into the pcDNA5/FRT/TO vector as described in previous sections for subsequent use in the Flp-In™ T-REx™ system.

2.2.8 Generation of Nanoluciferase-tagged FFA2 constructs

Development of the BRET-based binding assay (see section 2.4.5) required the generation of an hFFA2 construct N terminally tagged with Nanoluciferase (NLuc) in the pcDNA5/FRT/TO vector. For this purpose, the pcDNA5/FRT/TO-NLuc-hFFA4 plasmid developed for a previous BRET-based binding study was employed as an NLuc template (Christiansen et al., 2016) and pcDNA5/FRT/TO-hFFA2-eYFP as an hFFA2 template. The NLuc sequence was previously fused to an mGLUR signal at the N terminus to ensure correct insertion of the NLuc-tagged receptor into the plasma membrane. To amplify the NLuc insert a forward primer upstream of the multiple cloning site of the pcDNA5/FRT/TO vector was employed and a reverse primer was designed to introduce an *Xma*I restriction site downstream of the NLuc sequence. The hFFA2 sequence was amplified using a forward primer that introduced an *Xma*I restriction site upstream, to allow for ligation with the NLuc insert, and a reverse primer that introduced an *Xho*I restriction site downstream of the hFFA2 sequence.

pcDNA5/FRT/TO-MCS Forward Primer

5' CCACGCTGTTTTGACCTCCAT 3'

NLUC-*Xma*I Reverse Primer

5' ACTGACTGCCCGGGCGCCAGAATGCGTTCGCACAG 3'

***Xma*I-hFFA2 Forward Primer**

5' ACTGACTGCCCGGGATGCTGCCGGACTGGAAGAGC 3'

hFFA2-*Xho*I Reverse Primer

5' TTTTCTCGAGCTACTCTGTAGTGAAGTCCGA
ACTTGG 3'

The empty pcDNA5/FRT/TO vector was digested with *Hind*III and *Xho*I to generate sticky-end DNA necessary for ligation, while the amplified NLuc insert

was digested with *HindIII* and *XmaI*, and the amplified hFFA2 insert with *XmaI* and *XhoI*. The cloning procedure was followed as described in sections above and the resulting pcDNA5/FRT/TO-NLuc-hFFA2 plasmid was used in the Flp-In™ T-REx™ system.

2.2.9 Site-directed mutagenesis

To alter the wild type sequence of receptors by introducing point mutations, the Stratagene QuikChange® System was employed. Although the general procedure is akin to standard PCR described in section 2.2.6, it is actually a linear amplification technique as the reaction product is never used as a template. Oligonucleotide primers that contain the desired base substitution were designed using the online software PrimerX (www.bioinformatics.org/primerx), which screens for primers that are between 20-40 bp in length with a low GC content of $\leq 60\%$, when possible, and a $T_m \geq 75^\circ\text{C}$. The reactions were performed in a volume of 50 μL and set up in 500 μL PCR tubes with following final reagent concentrations:

- 1 x *Pfu* DNA Polymerase Buffer with MgSO_4 (Promega)
- 250 μM dNTP mixture
- 1 μM each forward and reverse primers
- 20 ng template DNA
- 2.5 units *Pfu* DNA Polymerase (Promega)

A thermal cycler was employed to subject the reaction mixtures to the following cycling programme:

1. Preheating	95 °C	5 min
2. Denaturing	95 °C	30 s
3. Annealing	42-65 °C	30 s
4. Extension	72 °C	≥ 2 min
5. Repeat steps 2-4 for 30 cycles		
6. Final extension	72 °C	5 min

As in the case of PCR described in section 2.2.6, the annealing temperature needs to be adjusted to the T_m of respective primers. For the extension time it

is recommended to allow approximately 2 min per 1 kb that need to be amplified. Following the reaction, the methylated parental template DNA was digested by adding 10 units of the *DpnI* restriction enzyme (Promega) to the reaction product and incubating the samples for 16 h at 37°C. To express and purify the desired plasmid DNA, 1 µL of digested product was used to transform XL1-Blue competent bacteria following the protocol described in section 2.2.3.

2.2.10 Generation of FFA2 point mutant constructs

The generation of hFFA2 and mFFA2 constructs that contain point mutations of interest was performed by site-directed mutagenesis. Depending on the application, different templates were used for generation of mutations, including pcDNA5/FRT/TO-hFFA2-eYFP, pcDNA5/FRT/TO-hFFA2-HA, pcDNA5/FRT/TO-NLuc-hFFA2 and pcDNA5/FRT/TO-mFFA2-eYFP. For generation of the same mutations in different plasmids, the same mutagenic primers were employed.

R180A (in pcDNA5/FRT/TO-NLuc-hFFA2)

Forward Primer: 5' GTGCTGCCCGTGGCGCTGGAGCTGTG 3'

Reverse Primer: 5' CACAGCTCCAGCGCCACGGGCAGCAC 3'

R255A (in pcDNA5/FRT/TO-NLuc-hFFA2)

Forward Primer: 5' GAAAAAGCCCCTGGTGGCGTCAATAGCCGTGGTG 3'

Reverse Primer: 5' CACCACGGCTATTGACCGCCACCAGGGGCTTTTTTC 3'

H242A (in pcDNA5/FRT/TO-NLuc-hFFA2)

Forward Primer: 5' CTTACAACGTGTCCCGCTGGTGGGGTATCAC 3'

Reverse Primer: 5' GTGATACCCACAGCGCGGACACGTTGTAAG 3'

K65A (in pcDNA5/FRT/TO-NLuc-hFFA2 and -hFFA2-HA)

Forward Primer: 5' CTGCTGCCCTTCGGATCATCGAGG 3'

Reverse Primer: 5' CCTCGATGATCGCGAAGGGCAGCAG 3'

K65R (in pcDNA5/FRT/TO-NLuc-hFFA2 and -hFFA2-HA)

Forward Primer: 5' GCTGCTGCCCTTCGTATCATCGAGGCTGC 3'

Reverse Primer: 5' GCAGCCTCGATGATACGGAAAGGGCAGCAGC 3'

K65E (in pcDNA5/FRT/TO-NLuc-hFFA2 and -hFFA2-HA)

Forward Primer: 5' CTGCTGCTGCCCTTCGAAATCATCGAGGCTGC 3'

Reverse Primer: 5' GCAGCCTCGATGATTTCGAAGGGCAGCAGCAG 3'

R65K (in pcDNA5/FRT/TO-mFFA2-eYFP)

Forward Primer: 5' GCTGCTGCTGCCCTTCAAAATCGTGGAAGCAGCATC 3'

Reverse Primer: 5' GATGCTGCTTCCACGATTTTGAAGGGCAGCAGCAGC 3'

To generate the dual R180A-R255A mutant two sequential site-directed mutagenesis reactions were performed. After confirming by DNA sequencing that correct base replacements have been introduced, the plasmids were either employed for transient transfection or generation of stable cell lines using the Flp-In™ T-REx™ system.

2.3 Mammalian cell culture

2.3.1 Cell line maintenance

All cell culture procedures were performed under sterile conditions in a class II laminar flow biosafety cabinet with culture medium and reagents pre-warmed in a water bath at 37°C, when possible.

Two variants of the human embryonic kidney 293 cells were employed, namely HEK293T cells, which stably express large T antigen that can enhance protein production by binding to SV40 enhancers of expression vectors, and HEK293A cells, which stably express E1 proteins required to generate recombinant adenovirus. Both cell lines were maintained in Dulbecco's Modified Eagle's Medium supplemented with 10% (v/v) heat-inactivated foetal calf serum (FCS), 2 mM L-glutamine, 100 units/mL penicillin and 100 µg/mL streptomycin (Sigma) at 37°C and 5% CO₂ in a humidified atmosphere.

Before stable transfection of receptors of interest, parental Flp-In™ T-Rex™ 293 cells (Life Technologies) were maintained in Dulbecco's Modified Eagle's Medium with high glucose and without sodium pyruvate supplemented with 10% (v/v) heat-inactivated FCS, 100 units/mL penicillin, 100 µg/mL streptomycin and 5 µg/mL blasticidin at 37°C and 5% CO₂ in a humidified atmosphere.

To passage cell lines, the respective culture medium was aspirated and cells were washed with sterile PBS (137 mM NaCl, 2.7 mM KCl, 1.8 mM KH₂PO₄ and 10 mM Na₂HPO₄ at pH 7.4), followed by incubation with 0.25% trypsin-EDTA for a maximum of 5 min at RT. Upon detachment of cells from the culture vessel, proteolytic cleavage was inhibited by addition of culture medium and the volume of cell suspension required to achieve the desired dilution for cell passaging was transferred into a sterile culture vessel with an appropriate volume of fresh culture medium added.

For long-term storage cell lines were cryopreserved and stored in liquid nitrogen. After detachment of cells as described above, cells were centrifuged at 300 x g for 5 min and the resulting pellet was resuspended in 2 mL FCS with 10% (v/v) DMSO (for a confluent 75 cm² flask of HEK293 cells). Aliquots of 1 mL were frozen at -80°C for 24 h prior to transfer into liquid nitrogen storage. To revive cryopreserved cells, aliquots were rapidly thawed in a water bath at 37°C and transferred into a flask with 10 mL fresh culture medium. Cells were allowed to attach for 1-2 h and medium was replaced to remove DMSO.

2.3.2 Transient transfection

Transient transfection of cells was executed with polyethyleimine (PEI) as a transfection reagent and commonly performed in 10 cm dishes. To transfect respective DNA plasmids, 5 µg of DNA was diluted in 250 µL of 150 mM NaCl and mixed with 250 µL of 150 mM NaCl containing 30 µg PEI. The mixture was vortexed and incubated for 10 min at RT, followed by dropwise addition to the dish. To transfect cells grown in smaller culture vessels, the procedure was scaled down accordingly. Cells were incubated with PEI for 24 h at 37°C and 5% CO₂ in a humidified atmosphere and depending on the downstream application either employed for assays directly, or the medium was replaced and cells were used after passage into appropriate culture vessels and a further 24 h incubation.

2.3.3 Generation of stably transfected Flp-In™ T-REx™ 293 cell lines

Most assays made use of Flp-In™ T-REx™ 293 cells, which contain a doxycycline-controlled flippase recognition target (FRT) site that allows stable integration of

DNA plasmids in the pcDNA5/FRT/TO vector when co-transfected with the Flp recombinase-encoding pOG44 vector. In addition to the receptor of interest, the pcDNA5/FRT/TO plasmid also confers hygromycin resistance to positively transfected cells, which serves as a means of selection. Parental cells were cultured to reach 50-60% confluency in a 10 cm dish and co-transfected with 8 µg of DNA, including the receptor of interest in the pcDNA5/FRT/TO vector and pOG44 at a ratio of 1:8, using PEI. The medium was changed after 24 h and following a further 24 h incubation cells were subcultured at ratios of 1:10, 1:25 and 1:50. Selection of positively transfected cells was initiated by addition of 200 µg/mL hygromycin to the basal Flp-In™ T-REx™ 293 medium, which was maintained upon positive clonal selection. The culture medium was changed every 2-3 days until cell colonies could be detected by eye (14-28 days). Cells were detached as described previously and colonies were combined to yield polyclonal cell lines in which expression of the integrated gene could be stimulated by incubation with 100 ng/mL doxycycline for 16 h.

To confirm successful clonal selection, different approaches were employed depending on the fusion tag of the respective receptor. For eYFP-tagged constructs, cells were visualised under the epifluorescent Nikon ECLIPSE Ti microscope with a mercury light source and an eYFP filter set situated above the objective lens. The employed filter consists of an exciter with 500 nm peak and 20 nm bandwidth, a dichroic Q515LP mirror that allows passing of wavelengths above 515 nm and an emitter with 535 nm peak and 30 nm bandwidth. Alternatively, expression levels were assessed by determining eYFP fluorescence by excitation of doxycycline-induced cells with light at 500 nm and measuring emission at 530 nm using a POLARstar Omega Plate Reader (BMG LABTECH). As NLuc is capable of bioluminescence upon addition of the Nano-Glo® Luciferase Assay Substrate (Promega), NLuc-tagged receptor expression was assessed by measuring NLuc luminescence at 470 nm using a PHERAStar FS Plate Reader (BMG LABTECH). Although measurement of eYFP fluorescence and NLuc luminescence is not quantitative, it provides qualitative information on the comparability of expression levels in different cell lines. Receptor functionality and expression in HA-tagged receptor cell lines was confirmed in functional assays and directly quantified in radioligand binding studies.

2.4 Biochemical assays

2.4.1 Preparation of cellular membranes

Membranes required for biochemical assays were generated from Flp-In™ T-REx™ 293 cells treated in confluent 10 cm dishes with 100 ng/mL doxycycline for 16 h under sterile conditions to induce expression of the receptor of interest. Cells were washed once with non-sterile ice cold PBS, detached from the dish in 3 mL PBS by scraping, and centrifuged at 1,800 x g for 5 min at 4 °C. Pellets were incubated at -80 °C for a minimum of 30 min and then resuspended in TE buffer (10 mM Tris and 0.1 mM EDTA at pH 7.4) containing cOmplete™ EDTA-free Protease Inhibitor Cocktail (Roche), followed by homogenisation by passing the cell suspension through a 5 mL hand-held Dounce homogeniser 50 times. The cell lysate was then passed 5 times through a 25-gauge needle and centrifuged at 450 x g for 5 min at 4 °C to pellet cell debris. The plasma membrane-containing supernatant was then transferred to ultracentrifuge tubes and subjected to a centrifugation at 90,000 x g for 30 min at 4 °C. The pellet was resuspended in TE buffer with protease inhibitor and passed 5 times through a 25-gauge needle. Membrane preparations were either used immediately or aliquoted and stored at -80 °C.

2.4.2 Determination of membrane protein concentration

After membrane preparation, the concentration of protein was quantified to allow appropriate dilution for downstream applications. The bicinchoninic acid (BCA) assay was employed for protein quantification, using a standard curve of 0.25-3 µg/µL bovine serum albumin (BSA). Samples were diluted 1:2 and 10 µL of diluted sample or undiluted standard was added to a clear 96-well plate. Proteoquant BCA Reagent B (Expedeon) was diluted 1:50 in Proteoquant BCA Reagent A (Expedeon) and 200 µL/well were added to the samples and standards. The plate was incubated at 37 °C for 20 min and absorbance at 562 nm was measured on a POLARStar Omega Plate Reader (BMG Labtech). Diluted sample concentrations were interpolated from the linear BSA standard curve and multiplied by 2 to determine protein concentrations.

2.4.3 [³⁵S]-GTPγS binding assay

To assess coupling of G_i subtype G proteins to FFA2, the [³⁵S]-GTPγS binding assay was employed. GTPγS is a non-hydrolysable analogue of GTP and remains bound to Gα_i upon nucleotide exchange induced by an actively signalling GPCR. By radiolabelling GTPγS with [³⁵S], the extent of Gα_i protein activation can be quantified with an approach comparable to radioligand binding. Assays were performed in glass tubes in a total volume of 250 μL using a water bath at 25 °C. Initially, 10 μg of membrane protein were pre-incubated for 15 min in assay buffer (50 mM Tris, 10 mM MgCl₂, 100 mM NaCl, 1 mM EDTA, 1 μM GDP, 30 μg/ml saponin and 0.1% (w/v) fatty acid-free BSA at pH 7.4) containing the indicated ligand concentrations. The reaction was then initiated by addition of [³⁵S]-GTPγS at 50 nCi per tube, and the reaction was terminated after a further 45 min incubation by rapid filtration through GF/C glass filters (Alpha Biotech), which were pre-soaked in ice-cold wash buffer (50 mM Tris and 10 mM MgCl₂ at pH 7.4), using a 24-well Brandel cell harvester (Alpha Biotech). This filtration allows separation of free [³⁵S]-GTPγS and G_i-bound [³⁵S]-GTPγS, which will be unable to pass through the glass filter. Unbound radioligand was removed from filters by washing 3 times with ice-cold wash buffer and filters were dried for a minimum of 30 min at RT. Dried filters were transferred to 6 mL polyethylene (PE) Pony Vials (PerkinElmer) and 3 mL of Ultima Gold™ XR liquid scintillation cocktail (PerkinElmer) were added per vial. To quantify [³⁵S]-GTPγS binding, a Tri-Carb® liquid scintillation counter was employed to measure [³⁵S] counts per minute (CPM) with a maximum quantification time of 5 min. For data analysis, CPM was plotted against ligand concentrations on a logarithmic scale.

2.4.4 Radioligand binding assay

All radioligand binding assays using [³H]-GLPG0974 were conducted in binding buffer (50 mM Tris, 100 mM NaCl, 10 mM MgCl₂ and 1 mM EDTA at pH 7.4) in glass tubes at a total volume of 200 μL and using a water bath at 25 °C. Nonspecific binding of the radioligand was determined in the presence of 10 μM unlabelled GLPG0974 or CATPB, as stated in respective figure legends. The indicated incubation time of radioligand with membrane protein, generated from doxycycline-induced Flp-In™ T-REX™ cells, and other experiment-specific additions was followed by separation of receptor-bound and free [³H]-GLPG0974

by rapid vacuum filtration through PBS-soaked GF/C glass filters (Alpha Biotech) using a 24-well Brandel cell harvester (Alpha Biotech). As in case of [³⁵S]-GTPγS assays, receptor-bound radioligand will be unable to pass through the glass filter. To remove remaining unbound radioligand, the filter was washed 3 times with ice-cold PBS. After drying for a minimum of 30 min, cut filters were transferred to 6 mL PE Pony Vials (PerkinElmer) and 3 ml of Ultima Gold™ XR liquid scintillation cocktail (PerkinElmer) were added to each sample vial. Radioactivity of receptor-bound [³H]-GLPG0974 was quantified by using the Tri-Carb® liquid scintillation counter to measure [³H] disintegrations per minute (DPM) with a maximum quantification time of 3 min. Corresponding standards of [³H]-GLPG0974 concentrations used in respective assays were also quantified to define the concentration of [³H]-GLPG0974 added per tube:

$$\frac{\text{Standard (DPM)}}{\text{Specific activity} \left(\frac{\text{DPM}}{\text{fmol}} \right)} \times \frac{1}{200 \text{ (Assay volume)}} = \frac{\text{fmol}}{\mu\text{L}} = \frac{\text{nmol}}{\text{L}} = \text{nM}$$

Radioligand binding data analysis usually includes the calculation of specific binding by subtracting nonspecific binding from total binding, which is appropriate as total radioligand binding never exceeded more than 10% of that added, thereby avoiding complications associated with free radioligand depletion (Hulme and Birdsall, 1992). To quantify specifically bound [³H]-GLPG0974 in context of the protein concentration the following formula was used:

$$\frac{\text{Specific binding (DPM)}}{\text{Specific activity} \left(\frac{\text{DPM}}{\text{fmol}} \right)} \times \frac{1000}{\text{Protein} \left(\frac{\mu\text{g}}{\text{tube}} \right)} = \text{Specific binding} \left(\frac{\text{fmol}}{\text{mg}} \right)$$

Availability of a radioligand allows for various different approaches to radioligand binding including assessment of saturation and competition binding or kinetic studies. The methods described above apply for all radioligand binding assays, while experiment-specific procedures will be described in the following paragraphs. Detailed data analysis and calculations of respective parameters are described in section 2.7.3.

To construct **saturation binding** isotherms, which allow calculation of radioligand affinity in terms of the dissociation constant (K_d), increasing concentrations of [^3H]-GLPG0974 were incubated with 5 μg of membrane protein for 2 h followed by filtration and quantification. For data analysis, specific binding was plotted against quantified [^3H]-GLPG0974 concentrations.

Competition binding assays are a valuable tool for calculation of unlabelled ligand affinity in terms of K_i by assessing their ability to displace the radioligand from the receptor. To perform such an assay, [^3H]-GLPG0974 at K_d concentration and increasing concentrations of unlabelled ligand of choice were co-added to 5 μg of membrane protein. The reactions were incubated for 2 h and processed following standard protocol. To analyse the resulting data, specific binding was plotted against unlabelled ligand concentrations and [^3H]-GLPG0974 concentration to be displaced was quantified.

Dissociation and association **kinetic binding** assays were performed using a reverse time protocol. To measure radioligand **dissociation** [^3H]-GLPG0974 at K_d concentration was incubated with 5 μg of membrane protein for 1 h to allow pre-association of the radioligand with the receptor. To induce radioligand dissociation two different approaches were employed. Either 10 μM CATPB was added to monitor displacement of [^3H]-GLPG0974 by competition (standard procedure) or an “infinite dilution” approach was used, in which the reaction mixture was scaled down to 100 μL and diluted 70-fold. This was performed in a time-staggered fashion to capture time points between 5 and 240 min. For determination of **association** kinetics, [^3H]-GLPG0974 was added to 5 μg membrane protein in a time-staggered protocol to measure 5-240 min time points. For both kinetic binding assays filters were processed simultaneously, while measuring the time required per filter to correct for increased incubation time, and processed according to standard protocol. Before data analysis, specific binding was plotted against time and for association kinetics calculations, the employed [^3H]-GLPG0974 concentration was quantified.

Competitive kinetic binding assays can be employed to determine the kinetic binding parameters of unlabelled ligands by assessing radioligand association in presence of different concentration of competing ligands (Dowling and Charlton, 2006). Three concentrations of competing ligand at 1-, 3-, and 10-fold K_i were

co-added with a K_d concentration of [^3H]-GLPG0974 and 5 μg of membrane protein was added at indicated time points. As in the case of regular kinetic binding assays, specific radioligand binding was plotted against time for data analysis.

2.4.5 BRET-based binding assay

The BRET-based binding assay was developed to measure binding of fluorescent ligands to FFA2 tagged N-terminally with NLuc. This approach has already been successfully applied previously (Christiansen et al., 2016) and the described approach has been followed. This technique combines features of radioligand binding assays (see section 2.4.4) with BRET-based methodology (see section 2.5.4). The underlying mechanism of the binding assay itself will be described in detail in chapter 5 and this section aims to outline the experimental procedures. For data analysis the BRET ratio was calculated, which corresponds to division of emission at 545 nm (substrate emission wavelength) by 460 nm (NLuc emission wavelength). Apart from the data processing, the underlying approach to measuring saturation, competition and kinetic binding is identical to the radioligand binding, therefore the following paragraphs will briefly highlight differences in experimental setup and detection.

For **equilibrium BRET binding** assays, which include saturation and competition binding, membrane protein was suspended in binding buffer and transferred into a white 96-well plate at 2.5 μg membrane protein/well. The reaction was performed in a total volume of 100 μL and respective reagents were added at 10 μL /well. Fluorescent ligand was added at increasing concentrations for saturation binding, or K_d concentration for competition binding in presence of increasing concentrations of unlabelled ligand. Nonspecific binding was determined by addition of an appropriate competitive unlabelled ligand, in an optimal case a fluorescent ligand analogue without attached fluorophore, at fully displacing concentration. Incubations were performed at 30°C for 2 h in a gently shaking incubator at 50 rpm. Following incubation, the Nano-Glo® Luciferase Assay Substrate (Promega) was added at a final dilution of 1:800 and after a further 5 min incubation bioluminescent emission at 460 and 545 nm was measured using a CLARIOstar Plate Reader (BMG LABTECH). The resulting specific BRET ratio (nonspecific signal subtracted from total signal) was plotted

against fluorescent ligand concentration or displacing unlabelled ligand concentration.

For **kinetic BRET binding** assays, cell membranes were distributed in white 96-well microplates at 2.5 μg membrane protein/well, as before. The substrate was then added (1:800 final dilution) and after incubation for 5 min at 30°C, plates were inserted into a CLARIOstar Plate Reader, with temperature set to 30 °C. Emission at 460 and 545 nm was then measured at 90 s intervals. For **association** experiments, fluorescent ligand was added manually to the plate after 60 s of measurement to a final concentration of 100, 300, 500, or 1000 nM. Measurement was resumed and continued at 90 s intervals for the indicated time period. For **dissociation** experiments, the reaction was incubated for 2 h at 30°C followed by two washes with binding buffer, including centrifugation at 20,000 $\times g$ at 4°C for 15 min, to induce fluorescent ligand dissociation. The membrane pellet was then resuspended in binding buffer pre-warmed to 37°C, transferred into a white 96-well microplate at 90 μL /well and after pre-incubation with substrate for 5 min at 30°C, emission at 460 and 545 nm was measured as before at 90 s intervals. In all kinetic experiments, nonspecific binding was assessed in parallel by preparing wells with pre-added competing unlabelled ligand at fully displacing concentration. Kinetic binding data were then plotted as specific BRET ratio against time.

Competitive kinetic binding assays were also performed using the BRET-based binding system. Membrane protein was pre-incubated for 5 min with substrate, in this case coelenterazine h (Nanolight Tech), followed by simultaneous addition of a K_d concentration of fluorescent ligand and three different concentrations of competing unlabelled ligand, namely 1-, 3-, or 10-fold of K_i , were added simultaneously. As in the case of other kinetic assays, readings were then continued at 90 s intervals for 60 min and the specific BRET ratio was plotted against time for data analysis.

2.5 Cell-based assays

2.5.1 IP1 accumulation assay

To measure G_q G protein-induced production of IP1 an IP-One Tb kit (Cisbio Bioassays) was used, which is based on detection of homogeneous time-resolved FRET (fluorescence resonance energy transfer) or HTRF, according to manufacturer's instruction. Briefly, Flp-In™ T-REx™ cells were plated in culture vessels of appropriate size and treated with 100 ng/mL doxycycline for 16-24 h to induce expression of receptor of interest. Test compounds were prepared in provided IP1 Stimulation Buffer (10 mM HEPES, 1 mM CaCl₂, 0.5 mM MgCl₂, 4.2 mM KCl, 146 mM NaCl, 5.5 mM glucose and 50 mM LiCl 50 mM at pH 7.4), which includes LiCl to prevent degradation of IP1, at 2 x final concentration and 7 µL were added to white low-volume 384-well plates according to the desired plate layout. In addition, an IP1 standard curve with final concentrations of 11 to 11,000 nM was prepared and added at 14 µL/well. Cells were counted in HBSS (Hank's Balanced Salt Solution: 137 mM NaCl, 5.3 mM KCl, 0.34 mM Na₂HPO₄, 0.44 mM KH₂PO₄, 4 mM NaHCO₃, 1.26 mM CaCl₂, 0.5 mM MgCl₂ and 0.4 mM MgSO₄ at pH 7.3) and an appropriate volume was centrifuged at 300 x g for 5 min, followed by resuspension in IP1 Stimulation Buffer and addition of 7 µL of cell suspension to test compounds resulting in a concentration of 7,500 cells/well. For testing of agonists, cells were incubated with test compound for 2 h at 37°C. To assess ability of antagonists to inhibit agonist responses, cells were incubated with 3.5 µL of test compound per well for 30 min at 37°C prior to addition of an EC₈₀ concentration of agonist at 3.5 µL/well, followed by a 2 h incubation at 37°C. Prepared antagonist and agonist test compound concentrations were adjusted accordingly to the increased dilution factor. To terminate the reaction and enable measurement of accumulated IP1, synthetic IP1 coupled to dye d2 and an anti-IP1 antibody labelled with Lumi4™-Tb cryptate were employed. The FRET reaction takes place between Lumi4™-Tb cryptate and dye d2, therefore competition between d2-labelled IP1 and IP1 produced in response to test compounds results in reduction of the FRET signal with increasing concentration of produced IP1. Both reagents were diluted as instructed (1:20) and added in cell lysis buffer at 3 µL/well. As a negative control, lysis buffer instead of d2-labelled IP1 was added to a selected triplicate of wells. Plates were

incubated for 1 h at RT and then fluorescence at 620 (Lumi4TM-Tb cryptate) and 665 nm (dye d2) and was quantified using a PHERAstar FS plate reader.

For data analysis, the ratio of fluorescence at 665 over 620 nm was calculated for sample wells and the negative control ($Ratio_{neg}$). To correct for basal fluorescence, the Delta F was calculated using the following formula:

$$\Delta F = \frac{Ratio_{standard\ or\ sample} - Ratio_{neg}}{Ratio_{neg}} \times 100$$

The concentration of IP1 in sample wells was then interpolated from the sigmoidal IP1 standard curve and plotted as concentration of IP1 in nM against tested compound concentrations on a logarithmic scale.

2.5.2 cAMP inhibition assay

To measure G_i G protein-mediated inhibition of cyclic adenosine monophosphate (cAMP) production, the cAMP Dynamic 2 kit (Cisbio Bioassays) was employed, which uses an equivalent technology and approach to the IP-One Tb kit described in section 2.5.1, and was performed according to manufacturer's instructions. Due to the similarity to the IP-One TB kit, significant differences in procedure are described briefly below. Doxycycline-inducible cells were prepared a day prior to the experiment as for the IP1 assay. Test compounds were diluted in HBSS with 500 nM IBMX (3-isobutyl-1-methylxanthine), which induces cAMP accumulation by inhibiting phosphodiesterase-mediated degradation, at 2 x final concentration and added to a white low-volume 384-well plate at 5 µL/well. Additionally, a cAMP standard curve was also prepared with concentrations ranging from 0.17 to 712 nM and added to the plate at 5 µL/well. Cells were counted in HBSS and diluted to a concentration of 400,000 cells/mL in HBSS with 2 µM forskolin, which non-specifically activates adenylyl cyclase and thereby induces cAMP production. The cell suspension was then added to the plate at 5 µL/well, thereby reaching a final concentration of 2,000 cells/well. For testing of agonists, cells were incubated with test compounds for 30 min at RT. As in the case of the IP1 assay, antagonists were pre-incubated with stimulated cells at 2.5 µL/well for 30 min at RT prior to addition of 2.5 µL agonist per well. Again, agonist and antagonist concentrations

were adjusted according to the increased dilution factor. The stimulation was terminated by addition of anti-cAMP antibody labelled with Eu^{3+} cryptate and synthetic cAMP conjugated to dye d2 in lysis buffer at 5 μL /well. The assay mechanism is equivalent to IP1 detection, with Eu^{3+} cryptate acting as the FRET donor and cAMP-d2 as the acceptor. Plates were incubated for 1 h at RT, followed by a fluorescence measurement at 620 (Eu^{3+} cryptate) and 665 nm (dye d2) using the PHERAstar FS plate reader. For data analysis the resulting FRET ratio was analysed in the same fashion as described for the IP1 assay to calculate the concentration of cAMP per well. As FFA2 is a G_i -coupled receptor and therefore has a negative effect on cAMP production, data was plotted as inhibition of the basal cAMP level as follows:

$$\text{Inhibition (\%)} = \frac{cAMP_{\text{basal}} - cAMP_{\text{sample}}}{cAMP_{\text{basal}}} \times 100$$

The inhibition of the basal cAMP level in percent was then plotted against test compound concentrations on a logarithmic scale for further data analysis.

2.5.3 ERK phosphorylation assay

To detect the phosphorylation of ERK1/2 a Phospho-ERK1/2 kit (Cisbio Bioassays) was used, which uses an equivalent approach to the IP-One Tb (see section 2.5.1) and cAMP Dynamic 2 (see section 2.5.2) kits and was performed according to manufacturer's instructions. Briefly, Flp-In™ T-REx™ cells were plated in culture vessels of appropriate size and treated with 100 ng/mL doxycycline for 16-24 h to induce expression of the receptor of interest. Antagonist compounds were prepared in HBBS at 6 x final concentration and 2 μL were added to white low-volume 384-well plates according to the desired plate layout. Cells were counted in HBSS and diluted to a concentration of 1,875,000 cells/mL and 8 μL /well were added to test compounds resulting in a concentration of 15,000 cells/well. Cells were incubated with antagonist compounds for 1 h at 37°C, followed by addition of 2 μL of a 6 x final concentration of agonist compounds and a further incubation for 30 min at 37°C. Cell lysis buffer was prepared by diluting the blocking reagent stock solution 25-fold with 4 x lysis buffer. To terminate the reaction, 4 μL of supplemented lysis buffer was added per well and the plate was incubated for 30 min at RT under shaking. A 1:1

solution of two anti-pERK (phosphorylated ERK) antibodies, one labelled with Eu^{3+} cryptate and the other conjugated to dye d2, was prepared in detection buffer and added at 4 μL /well to lysed cells. The antibodies bind to different epitopes of pERK and the donor Eu^{3+} cryptate triggers FRET towards the acceptor dye d2 when in close proximity, therefore the FRET signal increases with stimulation of ERK phosphorylation. Plates were incubated for 2 h at RT and then fluorescence at 620 (Eu^{3+} cryptate) and 665 nm (dye d2) and was quantified using a PHERAstar FS plate reader. For data analysis, the ratio of fluorescence at 665 over 620 nm was calculated for sample wells and plotted against the logarithm of agonist compound concentrations.

2.5.4 BRET-based β -arrestin recruitment assay

The BRET-based β -arrestin recruitment assay measures the interaction of RLuc-tagged β -arrestin with a receptor fused with eYFP at its C terminus. In presence of its substrate, RLuc acts as a BRET donor by emitting light at a wavelength that is able to excite the BRET acceptor eYFP, if in close enough proximity. HEK293T cells were co-transfected in 10 cm dishes at a 4:1 ratio with plasmids encoding an eYFP-tagged receptor and RLuc-tagged β -arrestin 2, using PEI as a transfection reagent (see section 2.3.2). For data analysis the BRET donor luminescence in absence of its acceptor is required (RLuc only control), therefore one 10 cm dish was transfected with RLuc-tagged β -arrestin 2 and pcDNA3.1 instead of eYFP-tagged receptor. After incubating transfected cells for 24 h, they were detached as described in section 2.3.1, resuspended in 20 mL media and added at 100 μL /well to white 96-well plates. Prior to addition of cells, the plates were coated with poly-D-lysine to facilitate cell attachment by preparing a 50 $\mu\text{g}/\text{mL}$ solution of poly-D-lysine hydrobromide (Sigma-Aldrich) in cell culture medium from a 1 mg/mL stock solution, which was added at 40 μL /well, and coated plates were incubated at RT for a minimum of 15 min. At 48 h post-transfection, cells were washed and the culture medium was replaced with 70 or 80 μL HBSS depending on further additions to reach a final volume of 100 μL , allowing cells to equilibrate for a minimum of 30 min at 37°C prior to conducting the assay. Test compounds were prepared in HBSS at 10 x final concentration and added to the plate at respective time points at 10 μL /well. To investigate agonist activation, test compounds were added for 5 min at 37°C prior to measurement. For assessment of the inhibitory ability of antagonists,

cells were pre-incubated with test compounds for 15 min at 37°C before addition of an EC₈₀ concentration of agonist. To measure β -arrestin 2 recruitment, 10 μ L of the RLuc substrate coelenterazine h was added per well to a final concentration of 2.5 μ M at a time point 15 min prior to measurement. The luminescence resulting from BRET between β -arrestin 2-RLuc and FFA2-eYFP was assessed by measuring luminescence at 535 (eYFP) and 475 nm (RLuc) using a PHERAstar FS plate reader. The BRET ratio was calculated by dividing luminescence at 535 nm by luminescence at 475 nm, subtracted by the BRET ratio of the RLuc only control and multiplied by 1000 to calculate mBRET values. For data analysis, mBRET values were plotted against test compound concentrations on a logarithmic scale.

2.5.5 TGF α shedding assay

For a standard TGF α shedding assay, a mixture of 250 ng alkaline phosphatase (AP)-tagged TGF α and 100 ng receptor of interest plasmids were transfected using PEI into one well of HEK293A cells cultured in a 12-well plate. Depending on the experimental aim, 50 ng of G α plasmid was co-transfected with the AP-TGF α and receptor plasmids. If a larger number of cells was required, quantities were increased according to surface of culture vessel. After 24 h incubation transfected cells were washed with PBS and detached by adding 200 μ L 0.05% trypsin-EDTA. The proteolytic cleavage was inhibited by addition of 300 μ L culture medium and cell suspension was centrifuged at 190 x g for 5 min. The cell pellet was resuspended in 3.5 mL HBSS+H (HBSS with 5 mM HEPES at pH 7.4) and incubated for 15 min at RT to allow for equilibration of cells. After a second centrifugation at 190 x g for 5 min, pelleted cells were resuspended in 3.5 mL HBSS+H per well (for a 12-well plate). The cell suspensions were plated at 90 μ L per well in a clear 96-well plate and incubated at 37°C with 5% CO₂ for 30 minutes. During the equilibration period test compounds were prepared at 10 x final concentration in HBSS with 0.01% (w/v) fatty acid-free BSA. To stimulate TGF α shedding, compounds were added to cells at 10 μ L/well and incubated for 1 h at 37°C with 5% CO₂. Plates were then centrifuged at 190 x g for 2 min and 80 μ L of supernatant was transferred into another clear 96-well plate using a multichannel pipette. To quantify the amount of AP-TGF α , a solution containing its substrate, p-nitrophenyl phosphate (10 mM p-NPP, 40 mM Tris-HCl (pH 9.5), 40 mM NaCl and 10 mM MgCl₂), was added at 80 μ L per well into plates

containing only medium or cells. Absorbance at 405 nm of both plates was read before and after a 2 h incubation at 37°C using a VersaMax microplate reader (Molecular Devices) or a POLARstar Omega plate reader.

The specific alkaline phosphatase activity was calculated by subtracting the absorbance measured at 0 h from the absorbance measured at the 2 h time point for conditioned medium and cell plates. To calculate the percentage of total AP-TGF α shed into the medium the following formula was employed, which also corrects for the different volumes in conditioned medium (CM) and cell (C) plates.

$$Shedding_{CM} (\%) = \frac{AP_{CM}}{AP_{CM} + AP_C} \times 125$$

The data was baseline-corrected by subtracting the basal level of shedding in vehicle-treated wells from shedding in compound-treated wells and plotted against test compound concentrations on a logarithmic scale.

2.6 Structural studies

2.6.1 Homology modelling

All structural studies were performed by Dr Hansen within Professor Ulven's laboratory group in the Department of Physics, Chemistry and Pharmacy at the University of Southern Denmark. The following sections aim to provide a short summary of the software and methodology employed to construct homology models discussed in this thesis to serve as a reference for future modelling efforts.

The hFFA2 homology model was generated by using the crystal structure of the hFFA1 receptor (PDB ID: 4PHU) as a template (Srivastava et al., 2014). Manual alignment was performed with the SeaView software (Gouy et al., 2010). Initially, the T4 lysozyme fusion protein fused into ICL3 of hFFA1 for enhanced crystallisation potential was deleted. The final template was optimized using the Protein Preparation Wizard programme (Schrödinger, LLC) in which bond orders and partial charges were assigned, hydrogen atoms added, and water molecules deleted. Hydrogen bond assignment was generated at pH 7.0 using PROPKA

software (Olsson et al., 2011). Restrained minimization until heavy atoms converged to a root mean square deviation of 0.3 Å was executed using the OPLS-2005 force field (Banks et al., 2005). The homology models of hFFA2, mFFA2 and respective mutant receptors were constructed using the homology modelling module within the Prime software package (Schrödinger, LLC). Final models were subjected to restrained minimization using OPLS-2005 force field in Protein Preparation Wizard.

2.6.2 Ligand docking

One important function of homology models is the prediction of ligand binding modes to the respective receptors. Ligands were prepared for docking by using the OPLS-2005 force field in LigPrep (Schrödinger, LLC) and ionization states were predicted using Epik at pH 7.0 ± 2.0 (Schrödinger, LLC). Induced-fit docking was performed using the IFD 2006 protocol using Glide and Prime software (Schrödinger, LLC). Depending on the binding site under investigation, residues within 3 Å of each docked ligand were defined as potential interacting residues and were initially refined during ligand docking. In certain cases, selected residues of interest were not included in the refinement, based on crucial interactions observed in the hFFA1 template structure. During ligand conformational sampling and docking in Glide, default settings were employed and a maximum number of 20 poses per ligand were allowed. The protein-ligand complexes were ranked to determine the five models with lowest energy complexes, which were then re-docked in standard precision mode, and residue refinement was set within 5 Å of each ligand.

2.7 Data analysis

All data are presented as mean \pm SEM of at least three independent experiments unless stated otherwise. For data and statistical analysis, the GraphPad Prism software package version 5.02 (GraphPad) was employed. Below, curve fitting and calculations for different experimental aims are outlined briefly and include models in GraphPad Prism software used for analysis.

2.7.1 Analysis of functional agonist and antagonist assays

Agonist and antagonist response curves both follow sigmoidal functions and data are fit accordingly, which allows for calculation of the pharmacological parameters of respective ligands. In both cases the slope of the sigmoidal curve (Hill slope) was restricted to equal unity, which would be expected when a ligand binds to a receptor following the law of mass action. This constrain improves the quality of the fit in cases of modest data quality and restricted number of data points. In most cases, experiments were designed to test seven concentrations of test compounds and one vehicle control, which was plotted one log unit lower than the lowest concentration of test compound.

For **agonist** ligands, the following formula was employed to fit such a three-parameter sigmoidal curves by nonlinear regression analysis. It allows calculation of the bottom and top asymptotes of the curve with the top asymptote representing the maximal response E_{max} , a means of determining agonist efficacy. Most importantly, agonist potency in terms of EC_{50} can be determined from the $\log EC_{50}$, which corresponds to the agonist concentration required to induce a half-maximal response. As curves were generated from semi-logarithmic plots and parametric tests were employed for statistical analysis, agonist potency was presented and analysed in terms of pEC_{50} , the negative logarithm of the EC_{50} , which is normally distributed.

$$Response (Y) = Bottom + \frac{Top - Bottom}{1 + 10^{LogEC_{50} - [Ligand] (X)}}$$

For **antagonist** ligands, an equivalent formula was employed to fit the inhibition curve to calculate IC_{50} values rather than EC_{50} values, which equals the concentration of antagonist required to reduce the agonist response by half. As in case of agonist ligands, data were presented and analysed in terms of pIC_{50} .

2.7.2 Global Gaddum/Schild analysis

To investigate whether an antagonist ligand is competitive, and therefore likely orthosteric, or non-competitive, and hence likely allosteric, with orthosteric agonists, the effect of a constant concentration of antagonist on the agonist concentration response was investigated. By performing such an experiment with

at least three concentrations of antagonist, the Schild model can be applied to the resulting set of curves, if the antagonist behaves in a competitive manner (Colquhoun, 2007). The underlying pharmacological principles and possible interpretations will be discussed in more detail in chapter 3. The following set of formulas is employed by GraphPad Prism to fit a set of antagonist-treated agonist response curves.

$$Response (Y) = \frac{Top - Bottom}{1 + 10^{\left(\left(\log \left(10^{LogEC_{50}} \times \left(1 + \frac{[Antagonist]^{Schild\ slope}}{10^{-1 \times pA_2}} \right) \right) \right) \right) \times Hill\ slope}}$$

This model generates a global fit of the set of curves to provide top and bottom asymptote fits and calculate the EC₅₀ of the agonist in absence of the antagonist. The Hill slope is commonly constrained to unity for reasons described in section 2.7.1, while the Schild slope indicates how well the shift induced by the antagonist corresponds to the competitive inhibition model and would equal unity in a perfect case. The pA₂ corresponds to the negative logarithm of the antagonist concentration required to induce a shift of the agonist response curve by a factor of 2 and provides a measure of antagonist affinity for the receptor if Hill and Schild slope are close to unity.

2.7.3 Analysis of binding parameters

Binding studies can provide important pharmacological parameters and allow the direct measurement of affinity for labelled and unlabelled ligands. In this thesis both radioligand (section 2.4.4) and fluorescent binding (section 2.4.5) studies have been employed and despite the different methodology underlying these approaches, the data analysis of binding parameters is identical, as the resulting data represents ligand binding to the receptor.

The **saturation binding** assay assesses the specific binding of a labelled ligand (probe) at increasing ligand concentrations. The resulting curve follows a rectangular hyperbola, also known as the Michaelis-Menten equation, which was initially defined to measure the activity of an enzyme as a function of substrate concentration. In the context of radioligand binding, the maximum specific binding in terms of B_{max} can be calculated and corresponds to receptor

expression in membranes if the specific binding is plotted in units such as fmol/mg. In the case of BRET binding assays, the B_{max} is dependent on the nature of the BRET reaction such as the distance between donor and acceptor. Furthermore, the equilibrium binding constant K_d is calculated and corresponds to the concentration of ligand required to occupy half of all receptor sites, which serves as a measure of ligand affinity. The following equation is used to determine the described parameters.

$$\text{Specific binding } (Y) = \frac{B_{max} \times [Probe](X)}{K_d + [Probe](X)}$$

The **competition binding** assay is an important tool for determining the affinity of unlabelled ligands. Essentially, the displacement curve of the radioligand by the unlabelled competing ligand is fit to an inverse sigmoidal curve in a similar fashion to antagonist inhibition curves from which an IC_{50} can be calculated. However, as the affinity and exact concentration of the displaced labelled ligand is known, a model can be applied which allows calculation of unlabelled ligand affinity in terms of K_i as described in the formulas below. It is important to consider that this value is only an accurate representation of unlabelled ligand affinity if the competing and labelled ligand are truly competitive.

$$\text{Specific binding } (Y) = \text{Bottom} + \frac{\text{Top} - \text{Bottom}}{1 + 10^{[Competitor](X) - \text{Log}\left(10^{\text{Log}K_i} \times \frac{1 + [Probe]}{K_d}\right)}}$$

In **kinetic binding** assays labelled ligand association and dissociation curves fit a simple one phase exponential association or decay, respectively. However, to calculate the association rate K_{on} ($M^{-1} \text{ min}^{-1}$) and dissociation rate K_{off} (min^{-1}) the curves need to be analysed with specific models. In the case of **dissociation** the model is relatively simple, as it can be calculated independently of labelled ligand concentration and affinity. The model requires the nonspecific (NS) binding, which will be constant throughout the experiment, and the rate constant K , which equals the \ln of 2 (0.693) divided by the half-life.

$$\text{Specific binding } (Y) = (Y_{0h} - NS) \times e^{-K \times \text{Time}(X)} + NS$$

The **association** model is significantly more complicated, as it depends on the employed labelled ligand concentration (L), and the ligand K_{off} must be known. Once both dissociation and association constants have been determined, the K_d can be calculated by dividing the K_{off} by the K_{on} , which provides a further means of K_d determination in addition to saturation binding assays.

$$\text{Specific binding } (Y) = \frac{L}{L + K_d} \times B_{max} \times (1 - e^{-1 \times (K_{on} \times L + K_{off}) \times \text{Time}(x)})$$

To determine the kinetic parameters of unlabelled ligands by using the **competitive kinetic** binding assay (Dowling and Charlton, 2006), the K_{on} (K_1) and K_{off} (K_2) of the labelled ligand must be known as well as the concentration of labelled ligand (L) and unlabelled ligand (I). By employing the model outlined below the unlabelled ligand K_{on} (K_3) and K_{off} (K_4) can then be calculated. To allow for a better overview, the complete model (7) was broken down into separate equations (1-6), defining respective factors.

$$(1) K_A = K_1 \times L + K_2$$

$$(2) K_B = K_3 \times I + K_4$$

$$(3) S = \sqrt{((K_A - K_B)^2 + 4 \times K_1 \times K_3 \times L \times I)}$$

$$(4) K_F = 0.5 \times (K_A + K_B + S)$$

$$(5) K_S = 0.5 \times (K_A + K_B - S)$$

$$(6) Q = \frac{B_{max} \times K_1 \times L}{K_F - K_S}$$

$$(7) Y = Q \times \left(\frac{K_4 \times (K_F - K_S)}{K_F \times K_S} + \frac{K_4 - K_F}{K_F} \times e^{-K_F \times X} - \frac{K_4 - K_S}{K_S} \times e^{-K_S \times X} \right)$$

2.7.4 Calculation of signalling bias

Studies described in chapter 6 focus on mutations of hFFA2 that appear to induce receptor signalling bias. To quantify this signalling bias the bias factor β

was calculated by determining the logarithm of the ratio of relative intrinsic activities for a ligand at two different assays (Rajagopal et al., 2011). This approach is relatively simple compared to the use of an operational model and requires only EC_{50} and E_{max} values of the ligands in two pathways to be compared at wild type and mutant receptors. The underlying reason for choosing such an equiactive comparison over equimolar comparison and the operational model will be discussed in section 6.2.5. Typically, such calculations assess signalling of a ligand of interest in comparison to a reference endogenous agonist, but in this case the response of the agonist at the wild type receptor serves as the reference to calculate the effect on the signalling bias induced by respective mutations using the following equation.

$$\beta = \text{Log} \left(\left(\frac{E_{\max(P1)} EC_{50(P2)}}{EC_{50(P1)} E_{\max(P2)}} \right)_{WT} \times \left(\frac{E_{\max(P2)} EC_{50(P1)}}{EC_{50(P2)} E_{\max(P1)}} \right)_{Mutant} \right)$$

2.7.5 Statistical analysis

Graphpad Prism software was employed to perform statistical analyses. As data were assumed to be normally distributed, pharmacological parameters of different ligands or altered forms of a receptor were compared using appropriate parametric tests: Two-tailed unpaired Student's t test for two groups, or one-way analysis of variance (ANOVA) for three or more groups followed by a Tukey's or Dunnett's post-test, which gives more power to detect differences due to consideration of scatter among the analysed groups (McHugh, 2011). Tukey's post-test was used to compare all means to one another, while Dunnett's post-test was employed to compare means to a reference mean, such as data generated at the wild type receptor. Analyses were performed on data with at least three biological replicates, representing independent experiments carried out on separate occasions with cells of different passage number, and a P value of <0.05 was considered statistically significant. However, due to the highlighted limitations of insufficient n numbers and P values (Lew, 2012), differences supported by P values above 0.01 were treated with caution and scientific conclusions were always drawn in conjunction with data generated by alternative means such as homology modelling or by demonstrating the same trends in different assay systems that represent the same signalling pathways. Furthermore, data were exclusively generated in recombinant cell line systems

and no studies using primary cells or animals were performed, which inherently display increased variability. Therefore, an n of 3 was deemed sufficient to allow statistical analysis and ensure reproducibility of generated data.

3 Exploring the structure-activity relationships of FFA2 agonists and antagonists

3.1 Introduction

As discussed in section 1.1.2, selection of an appropriate assay system to test ligands for potential therapeutic targets such as GPCRs is an important step in the drug discovery process and may play a role in target validation as well as in screening for hit and lead compounds. Radioligand binding assays are a popular choice, if there is a radioactive probe available for the receptor of interest, as these can be performed in a high-throughput, cell-free system with membranes isolated from, in the case of ligand screening, cells artificially overexpressing the receptor of interest (Bylund and Toews, 1993). While radioligand binding assays are invaluable tools for investigation of ligand binding pockets and screening for compounds binding to specific sites, they do not provide mechanistic information directly, for example whether a ligand is an agonist or antagonist. Therefore, functional assays that detect GPCR signalling are usually employed either in conjunction with radioligand binding studies or after identification of high-affinity ligands (Thomsen et al., 2005). For GPCRs that signal by coupling to only one G protein subtype, the selection of an appropriate functional screening system is relatively straightforward. Most G proteins affect production of specific secondary messengers in a positive or negative fashion, which can be detected using a range of approaches. Such platforms utilise second messenger-sensitive proteins such as aequorin, which detects $G_{q/11}$ activation by producing bioluminescence in the presence of its substrate in response to calcium ions (Stables et al., 2000), or HTRF-based detection of downstream products of GPCR activation such as IP1 ($G_{q/11}$), cAMP (elevated by G_s and inhibited by $G_{i/o}$) or phosphorylated ERK1/2 (Norskov-Lauritsen et al., 2014). Phosphorylation of ERK1/2 can occur in response to activation of multiple G protein subtypes, including G_s , $G_{i/o}$ and $G_{q/11}$ (Leroy et al., 2007), and β -arrestin-mediated signalling (Lefkowitz and Shenoy, 2005). The [35 S]-GTP γ S binding assay is a more direct means of measuring G protein recruitment, in particular of the $G_{i/o}$ subfamily, due to its high rates of basal guanine nucleotide exchange (Milligan, 2003). GTP γ S is a poorly-hydrolysable analogue of GTP and remains bound to the $G\alpha$ protein after the release of GDP and binding of this analogue of GTP has been facilitated by an actively signalling GPCR. Labelling of

the GTP γ S molecule with the radioactive isotope [³⁵S] allows monitoring of its incorporation into G proteins by liquid scintillation spectrometry. Alternatively, to achieve a higher throughput and eliminate the filtration step necessary for [³⁵S]-GTP γ S binding assays, scintillation proximity assays can be performed, in which a primary anti-G α antibody is employed that is captured by anti-IgG antibody-coated scintillant-containing beads (DeLapp, 2004).

Detection of an interaction between a GPCR and β -arrestin can serve as an alternative screening approach to the measurement of G protein-dependent signalling. Although β -arrestins play an increasingly important role in mediating G protein-independent signalling of a selection of GPCRs, the recruitment of β -arrestin itself is an essential component of GPCR desensitisation and the majority of GPCRs interact with β -arrestin 1 and/or 2 (DeWire et al., 2007). Therefore, β -arrestin recruitment conceptually represents a more universal pathway that can be of particular value when developing a screening system for poorly characterised receptors, where G protein coupling is not yet fully understood (Oakley et al., 2006, Southern et al., 2013). Methods to monitor the interaction of β -arrestins with GPCRs have developed significantly over the last decade and include proximity-based systems that utilise BRET methodology using a *Renilla reniformis* luciferase (RLuc)-tagged receptor serving as a BRET donor and a fluorescent protein-tagged β -arrestin as BRET acceptor (Kocan et al., 2010). Another example of a commonly employed β -arrestin recruitment assay in the drug discovery industry is the PathHunter™ assay developed by DiscoverX (Zhao et al., 2008), which is based on an enzyme fragment complementation approach. A catalytically inactive N-terminal deletion mutant of the β -galactosidase enzyme is fused to β -arrestin and is complemented by a GPCR tagged with the respective deleted N-terminal β -galactosidase sequence. Both components of the β -galactosidase are brought into proximity by the GPCR- β -arrestin interaction, thereby regenerating the enzyme and producing a chemiluminescent signal upon cleavage of a suitable substrate.

Considering the variety of different assay systems available for screening of ligands at GPCRs, the selection of an appropriate assay for promiscuous receptors such as FFA2, which couples to multiple G proteins, can be challenging. FFA2 has been shown to couple to G_{q/11}, G_{i/o} and G_{12/13} G α subtypes

(Brown et al., 2003) and recruitment of β -arrestin 2 in response to agonist treatment has also been demonstrated (Hudson et al., 2013a). However, due to the lack of availability of a labelled probe, the affinity of endogenous and synthetic FFA2 ligands remains to be determined. Understanding the structure-activity relationship (SAR) of synthetic ligands can be an important step in drug development, as it provides information on how specific structural modifications in a molecule correlate with changes in pharmacological action. However, relying on functional potency data alone to define the SAR of compound series can be problematic and does not always yield conclusive data. An investigation of the SAR of the compound 1 FFA2 agonist series identified analogues which had diverse effects in $G_{i/o}$ -coupled assays, with a selection of ligands showing agonism in [^{35}S]-GTP γ S binding assays, but inverse agonism in a yeast-based $G_{i/o}$ coupling assay (Brown et al., 2015). As outlined in section 1.2.4, functional studies require additional considerations such as the level of receptor reserve in the respective systems employed and the extent of signal amplification underlying the measurement.

This chapter aims to assess functional assay systems available for FFA2, including $G_{i/o}$ -coupled [^{35}S]-GTP γ S binding and cAMP inhibition, $G_{q/11}$ -coupled IP1 accumulation and BRET-based β -arrestin 2 recruitment. To investigate how potency values correlate with binding affinity, a direct binding assay was developed based on a tritiated form of GLPG0974 recently obtained from a collaboration with AstraZeneca. The endogenous SCFA C3, the synthetic agonist compound 1 and the two synthetic antagonists CATPB and GLPG0974 served as reference ligands for initial characterisation of the respective assays (**Figure 3.1**). Following this initial assessment, a detailed SAR analysis of compound 2 (**Figure 3.1**), an FFA2 agonist recently used in an *in vivo* study in mice to investigate the role of FFA2 in gut health and obesity (Forbes et al., 2015), was performed and employed for a more extensive evaluation of functional versus binding assays for ligand screening at FFA2. In addition to the investigation of FFA2 agonists, the pharmacology of the antagonist GLPG0974 in comparison to CATPB was also explored in selected assay systems. From an SAR perspective, it is not clear whether the carboxylate moiety typical of orthosteric FFA2 agonist ligands (**Figure 3.1**) is also required for the action of FFA2 antagonist series.

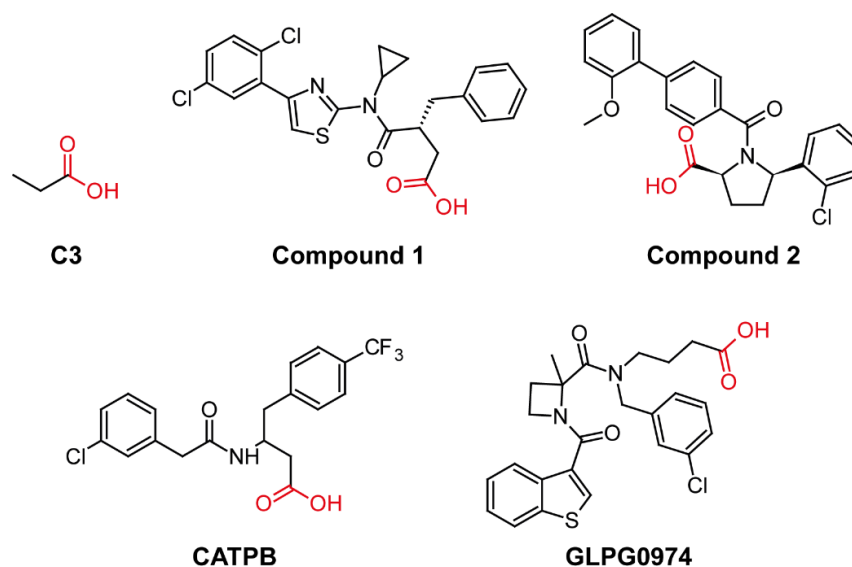


Figure 3.1 FFA2 reference compounds Chemical structures are shown with the carboxyl moiety highlighted in red. C3 and compounds 1 and 2 act as agonists at FFA2, while CATPB and GLPG0974 are antagonists.

Therefore, the effect of different modifications in this position on the functional inhibition of hFFA2 responses to agonists was investigated. The overarching purpose of the work described in this chapter is to provide an introductory overview of the complex pharmacology of FFA2 and its ligands and serve as a guide for future assay selection and development.

3.2 Results

3.2.1 Selection of assay systems to screen FFA2 ligands

To expand the available repertoire of FFA2 ligand screening systems, a radioligand binding assay was developed using a tritiated form of GLPG0974. Kinetic binding studies in membranes isolated from Flp-In™ T-REX™ 293 cells induced to express hFFA2-eYFP were performed to determine the rate of association and dissociation of [³H]-GLPG0974, which is necessary to define the time required to reach equilibrium binding. To measure radioligand dissociation, 10 μM of antagonist CATPB, which originates from a distinct chemical series of FFA2 antagonists, was added to membranes with 10 nM of pre-associated [³H]-GLPG0974. The presence of an excess of competing ligand prevents the rebinding of [³H]-GLPG0974 to the receptor and allows monitoring of its dissociation. The ability of CATPB to compete with [³H]-GLPG0974 to the same level as 10 μM of GLPG0974, which was used to determine levels of nonspecific

binding, suggests that these ligands bind to the same site and allows the use of CATPB as a competing ligand in dissociation studies (Hulme and Trevethick, 2010). The determined K_{off} at 25 °C was $0.014 \pm 0.001 \text{ min}^{-1}$, which corresponds to a half-time of 70 min (Figure 3.2A). The K_{on} value was then determined from an association experiment using the calculated K_{off} and was equal to $1,730,000 \pm 74,000 \text{ M}^{-1} \text{ min}^{-1}$ with a half-time of 40 min for association of 6 nM [^3H]-GLPG0974 (Figure 3.2B). Using the determined rate constants a first estimate of [^3H]-GLPG0974 affinity could be obtained by division of the K_{off} by the K_{on} , yielding a predicted K_d of $8.1 \pm 0.9 \text{ nM}$. An equilibrium binding assay was then performed in which increasing concentrations of [^3H]-GLPG0974, which were selected based on the K_d derived from the kinetic studies, were incubated with membranes containing hFFA2-eYFP to obtain a saturation binding curve (Figure 3.2C). To allow for full equilibration of radioligand binding, an incubation time of 2 h at 25 °C was selected, based on the half-time of 6 nM [^3H]-GLPG0974

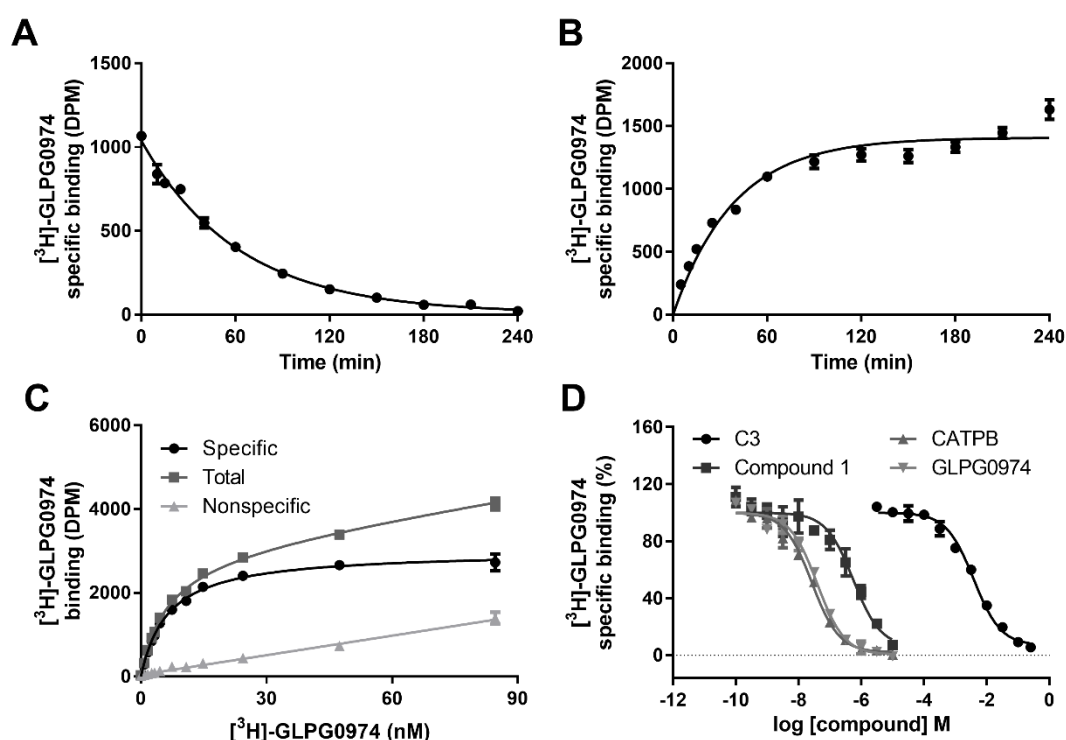


Figure 3.2 Characteristics of [^3H]-GLPG0974 binding to wild type hFFA2 Binding of [^3H]-GLPG0974 to membranes purified from Flp-InTM T-RExTM 293 cells induced to express hFFA2-eYFP was assessed and data from representative experiments are illustrated. Dissociation (A) and association (B) of 6 nM [^3H]-GLPG0974 is shown. To monitor [^3H]-GLPG0974 dissociation 10 μM CATPB were added after 60 min pre-association of the radioligand. The ability of increasing concentrations of [^3H]-GLPG0974 to bind to hFFA2 was assessed (C). The capacity of varying concentrations of C3, compound 1, CATPB and GLPG0974 to compete with 10 nM of [^3H]-GLPG0974 is shown (D). Nonspecific binding was determined in presence of 10 μM GLPG0974 and subtracted from total binding to calculate specific binding.

association, and nonspecific binding was determined by addition of 10 μM CATPB. [^3H]-GLPG0974 showed a good total to nonspecific binding ratio and the resulting specific binding curve fit a one-site, but not a two-site, binding model suggesting that [^3H]-GLPG0974 binds to a single site on the receptor. The radioligand concentration that results in half-maximal occupation of the receptor corresponds to the K_d of [^3H]-GLPG0974, which was equal to 7.5 ± 0.4 nM and is hence in agreement with the value derived from the kinetic studies. In the context of ligand screening and drug discovery the most relevant radioligand-based assay is perhaps the displacement assay, in which the affinity of unlabelled ligands can be calculated based on their capacity to compete with the radioligand, so long as the unlabelled ligands and radioligand bind to the same site (Sweetnam et al., 1993). To assess whether [^3H]-GLPG0974 is an appropriate radioligand for use in such an assay system, the ability of SCFA C3, synthetic agonist compound 1 and the synthetic antagonists CATPB and GLPG0974 to compete with the radioligand was determined (**Figure 3.2D**). All unlabelled ligands were able to fully outcompete [^3H]-GLPG0974, suggesting that they bind to the same site as the radioligand. The SCFA C3 was included in the panel of tested ligands to serve as a probe for the endogenous orthosteric binding site and its ability to fully displace [^3H]-GLPG0974 indicates that the radioligand, and the unlabelled ligands able to displace it, also bind in an orthosteric fashion. As expected from previous functional studies (Stoddart et al., 2008, Schmidt et al., 2011, Hudson et al., 2013a), C3 displayed relatively modest affinity with a calculated pK_i of 2.96 ± 0.11 ($= 1.10$ mM), while compound 1 showed affinity approximately 9000-fold greater, with a pK_i of 6.91 ± 0.12 ($= 123$ nM) (**Table 3.1**). The affinities of CATPB and GLPG0974 were essentially equivalent to each other with pK_i values of 7.87 ± 0.08 and 7.88 ± 0.08 ($= 13$ mM), respectively. In addition to providing information on the affinity of unlabelled ligands, radioligands can also be employed for more detailed investigations of ligand binding and [^3H]-GLPG0974 will be used to explore the binding site and kinetics of FFA2 agonists and antagonists in chapter 4.

Prior to [^3H]-GLPG0974 no labelled FFA2 ligand probes were available. As such, functional studies have played a key role in defining the pharmacology of FFA2 ligands (Stoddart et al., 2008, Hudson et al., 2013a). A selection of different assay systems was used to assess FFA2 agonists, which reflect the promiscuity of

Table 3.1 Affinity and potency of hFFA2 reference ligands

Assay	Agonist ^a		Antagonist ^b	
	C3	Compound 1	CATPB	GLPG0974
Binding (pKi)	2.96 ± 0.11	6.81 ± 0.09	7.87 ± 0.08	7.88 ± 0.08
[³⁵S]-GTPγS binding (pE/IC ₅₀)	3.95 ± 0.02 ^{\$\$\$}	6.66 ± 0.09	6.60 ± 0.08 ^{\$\$\$}	6.70 ± 0.10 ^{\$\$\$}
cAMP inhibition (pE/IC ₅₀)	3.97 ± 0.06 ^{\$\$\$}	6.66 ± 0.14	6.32 ± 0.13 ^{\$\$\$}	6.27 ± 0.03 ^{**/\$\$\$}
IP1 accumulation (pE/IC ₅₀)	4.16 ± 0.05 ^{*/\$\$\$}	7.16 ± 0.07 ^{**}	6.71 ± 0.11 ^{\$\$\$}	6.94 ± 0.04 ^{\$\$\$}
β-arrestin 2 (pE/IC ₅₀)	3.35 ± 0.05 ^{***/\$\$\$}	5.75 ± 0.07 ^{***/\$\$\$}	6.65 ± 0.04 ^{\$\$\$}	7.42 ± 0.07 ^{**/\$\$\$}

^a Data shown as pK_i and pEC₅₀.

^b Data shown as pK_i and pIC₅₀.

* Analysis of pE/IC₅₀ values of one compound in different assays by one-way ANOVA followed by Tukey's test with significant differences denoted as P = * ≤ 0.05 and P = *** ≤ 0.001

§ Comparison of all pK_i and pE/IC₅₀ values of one compound by a one-way ANOVA followed by a Dunnett's test with the pK_i as a reference with significant differences denoted as P = \$\$\$ ≤ 0.001.

FFA2 signalling. The [³⁵S]-GTPγS binding assay was performed in membranes isolated from Flp-InTM T-RExTM 293 cells, which were induced with doxycycline to express stably harboured hFFA2-eYFP. The reactions were set up in single glass tubes and bound [³⁵S]-GTPγS was separated from unbound radioligand by filtration, therefore this assay system is relatively low-throughput compared to other assays employed. The cAMP inhibition and IP1 accumulation assays are based on detection of cAMP or IP1 levels by HTRF technology developed by Cisbio Bioassays. These assays were performed in 384-well plates and required only small amounts of reagents and doxycycline-induced cells, therefore they are more suitable for screening of larger numbers of compounds. Increasing concentrations of C3 and compound 1 were able to induce FFA2 signalling through G_{i/o}-coupled pathways, as reflected in increasing [³⁵S]-GTPγS incorporation (**Figure 3.3A**) and cAMP inhibition (**Figure 3.3B**) upon agonist treatment. FFA2 is also able to couple to the G_{q/11} family of G proteins and indeed C3 and compound 1 also promoted accumulation of IP1 in a concentration-dependent manner (**Figure 3.3C**). With an increasing body of evidence suggesting that β-arrestin also plays an important role in GPCR signalling (Daaka et al., 1998, Cahill et al., 2017), the ability of FFA2 to recruit β-arrestin 2 was assessed in a BRET-based system in which β-arrestin-2-RLuc, the BRET donor, and hFFA2-eYFP, the BRET acceptor, were transiently co-transfected into cells, which were seeded in 96-well plates. Activation of

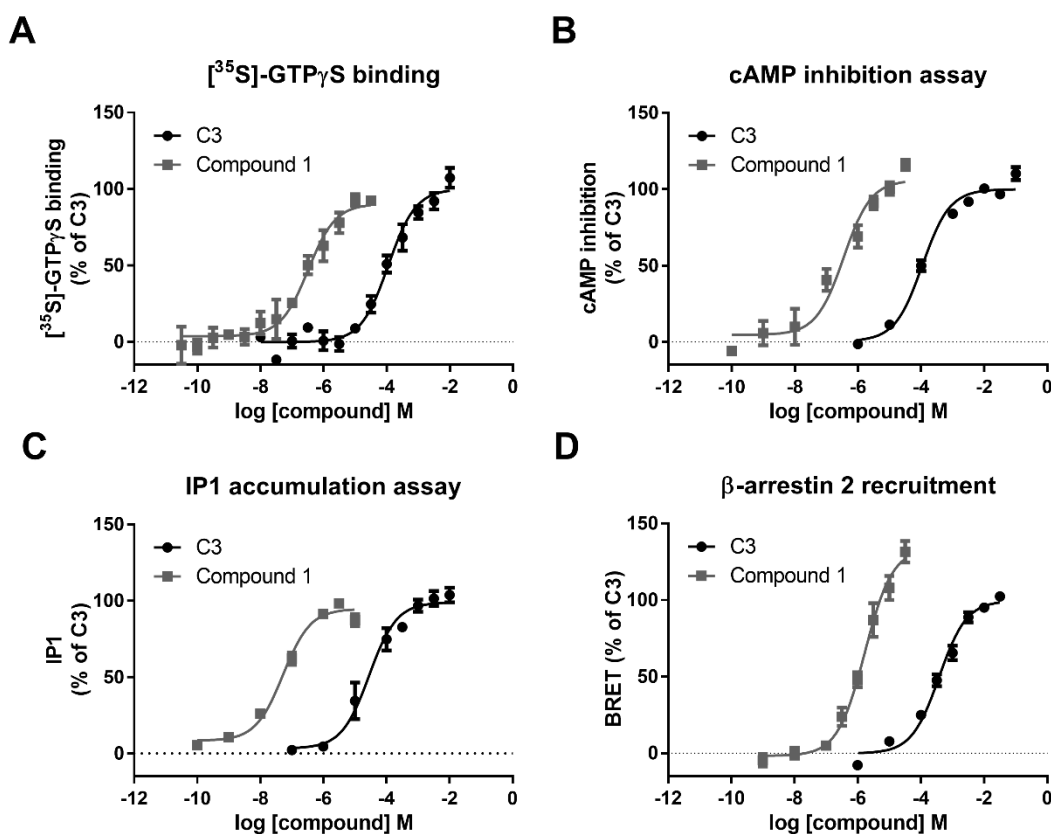


Figure 3.3 Assay systems for assessment of hFFA2 agonist signalling The potency of the endogenous SCFA C3 and the synthetic agonist compound 1 to activate hFFA2 in $[^{35}\text{S}]\text{-GTP}\gamma\text{S}$ binding (A), cAMP inhibition (B), IP1 accumulation (C) and β -arrestin 2 recruitment assays (D) is shown. Assays employed membranes (A) or cells (B, C) with a Flp-InTM T-RExTM 293 background that stably harbour hFFA2-eYFP and were induced to express the receptor. For β -arrestin 2 recruitment assays HEK293T cells were transiently co-transfected with hFFA2-eYFP and RLuc-tagged β -arrestin 2 (D). Results were normalised to the maximal C3 response. All data are means pooled from independent experiments ($n \geq 3$) that were performed in triplicate (A, B, D) or duplicate (C).

hFFA2-eYFP by C3 and compound 1 led to a concentration-dependent increase in the BRET signal, indicating recruitment of RLuc-tagged β -arrestin-2 within close enough proximity of eYFP to produce BRET (Figure 3.3D). However, while this demonstrates that activation of FFA2 results in binding of β -arrestin to the receptor, this does not necessarily confirm that FFA2 does induce β -arrestin-dependent signalling, as recruitment of β -arrestin is also a vital component of the GPCR downregulation cascade. As expected from the affinity of the respective ligands, compound 1 was consistently more potent than C3 (Table 3.1). However, across this set of assays some variation in potency could be observed. The $G_{i/o}$ -coupled $[^{35}\text{S}]\text{-GTP}\gamma\text{S}$ binding and cAMP inhibition assays yielded almost identical potency values for both C3 and compound 1. In the $G_{q/11}$ -coupled IP1 assay both agonists were more potent, while in the β -arrestin 2 recruitment assay the lowest potency values were observed. In the case of C3 its

potency in the β -arrestin 2 recruitment assay came closest to its determined affinity, while the measured affinity of compound 1 was more closely approximated by G protein-dependent signalling assays.

The same set of assays were also employed to assess the action of antagonists at FFA2. Synthetic antagonists CATPB and GLPG0974 were both able to inhibit the response of FFA2 to C3 in $[^{35}\text{S}]$ -GTP γ S binding, cAMP inhibition, IP1 accumulation and β -arrestin 2 recruitment assays in a concentration-dependent fashion (Figure 3.4). The concentration of C3 employed was selected to reflect the measured EC_{80} concentration in the respective assay system, which is an important consideration as the determined antagonist IC_{50} , the half-maximal inhibitory concentration, will depend on the agonist concentration employed.

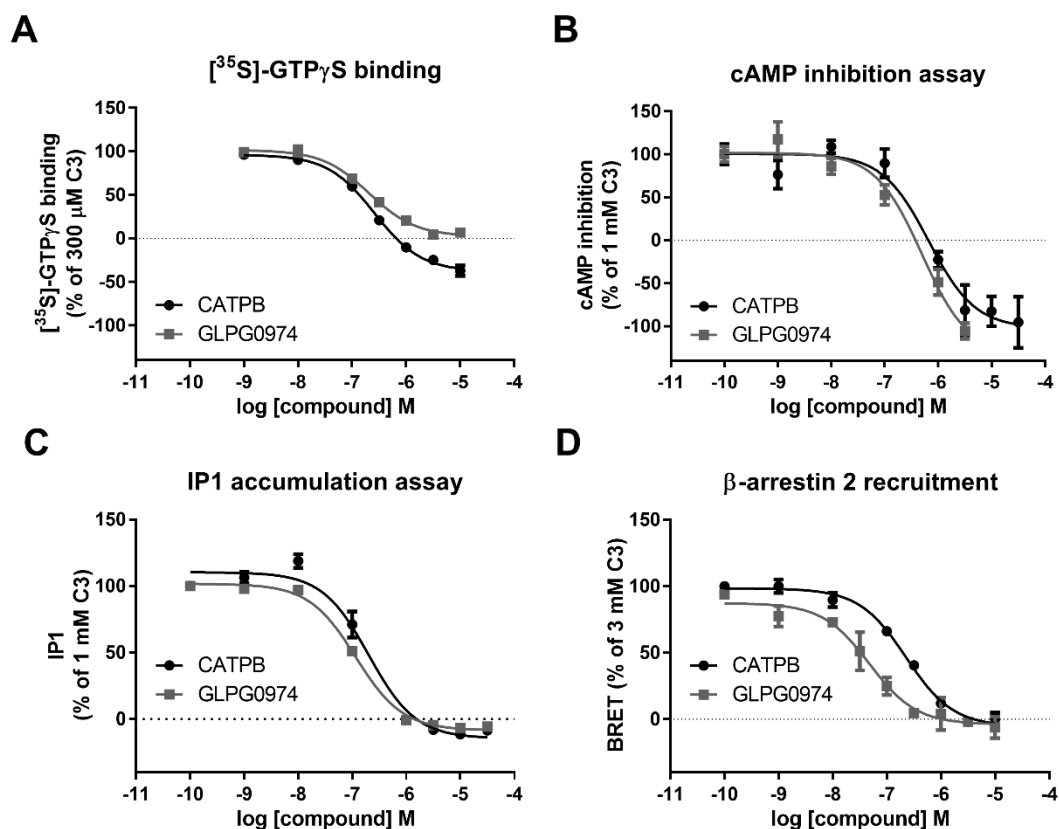


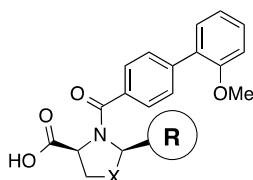
Figure 3.4 Assay systems for assessment of hFFA2 antagonists The ability of the synthetic antagonists CATPB and GLPG0974 to inhibit the response of hFFA2 to indicated C3 concentrations in $[^{35}\text{S}]$ -GTP γ S binding (A), cAMP inhibition (B), IP1 accumulation (C) and β -arrestin 2 recruitment (D) assays is shown. Assays employed membranes (A) or cells (B, C) with a Flp-InTM T-RExTM 293 background that stably harbour hFFA2-eYFP and were induced to express the receptor. For β -arrestin 2 recruitment assays, HEK293T cells were transiently co-transfected with hFFA2-eYFP and RLuc-tagged β -arrestin 2 (D). Results were normalised with vehicle-treated cells set to 0% and response to indicated C3 concentrations set to 100%. All data are means pooled from independent experiments ($n \geq 3$) that were performed in triplicate (A, B, D) or duplicate (C).

Some antagonists can act as inverse agonists, which is reflected in an inhibition of the basal signalling of the receptor. This appeared to be the case for CATPB in the $G_{i/o}$ -coupled [^{35}S]-GTP γ S binding and cAMP inhibition assay (**Figures 3.4A and B**), but not for $G_{q/11}$ -coupled IP1 accumulation or β -arrestin 2 recruitment assays (**Figures 3.4C and D**). In contrast, inverse agonism of GLPG0974 was only observed in the cAMP inhibition and not the [^{35}S]-GTP γ S binding assay (**Figures 3.4A and B**). When comparing functional IC_{50} values of antagonists with their affinities, the IC_{50} values were consistently lower than affinity values with at least a 10-fold difference (**Table 3.1**). Furthermore, although CATPB and GLPG0974 have essentially equivalent affinity for FFA2, their IC_{50} values in the β -arrestin 2 recruitment assay were almost 6-fold different.

3.2.2 Screening of a structurally unexplored FFA2 agonist series

Compound 1 has played an important role in understanding the SAR of FFA2 agonists (Hudson et al., 2013a), but it has not been employed in any published *in vivo* studies to investigate the physiological role of FFA2, potentially due to its reduced potency at mFFA2 and potential concerns regarding the chemical stability of the compound. Consequently, there is still need for exploration of alternative FFA2-specific agonist series. A recent investigation of the role of FFA2 in obesity and diabetes employed a different synthetic FFA2 agonist, here referred to as compound 2, *in vivo* to demonstrate that FFA2 activation induced PYY-dependent reduction in gut motility and food intake (Forbes et al., 2015). However, this study focussed on a physiological aspect of FFA2 activation and did not explore any structural analogues of compound 2. To investigate the SAR of this ligand series with the aim to identify compounds with improved potency, a range of different analogues with structural modifications in different areas of the molecule were tested. The investigation of reference ligands for FFA2 in functional assays revealed that agonists tend to show variations in potency in different assay systems. Furthermore, screening compounds in multiple assay systems allows detection of potential bias in ligand-induced signalling. Therefore, the analogues were tested in two different assays to reflect both G protein and β -arrestin coupling. Initial replacement of the central pyrroline with a thiazolidine and modifications at the eastern part of the molecule did not result in improved potencies in the β -arrestin 2 recruitment or cAMP inhibition assays (**Table 3.2**). However, replacement of the northern anisole group of the

Table 3.2 Screening of compound 2 analogues with eastern part variations



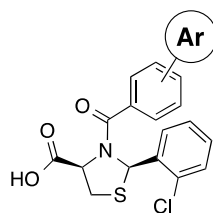
Compound	Structure		Potency/pEC ₅₀ (Efficacy/E _{max}) ^a		CLogP ^b
	X	R	β-arrestin 2 recruitment	cAMP inhibition	
2	CH ₂		5.91 ± 0.21 (127)	6.28 ± 0.19 (96)	5.13
2-1	S		5.60 ± 0.10 (116)	5.61 ± 0.06 (96)	5.13
2-2	S		4.91 ± 0.29 (93)	5.15 ± 0.19 (106)	5.13
2-3	S		4.73 ± 0.29 (136)	5.55 ± 0.19 (80)	5.13
2-4	S		5.65 ± 0.18 (108)	5.45 ± 0.11 (90)	5.28
2-5	S		5.53 ± 0.16 (116)	6.03 ± 0.15 (88)	4.42
2-6	S		4.83 ± 0.09 (124)	5.87 ± 0.10 (75)	2.92
2-7	S		4.74 ± 0.38 (68)	5.66 ± 0.19 (70)	3.60
2-8	S		< 4	< 4	4.56
2-9	O		< 4	< 4	4.18

^a E_{max} values were normalised as percentage of C3 response

^b ClogP values were calculated using ChemBioDraw

thiazolidine-based compound 2-1 with a 3,5-dimethyl-2,3-dihydro-1,2-oxazole moiety produced compound 2-23, which showed greatly improved potency in the cAMP inhibition assay with an almost 10-fold increase and a more modest 1.5-fold improvement in the β-arrestin 2 recruitment assay (Table 3.3). The ClogP value, which is a computationally determined measure of compound hydrophilicity calculated from the logarithm of the ratio of predicted compound partition coefficients in octanol and water, was also reduced from 5.13 for compound 2 to 3.73 for compound 2-23, suggesting a potentially improved pharmacokinetic profile for compound 2-23. Interestingly, a switch of the

Table 3.3 Screening of compound 2 analogues with northern part variations



Compound	Structure		Potency/pEC ₅₀ (Efficacy/E _{max}) ^b		CLogP ^c
	ArS ^a	R	β-arrestin 2 recruitment	cAMP inhibition	
2-10	(4)		< 4	< 4	3.82
2-11	(4)		5.09 ± 0.05 (146)	5.00 ± 0.20 (93)	5.71
2-12	(3)		4.59 ± 0.13 (141)	5.40 ± 0.04 (91)	5.71
2-13	(4)		5.32 ± 0.23 (122)	5.04 ± 0.18 (82)	5.74
2-14	(4)		4.66 ± 0.16 (174)	5.35 ± 0.15 (87)	5.69
2-15	(4)		6.09 ± 0.04 (103)	5.68 ± 0.07 (90)	5.21
2-16	(4)		5.89 ± 0.08 (95)	5.89 ± 0.13 (95)	5.18
2-17	(4)		5.14 ± 0.24 (143)	6.04 ± 0.16 (74)	6.19
2-18	(4)		5.36 ± 0.12 (146)	5.40 ± 0.19 (82)	5.91
2-19	(4)		5.04 ± 0.17 (212)	5.32 ± 0.15 (89)	6.09
2-20	(4)		5.22 ± 0.12 (130)	5.68 ± 0.09 (83)	6.46
2-21	(4)		4.80 ± 0.35 (99)	5.65 ± 0.09 (89)	6.38
2-22	(4)		6.01 ± 0.04 (103)	6.67 ± 0.12 (77)	4.10
2-23	(4)		6.10 ± 0.07 (99)	7.11 ± 0.08 (86)	3.73

^a Aromatic substitution at meta (3) or para (4) position

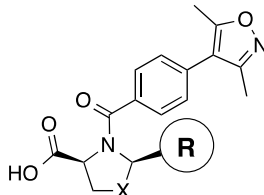
^b E_{max} values were normalised as percentage of C3 response

^c ClogP values were calculated using ChemBioDraw

thiazolidine core back to a pyrroline in compound 2-24, which is the basis of increased potency of compound 2 compared to compound 2-1 (Table 3.2), did not result in an improvement in potency and other modifications of the eastern region of the molecule also failed to produce a more potent agonist than compound 2-23 (Table 3.4). Concentration response curves of a selected set of these compounds in the β -arrestin 2 recruitment and cAMP inhibition assays are shown in figure 3.5.

The radioligand competition assay described in section 3.2.1 was then employed to determine the affinity of a set of compound 2 analogues, which were selected to reflect different types of structural modifications. Compounds 2 and 2-1 represent the “parent ligands” with pyrroline (2) and thiazolidine (2-1) cores. Compounds 2-5 and 2-11 both have thiazolidine cores and a nonpolar benzene group in the eastern (2-5) and northern (2-11) part. Thiazolidine-based compound 2-23 showed the highest potency across both functional assays, while compound 2-24 is the pyrroline core equivalent to compound 2-23. All ligands

Table 3.4 Screening of compound 2 analogues with isoxazole and eastern part variations



Compound	Structure		Potency/pEC ₅₀ (Efficacy/E _{max}) ^a		CLogP ^b
	X	R	β -arrestin 2 recruitment	cAMP inhibition	
2-24	CH ₂		5.97 ± 0.08 (90)	6.82 ± 0.07 (85)	3.73
2-25	S		5.64 ± 0.04 (79)	5.84 ± 0.08 (94)	3.02
2-26	S		5.99 ± 0.21 (73)	5.46 ± 0.12 (49)	3.29
2-27	S		5.09 ± 0.11 (79)	5.78 ± 0.04 (83)	2.94
2-28	S		4.45 ± 0.04 (102)	< 4	1.52

^a E_{max} values were normalised as percentage of C3 response

^b ClogP values were calculated using ChemBioDraw

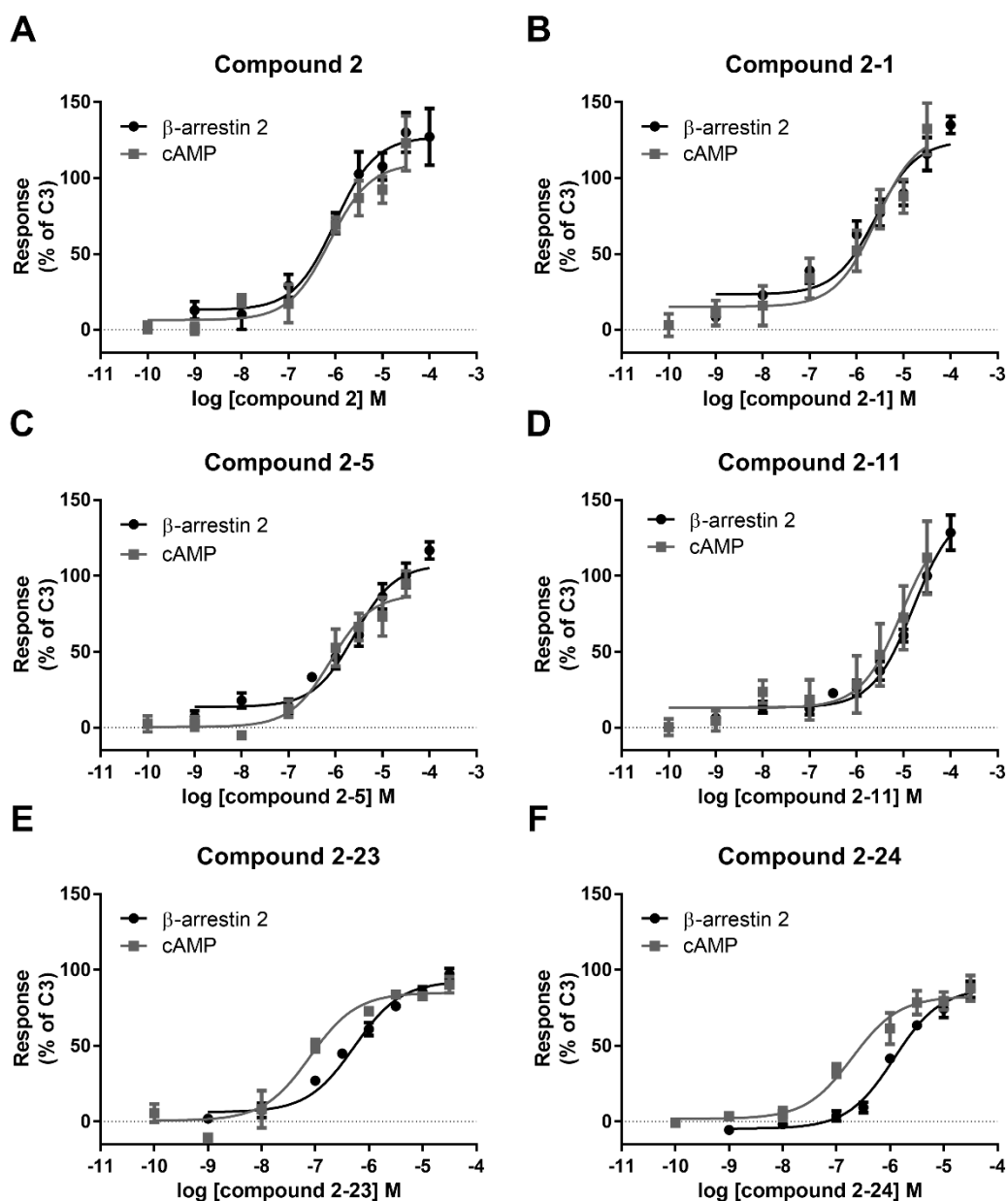


Figure 3.5 Assessment of an hFFA2 agonist series based on compound 2 in functional assays The capacity of compound 2 (A) and a selection of analogues (B-F) to activate hFFA2 in β -arrestin 2 recruitment and cAMP inhibition assays is shown. To measure cAMP inhibition, Flp-In™ T-REx™ 293 cells were induced to express hFFA2-eYFP, while for β -arrestin 2 recruitment assays HEK293T cells were transiently co-transfected with hFFA2-eYFP and RLuc-tagged β -arrestin 2. All data are means pooled from independent experiments ($n \geq 3$) that were performed in triplicate. RLuc = Renilla luciferase.

were all able to fully displace [3 H]-GLPG0974 (Figure 3.6), suggesting an orthosteric mode of binding akin to C3 and compound 1. The increased potency of compound 2-23 was reflected in a 2.3-fold increase in affinity over “parent” compound 2 (Table 3.5).

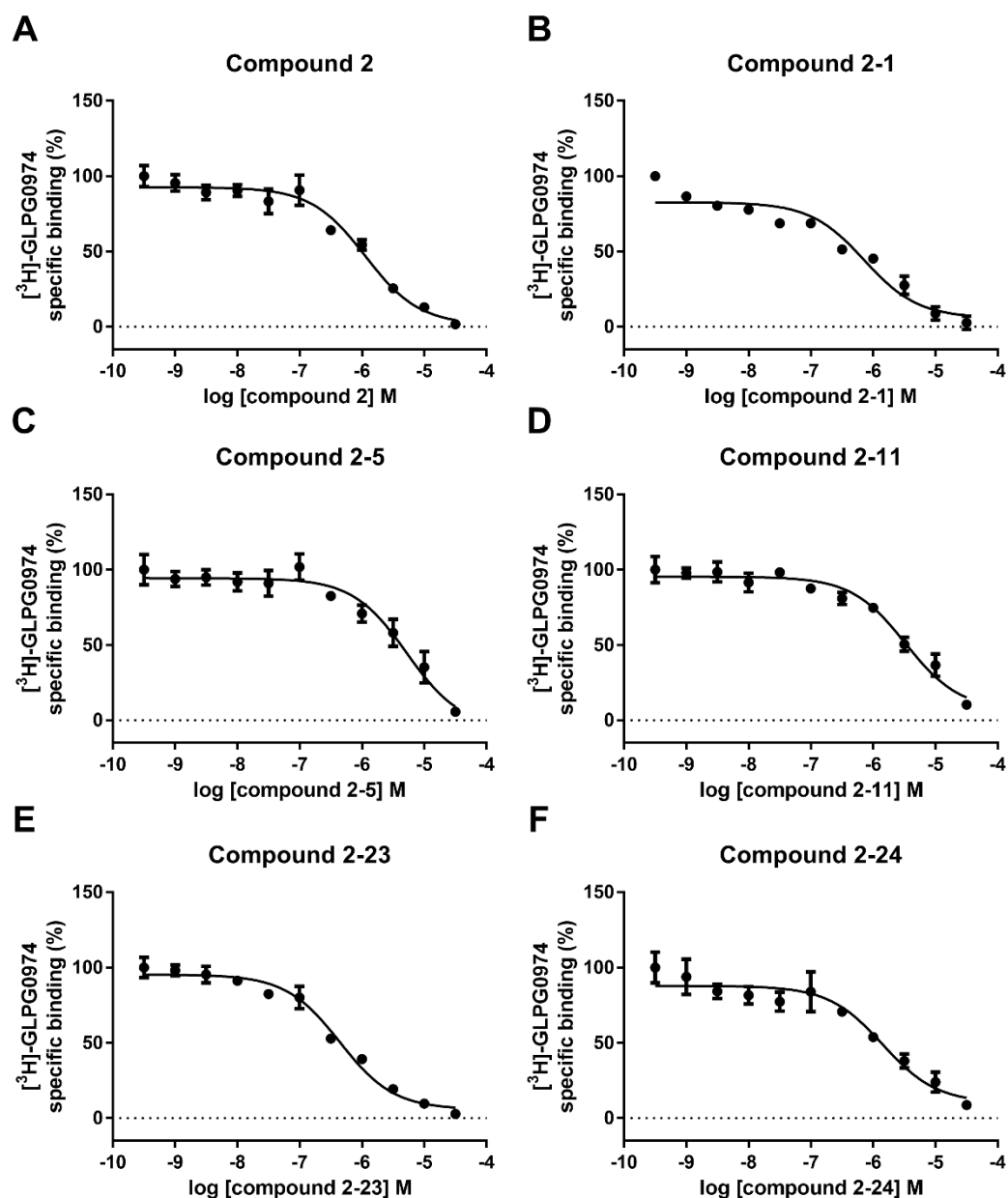


Figure 3.6 Screening of an hFFA2 agonist series based on compound 2 in competition binding assays The capacity of compound 2 (**A**) and a selection of analogues (**B-F**) to compete with [³H]-GLPG0974 for binding to membranes purified from Flp-In™ T-REx™ 293 cells induced to express hFFA2-eYFP is shown from representative experiments. To calculate specific binding, nonspecific binding was determined in the presence of 10 μM CATPB and subtracted from total binding.

Table 3.5 Affinity of compound 2 and representative analogues for hFFA2

Compound	Binding (pK _i)
2	6.32 ± 0.02
2-1	6.47 ± 0.06
2-5	5.92 ± 0.08
2-11	6.01 ± 0.02
2-23	6.69 ± 0.03
2-24	6.40 ± 0.06

To assess how the potency values between the two assays correlate and compare to affinity determined in binding assays, pEC₅₀ and pK_i values were shown as correlation plots with the r value indicating the correlation coefficient (**Figure 3.7**). When considering only the selected set of compounds, the pEC₅₀ values in the cAMP inhibition and β-arrestin 2 recruitment assays correlated well with a slope steeper than 1 (**Figure 3.7A**). This suggests that although a corresponding increase in potency can be observed in both assays, the spread of values differs.

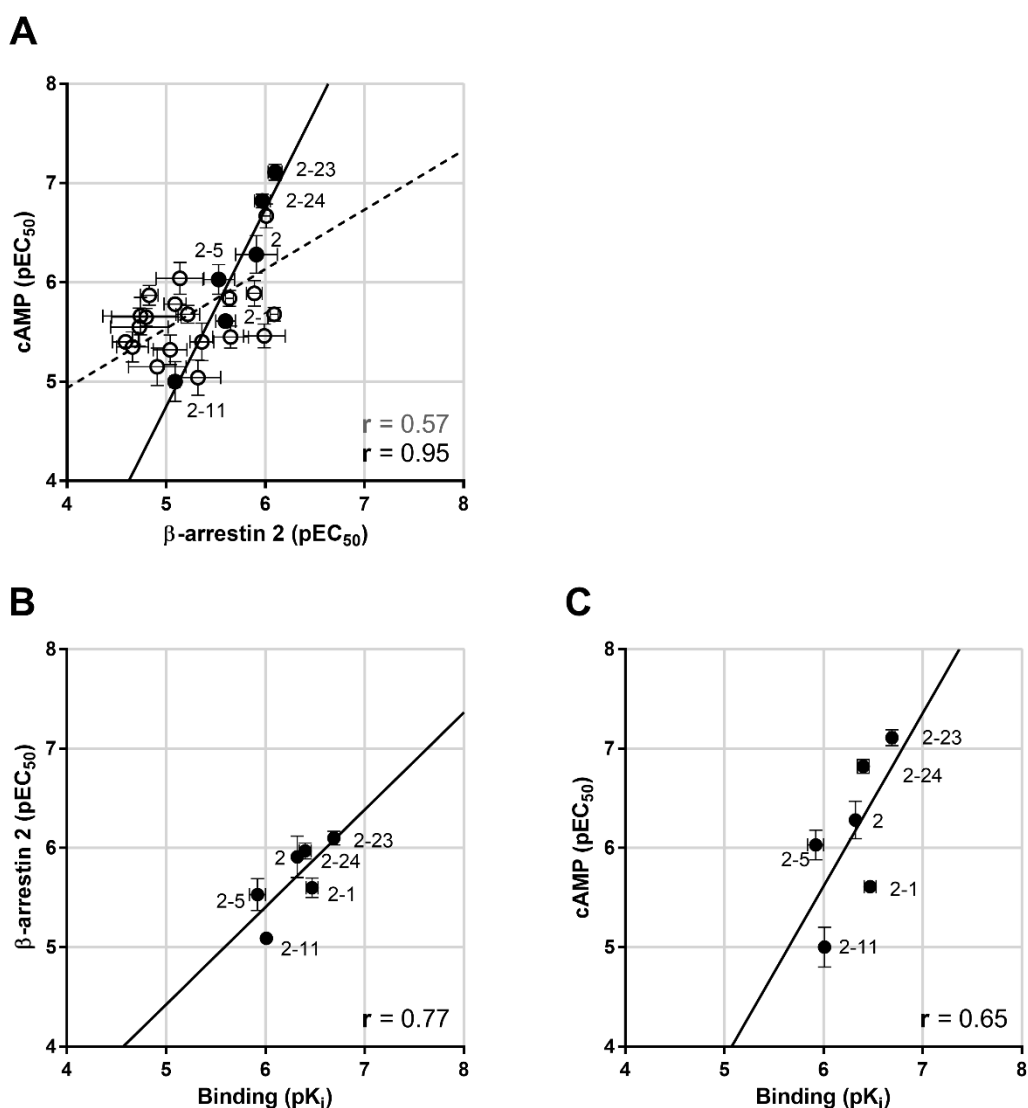


Figure 3.7 Correlation between hFFA2 agonist potencies and affinities Potency values in terms of pEC₅₀ of compound 2 and its analogues in cAMP inhibition and β-arrestin 2 recruitment assays are plotted (**A**). Selected compound numbers are shown in full circles and additional analogues screened are shown in open circles. Affinity values in terms of pK_i calculated from [³H]-GLPG0974 competition binding assays are plotted against potency of agonists in β-arrestin 2 recruitment (**B**) and cAMP inhibition assays (**C**). All data are means pooled from independent experiments (n ≥ 3) that were performed in triplicate (cAMP inhibition and β-arrestin 2 recruitment assays) or duplicate (radioligand displacement assay). Linear regression and correlation coefficient r for correlation of potencies and/or affinities of selected compounds (*black line*) or all analogues (*broken line*) is shown.

However, inclusion of the datasets for all analogues yields a comparatively poor correlation, perhaps due to the large error of some of the pEC₅₀ values. The linear regression of binding affinity and potency in the β -arrestin 2 recruitment (**Figure 3.7B**) or cAMP inhibition assay (**Figure 3.7C**) yielded respective *r* values of 0.77 and 0.65, which suggested a clear positive correlation. In the case of the cAMP inhibition assay the slope of the linear regression is considerably steeper compared to the β -arrestin 2 recruitment assay, therefore relative compound affinities were more closely approximated by ligand potencies in the β -arrestin 2 recruitment assay. Overall, it appears that a ligand such as compound 2-23, which clearly shows improved potency over the parent compound in two different assay systems, is likely to show higher affinity for the receptor. However, minor changes in potency between analogues did not necessarily seem to correlate between different functional assays and did not always translate into equivalent changes in affinity.

Model animals play an important role at multiple stages of the drug development pipeline and can be employed in target validation and lead compound optimisation, with rodents being the most commonly used species. To assess whether the compound 2 series contains agonists that could be of use in murine models of disease, compound 2 analogues were tested at mFFA2 in the cAMP inhibition assay. In the case of most ligands, the potency at mFFA2 versus hFFA2 was not significantly different (**Table 3.6**). However, selected compounds were notably selective for the murine versus the human orthologue and vice versa. Compound 2-1 displayed the highest potency at mFFA2 and was selective for the murine orthologue. The analogues 2-11, 2-13 and 2-18 also showed significant selectivity for the mFFA2, while compounds 2-5, 2-22 and 2-23 had a higher potency at hFFA2. Structurally, it appears that the polar modifications of the northern region that resulted in an improved potency of compounds 2-22 and 2-23 at hFFA2, did not correlate with potency values at mFFA2 and indicate potential species-specific differences in the SAR of this compound series. Although compound 2-23 did not show the highest potency at mFFA2, it was still relatively potent and its improved hydrophilicity may suggest a potential improvement over compound 2 for use *in vivo*.

Table 3.6 Comparing potency of compound 2 analogues at human and murine FFA2

Compound	cAMP inhibition at mFFA2 (pEC ₅₀)	Select ^a
2	6.40 ± 0.16	-0.12
2-1	6.92 ± 0.09	-1.31***
2-2	5.64 ± 0.22	-0.49
2-3	5.63 ± 0.23	-0.08
2-4	6.24 ± 0.36	-0.79
2-5	5.13 ± 0.17	0.9*
2-6	5.51 ± 0.07	0.36*
2-7	5.35 ± 0.29	0.31
2-11	5.96 ± 0.09	-0.96*
2-13	5.95 ± 0.16	-0.91*
2-14	5.79 ± 0.10	-0.44
2-15	5.87 ± 0.08	-0.19
2-16	5.80 ± 0.05	0.09
2-17	6.50 ± 0.06	-0.46
2-18	6.32 ± 0.21	-0.92*
2-19	5.44 ± 0.07	-0.12
2-20	5.59 ± 0.11	0.09
2-21	5.67 ± 0.11	-0.02
2-22	5.89 ± 0.15	0.78*
2-23	6.44 ± 0.13	0.67*

^a Selectivity represents comparison between species and was calculated by subtracting mFFA2 EC₅₀ values from hFFA2 EC₅₀ values

* Comparison of pEC₅₀ values of one compound at murine versus human FFA2 by unpaired *t* test with significant differences denoted as P = * ≤ 0.05 and P = *** ≤ 0.001

3.2.3 Comparing the pharmacology of FFA2 antagonists GLPG0974 and CATPB

The antagonist GLPG0974 is, to date, the only FFA2 compound to reach clinical development after preclinical studies in human blood demonstrated its ability to inhibit neutrophil migration through blockade of FFA2 (Pizzonero et al., 2014). Although GLPG0974 did not show significant efficacy in clinical trials in ulcerative colitis patients (Vermeire et al., 2015), it could still be of use as a tool compound for investigation of FFA2 function. Many questions remain regarding the physiological role of FFA2 (see section 1.4.2), which will likely have to be resolved prior to further clinical studies. Understanding the pharmacology and mode of action of GLPG0974 can contribute to facilitating its use as a tool compound. Therefore, its pharmacological behaviour in regard to the SCFA C3 and compound 1 was assessed and compared to CATPB (Figure 3.8). Surprisingly, increasing concentrations of C3 were unable to overcome the efficacy-reducing effect of increasing GLPG0974 concentrations in the β-arrestin

2 recruitment assay (Figure 3.8A), which was not the case for CATPB (Figure 3.8B). Conceptually insurmountable antagonism indicates a non-competitive relationship between agonist and antagonist, but in the case of GLPG0974 this would be surprising, as C3 is able to fully compete with the radioligand [³H]-GLPG0974 for binding to hFFA2 (Figure 3.2D). Indeed, in an equivalent experiment with compound 1 as an agonist ligand, the inhibitory effect of GLPG0974 was surmountable (Figure 3.8C) and mirrored the pattern of curves observed for CATPB (Figure 3.8D).

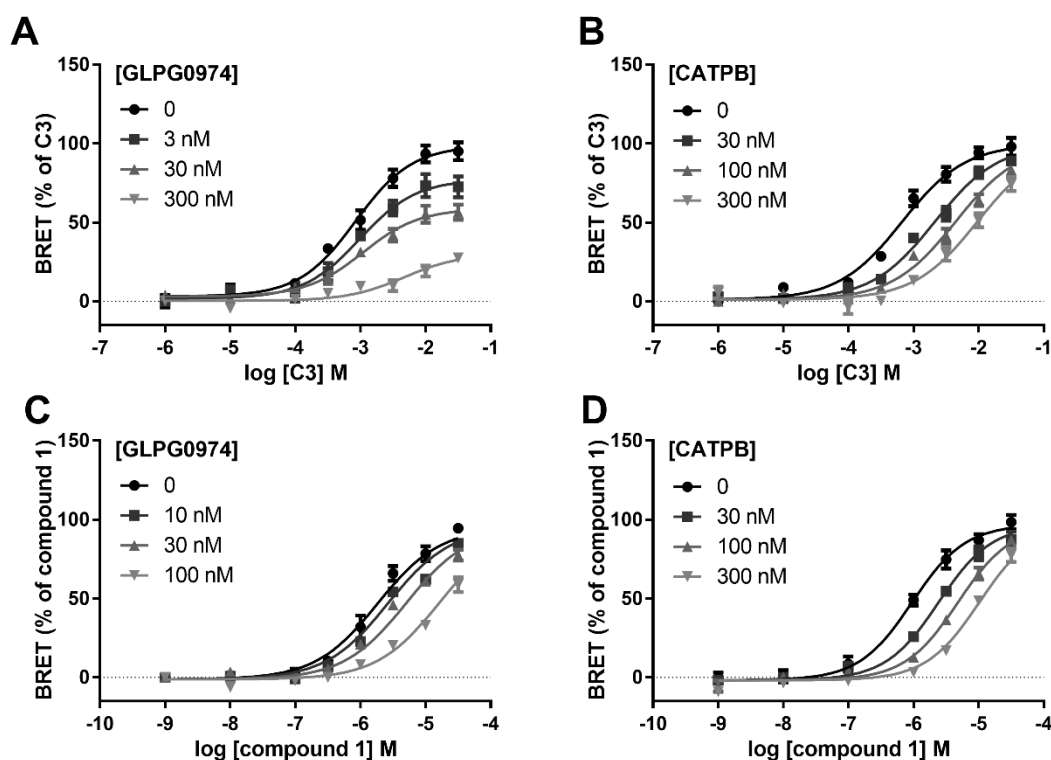


Figure 3.8 Effect of hFFA2 antagonists on agonist responses in a β -arrestin 2 recruitment assay The capacity of increasing concentrations of C3 (A, B) or compound 1 (C, D) to promote recruitment of β -arrestin 2 and how this was altered by the co-addition of the indicated concentrations of either GLPG0974 (A, C) or CATPB (B, D) is shown. To measure the interaction between receptor and β -arrestin 2, HEK293T cells were transiently co-transfected with hFFA2-eYFP and RLuc-tagged β -arrestin 2. All data are means pooled from independent experiments ($n \geq 3$) that were performed in triplicate and are fit using a three-parameter sigmoidal curve (A) or global Gaddum/Schild model (B-D).

The insurmountable effect of GLPG0974 on the C3 concentration response in the β -arrestin 2 recruitment assay was unexpected and was not observed with the synthetic orthosteric agonist compound 1. To confirm whether the same result would also be observed in a different assay, the ERK1/2 phosphorylation assay was employed as an alternative. Here, C3 and compound 1 had significantly

higher potencies than in the β -arrestin 2 recruitment assay with pEC_{50} values of 4.83 ± 0.11 and 7.59 ± 0.01 , respectively, making it possible to detect a further rightward shift of the concentration response curve with increasing antagonist concentrations. In this assay system increasing concentrations of C3 were able to overcome the inhibitory effect of GLPG0974 (Figure 3.9A), as anticipated for competitive antagonism. Fitting of the corresponding Schild plot resulted in a linear regression with a slope of 0.98, which is very close to unity and therefore a further indication of a competitive relationship between agonist and antagonist (Figure 3.9B). Furthermore, the negative x-intercept provides an estimation of antagonist affinity in terms of a pA_2 , which in this case was 8.14 (= 7.2 nM). These observations were mirrored by an equivalent experiment performed with compound 1 showing clearly surmountable effects of GLPG0974

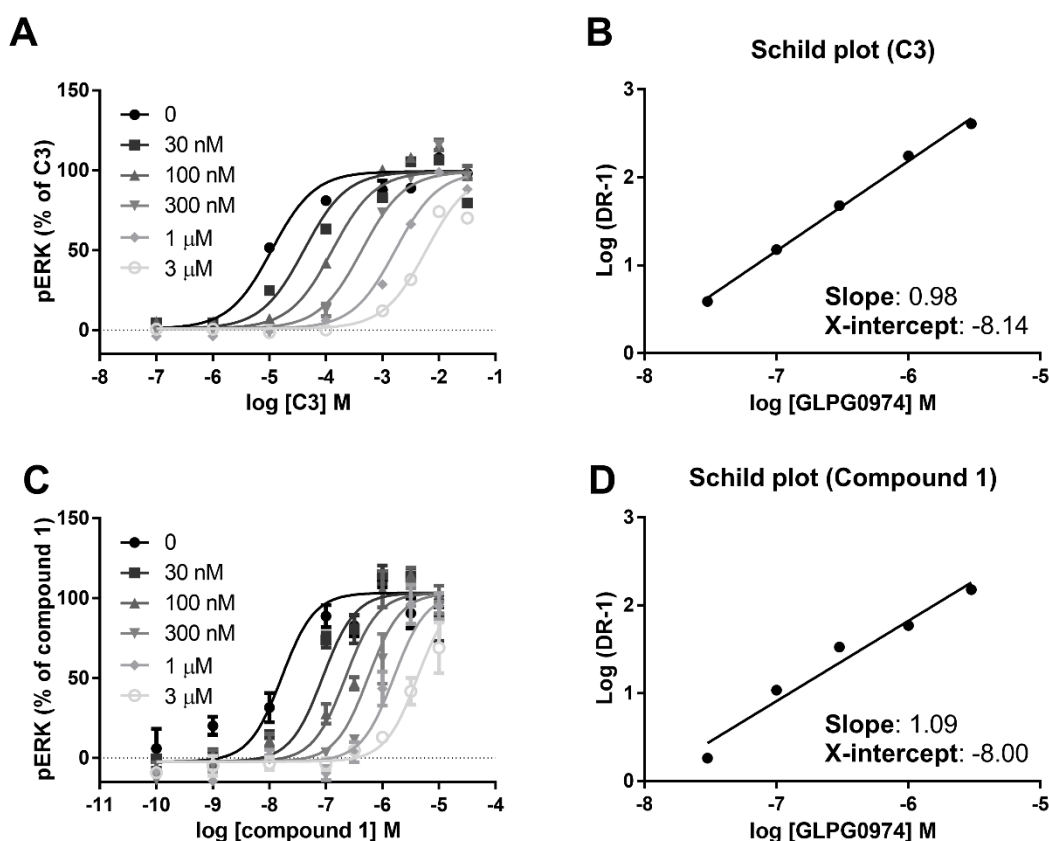


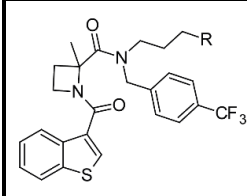
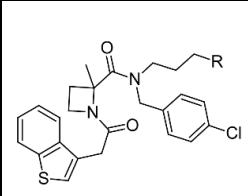
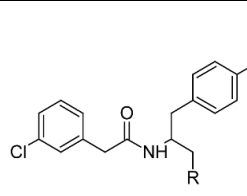
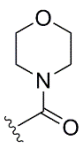
Figure 3.9 Effect of hFFA2 antagonists on agonist response in an ERK1/2 phosphorylation assay The ability of increasing concentrations of C3 (A) or compound 1 (C) to induce ERK1/2 phosphorylation and how this was altered by the co-addition of GLPG0974 is shown. Experiments employed Flp-InTM T-RExTM 293 cells induced to express hFFA2-eYFP. All data are means pooled from independent experiments ($n \geq 3$) that were performed in triplicate and are fit using a global Gaddum/Schild model. The Schild plots for GLPG0974 versus C3 (B) and compound 1 (D) are shown. The dose ratio (DR) equals A'/A with A representing the agonist EC_{50} without antagonist and A' the agonist EC_{50} with antagonist. Values were calculated for each agonist concentration response with antagonist present and plotted against the logarithm of antagonist concentration. The slope and X-intercept were determined by linear regression.

(Figure 3.9C) and a Schild slope of 1.09 with an estimated pA_2 of 8.0 (= 10 nM) (Figure 3.9D). These pA_2 values match very well with the affinity determined in the [3H]-GLPG0974 binding assay ($K_d = 7.5 \pm 0.4$ nM), which is a further indication of competitive antagonism.

3.2.4 Effect of carboxylate moiety modifications on FFA2 antagonists

Almost all available orthosteric FFA2 ligands contain a carboxylate moiety, which is thought to be important for the orthosteric interaction of the SCFA carboxylate with a pair of arginines, Arg180^{5.39} and Arg255^{7.35}, within the core orthosteric binding pocket (Stoddart et al., 2008, Hudson et al., 2013a). However, the recently published BTI-A series of FFA2 antagonists behave as orthosteric ligands despite the lack of a carboxylate group (Park et al., 2016). To explore the importance of this structural feature for binding and function of the GLPG0974 and CATPB series, the carboxylate moiety of two GLPG0974 analogues, GLPG-1 and GLPG-2, and of CATPB was replaced with a methyl ester (Me) (Table 3.7). In the case of GLPG-2 a further analogue was generated with a

Table 3.7 Impact of carboxylate moiety modifications on hFFA2 antagonist function

	 GLPG-1^a	 GLPG-2^a	 CATPB^a
 Carboxyl	6.98 ± 0.03	7.31 ± 0.01	6.65 ± 0.04
 Methyl ester (Me)	5.87 ± 0.08***	6.08 ± 0.07***	5.70 ± 0.11***
 Morpholine (Mo)		6.23 ± 0.06***	

^a Data shown as pIC_{50} values determined in β -arrestin 2 recruitment assays in presence of an approximate EC_{80} concentration of C3

* Statistical significance was determined by unpaired t test comparing analogue pIC_{50} to carboxylate pIC_{50} is denoted as $P = *** \leq 0.001$

morpholine (Mo) in place of the carboxylate, which features a heterocycle and is therefore significantly bulkier than the carboxylate moiety. All methyl ester analogues retained the ability to inhibit the C3-induced responses of hFFA2 in a concentration-dependent fashion (**Figure 3.10**), however, with an approximately 10-fold reduction in pIC_{50} (**Table 3.7**). Interestingly, replacement of the carboxylate moiety with a morpholine instead of a methyl ester had a similar effect (**Figure 3.10B**) and the pIC_{50} value of MoGLPG-2 was slightly higher than that of MeGLPG-2 (**Table 3.7**).

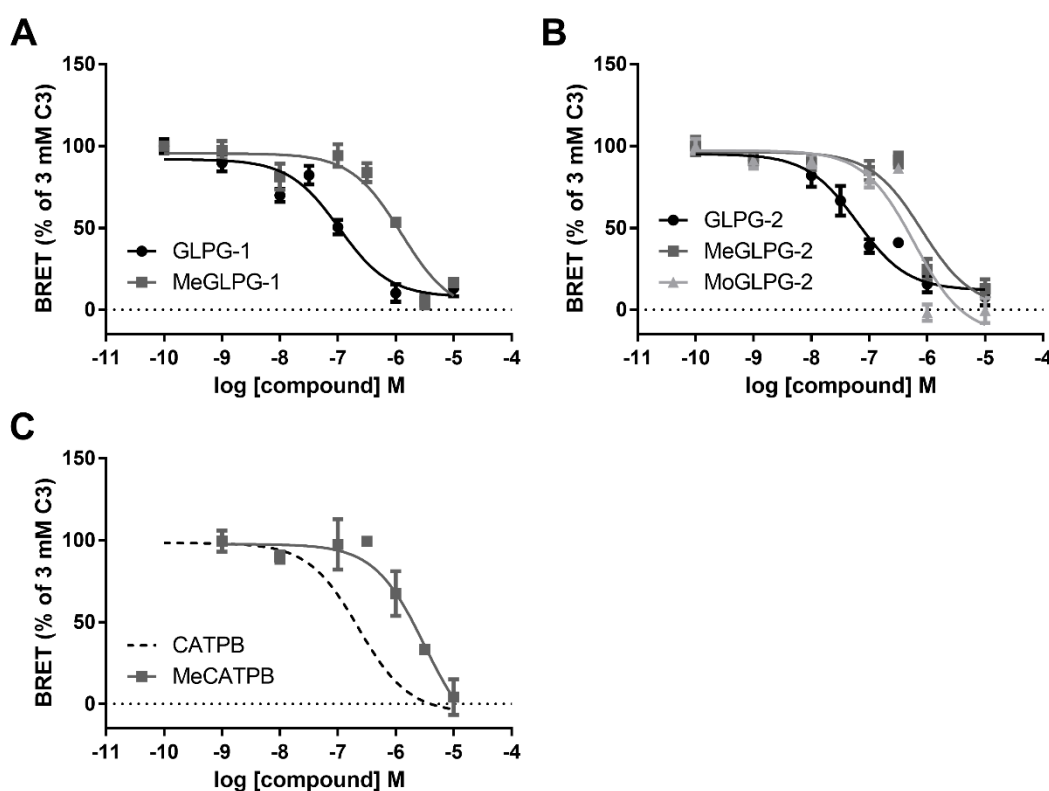


Figure 3.10 Importance of carboxylate moiety for hFFA2 antagonist action The capacity of the synthetic antagonists GLPG-1 and MeGLPG-1 (**A**); GLPG-2, MeGLPG-2 and MoGLPG-2 (**B**); and CATPB and MeCATPB (**C**) to inhibit the response of hFFA2 to C3 in β -arrestin 2 recruitment assays is shown. HEK293T cells were transiently co-transfected with hFFA2-eYFP and RLuc-tagged β -arrestin 2. All data are means pooled from independent experiments ($n \geq 3$) that were performed in triplicate. Dashed lines indicate that data was shown previously, in this case in figure 3.4D. Me = methyl ester; Mo = morpholine.

3.3 Discussion

3.3.1 Use of multiple screening assays is important for promiscuous receptors

The important role of GPCRs in therapeutic development as the largest family of drug targets in the human genome (see section 1.1.3) has certainly contributed

to motivating scientific advances in assay systems that can be employed to investigate GPCR signalling and to test compound series. Depending on the aim different priorities apply to selection of an assay format (Hughes et al., 2011), however likely the most important properties are reproducibility, resulting data quality and translational relevance in the context of the disease to be treated, if known. For GPCRs that couple to multiple signalling pathways it can be particularly important to assess ligands in several assays, however it is not always feasible or necessary to perform screening across all available formats. As FFA2 is able to couple to multiple G proteins and recruits β -arrestin 2 in response to agonists (Stoddart et al., 2008, Hudson et al., 2013a, Brown et al., 2003), a selection of relevant assays were employed to assess available reference ligands: Radioligand competition to measure affinity; and $G_{i/o}$ -coupled [^{35}S]-GTP γ S binding and cAMP inhibition, G_q -coupled IP1 accumulation and β -arrestin 2 recruitment assays to detect functional responses. [^{35}S]-GTP γ S binding and cAMP inhibition resulted in equivalent potencies for both C3 and compound 1 in these assays, which is in agreement with the ability of both assays to detect activation of $G_{i/o}$ G proteins. This perhaps appears unexpected as [^{35}S]-GTP γ S assays detect an early event after GPCR activation and were therefore thought to be less subject to amplification, which is certainly the case for inhibition of cAMP (Zhang and Xie, 2012). However, it has been demonstrated that a GPCR is capable of activating more than a single copy of a G protein, depending on the respective receptor and G protein subtype (Ross, 2014). Therefore, measurement of [^{35}S]-GTP γ S incorporation may also be subject to amplification. It also appears to be a suitable assay for measurement of inhibition of agonist responses by antagonists and in the case of FFA2 it also allows detection of inverse agonists. The cAMP inhibition assay measures the inhibition of adenylyl cyclase by $G_{i/o}$ G proteins. Detection of G_s -dependent cAMP production is relatively straightforward, but to measure cAMP inhibition it first needs to be stimulated, commonly by treatment with forskolin that activates adenylyl cyclase (Zhang and Xie, 2012). This does not appear to be an issue for assessment of FFA2 agonists, as measured potencies mirrored values in the [^{35}S]-GTP γ S binding assay, making the cAMP inhibition assay a good alternative measure of $G_{i/o}$ activation that does not require use of radioactivity or a filtration step. However, the requirement for pre-stimulation with forskolin makes detection of antagonist action more problematic, as it involves the

reversal of the inhibition of an artificially stimulated signal. The extreme inverse agonism produced by FFA2 antagonists, and the corresponding reduced pIC_{50} values compared to the [^{35}S]-GTP γ S binding assay, is hence more likely to be an assay artifact rather than true pharmacological behaviour, therefore a different assay format for assessment of FFA2 antagonists is recommended.

The IP1 accumulation assay detects the level of inositol monophosphates, which reflects degradation of inositol 1,4,5-trisphosphate (IP $_3$) produced by $G_{q/11}$ -dependent hydrolysis of phosphatidylinositol-4,5-bisphosphate (PIP $_2$) into IP $_3$ and diacylglycerol by phospholipase C (Berridge, 1993). FFA2 agonists showed the highest potency in this assay, most likely due to the high level of amplification from GPCR activation (Bergsdorf et al., 2008), and it also appears to be an appropriate assay for detection of antagonist inhibition. Due to the relatively slow binding kinetics of GLPG0974, the IP1 assay is preferable to a Ca $^{2+}$ release assay, which is a more rapid and transient $G_{q/11}$ -dependent response that allows little time for ligand binding equilibration (Zhang and Xie, 2012). Finally, the BRET-based β -arrestin 2 recruitment assay measures a G protein-independent result of GPCR activation. Each GPCR can only bind one β -arrestin adapter protein (Lohse and Hoffmann, 2014), therefore the potency of agonists in a β -arrestin recruitment assay should conceptually be a close estimate of their affinity. This was indeed the case for C3, with its potency in the β -arrestin 2 recruitment assay coming closest to its measured affinity. In contrast, compound 1 showed a significantly lower potency in the β -arrestin 2 recruitment assay compared to its affinity. This divergence could perhaps be explained by differences in binding kinetics of compound 1 versus C3. SCFAs are small compounds and will likely bind the receptor with a diffusion-limited rate. In contrast, compound 1 will undoubtedly interact with additional residues within the binding pocket, resulting in an increased affinity over C3, but it is likely to require more time to fully associate with the receptor. However, more detailed studies would be necessary to investigate this hypothesis. For antagonists the pIC_{50} does not serve as an estimate of affinity, as it is dependent on the concentration of agonist, and other experimental approaches are usually employed to obtain an estimate of affinity in terms of pA_2 from functional assays, as will be discussed in the following section (Lazareno and Birdsall, 1993). The pIC_{50} values of CATPB were not significantly different across the assay

systems employed, in contrast GLPG0974 showed more variation. While the low IC_{50} in the cAMP inhibition assay is likely due to the observed artificial inverse agonism, the significantly higher value in the β -arrestin 2 recruitment assay is more difficult to explain. However, it may relate to observations that will be discussed in the next section.

Based on the knowledge gained from the screening of reference agonists in selected assay systems, the cAMP inhibition and β -arrestin 2 recruitment assays were selected to screen a series of ligands based on compound 2, which has recently been employed in an *in vivo* study in mice (Forbes et al., 2015). Thereby, the capacity of the tested compounds to activate pathways dependent and independent of G protein signalling were assessed. Various modifications of different regions of the molecule resulted in the synthesis of compound 2-23, an FFA2 agonist with highly improved potency in the cAMP inhibition assay and modest potency improvement in the β -arrestin 2 recruitment assay. Introduction of a more polar group in the northern part of the molecule resulted in a reduction of the compound ClogP to 3.73, suggesting improved hydrophilicity and placing compound 2-23 within the Lipinski Rules for drug-like molecules (Lipinski et al., 2001). The correlation of compound 2-23 potencies and affinity is similar to that of compound 1, with a lower potency in the β -arrestin 2 recruitment assay compared to the cAMP inhibition assay and its affinity more closely approximated by the G protein-dependent assay system. Perhaps this may, as proposed for compound 1, be explained by differences in the ligand binding kinetics compared to C3. In general, when considering the full selection of screened compounds, it is difficult to construct a full SAR of the compound 2 ligand series as most of the compounds have relatively similar potency with a fairly flat SAR and as a result it is difficult to define clear trends. The core structure of the compound series consists of one central pyrroline or thiazolidine and two northern and one eastern aromatic rings with five or six carbon members and different substitutions. Replacement of either of the terminal aromatic rings with a hydrogen (compound 2-10) or butyl groups (compounds 2-8 and 2-9) resulted in loss of agonist action. Furthermore, the variation of potencies between the different functional analogues was relatively small and considering the, in some cases, high error it is challenging to pinpoint which structural changes relate to effects on potency, in particular due to the poor

correlation between the two functional assay systems when including all tested compounds.

Although compound 2-23 can be considered an improvement of compound 2, its potential use in the physiological characterisation of FFA2 is limited by species-specific differences. Screening of a selection of compound 2 analogues at the murine orthologue of FFA2 demonstrated a different potency rank order compared to the human receptor. Perhaps this is not surprising, considering that even SCFAs have a different rank order of potency at mFFA2 compared to hFFA2 and there are clear differences in constitutive receptor activity between the two orthologues (Hudson et al., 2012b). Furthermore, an analogue of compound 1 (here referred to as compound 1-2) also showed a reduced potency at mFFA2 compared to hFFA2 (Hudson et al., 2013a).

Based on these results, which assay could be recommended for screening of FFA2 agonist ligands? As the ability to activate the receptor is an essential feature of an agonist, performing an initial screen in a functional assay system seems reasonable. The use of an assay further downstream of GPCR activation, such as cAMP inhibition, appears to yield a larger spread of potency values due to increased amplification, which may facilitate SAR investigations of the tested compound series. Although screening of selected compounds in multiple assay systems can be of value to obtain more information on compound SAR and aids the identification of ligands with a biased signalling profile, conflicting potency trends can complicate chemistry decisions. Therefore, it would likely be best to base medicinal chemistry optimisation on only one assay system, however screening selected key compounds with representative structural modifications in an additional assay to confirm whether the SAR is conserved across multiple systems would be recommended. Another crucial consideration of ligand screening that is easily overlooked is whether the assay end point is close to equilibrium binding of the ligands. A recent study on dopamine receptor agonists revealed that apparent signalling bias can be heavily dependent on agonist kinetics and the time point at which agonist response is measured (Klein Herenbrink et al., 2016). Choosing an assay system that allows a long test compound incubation time at a reasonably high temperature could circumvent bias artifacts due to non-equilibrated ligand binding.

3.3.2 Hemi-equilibrium conditions can affect investigations of antagonist pharmacology

Although many questions remain regarding the physiological role of FFA2, its ability to promote recruitment of neutrophils to sites of infection seems to be generally accepted and has raised interest in FFA2 antagonists as potential therapeutics (Pizzonero et al., 2014). GLPG0974 was the first FFA2 antagonist to reach clinical trials (Vermeire et al., 2015), however apart from its ability to inhibit neutrophil migration and its selectivity for the human over rodent forms of FFA2 (Pizzonero et al., 2014), there is little information available on its pharmacology. A common means of investigating antagonist pharmacology in the context of the employed agonist is to assess the effect of increasing antagonist concentrations on the agonist concentration response (Lazareno and Birdsall, 1993). This provides information not only on whether the antagonist effect is surmountable and, therefore, most likely competitive with the tested agonist, but also allows estimation of antagonist affinity. Initial radioligand binding assays employing a tritiated form of GLPG0974 indicated competitive behaviour with SCFA C3 and synthetic orthosteric agonist compound 1, which supports a competitive relationship. However, an initial experiment in a β -arrestin 2 recruitment assay showed that GLPG0974 antagonism was insurmountable by C3 and that increasing concentrations of GLPG0974 induced a depression in maximal response. Such a curve pattern is typical of allosteric non-competitive antagonists or competitive antagonists that bind irreversibly (Vauquelin et al., 2002). This would be highly unexpected for GLPG0974, in particular as this was not observed with compound 1. What hypothesis would be able to explain these observations? Although GLPG0974 being an allosteric ligand is perhaps the first conclusion to be drawn, other pharmacological concepts can also explain such observations (Vauquelin et al., 2002). Kinetic binding assays with [^3H]-GLPG0974 showed that GLPG0974 has a slow dissociation rate and perhaps the β -arrestin 2 recruitment assay does not allow for sufficient equilibration time between agonist and antagonist binding, resulting in a measurement at a state of hemi-equilibrium, as the recruitment of β -arrestin is measured only 5 min after agonist addition with a 15 min pre-incubation with antagonist. This is a well-known problem for calcium release assays, which is usually measured rapidly after ligand addition (Charlton and Vauquelin, 2010). Furthermore, a state of

hemi-equilibrium could also account for the increased pIC_{50} value of GLPG0974 observed in the β -arrestin 2 recruitment assay compared with CATPB.

To assess whether a state of hemi-equilibrium is indeed the reason for the apparent insurmountable antagonism of GLPG0974 on C3, a different assay system was employed to perform the experiment, which detects the accumulation of phosphorylated ERK1/2 MAP kinases. This assay was selected as it allows longer incubation times of agonist and antagonist and in this case, antagonist was pre-incubated for 1 h followed by a 30 min incubation with agonist. When performing experiments in this fashion, GLPG0974 induced a rightward shift of the C3 concentration response curve and increasing concentrations of C3 were able to overcome inhibition by GLPG0974, fully in agreement with expectations of competitive antagonism (Colquhoun, 2007). The slope of the resulting Schild plot also approximated unity, a further indication of competitive antagonism, and the pA_2 values from Schild plots against C3 and compound 1 matched the affinity of [3H]-GLPG0974 determined in saturation binding assays very closely.

In contrast to GLPG0974, CATPB behaved as a competitive antagonist in the β -arrestin 2 recruitment assay. If the insurmountable antagonism of GLPG0974 was indeed a reflection of slow dissociation kinetics this would imply that the dissociation rate of CATPB is faster compared to GLPG0974, despite the essentially identical affinity of the two antagonists for the receptor. The residence time of ligands at their receptor is an emerging topic in drug discovery and is thought to be an increasingly important consideration for successful drug development (Hothersall et al., 2016, Hoffmann et al., 2015). Chapter 4 will explore this hypothesis further and employ [3H]-GLPG0974 to investigate the binding kinetics of different FFA2 ligands.

3.3.3 Carboxylate moiety contributes to binding of FFA2 antagonists, but is not essential

One structural feature shared by most orthosteric FFA2 ligands is a carboxylate moiety. SCFAs, whose only functional group is a carboxylate, bind to FFA2 by interacting with a pair of arginine residues, Arg180^{5.39} and Arg 255^{7.35}, and histidine residue His242^{6.55} (Stoddart et al., 2008), whilst activation of FFA2 by

synthetic agonist compound 1 is also dependent on the same residues (Hudson et al., 2013a). The agonism of the allosteric FFA2 ligands 4-CMTB (Smith et al., 2011) and AZ1729 (Bolognini et al., 2016a) is, by contrast, not affected by alanine replacement of these residues and their structures do not contain a carboxylate moiety, therefore this structural feature has been hypothesised to be defining for orthosteric FFA2 ligands. However, the lack of agonist action at respective alanine replacement mutants prohibited the testing of antagonist inhibition, therefore the importance of the carboxylate moiety in antagonist ligands remained unexplored. Interestingly, a recently published antagonist series lacked a carboxylate moiety and still appeared to behave as competitive antagonists of C3 (Park et al., 2016). An exploration of the GLPG0974 and CATPB compound series revealed that replacement of the carboxylate with a methyl ester moiety resulted in reduced pIC₅₀ values for both antagonist series. However, the compounds retained the ability to inhibit the FFA2 response to C3 in a concentration-dependent manner. Interestingly, larger modifications, i.e. introduction of a morpholine in the case of MoGLPG-2, did not significantly affect the pIC₅₀ in comparison to the methyl ester analogue MeGLPG-2. Nevertheless, the significant reduction in pIC₅₀ upon replacement of the carboxylate moiety suggests that the arginine pair potentially serves as an important point of antagonist interaction with the receptor that contributes to their high affinity but is not required for binding and receptor blockade. Interestingly, replacement of the compound 1-2 carboxylate with a methyl and *tert*-butyl ester rendered the ligand non-functional (Hudson et al., 2013a). This served as a first indication of potentially different interactions of agonists and antagonists with the receptor. Availability of a labelled probe such as [³H]-GLPG0974 provides a great opportunity to explore the binding of FFA2 antagonists in more detail and will be discussed in chapter 4. Following this investigation, the development of GLPG0974 was published and, interestingly, the original hit compound did also not contain a carboxylate moiety, supporting that activity of the GLPG0974 compound series is indeed not dependent on the presence of a carboxylate (Pizzonero et al., 2014).

3.3.4 Conclusions

One of the key questions that needs to be addressed for successful FFA2 drug development is whether FFA2 is indeed a realistic therapeutic target and which

pharmaceutical action in which disease context would be desirable for therapeutic benefit. The physiological roles of FFA2 remain to be fully understood (see section 1.4.2) and that makes it difficult to answer this question. While studies in KO animals can and have provided important information on the function of FFA2, the lack of appropriate tool compounds has hindered confirmation of the therapeutic potential of FFA2 in animal models of disease. Identification of novel ligands often falls to pharmaceutical companies capable of performing high-throughput screening of large compound libraries, usually with the aim to identify a hit compound that can be developed into a therapeutic candidate. Medicinal chemistry optimisation of compound series plays an important role in this process and can lead to development of improved ligands, as here demonstrated with compound 2-23. However, cross-screening of compound 2 analogues at the murine orthologue of FFA2 has highlighted one important issue: Compound SAR can differ between species. This suggests that development of a potential therapeutic that acts on human FFA2 does not necessarily coincide with an improved ligand that can be employed in rodent studies. However, there is a great need for such tool compounds to confirm the therapeutic potential of FFA2, therefore it may be of interest to perform an SAR study at the murine orthologue with the aim to develop a ligand specifically for *in vivo* use in animal models of disease. Particularly the development of ligands biased towards specific pathways such as $G_{i/o}$ - or $G_{q/11}$ -mediated signalling could provide further information on which pathways mediate which physiological effects of FFA2, which could in turn guide the selection of an appropriate screening system for the desired signalling profile. Species selectivity of ligands is even more relevant for the development of FFA2 antagonists, as all currently available antagonists are selective for the human orthologue. The molecular basis of this will be considered in chapter 6.

The screening of FFA2 agonists and pharmacological investigation of the mode of action of FFA2 antagonists also revealed that considering the kinetics of ligand association and dissociation can be very important. While the aspect of ligand kinetics may not play as crucial a role when single concentrations of ligands are tested for activity in high-throughput systems, the lack of kinetic considerations can lead to skewed potency values upon closer investigation and can even result in erroneous conclusions, such as the insurmountable inhibitory effect of

GLPG0974 on C3 in the β -arrestin recruitment assay that may be interpreted as non-competitive antagonism. Therefore, conditions of hemi-equilibrium should be avoided when possible and carefully considered when drawing conclusions regarding ligand pharmacology.

4 Defining molecular and kinetic determinants of FFA2 ligand binding using [³H]-GLPG0974

4.1 Introduction

Mapping the ligand binding sites of GPCRs can play an important role in drug discovery, in particular in the process of compound optimisation. Although it is not essential to define the entire binding site of a future therapeutic, it can greatly contribute to the development of a lead compound and is an important component of the structure-based drug design approach. Detailed information on ligand-receptor interactions can be obtained from crystal structures of GPCRs complexed with respective ligands, however these only exist for a small number of GPCRs with a total of only 43 unique receptor-ligand complexes published to date (Isberg et al., 2016). Therefore, the majority of efforts to define the binding site of GPCR ligands are based on functional and binding data, which often include the use of site-directed mutagenesis to generate specific mutations in the receptor of interest and the assessment of their effect on ligand affinity and efficacy. Due to a lack of structural information on FFA2, such an approach has been employed to assess its orthosteric and allosteric binding sites (Stoddart et al., 2008, Schmidt et al., 2011, Smith et al., 2011, Hudson et al., 2013a, Bolognini et al., 2016a). FFA2 is endogenously activated by SCFAs, which can form an electrostatic interaction with positively charged residues through their carboxylate moiety. In an effort to identify the point of SCFA carboxylate interaction with FFA2, the effect of alanine replacement of positively charged residues that were thought to be ligand-accessible was investigated and resulted in the identification of two arginine residues, Arg180^{5.39} and Arg255^{7.35} (Stoddart et al., 2008). Mutation of either of these arginines resulted in loss of FFA2 activation by SCFAs (Stoddart et al., 2008) and synthetic agonist compound 1 (Hudson et al., 2013a). Furthermore, His242^{6.55} was also essential for activation of FFA2 by SCFAs (Stoddart et al., 2008) and compound 1 (Hudson et al., 2013a). These observations seemed to define the essential importance of the carboxylate moiety for FFA2 agonist activity. Replacement of the carboxylate of SCFAs with an amine renders them inactive (Schmidt et al., 2011) and methyl and *tert*-butyl ester analogues of compound 1-2 lack ability to activate FFA2 (Hudson et al., 2013a). Therefore, there is a consensus that orthosteric FFA2 agonists are defined by their ability to form an

interaction with Arg180^{5.39} and Arg255^{7.35} through their carboxylate moiety. This hypothesis is further supported by the fact that allosteric agonists of FFA2, 4-CMTB (Smith et al., 2011) and AZ1729 (Bolognini et al., 2016a), do not contain a carboxylate and retained the capacity to activate R180A and R255A hFFA2.

While agonist binding to hFFA2 appears to be relatively well understood, there is little information on the binding determinants of the FFA2 antagonists GLPG0974 and CATPB. Defining how antagonists interact with hFFA2 is of high importance, as the lack of available antagonists at rodent FFA2 has hindered progress in dissecting the physiological role of FFA2 (Hudson et al., 2012b, Pizzonero et al., 2014, Milligan et al., 2017). Selected studies (Pizzonero et al., 2014, Park et al., 2016) and data presented in chapter 3 suggested that the carboxylate interaction with the orthosteric arginine pair is of lesser importance for FFA2 antagonists than agonists. Replacement of the carboxylate of GLPG0974 analogues with a methyl ester or morpholine group only had a modest effect on their ability to inhibit the hFFA2 response to C3 (see section 3.2.4) and multiple active non-carboxylate analogues were synthesised during the development of GLPG0974 (Pizzonero et al., 2014). Furthermore, the recently published BTI-A series of FFA2 antagonists also do not contain a carboxylate moiety (Park et al., 2016). However, it is difficult to assess whether binding of FFA2 antagonists is similarly affected by orthosteric arginine mutations as the potency of FFA2 agonists, because the loss of agonist action at respective mutants prohibits assessment of the inhibitory action of antagonists.

Another aspect of GPCR ligand binding that has recently attracted a lot of attention is binding kinetics (Hoffmann et al., 2015). There is a body of evidence developing which suggests that in the case of agonists an increased residence time at the receptor positively correlates with functional efficacy (Guo et al., 2012) and that optimising agonist kinetics to achieve a prolonged residence time could contribute to improvement of sustained signalling by internalised receptors (Hothersall et al., 2016). However, there is also evidence that the binding kinetics of antagonists plays an important role in defining their therapeutic benefit. There seems to be a clear relationship between antagonist residence time and its clinical application (Guo et al., 2014). The muscarinic M₃ receptor antagonist tiotropium, which has a residence time of 35 h, is best-in-

class for management of chronic obstructive pulmonary disease and provides a durable bronchodilatory effect (Casarosa et al., 2009). In contrast, for targeting of the dopamine D₂ receptor in psychotic disorders with antagonists, a shorter residence time is more desirable to prevent on-target side effects. The D₂R antagonist JNJ-37822681 was specifically developed using a kinetic screening assay to optimise for a short residence time and showed a dissociation half-time of 6.5 s in kinetic radioligand binding studies (Langlois et al., 2012). In following clinical trials an improved tolerability over haloperidol, which has a half-time of 72 s (Schmidt et al., 2012), could be observed. These studies represent only some of the examples that suggest that residence time can be an important factor in the clinical success of therapeutics (Guo et al., 2014). Although in the case of FFA2 it is perhaps not clear whether a short or long drug residence time would be therapeutically beneficial, defining the kinetic profile of antagonists is undoubtedly important and may contribute to targeted development of a potential therapeutic. In addition, furthering the understanding of the kinetic profile of FFA2 activation or inhibition that would be desirable in the respective disease context could serve as a guide for future drug development.

This chapter aims to characterise two important aspects of FFA2 ligand binding: (1) The determinants of FFA2 agonist and antagonist binding and (2) the kinetic profile of FFA2 antagonists. The tritiated FFA2 antagonist [³H]-GLPG0974 played a key role in this investigation, as it allowed the assessment of antagonist binding to orthosteric binding site mutants R180A, R255A and H242A hFFA2 and the effect of respective mutations on the affinity of unlabelled ligands C3, compound 1 and CATPB. Furthermore, the contribution of the FFA2 antagonist carboxylate moiety to binding affinity was investigated using a selection of analogues and served as a support for data from functional studies (see section 3.2.4). To rationalise observations described in previous chapters and functional studies (Stoddart et al., 2008, Hudson et al., 2013a), a homology model of hFFA2 was constructed using the recently published crystal structure of hFFA1 as a template (Srivastava et al., 2014). Various aspects of [³H]-GLPG0974 kinetics were also investigated, including the role of the orthosteric arginine pair in regulating the kinetics of radioligand binding and how different FFA2 ligands impact the dissociation rate of [³H]-GLPG0974. Furthermore, the kinetic profile

of the GLPG0974 and CATPB antagonist series was defined in an effort to understand previous observations in functional studies (see section 3.2.3).

4.2 Results

4.2.1 Binding of [³H]-GLPG0974 to hFFA2 does not require both orthosteric arginine residues

In chapter 3 a hFFA2 binding assay was developed using the tritiated antagonist [³H]-GLPG0974 and served as a tool to determine the affinity of compounds in an agonist screen (see section 3.2.2). However, in addition to compound screening, radioligands can also play a crucial role in the mapping of ligand binding sites. While the importance of the orthosteric residues Arg180^{5.39}, Arg255^{7.35} and H242^{6.55} for hFFA2 activation by agonists has been demonstrated (Stoddart et al., 2008, Hudson et al., 2013a), to date it is not clear whether antagonist binding also relies on electrostatic interaction between the carboxylate moiety and the Arg180-Arg255-His242 triad. Therefore, [³H]-GLPG0974 was employed as a representative antagonist to examine its binding to membranes purified from cells expressing orthosteric binding site mutants of hFFA2. Interestingly, [³H]-GLPG0974 retained the ability to bind the single mutants R180A (**Figure 4.1B**) and R255A (**Figure 4.1C**) hFFA2 with a relatively minor decrease in binding affinity of 2.9- and 1.7-fold, respectively (**Table 4.1**). Alanine replacement of Arg180^{5.39} affected binding of [³H]-GLPG0974 to a larger extent, therefore it perhaps plays a more important role than Arg255^{7.35} in anchoring the radioligand. In contrast, specific binding of [³H]-GLPG0974 to the dual mutant R180A-R255A hFFA2 could not be detected at concentrations of up to 80 nM (**Figure 4.1D**), suggesting that [³H]-GLPG0974 binding requires at least one orthosteric arginine. Mutation of His242^{6.55}, a further residue necessary for hFFA2 activation by agonists, to alanine did also not negatively impact [³H]-GLPG0974 affinity (**Figure 4.1E**). On the contrary, affinity of the radioligand was increased by 2-fold compared to wild type hFFA2 (**Table 4.1**). To confirm that the lack of specific binding of [³H]-GLPG0974 to hFFA2-R180A-R255A was not related to a lack of expression of this hFFA2 mutant, receptor expression was assessed by measuring the fluorescence intensity of the eYFP tag in purified membranes. Indeed, all orthosteric binding site mutants of hFFA2 were expressed at a similar or even increased level compared to the wild type receptor (**Table 4.1**).

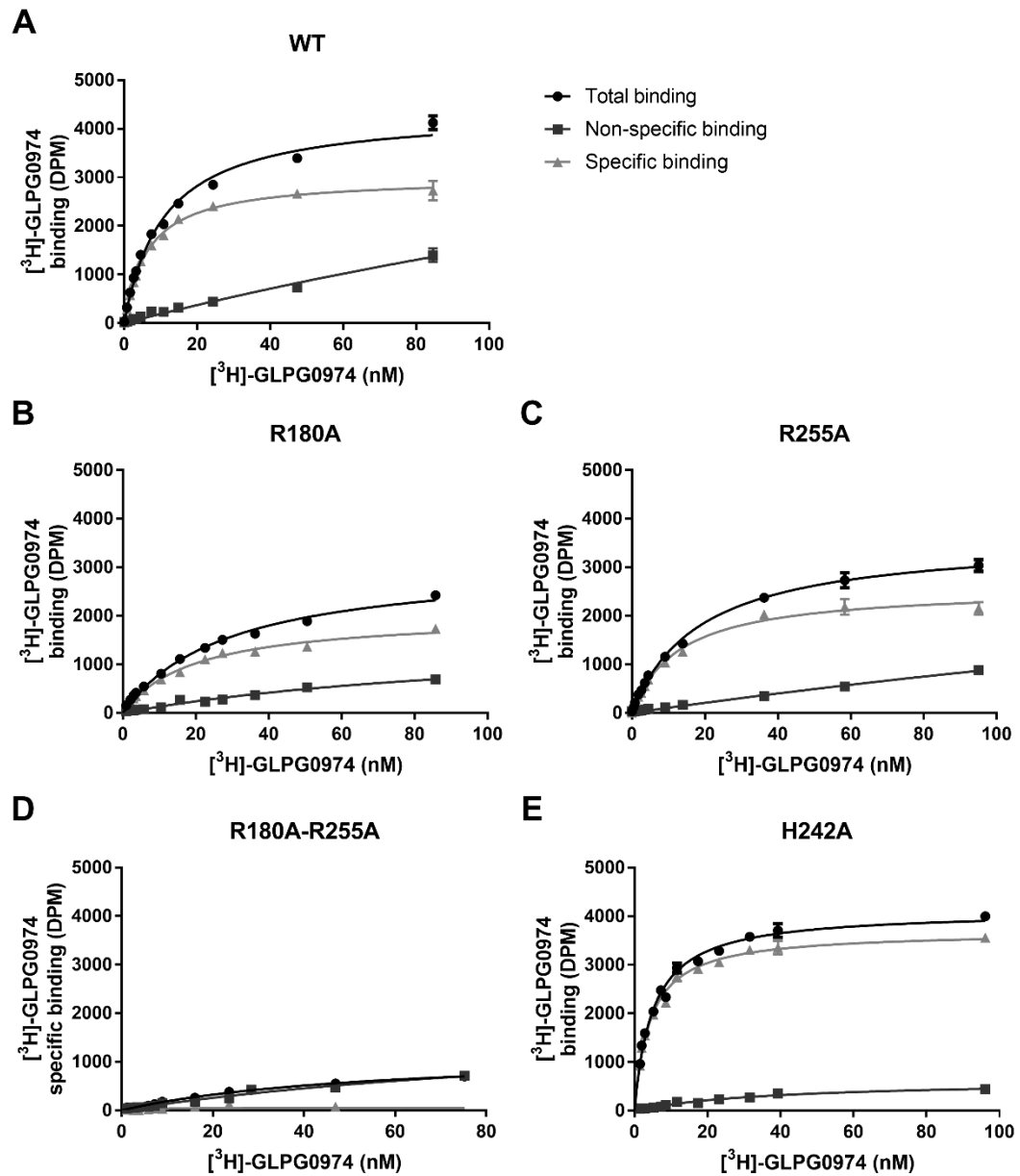


Figure 4.1 Binding characteristics of $[^3\text{H}]\text{-GLPG0974}$ to orthosteric binding site mutants of hFFA2 Binding of $[^3\text{H}]\text{-GLPG0974}$ to membranes purified from Flp-InTM T-RExTM 293 cells induced to express wild type (A) or mutant forms of hFFA2-eYFP with alanine replacement of Arg180^{5.39} (B), Arg255^{7.35} (C) Arg180^{5.39} and Arg255^{7.35} (D) or His242^{6.55} (E) is illustrated from representative experiments. No specific binding to hFFA2-R180A-R255A could be measured. Nonspecific binding was determined in presence of 10 μM CATPB and subtracted from total binding to calculate specific binding. Data in panel A was previously shown in figure 3.2C.

Therefore, loss of specific radioligand binding at hFFA2-R180A-R255A cannot be attributed to lack of receptor expression and confirms loss of $[^3\text{H}]\text{-GLPG0973}$ binding to this mutant.

Table 4.1 Affinity of [³H]-GLPG0974 for orthosteric binding site mutants of hFFA2

Receptor	K _d (nM)	Expression ^a
WT	7.5 ± 0.4	373 ± 7
R180A	21.8 ± 1.3 ^{***}	409 ± 11
R255A	13.0 ± 0.5 ^{***}	465 ± 18
R180A-R255A	> 80	405 ± 7
H242A	3.7 ± 0.3 ^{**}	794 ± 38

^a Determined by measuring eYFP fluorescence of 5 µg membrane preparation and shown in relative fluorescent units.

* Analysis of K_d values by one-way ANOVA followed by Dunnett's test with the K_d at WT hFFA2 as a reference with significant differences denoted as P = ** ≤ 0.01 and P = *** ≤ 0.001

4.2.2 FFA2 agonists and antagonists have different binding determinants

Because [³H]-GLPG0974 retained the ability to bind to single orthosteric binding site mutants of hFFA2, the importance of these residues for binding of other hFFA2 ligands could be examined using a radioligand competition binding assay. Initially, the capacity of increasing concentrations of the agonists C3 (**Figure 4.2A**) and compound 1 (**Figure 4.2B**) to compete with [³H]-GLPG0974 at each of R180A, R255A and H242A hFFA2 was assessed. Only minimal displacement of [³H]-GLPG0974 at the orthosteric binding site mutants was observed at the highest concentrations of C3 and compound 1 employed, suggesting that the affinity of FFA2 agonists was markedly reduced. Therefore, the loss of agonist function at each of these mutants described previously (Stoddart et al., 2008, Hudson et al., 2013a) resulted from a decrease in agonist affinity and was not due to an inability of ligand binding to induce receptor activation.

In contrast, the hFFA2 antagonist CATPB, which is structurally distinct from GLPG0974, retained the ability to displace [³H]-GLPG0974 from mutant forms of the receptor (**Figure 4.2C**). The effects of orthosteric binding site mutations on CATPB affinity were much more modest with a 3.5-fold reduction at R180A FFA2 and a decrease of 7.8-fold at R255A hFFA2, suggesting that CATPB might preferentially interact with Arg255^{7.35} (**Table 4.2**). Interestingly, this trend is opposite to the impact of the respective arginine mutations on [³H]-GLPG0974 affinity, which was most affected by alanine replacement of Arg180^{5.39} (**Table 4.1**). In the case of the H242A hFFA2 mutant, affinity of CATPB was not significantly affected, hence this residue is not likely to play a role in CATPB binding (**Table 4.2**). An equivalent competition experiment was performed with

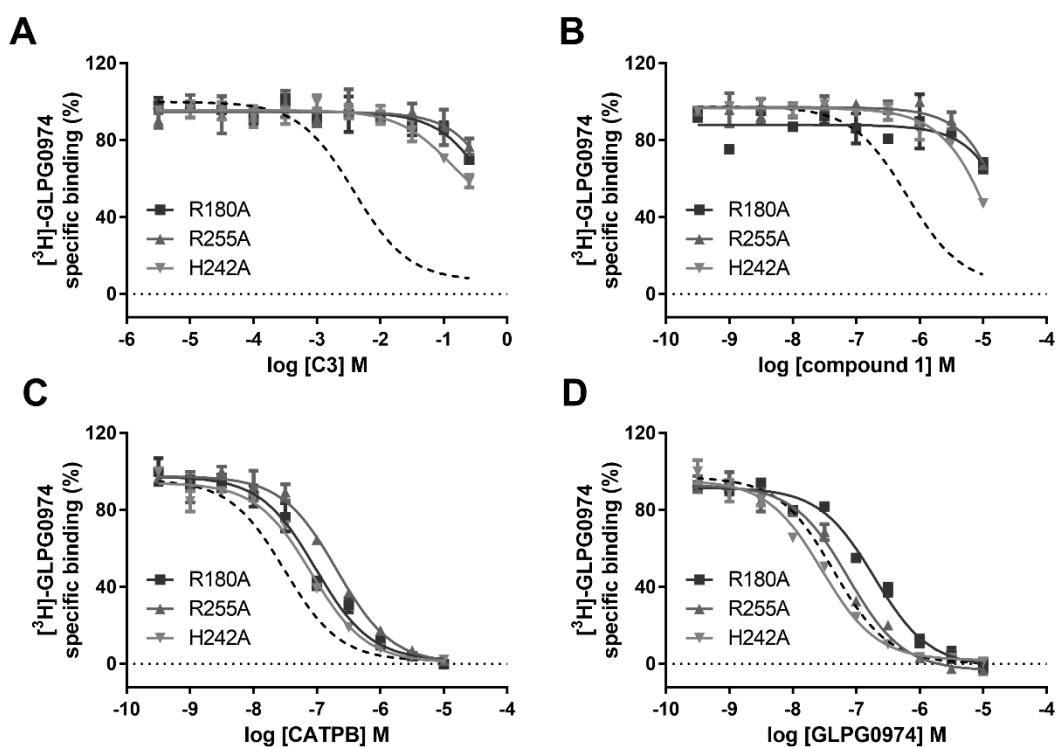
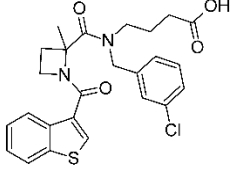
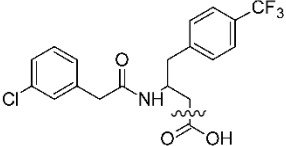
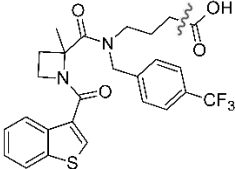
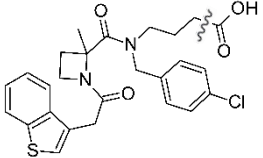


Figure 4.2 Agonists but not antagonists of hFFA2 show reduced ability to compete with $[^3\text{H}]$ -GLPG0974 at receptor binding site mutants The capacity of C3 (A), compound 1 (B), CATPB (C) and GLPG0974 (D) to compete with $[^3\text{H}]$ -GLPG0974 for binding to R180A, R255A or H242A hFFA2-eYFP is shown from representative experiments. For comparison the displacement of $[^3\text{H}]$ -GLPG0974 by respective ligands at WT is also illustrated (---) with original data shown in figure 3.2 of chapter 3. Nonspecific binding was determined in presence of 10 μM CATPB and subtracted from total binding to calculate specific binding.

GLPG0974 as the displacing ligand (Figure 4.2D). No significant loss in affinity of GLPG0974 was observed at R255A or H242A hFFA2, however the R180A mutation resulted in a 5.5-fold reduction in affinity (Table 4.2). These observations are in agreement with the saturation binding data obtained for $[^3\text{H}]$ -GLPG0974 and although the minor reduction in GLPG0974 affinity at R255A and increase at H242A were not statistically significant, the same trend could be observed in the $[^3\text{H}]$ -GLPG0974 saturation binding experiments. The differences in affinity of CATPB and GLPG0974 at the orthosteric arginine mutants suggest that although both antagonists had the same affinity for the wild type receptor, they might adopt different binding poses, with CATPB interacting preferentially with Arg255^{7,35} and GLPG0974 with Arg180^{5,39}.

Table 4.2 Affinity of hFFA2 antagonist analogues for wild type and orthosteric binding site mutants of hFFA2

Compound	Receptor ^a			
	WT	R180A	R255A	H242A
 GLPG0974	7.88 ± 0.08	7.14 ± 0.06 ^{***}	7.59 ± 0.09	8.04 ± 0.04
 CATPB	7.87 ± 0.08	7.32 ± 0.06 ^{***}	6.98 ± 0.06 ^{***}	7.63 ± 0.07
 MeCATPB	6.74 ± 0.14 ^{\$\$}	6.52 ± 0.14	7.08 ± 0.10	
 GLPG-1	7.39 ± 0.04	7.01 ± 0.10 [*]	7.06 ± 0.09 [*]	
 MeGLPG-1	6.22 ± 0.09 ^{\$\$\$}	6.89 ± 0.07 ^{**}	6.80 ± 0.08 ^{**}	
 GLPG-2	7.65 ± 0.08			
 MeGLPG-2	7.16 ± 0.06 ^{\$\$\$}			
 MoGLPG-2	7.36 ± 0.08			

^a Data shown as pK_i values of respective antagonists determined in [³H]-GLPG0974 competition assays

^{*} Analysis of pK_i values by one-way ANOVA followed by Dunnett's test with the pK_i at WT hFFA2 as a reference with significant differences denoted as P = * ≤ 0.05, P = ** ≤ 0.01 and P = *** ≤ 0.001

[§] Comparison of methyl ester (Me) or morpholine (Mo) analogue pK_i values with carboxylate compound by unpaired *t* test with significant differences denoted as P = \$\$ ≤ 0.01 and P = \$\$\$ ≤ 0.001

4.2.3 Carboxylate moiety present in FFA2 antagonists is not necessary for high-affinity binding

The ability of CATPB and GLPG0974 to bind to single arginine mutants of hFFA2 supported the hypothesis that the interaction between ligand carboxylate and orthosteric binding pocket arginines is of less importance for antagonist than agonist binding. Indeed, functional studies in chapter 3 demonstrated that CATPB and GLPG0974 analogues with a methyl ester or morpholine in place of the carboxylate moiety retained the ability to inhibit the hFFA2 response to C3 at wild type hFFA2, albeit with a reduced pIC₅₀ (see section 3.2.4). To define whether this observation could be explained by a loss of antagonist affinity for the receptor, [³H]-GLPG0974 competition binding assays were performed with methyl ester (Me) analogues of GLPG0974 analogues GLPG-1 (Figure 4.3A) and GLPG-2 (Figure 4.3B), and CATPB (Figure 4.3C). In agreement with functional studies, the replacement of the carboxylate moiety led to a loss of affinity

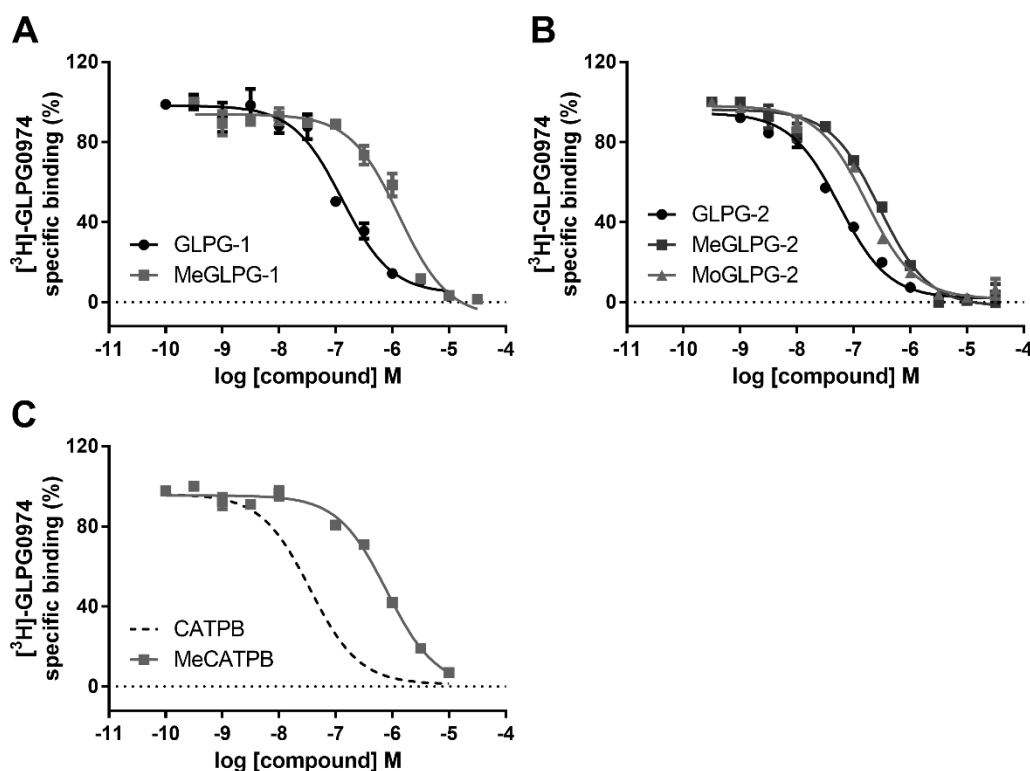


Figure 4.3 Modification of the carboxylate moiety of hFFA2 antagonists results in loss of binding affinity The ability of various concentrations of GLPG-1 and MeGLPG-1 (A); GLPG-2, MeGLPG-2 and MoGLPG-2 (B); and CATPB and MeCATPB (C) to compete with [³H]-GLPG0974 for binding to hFFA2-eYFP is shown from representative experiments. Nonspecific binding was determined in presence of 10 μM CATPB and subtracted from total binding to calculate specific binding. Dashed lines indicate that data was shown previously, in this case in figure 3.2. Me = Methyl ester; Mo = Morpholine.

compared to the carboxylate-containing compound with a 13-fold reduction in K_i of MeCATPB, a 15-fold reduction in K_i of MeGLPG-1 and a 3-fold reduction in K_i of MeGLPG-2 (Table 4.2). These results show that the affinity of GLPG-2 was least affected by modification of the carboxylate moiety. To examine this further, an analogue of GLPG-2 with a relatively bulky morpholine (Mo) amide in place of the carboxylate was employed (Figure 4.3C). Interestingly, the affinity of MoGLPG-2 was higher than that of MeGLPG-2 (Table 4.2), which was also observed in functional studies (see section 3.4.2). This might suggest that the morpholine moiety of MoGLPG-2 was able to make additional contacts with the receptor binding pocket compared to the methyl ester analogue MeGLPG-2.

Although methyl esters are less electronegative than carboxylates and are not negatively charged, they retain the ability to act as hydrogen bond acceptors and may still interact with the orthosteric arginine residues. To examine whether this is the case, the affinity of MeCATPB and MeGLPG-1 was assessed at R180A and R255A hFFA2 (Figure 4.4). Interestingly, the affinity of MeCATPB was not significantly affected by these mutations and, although not quite reaching statistical significance, a 2.2-fold increase in affinity was observed at R255A hFFA2 compared to the wild type receptor (Table 4.2). This positive trend was more prominent and significant in the case of MeGLPG-1 with a 4.8-fold increase in affinity at R180A hFFA2 and a 3.8-fold increase at R255A hFFA2. These

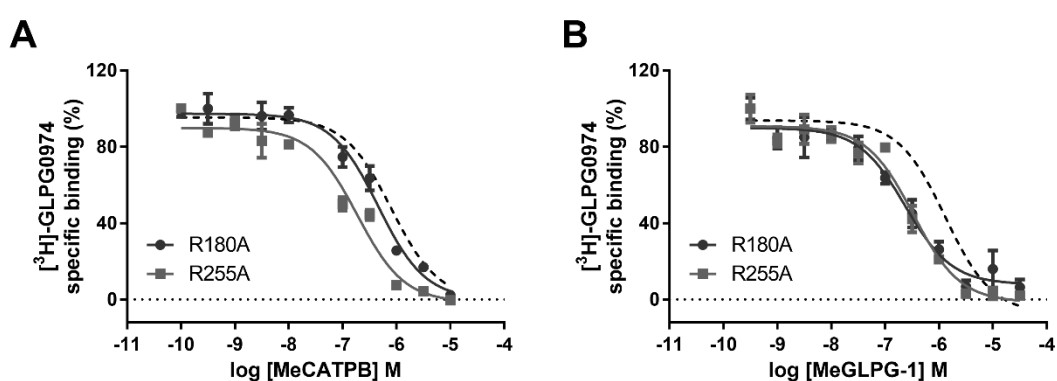


Figure 4.4 Methyl ester analogues of hFFA2 antagonists display higher affinity at orthosteric binding site mutants of hFFA2 The capacity of MeCATPB (A) and MeGLPG-1 (B) to displace [³H]-GLPG0974 from R180A and R255A hFFA2-eYFP is shown from representative experiments. For comparison the effect of each ligand at WT is also shown (--) with original data displayed in figure 4.3. Me = Methyl ester.

observations suggest that the presence of two orthosteric arginine residues was not required for binding of methyl ester analogues and was instead more likely to have a negative impact on binding affinity.

4.2.4 FFA2 homology model and ligand docking supports diverse binding poses of FFA2 agonists and antagonists

In initial binding studies (see section 4.2.2) clear differences in binding determinants of FFA2 agonists and antagonists could be observed with agonists requiring both orthosteric arginines and histidine, while antagonists only required one arginine residue. Furthermore, distinct antagonist series potentially showed differences in arginine preference. These observations provided important information on the binding mode of FFA2 ligands, which were applied and examined in more detail by generating a homology model of hFFA2. The recently published crystal structure of hFFA1 complexed with the allosteric partial agonist TAK-875 (Srivastava et al., 2014) was employed as the template, which also provides a good opportunity to improve upon currently available homology models that were based on the lower-similarity template structure of the β_2 -adrenergic receptor (Schmidt et al., 2011).

Docking studies of FFA2 agonists C3 (**Figure 4.5A**) and compound 1 (**Figure 4.5B**) into the constructed hFFA2 homology model resulted in agonist carboxylates being positioned in a highly similar fashion, engaging Arg180^{5.39} and Arg255^{7.39} simultaneously in a strong electrostatic interaction that included multiple hydrogen bonds. These binding poses were in agreement with the loss of agonist binding observed at R180A and R255A hFFA2 mutants. In addition, both agonist carboxylates also acted as hydrogen bond donors to Tyr238^{6.51} (**Figures 4.5A and B**). In previous functional studies mutation of this tyrosine residue resulted in a significant loss of C3 and compound 1 potency (Hudson et al., 2013a). Interestingly, His242^{6.55}, which is also essential for agonist binding, did not directly interact with the agonist carboxylate (**Figures 4.5A and B**). Instead, His242^{6.55} was hydrogen bonded to Arg255^{7.39} and may therefore be important for positioning Arg255^{7.39} for interaction with the agonist. While the residues described above comprised the binding pocket of C3, compound 1 interacted with additional residues, as would be expected from its increased affinity over C3 (see section 3.2.1). The binding site of compound 1 also included His140^{4.56}

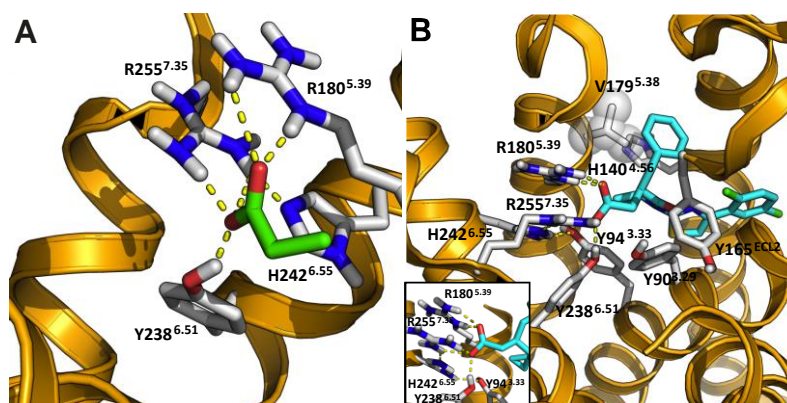


Figure 4.5 Modelling of orthosteric FFA2 agonist binding poses Docking of C3 (**A**) or compound 1 (**B**) into a homology model of hFFA2 is illustrated. The carboxylate moiety of C3 and compound 1 is anchored by Arg180^{5.39} and Arg255^{7.35}, which are both required for agonist binding and activation of FFA2. His242^{6.55} appears to play a stabilising role in the binding pocket by interacting with and thereby positioning Arg255^{7.35} for interaction with agonists. In addition to the Arg180-Arg255-His242 triad, C3 also interacts with Tyr238^{6.51}. Binding of compound 1 is additionally supported by interaction with Tyr90^{3.33}, His140^{4.56}, Tyr165^{ECL2}, Val179^{5.38} and Tyr238^{6.51}, whose mutation has been shown to affect activation of hFFA2 by compound 1 (Hudson et al., 2013a). The inset in **B** shows greater detail of electrostatic interactions of the compound 1 carboxylate with the hFFA2 binding pocket. These figures are the work of Dr Hansen generated in collaboration with Professor Ulven's group at the University of Southern Denmark.

and Val179^{5.38}, which were in close proximity to its phenyl group, as well as Tyr90^{3.29}, Tyr94^{3.33} and Tyr165^{ECL2}. The importance of Tyr90^{3.29}, His140^{4.56}, Tyr165^{ECL2} and Val179^{5.38} was also demonstrated in previous functional studies, in which alanine replacement of these respective residues resulted in a reduction of compound 1 potency (Hudson et al., 2013a).

Docking studies carried out for CATPB and GLPG0974 showed distinct binding poses, compared to FFA2 agonists (**Figure 4.6A**). Interestingly, lower-energy poses were obtained for CATPB when interacting with Arg255^{7.35} and for GLPG0974 when interacting with Arg180^{5.39}, which is in agreement with the effect of the respective mutations observed in binding studies (**Table 4.2**). The hypothesis that CATPB and GLPG0974 prefer to interact with different arginine residues was further supported by the observation that mutation of His242^{6.55}, which positioned Arg255^{7.35} in the homology model through a hydrogen bond interaction, resulted in a 1.7-fold reduction in CATPB affinity, albeit this was not quite statistically significant (**Table 4.2**). This supporting interaction was modelled based on equivalent positioning of corresponding residues in hFFA1, in which Asn255^{6.55} forms a stabilising interaction with Arg258^{7.35} (Srivastava et al., 2014). The affinity of CATPB and GLPG0974 was affected by less than 10-fold by alanine replacement of either orthosteric arginine (**Table 4.2**), which may be explained by a compensatory interaction of the antagonist carboxylate with the

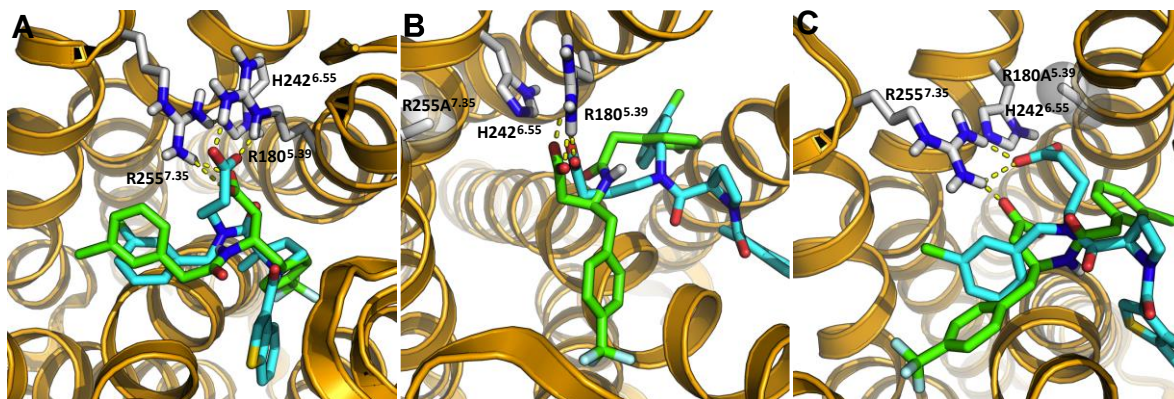


Figure 4.6 Modelling of orthosteric hFFA2 antagonist binding poses Docking of CATPB (green) and GLPG0974 (cyan) into hFFA2 demonstrated preferred interaction of GLPG0974 with Arg180^{5.39} and CATPB with Arg255^{7.35} (A). Representative poses of CATPB and GLPG0974 in alanine replacement mutants of Arg255^{7.35} (B) and Arg180^{5.39} (C) show that the antagonists are able to adapt their binding pose to interact with the respective remaining arginine residue. These figures are the work of Dr Hansen generated in collaboration with Professor Ulven's group at the University of Southern Denmark.

remaining, less favourable, arginine. To examine this hypothesis further, the effect of R255A (Figure 4.6B) and R180A (Figure 4.6C) mutations on the docking of CATPB and GLPG0974 into the hFFA2 binding pocket was investigated. Indeed, both antagonists were able to adapt their binding pose to allow for hydrogen bond interaction between the carboxylate moiety and the remaining arginine residue (Figures 4.6B and C). In the case of CATPB, the favoured binding pose at R255A (Figure 4.6B) and R180A (Figure 4.6C) hFFA2 mutants was significantly altered compared to wild type hFFA2 (Figure 4.6A) with respective functional groups adopting different conformations. In contrast, GLPG0974 favoured a similar binding pose to wild type hFFA2 (Figure 4.6A) at the R180A hFFA2 mutant (Figure 4.6C), while at R255A hFFA2 the conformation of GLPG0974 was drastically changed (Figure 4.6B). This may appear to be inconsistent with the higher affinity of GLPG0974 for R255A hFFA2, however the length and orientation of the hydrogen bond between GLPG0974 and Arg255^{7.35} seemed to be less optimal than that between GLPG0974 and Arg180^{5.39}. As hydrogen bond distance and orientation are some of the deciding factors of hydrogen bond strength (Hubbard et al., 2016), the interaction between GLPG0974 and R255A hFFA2 may be weaker than that between GLPG0974 and R180A, although GLPG0974 adopts a similar conformation as at wild type hFFA2.

4.2.5 Orthosteric arginine pair may regulate antagonist release from the FFA2 binding pocket

The affinity of a ligand is directly related to the speed at which it associates and dissociates from the receptor, with the ratio of K_{off} and K_{on} corresponding to the K_d . To examine how R180A and R255A mutations affect the kinetics of [3 H]-GLPG0974, the dissociation (Figure 4.7A) and association (Figure 4.7B) of the radioligand was assessed at respective mutants. Although the affinity of [3 H]-GLPG0974 was only modestly affected at R180A and R255A hFFA2, a drastic increase in K_{off} and K_{on} rates could be observed at the mutant receptors. The dissociation rate of [3 H]-GLPG0974 is significantly increased by 15- and 7.6-fold at R180A and R255A hFFA2, respectively (Table 4.3). Although the enhancing effect of R180A and R255A on radioligand association appears to be very pronounced when visually comparing data at mutant and wild type FFA2 (Figure 4.7B), the impact on the association rate was not quite statistically significant, albeit a positive trend was observed with increases of 3.9- and 2-fold at R180A and R255A hFFA2, respectively (Table 4.3). The half-time of ligand association is dependent on its dissociation rate and binding equilibrium is reached more quickly if the ligand has a fast dissociation rate, therefore the impact of R180A and R255A mutations on the association curve of [3 H]-GLPG0974 does not translate into a statistically significant effect on the K_{on} . These observations demonstrated that that orthosteric arginine mutations primarily affected the

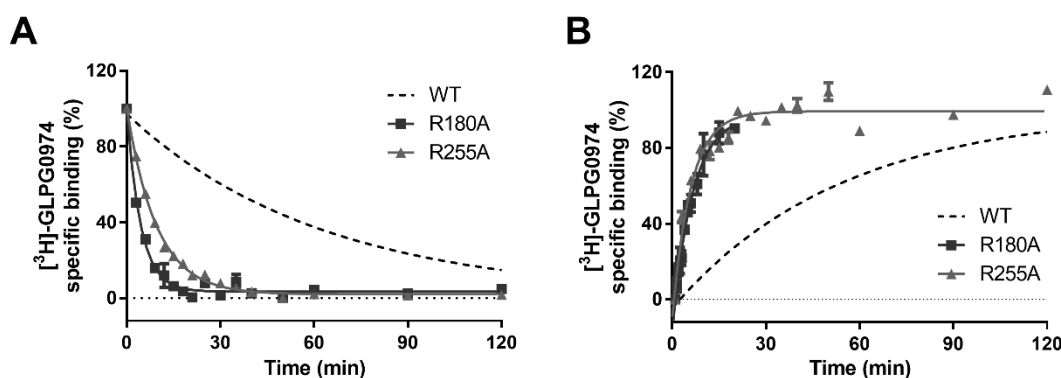


Figure 4.7 Alanine replacement of orthosteric arginines increases the speed of [3 H]-GLPG0974 binding kinetics Dissociation (A) and association (B) of 6 nM [3 H]-GLPG0974 at WT, R180A and R255A hFFA2-eYFP is shown from representative experiments. To induce [3 H]-GLPG0974 dissociation 10 μ M CATPB were added after 60 min pre-association of the radioligand.

Table 4.3 Kinetic parameters of [³H]-GLPG0974 binding to wild type and orthosteric arginine mutants of hFFA2

Parameter	WT	R180A	R255A
K_{off} (min ⁻¹)	0.014 ± 0.001	0.221 ± 0.004***	0.107 ± 0.009***
K_{on} (M ⁻¹ min ⁻¹)	1,730,000 ± 74,000	6,794,000 ± 3,388,000	3,480,000 ± 167,000
K_{d}^{a} (nM)	8.1 ± 0.9	32.5 ± 16.8	30.7 ± 4.1

^a Determined by dividing the K_{off} by the K_{on} value of at least three independent kinetic binding experiments.

* Analysis of K_{off} and K_{on} values by one-way ANOVA followed by Dunnett's test with the value at WT hFFA2 as a reference with significant differences denoted as $P = *** \leq 0.001$

release of [³H]-GLPG0974 from the receptor, which might suggest that Arg180^{5,39} and Arg255^{7,35} play a role in retaining [³H]-GLPG0974 at the binding pocket of wild type hFFA2.

4.2.6 Competitive kinetic binding experiments indicate distinct kinetics of GLPG0974 and CATPB despite similar affinity

The investigation of GLPG0974 and CATPB pharmacology in chapter 3 indicated that differences in GLPG0974 and CATPB binding kinetics might account for the diverse effects of these antagonists observed in functional assays (see section 3.2.3). To examine this hypothesis further, a competitive kinetic binding assay of [³H]-GLPG0974 was performed in the presence of CATPB (**Figure 4.8A**) or GLPG0974 (**Figure 4.8B**). Increasing concentrations of the competing ligand were added to membranes containing hFFA2-eYFP simultaneously with [³H]-GLPG0974 and the association of the radioligand was measured, which will be affected in defined ways depending on the binding kinetics of the competing ligand (Dowling and Charlton, 2006). Interestingly, CATPB did indeed show significantly faster binding kinetics than GLPG0974 with a 4.5-fold increase in K_{off} and a 5.2-fold increase in K_{on} (**Table 4.4**), which supports the hypothesis that GLPG0974 requires a longer incubation time with the receptor to reach equilibrium (see section 3.2.3). This result also exemplified that ligands with equal affinities can have relatively different kinetic profiles, which may result in different pharmacology. Furthermore, kinetic parameters determined for GLPG0974 in the competitive kinetic binding assay (**Table 4.4**) correlated well with association and dissociation rates determined in [³H]-GLPG0974 kinetic binding assays (**Table 4.3**), which suggests that the kinetic binding rates calculated from competitive kinetic binding studies are a good representation of the true kinetic profile of unlabelled ligands.

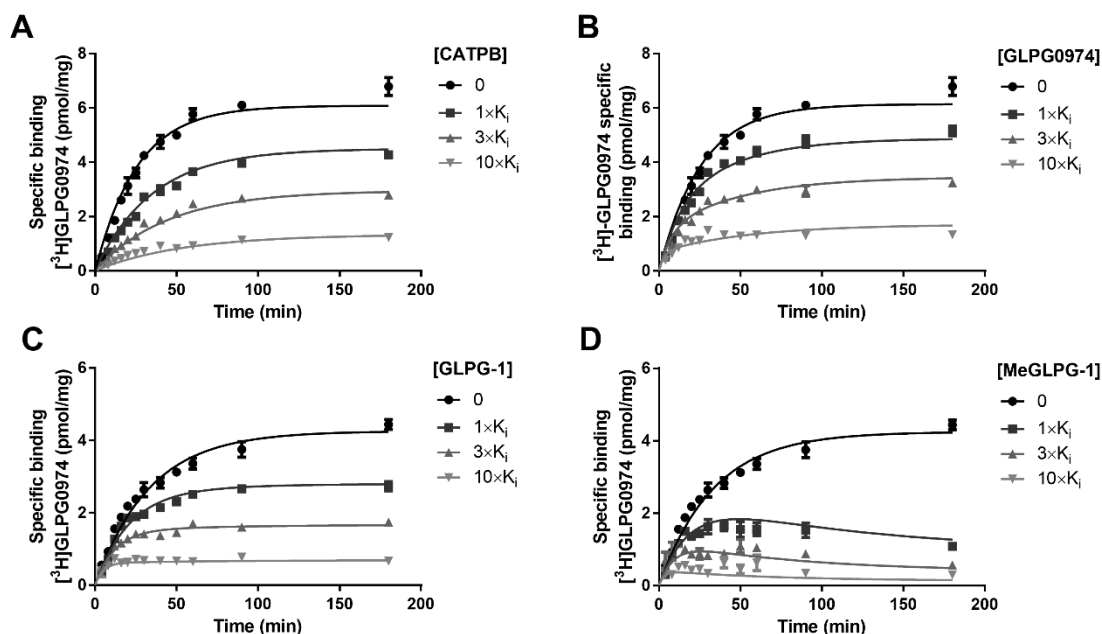


Figure 4.8 Effects of hFFA2 antagonists on $[^3\text{H}]$ -GLPG0974 association demonstrate different kinetic parameters for the antagonist series The association of 10 nM $[^3\text{H}]$ -GLPG0974 to hFFA2-eYFP in absence or presence of indicated concentrations of CATPB (A), GLPG0974 (B), GLPG-1 (C) and MeGLPG-1 (D) is shown from representative experiments. A competitive kinetic binding model (Dowling and Charlton, 2006) was used to fit shown data to estimate the kinetic parameters of unlabelled competing ligands and resulting analysis is shown in table 4.3. Respective K_i values of antagonists are shown in table 4.2. Experiments were performed in collaboration by Dr Mackenzie in Professor Milligan's laboratory group. Me = Methyl ester.

As the orthosteric arginine residues seemed to play a role in regulating the kinetics of $[^3\text{H}]$ -GLPG0974, the carboxylate/methyl ester analogue pair GLPG-1/MeGLPG-1 was selected to investigate how the potentially weakened interaction of MeGLPG-1 with R180A and R255A affected the ligand binding kinetics at wild type hFFA2. Therefore, competitive kinetic binding assays were performed in the presence of increasing concentrations of GLPG-1 (Figure 4.8C) and MeGLPG-1 (Figure 4.8D). Interestingly, the dissociation rate was not significantly affected by replacement of the carboxylate moiety with a methyl

Table 4.4 Kinetic parameters of antagonist binding to wild type hFFA2

Parameter	GLPG0974	CATPB	GLPG-1	MeGLPG-1
K_{off} (min^{-1})	0.021 ± 0.002	$0.094 \pm 0.026^*$	0.016 ± 0.001	0.011 ± 0.007
$t_{1/2}^a$ (min)	48	11	63	91
K_{on} ($\text{M}^{-1} \text{min}^{-1}$)	$1,220,000 \pm 87,000$	$6,360,000 \pm 1,540,000^*$	$398,000 \pm 16,200$	$26,900 \pm 9800^{***}$
K_d^b (nM)	17.2 ± 0.6	14.5 ± 0.7	39.9 ± 1.7	638 ± 259

^a Half-time of ligand dissociation calculated by dividing unity by K_{off} .

^b Determined by dividing the K_{off} by the K_{on} value of at least three independent kinetic binding experiments.

* Comparison of K_{off} and K_{on} rates of GLPG0974 and CATPB or GLPG-1 and MeGLPG-1 by unpaired t test with significant differences denoted as $P = * \leq 0.05$ and $P = *** \leq 0.001$.

ester, while the association rate was significantly reduced by 15-fold (**Table 4.4**). This observation might suggest that weakened interaction with orthosteric arginines has little effect on the release of ligands from the hFFA2 binding pocket, however more time is required for the methyl ester analogue to bind to the receptor and adopt its final conformation. In addition, the replacement of the chlorobenzene moiety of GLPG0974 with a trifluoromethylbenzene in GLPG-1, which led to a reduction in affinity by 3-fold (**Table 4.2**), primarily affected the association and not the dissociation rate with a 3-fold reduction compared to GLPG0974.

4.2.7 Binding of FFA2 agonists appears to have a cooperative effect on [³H]-GLPG0974 kinetics

All functional and competition binding studies shown so far in chapters 3 and 4 indicate that GLPG0974, CATPB and their respective analogues are orthosteric ligands that bind to the same site as the agonists C3 and compound 1. Allosteric ligands are defined by their ability to bind to a distinct site on the receptor compared to endogenous ligands and usually display a positive or negative cooperative effect on the affinity or efficacy of other ligands (Wootten et al., 2013). The allosteric modulation of probe affinity is rooted in the capacity of allosteric ligands to change the association or dissociation rate of the respective probe. Therefore, measurement of radioligand dissociation induced by competition with an excess of unlabelled compound should serve as a means of investigating whether the unlabelled compound has any cooperative effect on radioligand dissociation (May et al., 2010). An alternative approach to measuring radioligand dissociation is to wash out the radioligand or add an excess of binding buffer to the reaction that contains pre-associated radioligand, an approach referred to as “infinite dilution” (Guo et al., 2017).

To measure [³H]-GLPG0974 dissociation independently of the competing ligand, an infinite dilution experiment was performed and yielded a similar K_{off} compared to dissociation measured by competition with 10 μ M CATPB (**Figure 4.9A**). To assess whether this is also the case when employing methyl ester analogues, which likely have a distinct mode of binding compared to GLPG0974, 10 μ M of MeCATPB or MeGLPG-1 were employed for competition (**Figure 4.9B**). Indeed, the resulting K_{off} values were in a similar range compared to values

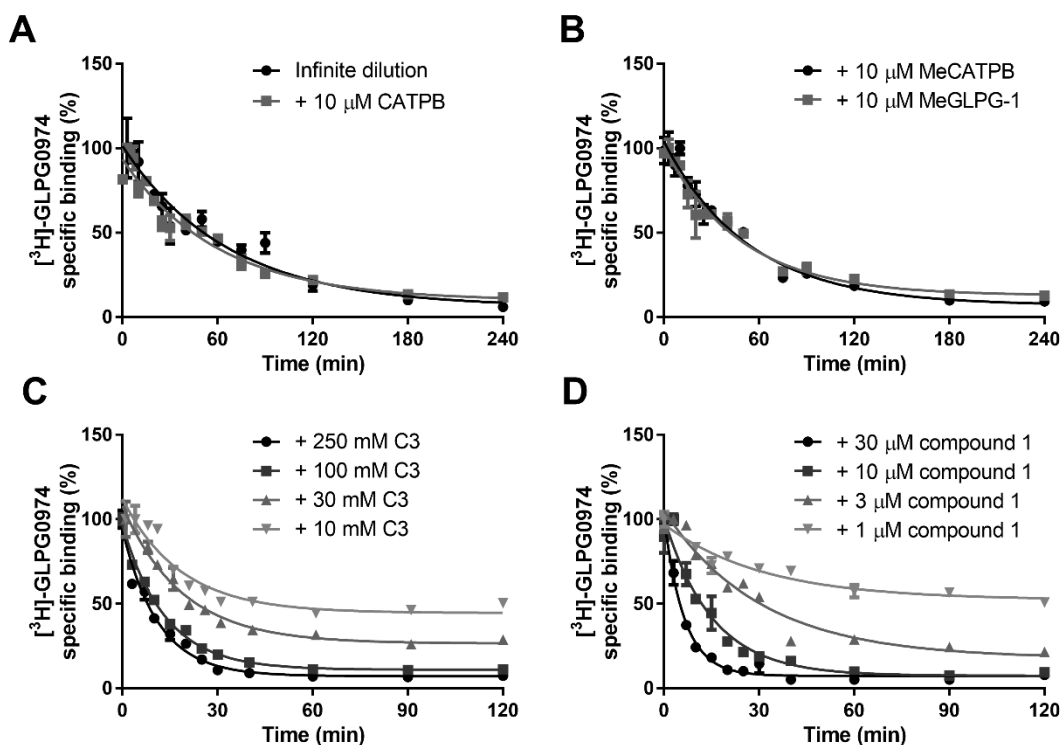


Figure 4.9 FFA2 agonists increase the dissociation rate of $[^3\text{H}]\text{-GLPG0974}$ The dissociation of $[^3\text{H}]\text{-GLPG0974}$ from hFFA2-eYFP was induced by using an “infinite dilution” approach (70-fold) or by competition with 10 μM CATPB (**A**) or 10 μM methyl ester analogues of hFFA2 antagonists (**B**). The capacity of increasing concentrations of C3 (**C**) or compound 1 (**D**) to affect dissociation of $[^3\text{H}]\text{-GLPG0974}$ is illustrated. Data shown is from representative experiments. Me = Methyl ester.

determined by infinite dilution and CATPB competition (**Table 4.5**). Although the dissociation experiments measured by infinite dilution and competition with MeCATPB or MeGLPG-1 were only performed once, the radioligand binding assay showed good consistency and it is likely that a drastic change in dissociation rate would have been detected in a single experiment. Regardless, it is important to keep in mind that additional repetitions are required to confirm these results.

Dissociation of $[^3\text{H}]\text{-GLPG0974}$ was also measured by competition with agonists C3 (**Figure 4.9C**) and compound 1 (**Figure 4.9D**). Surprisingly, the use of increasing concentrations of C3 (**Figure 4.9C**) or compound 1 (**Figure 4.9D**) resulted in a concentration-dependent increase in the dissociation rate of $[^3\text{H}]\text{-GLPG0974}$. This effect was most pronounced when 30 μM of compound 1 was present, which induced a significant 13-fold increase in the K_{off} of $[^3\text{H}]\text{-GLPG0974}$ (**Table 4.5**). When adding 250 mM of C3, only a 5.3-fold increase was observed, which was not quite statistically significant. These observations were unexpected, as increasing concentrations of C3 and compound 1 were both able to fully out-compete $[^3\text{H}]\text{-GLPG0974}$ (see section 3.2.1) and Schild plots

Table 4.5 Effect of different ligands on the [³H]-GLPG0974 dissociation rate

Parameter	70-fold dilution ^a	Antagonist ^b			Agonist ^b	
		CATPB	MeCATPB ^a	MeGLPG-1 ^a	C3	Compound 1
K_{off} (min ⁻¹)	0.013	0.014 ± 0.001	0.019	0.020	0.074 ± 0.015	0.187 ± 0.058*

^a Experiment performed once, therefore no SEM can be determined.

^b [³H]-GLPG0974 dissociation was monitored by addition of 10 μM of respective antagonist, 250 mM C3 or 30 μM compound 1.

* Analysis of values by one-way ANOVA followed by Dunnett's test with the value determined by addition of CATPB as a reference with significant differences denoted as P = ** ≤ 0.01 and P = *** ≤ 0.001.

suggested that GLPG0974 is a competitive, reversible antagonist of C3 and compound 1 (see section 3.2.3). Although it is challenging to interpret these results, discussion section 4.3.4 will attempt to provide hypotheses that may provide an explanation.

4.3 Discussion

4.3.1 FFA2 agonists are defined by their interaction with the Arg180-His242-Arg255 triad

The interactions formed between a ligand and its receptor are one of the defining factors of ligand pharmacology. Agonists engage the receptor in a fashion that causes the receptor conformation to favour an active state. In contrast, antagonists bind to the receptor but do not promote conformational rearrangements, unless the antagonist has the capacity to act as an inverse agonist that shifts the conformational equilibrium towards an inactive state. Therefore, although orthosteric agonists and antagonists by definition occupy the same endogenous binding pocket of the receptor, the nature of their interaction with the receptor must differ to allow for their distinct pharmacological actions. In the case of FFA2, the orthosteric arginine pair Arg180^{5,39} and Arg255^{7,39}, as well as His242^{6,55}, are thought to define the orthosteric binding site as their replacement with alanine resulted in loss of endogenous agonist action (Stoddart et al., 2008, Hudson et al., 2013a). SCFAs contain only one functional group, a carboxylate moiety, and its replacement with an amide renders SCFAs inactive at FFA2 (Schmidt et al., 2011). Therefore, a link between the FFA2 agonist carboxylate and the orthosteric Arg180-His242-Arg255 triad was established almost a decade ago. Furthermore, the importance of the orthosteric arginine pair is exemplified by the fact that it is conserved

between the majority of FFA receptor family members including FFA1 (Arg183^{5.39} and Arg258^{7.35}) and FFA3 (Arg185^{5.39} and Arg258^{7.35}). Alanine replacement of these arginines in FFA1 (Sum et al., 2007) or FFA3 (Stoddart et al., 2008) also affected agonist potency. Therefore, the carboxylate recognition by the orthosteric arginine pair does not only appear to be important for binding of SCFAs to FFA2 and FFA3, but also for binding of agonists to FFA1. However, all previous evidence on FFA2 has been based on investigation of agonist potency in functional assays. Although this information undoubtedly demonstrates that the Arg180-His242-Arg255 triad is important for agonist action, it does not allow differentiation between agonist affinity and efficacy. Therefore, it was not clear whether alanine replacement of Arg180^{5.39}, Arg255^{7.35} or His242^{6.55} resulted in a loss of agonist binding or agonist ability to promote an active receptor state.

By developing a radioligand competition assay using the tritiated FFA2 antagonist [³H]-GLPG0974, data presented in this chapter demonstrated that agonist binding is indeed lost at R180A, R255A and H242A hFFA2. Docking of the endogenous SCFA C3 and synthetic agonist compound 1 into a homology model of hFFA2 revealed that the agonist carboxylate is indeed strictly coordinated by the orthosteric arginine pair with His242^{6.55} potentially playing a coordinating role for Arg255^{7.35}. In contrast, antagonist binding poses showed a potentially weaker and differently oriented interaction with orthosteric arginines and no requirement of a carboxylate moiety for antagonist action, which will be discussed in more detail below. What could these observations suggest considering the different actions of agonists and antagonists? Potentially the engagement of the arginine pair observed in the FFA2 agonist docking represents the first step in the cascade of conformational rearrangements that result in an equilibrium shift to an active state receptor. In particular, considering that the functional groups of SCFAs are limited to a carboxylate, it is likely that this interaction with the receptor confers the activation mechanism. Interestingly, attempts to understand the molecular basis of differences in constitutive activity between FFA2 orthologues revealed that an ionic lock between a glutamic acid residue in the ECL2 of mFFA2 and orthosteric arginine residues was likely to be responsible for a reduced level of constitutive activity compared to hFFA2 (Hudson et al., 2012b). Similar results could be obtained for FFA1 in which two ionic locks between glutamic acid residues in ECL2 and the orthosteric

arginines limited the constitutive activity of the receptor and were thought to be broken by agonist binding (Sum et al., 2007). These studies provide further support for a role of Arg180^{5.39} and Arg255^{7.35} in FFA2 receptor activation. However, as the allosteric ligands 4-CMTB and AZ1729 retain the ability to activate R180A and R255A hFFA2, the receptor can still enter an active state conformation in the absence of the orthosteric arginine residues, perhaps through a different mechanism.

4.3.2 Key orthosteric binding site residues play limited role in hFFA2 antagonist binding

Multiple antagonists of hFFA2 also contain a carboxylate moiety, which was thought to be a defining factor of orthosteric FFA2 ligands. While the presence of a carboxylate moiety certainly contributes to increased affinity of antagonists, as demonstrated in sections 3.2.4 and 4.2.3, and in the development of GLPG0974 (Pizzonero et al., 2014), it is not an absolute requirement for antagonist binding. This was exemplified in the ability of [³H]-GLPG0974 to bind with comparably high affinity to R180A, R255A and H242A hFFA2 and the capacity of CATPB and GLPG0974 to fully out-compete the radioligand at respective mutants. The affinity of CATPB and GLPG0974 was only modestly affected at the alanine replacement mutants of the orthosteric arginines and was unchanged or even increased, in the case of GLPG0974, at H242A hFFA2. Furthermore, binding studies at R180A and R255A hFFA2 suggested that CATPB and GLPG0974 may prefer to interact with different arginine residues, with CATPB affinity being most affected by alanine replacement of Arg255^{7.35} and GLPG0974 by Arg180^{5.39}. This was reflected in binding poses obtained for hFFA2 antagonists in which CATPB and GLPG0974 showed lower-energy poses when interacting with Arg255^{7.35} and Arg180^{5.39}, respectively. However, the lack of specific [³H]-GLPG0974 binding to the dual arginine mutant R180A-R255A hFFA2 suggests that at least one arginine residue is required for antagonist interaction with the receptor. However, the concentration range of radioligand that can be employed in binding assays is limited by the increasing nonspecific binding at high radioligand concentrations. Therefore, it may be possible that [³H]-GLPG0974 binds to R180A-R255A hFFA2 with an affinity in the μM range, which cannot be detected in radioligand binding assays. An alternative hypothesis may be that mutation of both Arg180^{5.39} and Arg255^{7.35} to alanine

leads to a conformational rearrangement of the hFFA2 binding pocket, which could result in drastically reduced radioligand affinity.

To investigate the interaction between the hFFA2 antagonist carboxylate and the orthosteric arginines in an alternative fashion, analogues of GLPG0974 and CATPB with carboxylate modifications were employed. As anticipated from functional studies described in chapter 3 (see section 3.2.4), the affinity of methyl ester and morpholine analogues at wild type hFFA2 was indeed reduced compared to their carboxylate equivalents. Interestingly, the extent of the impact of carboxylate replacement appears to differ between different antagonist analogues. While CATPB and GLPG-1 affinities were reduced by over 10-fold by replacement of carboxylate with a methyl ester, the affinity of MeGLPG-2 was only reduced by 3-fold compared to GLPG-2. This indicates that GLPG-2 is likely to form additional interactions outside of the orthosteric binding pocket. Structurally, GLPG-2 contains one more carbon in the benzothiophene linker that may result in a different orientation of the benzothiophene group compared to GLPG-1, which could allow MeGLPG-2 to make additional interactions compared to MeGLPG-1. Interestingly, R180A and R255A mutations had little effect on methyl ester analogue affinity and the affinity of MeGLPG-1 was actually increased at both mutants. Potentially alanine replacement of one orthosteric arginine results in more space in the binding pocket to accommodate the methyl ester, which could form a hydrogen bond with the remaining arginine residue. This leads to one important question that remains: Do all or some methyl ester analogues have the ability to interact with R180A-R255A hFFA2? Unfortunately, without a labelled probe that binds the double arginine mutant of hFFA2 it is challenging to answer this question, however it will be addressed further in chapter 5.

4.3.3 Relationship between FFA2 antagonist interaction with orthosteric arginine residues and binding kinetics

The residence time of ligands at the receptor binding pocket has become an increasingly important factor to consider in drug discovery (Guo et al., 2014). Relating specific interactions between ligand and receptor with ligand binding kinetics could be a first step in the rational design of compounds with a desired kinetic profile. In the case of FFA2, the Arg180-Arg255 pair is one of the defining

factors of the orthosteric binding pocket that may translate receptor activation and limit the constitutive activity of the murine orthologue by forming an ionic lock with a glutamic acid residue in ECL2 (Hudson et al., 2012b). Interestingly, although alanine replacement of Arg180^{5.39} or Arg255^{7.35} did not have a major effect on [³H]-GLPG0974 affinity, its binding kinetics were more significantly affected. In particular the dissociation rate of [³H]-GLPG0974 was increased drastically compared to wild type hFFA2, suggesting that the orthosteric arginines play an important role in prolonging the residence time of [³H]-GLPG0974. This observation highlights that it can be of value to not only consider the effect of mutations on ligand affinity, but also on its binding kinetics as these may be affected even if ligand affinity is unchanged.

CATPB (Brantis et al., 2011) and GLPG0974 (Pizzonero et al., 2014) are currently the highest-affinity published hFFA2 antagonists and originate from different compound series. In particular GLPG0974 has attracted much attention as it is the first and only hFFA2 ligand that has entered clinical trials (Vermeire et al., 2015). However, even though the ability of GLPG0974 to inhibit neutrophil migration through FFA2 could be demonstrated in patients, it did not lead to improvement in ulcerative colitis symptoms. Although functional inhibition of the hFFA2 response to C3 (see section 3.2.1) and [³H]-GLPG0974 competition assays (see section 4.2.2) suggested that CATPB and GLPG0974 are equivalent in affinity for hFFA2, distinct pharmacological behaviour in the BRET-based β -arrestin 2 recruitment assay, which has a relatively short incubation time, suggested that CATPB and GLPG0974 may have different kinetic profiles. To examine this hypothesis further, a competitive kinetic binding assay was employed, in which the effect of increasing concentrations of an unlabelled ligand on [³H]-GLPG0974 association was assessed. Interestingly, this experiment indeed revealed that GLPG0974 and CATPB have different kinetic profiles with GLPG0974 associating and dissociating relatively slowly and CATPB showing significantly faster kinetics. The dissociation half-time of GLPG0974 equals 48 min, while the dissociation half-time of CATPB equals 11 min, which highlights that the two antagonists spend different amounts of time bound to the receptor (**Table 4.4**). How could this observation be explained structurally? When docking both antagonists into the homology model of hFFA2, CATPB and GLPG0974 adopted relatively similar poses. Perhaps the preferred interaction

with different arginines could result in different kinetic profiles? Alanine replacement of Arg180^{5,39} or Arg255^{7,35} did affect [³H]-GLPG0974 kinetics, as discussed above, so these residues do seem to play a role in regulating binding kinetics. However, additional studies are certainly required to dissect the determinants of GLPG0974 and CATPB binding kinetics more closely.

In an effort to understand how the interaction between antagonist carboxylate and orthosteric arginines defines binding kinetics, the kinetic profile of GLPG-1 and MeGLPG-1 was determined and compared. Interestingly, the replacement of the carboxylate with a methyl ester primarily affected ligand association such that MeGLPG-1 required more time to bind to the receptor than GLPG-1, while the association rate was not significantly changed. Therefore, the interaction between carboxylate and orthosteric arginines potentially serves as a guide for ligand association with the receptor that allows the ligand to adopt its final conformation more quickly.

4.3.4 Cooperative effect of hFFA2 agonists on [³H]-GLPG0974 kinetics may be rooted in co-binding or cross-dimer cooperativity

Functional studies described in chapter 3 and [³H]-GLPG0974 competition binding assays outlined here suggest that GLPG0974 is an orthosteric ligand that is a competitive, reversible antagonist at hFFA2. The surmountable right-shifted effect of increasing concentrations of GLPG0974 on the C3 and compound 1 concentration response curves is typical for a competitive antagonist (see section 3.2.3). Furthermore, resulting Schild plots had a slope close to unity and the pA₂ determined from the x-axis intercept of such plots was a good estimate of GLPG0974 affinity determined in [³H]-GLPG0974 saturation binding assays, which serves as additional support for competitive antagonism. C3 and compound 1 were also able to fully out-compete [³H]-GLPG0974 at wild type hFFA2, which suggests that they bind to the same orthosteric site on the receptor. Therefore, the enhancing effect of agonists on the dissociation rate of [³H]-GLPG0974 was surprising, as this is traditionally associated with negative cooperative modulation of co-bound ligand affinity by allosteric ligands (Leppik et al., 1998) and the majority of evidence supports that GLPG0974 is an orthosteric ligand. Of course, conceptually, it could be possible that GLPG0974 is

actually an allosteric ligand that has such a strong cooperative effect on C3 affinity, and vice versa, that it behaves like an orthosteric ligand in functional and binding assays (Christopoulos and Kenakin, 2002). However, although the dependence of agonist and antagonist binding on orthosteric arginine residues differs, mutation of Arg180^{5.39} or Arg255^{7.35} does impact antagonist binding kinetics and alanine replacement of both arginine residues results in loss of detectable [³H]-GLPG0974 binding, therefore it is very likely that GLPG0974 does indeed interact with Arg180^{5.39} or Arg255^{7.35}. Thus, what could serve as a feasible explanation for the cooperative effect of C3 and compound 1 on the dissociation of [³H]-GLPG0974?

If C3 or compound 1 and GLPG0974 were able to engage the receptor binding pocket simultaneously, this may result in a very strong negative cooperative effect and would explain why both agonists and GLPG0974 are affected by mutations of the orthosteric arginines. The pK_a of the arginine side chain is 12.5, which means that arginine will be positively charged at physiological pH and is thus able to form five hydrogen bonds through its protonated guanidinium group (Borders et al., 1994). Therefore, it could theoretically be possible for C3 and GLPG0974 to interact with the orthosteric arginine simultaneously, in particular as C3 is a relatively small molecule and could likely accommodate binding of GLPG0974. To assess the hypothesis, the effect of Arg180^{5.39} or Arg255^{7.35} alteration to a different positively charged residue such as lysine could be investigated, as such a mutation would retain the positive charge but allow less hydrogen bonding interactions. However, it is less likely that compound 1 and GLPG0974 can bind to the same site simultaneously as both are relatively bulky molecules and predicted binding poses in the hFFA2 homology model overlap. Furthermore, Schild plots assessing the effect of increasing GLPG0974 concentrations on the C3 and compound 1 concentration response curve showed a Schild slope close to unity and both agonists were able to fully outcompete [³H]-GLPG0974 in competition binding assays, which are clear indications of competitive antagonism that conceptually contradicts simultaneous binding.

A different explanation for the enhancing effect of agonists on the [³H]-GLPG0974 dissociation rate may be that hFFA2 contains two separate non-overlapping binding pockets that meet at the orthosteric arginine residues. As

both GLPG0974 and CATPB only require one of the two orthosteric arginine residues for interaction with the receptor, this would suggest that the remaining arginine is at least somewhat available to bind the carboxylate moiety of C3 or compound 1. Although both agonists required two arginine residues to fully bind to hFFA2, perhaps engagement of the first arginine residue increases the dissociation rate of the antagonists, which was observed for [³H]-GLPG0974 upon alteration of either Arg180^{5.39} or Arg255^{7.35} to alanine. This would allow agonists to engage the other arginine residue and fully bind. Thereby the orthosteric arginine residues would be required for binding to both pockets and when an agonist enters the pocket it could, in a sense, 'pull' the arginine away from the already bound antagonist. This would result in competitive behaviour as binding of agonists and antagonists is mutually exclusive, but account for the impact of agonist binding on antagonist dissociation rate. Molecular dynamics simulations may shine some light on this.

Finally, there is growing evidence that allosteric modulation can also occur across GPCR homodimers (Gherbi et al., 2015, Lane et al., 2014, May et al., 2011). The bitopic allosteric modulator of the dopamine D₂ receptor, SB269652, lost its allosteric effect when ligand binding to one of the protomers was impaired and engagement of the secondary pocket was a requirement for its allosteric behaviour (Lane et al., 2014). One could argue that GLPG0974, and indeed all synthetic orthosteric ligands of FFA2, are actually bitopic ligands as they will undoubtedly occupy a larger area of the binding pocket than SCFAs. Furthermore, a recent study demonstrated by utilising a FRET-based approach that FFA2 does form homodimers, as well as heterodimers with FFA3 (Ang et al., 2017). To explore this further, an assessment of the impact of C3 or compound 1 on [³H]-GLPG0974 dissociation in membranes that co-express wild type and R180A-R255A hFFA2 could be performed. The presence of a receptor form that cannot bind ligand, such as R180A-R255A hFFA2, should reduce the amount of wild type hFFA2 homodimers and would, conceptually, result in a reduction in the cooperative effect of C3 and compound 1 on [³H]-GLPG0974 dissociation, if this hypothesis is indeed true. An equivalent approach was successfully applied previously to confirm that cooperative interactions between two adenosine A₃ receptor ligands occurred across dimers (May et al., 2011).

4.4 Conclusions

Radioligands can be important tools in understanding ligand pharmacology at GPCRs and herein [³H]-GLPG0974 did indeed facilitate the analysis of hFFA2 ligand binding determinants and kinetics. While the Arg180-His242-Arg255 triad was essential for agonist binding to hFFA2, antagonist binding was less reliant on interaction with these key orthosteric residues, however at least one arginine was required to allow radioligand binding. This appears to be linked with the importance of the carboxylate moiety present in many orthosteric ligands of FFA2, which was crucial for agonist action (Schmidt et al., 2011, Hudson et al., 2013a) but not antagonist binding. Therefore, in future development of FFA2 ligands it should be ensured that a carboxylate moiety is set as a requirement for orthosteric agonist development, while this area of the molecule could be modified further for antagonists. Interestingly, different classes of hFFA2 antagonists show distinct kinetic profiles, which suggests that it may be possible to optimise antagonists for a long or short residence time. It could be of interest to relate structural features of antagonists with their kinetics to construct a “structure-kinetics relationship” for respective compound series. The use of ligands with different kinetic profiles in physiological systems could contribute to understanding the desired kinetic properties of ligands that target FFA2. However, the use of antagonists in rodent models of disease remains limited by the species-selectivity of antagonists for the human orthologue, which will be addressed in chapter 6. In conclusion, data presented in this chapter provides novel insights into the basis of FFA2 ligand pharmacology and can provide guidance for development of novel and improved tool compounds.

5 Development and characterisation of a fluorescent probe for FFA2

5.1 Introduction

Radioligand binding studies have played a tremendously important role in dissecting the pharmacology and function of GPCRs (Cooper et al., 2017). Applications of radioligands range from understanding the mode of ligand binding and defining receptor binding pockets (see chapter 4) to studying receptor oligomerisation (Ferreira et al., 2015) and tissue distribution (Sharif et al., 1999). However, radioligands have inherent limitations such as the safety requirements surrounding handling of radioactive materials. With recent advances in fluorescence-based methodologies for monitoring of protein-protein and protein-small molecule interactions, ligands that incorporate fluorophores have become established tools utilised to examine GPCR ligand binding and kinetics (Ma et al., 2014). The use of fluorescent probes has several advantages over conventional radioligand binding, including the circumvention of safety concerns regarding the use of radioactivity and the possibility to monitor ligand binding in real-time. Thereby the measurement of ligand binding kinetics can be greatly improved (May et al., 2011, Schiele et al., 2015), which is more difficult to achieve in a radioligand binding assay, and the interaction between ligand and receptor can even be visualised in a living cell (Daly et al., 2010). However, despite several advantages, fluorescent probes also have inherent limitations (Ma et al., 2014). Depending on the cell or tissue of interest, the emission spectrum of the fluorophore can fall into the spectrum of cellular autofluorescence, making it difficult to detect specific binding (Sklar et al., 2002). This limitation is enhanced by the often high level of nonspecific binding observed for fluorescent ligands, which can result in an unfavourable signal-to-noise ratio in applications such as cellular-based imaging (Leopoldo et al., 2009). One approach that can overcome issues arising from high nonspecific binding, combines fluorescent probes with proximity-based resonance energy transfer technology (Stoddart et al., 2015a, Christiansen et al., 2016). However, for detection of resonance energy transfer resulting from the fluorescent tracer binding to the receptor, the respective GPCR needs to be tagged with an appropriate fluorescence or bioluminescence donor such as in the case of bioluminescence, a luciferase enzyme. Therefore, such an approach is primarily

limited to heterologous expression systems. Taken together the benefits of using fluorescence over radioligand binding assay depend on the context of the study and the availability of a suitable fluorescent tracer. From a drug discovery perspective, fluorescence-based binding assays are attractive screening systems as they can, once established and optimised, be scaled up relatively easily to a high-throughput plate format and may be more cost-effective than radioligand binding assays (Janzen, 2014).

The investigation of FFA2 ligand binding determinants utilising the tritiated radioligand [³H]-GLPG0974 provided crucial information on the orthosteric binding pocket of FFA2 and the binding kinetics of distinct compound series (see chapter 4). Development of a fluorescent probe would expand the repertoire of tools available to examine FFA2 pharmacology and assess its drug target potential. A recent study successfully developed a BRET-based binding assay for FFA1 using a newly synthesised fluorescent tracer (Christiansen et al., 2016). This was achieved by linking an appropriate fluorophore to a FFA1 ligand that acted as a BRET acceptor and fusing a luciferase to the receptor N terminus, which served as a BRET donor in the presence of a substrate. For BRET-based assays that were employed previously to monitor β -arrestin recruitment, a luciferase cloned from sea pansy *Renilla reniformis* was fused to β -arrestin (see chapter 3). However, for the purpose of developing a BRET-based ligand binding assay, a different luciferase variant was utilised that was recently isolated from deep sea shrimp *Oplophorus gracilitostris* (Hall et al., 2012). The small luciferase subunit of the isolated enzyme was heavily engineered to develop the Nanoluciferase (NLuc), which has a relatively small size of 19 kDa, shows enhanced stability and produces a 150-fold brighter luminescent signal. The small size of NLuc and the fact that it has been engineered from a naturally secreted protein makes it less likely that N-terminal fusion will disrupt receptor trafficking and function (Hall et al., 2012). Indeed, in a study that developed a BRET binding assay for the β_2 AR, a signal representing specific ligand binding could only be detected using NLuc and not the *Renilla* luciferase variant RLuc8 (Stoddart et al., 2015a).

The basic requirement for a BRET reaction to take place is the overlap of donor emission and acceptor excitation spectra. Furthermore, the acceptor emission

spectrum should overlap as little as possible with the emission spectrum of the donor to avoid donor bleed-through during detection. These factors usually contribute to the selection of an appropriate luciferase and fluorophore pair. In the case of the BRET binding assay developed for FFA1, the nitrobenzoxadiazole (NBD) fluorophore was selected to complement NLuc-tagged FFA1 (Christiansen et al., 2016). How was this decision rationalised? Most importantly, the excitation spectrum of NBD matches the NLuc emission spectrum almost exactly, while there is little overlap with the NBD emission spectrum (**Figure 5.1A**). Furthermore, NBD is relatively small compared to other commonly employed fluorophores and therefore linking of NBD to a high-affinity ligand may be less likely to interfere with ligand binding. However, this will depend on the point of attachment and can be difficult to predict. Another important property of NBD is its solvatochromic behaviour, which refers to the solvent-dependence of NBD fluorescence. In a polar environment, such as common aqueous buffer solutions, NBD fluorescence is almost fully quenched, while in nonpolar environments, such as in organic solvents, or indeed deep ligand binding pockets or cell membranes, its fluorescence is high (Lin and Struve, 1991). Therefore, background fluorescence of NBD in aqueous environments is almost non-existent.

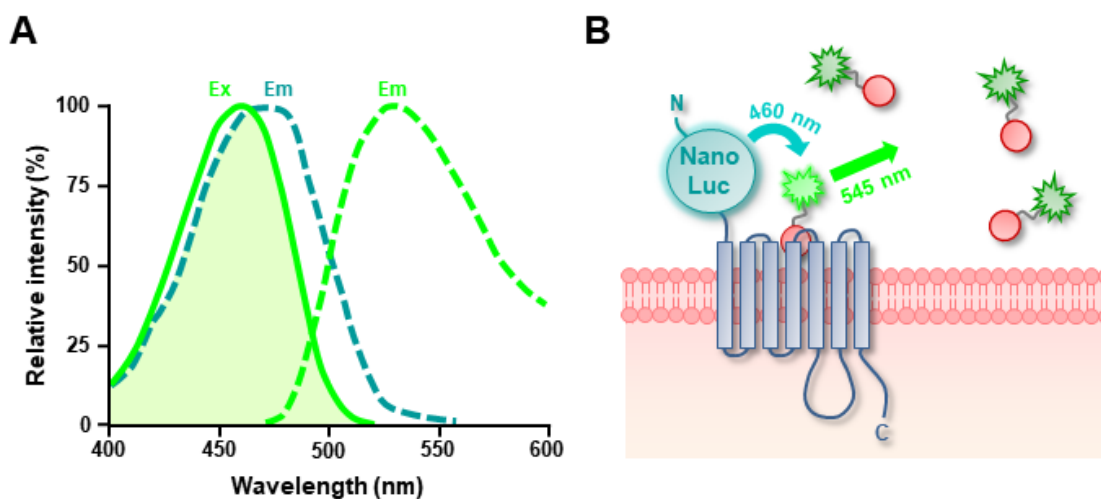


Figure 5.1 Principle of a BRET binding assay (A) The excitation (Ex) and emission (Em) spectra of fluorophore NBD (*green*) and emission spectrum of NLuc (*blue*) is shown. The overlap between the NBD excitation and NLuc emission spectra is highlighted in light green. **(B)** The Nanoluciferase (NLuc) that is fused to the N terminus of the receptor of interest emits light at 460 nm. When a suitable fluorophore such as NBD is in close enough proximity to NLuc, bioluminescence resonance energy transfer (BRET) takes place, which results in excitation of the fluorophore and emission of light centred at 545 nm. The BRET reaction depends on the distance between donor and acceptor, therefore unbound NBD-labelled ligand in the medium is not excited. The solvatochromic properties of NBD result in quenching of its fluorescence in an aqueous environment, therefore signal from unbound fluorophore should be minimal.

Furthermore, NBD has been employed previously for labelling of small molecules (Turcatti et al., 1995, Petrov et al., 2011). Therefore, NBD was selected as the complementing fluorophore for NLuc to develop a BRET binding assay (**Figure 5.1B**).

This chapter aimed to develop a fluorescent probe for the orthosteric binding site of FFA2 to be employed in a BRET binding assay. A selection of potential fluorescent tracers was synthesised by linking NBD to different parent molecules in collaboration with Dr Hansen in Professor Ulven's group at the University of Southern Denmark. After assessing how fluorophore attachment affected the function and binding affinity of resulting fluorescent probes, one candidate was selected for further studies. The fluorescent probe F-1 was utilised to develop a BRET binding assay, which was employed to measure the binding affinity and kinetics of unlabelled orthosteric antagonists for hFFA2. Furthermore, the binding site of F-1 was examined by assessing the effect of orthosteric binding site mutants of FFA2 on fluorescent probe affinity. Thereby, by following a strategy previously successfully applied for FFA1 (Christiansen et al., 2016), a BRET binding assay for FFA2 was successfully developed that could find use in a variety of applications. Furthermore, work presented in this chapter also highlights important considerations for development of fluorescent ligands and their suitability to explore ligand binding sites.

5.2 Results

5.2.1 Development of a FFA2 fluorescent ligand for BRET binding assays

Although NBD is a relatively small fluorophore, linking it to an existing FFA2 ligand is highly likely to affect the pharmacology and affinity of the parent molecule, hence the point of fluorophore attachment needs to be chosen with care. Structural investigations of the GLPG0974 and CATPB hFFA2 antagonist series showed that the carboxylate moiety was not necessary for high-affinity ligand binding and replacement of the carboxylate with larger functional groups was well tolerated, such as the morpholine group in MoGLPG-2 (see section 3.2.4 and 4.2.3). Therefore, the antagonist carboxylate moiety was selected for attachment of the linker and NBD fluorophore. Two potential fluorescent probes

were generated following this strategy: F-1, based on GLPG0974 analogue GLPG-3, which has an additional carbon in the benzothiophene linker and a para-trifluoromethyl substitution of the benzene ring in place of the meta-chlorobenzene in GLPG0974; and F-2, which is structurally related to CATPB (Figure 5.2A). Among available GLPG0974 analogues GLPG-3 was selected to generate a potential fluorescent tracer as its functional groups were least prone to secondary reactions during chemical synthesis and attachment of the fluorophore, thereby resulting in a higher yield. A further fluorescent probe was generated based on the structure of the FFA2 agonist compound 2-23, which showed highest potency among screened compound 2 analogues (see section 3.2.2). Modifications of the northern region were relatively well tolerated; therefore, the NBD fluorophore was attached with a short linker to the northern

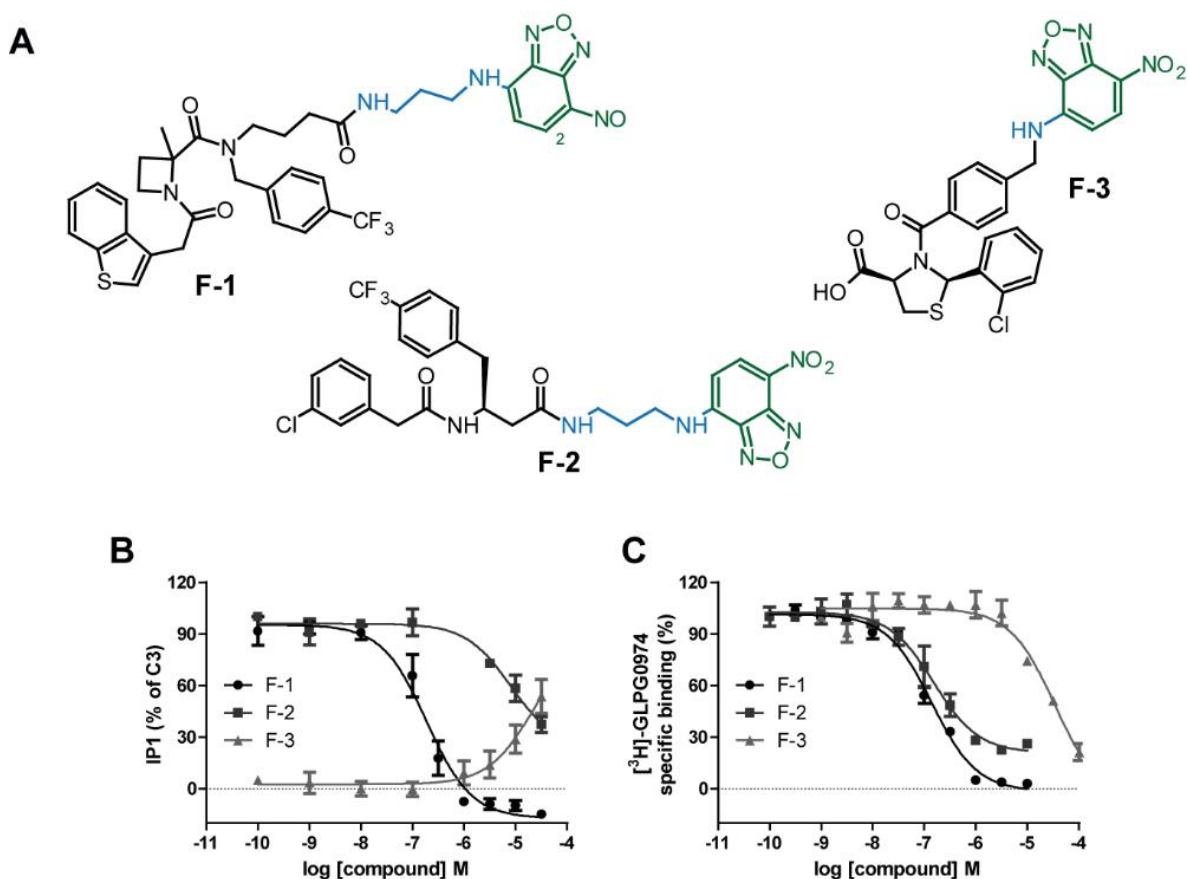


Figure 5.2 Assessment of function and binding of potential fluorescent tracers for hFFA2
Structures of potential fluorescent probes F-1, F-2 and F-3 are shown with the nitrobenzoxadiazole (NBD) fluorophore highlighted in green and the linker in blue (A). The ability of antagonist-based tracers F-1 and F-2 to inhibit the response of hFFA2 to 1 mM C3 in IP1 accumulation assays and the ability of the agonist-based tracer F-3 to induce accumulation of IP1 in Flp-In™ T-REx™ 293 cells induced to express hFFA2-eYFP was assessed (B). The capacity of increasing concentrations of F-1, F-2 and F-3 to compete with 10 nM [³H]-GLPG0974 for binding to membranes isolated from Flp-In™ T-REx™ 293 cells induced to express hFFA2-eYFP is shown from representative experiments (C). IP1 accumulation data was normalised to the response induced by 1 mM C3 for F-1 and F-2, and to the maximal response induced by C3 for F-3. Data are means pooled from independent experiments (n ≥ 3) that were performed in duplicate (B).

Table 5.1 Affinity and potency of potential fluorescent tracers for hFFA2

Assay	F-1 ^a	F-2 ^a	F-3 ^b
IP1 accumulation (pI/EC ₅₀)	6.57 ± 0.10	< 4.50	< 4.50
[³ H]-GLPG0974 competition (pK _i)	7.29 ± 0.07	7.26 ± 0.10	< 4.50
BRET saturation binding (K _d)	65.1 ± 1.8 nM	815 ± 192 nM	> 2 μM

^a IP1 accumulation assay data shown as pIC₅₀

^b IP1 accumulation assay data shown as pEC₅₀

benzene ring (**Figure 5.2A**). Following fluorescent ligand synthesis, the effect of the linker and NBD fluorophore addition on the pharmacological function and binding affinity of the prospective fluorescent tracers was examined. In IP1 accumulation assays F-1 and F-2 both retained the ability to inhibit the response of hFFA2 to an EC₈₀ concentration of C3 (**Figure 5.2B**). However, F-1 was at least 100-fold more potent than F-2 (**Table 5.1**) and inhibition by F-2 did not reach a plateau at concentrations of up to 30 μM (**Figure 5.2B**). The potency of the agonist-based fluorescent probe F-3 was also affected by attachment of the NBD fluorophore and F-3 was only able to induce IP1 accumulation at concentrations of 10 μM and above (**Figure 5.2B**). Although the affinity of F-1 and F-2 was not significantly different in [³H]-GLPG0974 competition binding assays (**Table 5.1**), F-2 was only able to outcompete approximately 80% of [³H]-GLPG0974 (**Figure 5.2C**), which suggested that F-2 may bind to a different site than [³H]-GLPG0974 and could therefore be acting in an allosteric fashion. Furthermore, the modest ability of F-2 to inhibit the response of hFFA2 to C3 in the IP1 accumulation assay did not correlate with the high affinity determined in the [³H]-GLPG0974 competition binding assay (**Table 5.1**), which also implied that F-2 has a complex pharmacology and may allosterically modulate [³H]-GLPG0974 binding and/or C3 potency or efficacy. F-3 was also not able to fully outcompete [³H]-GLPG0974 when using concentrations of up to 100 μM (**Figure 5.2C**), however, as the competition curve does not reach a plateau, this is most likely due to the low affinity of F-3 for hFFA2, which was anticipated from the poor potency of F-3 in the IP1 accumulation assay (**Figure 5.2B**).

Following this initial assessment, the suitability of F-1, F-2 and F-3 for a BRET binding assay was examined. For the purpose of the BRET binding assay, a Flp-In™ T-REx™ cell line was generated that stably expressed hFFA2 fused N-

terminally to NLuc in a doxycycline-inducible fashion. This cell line was extensively employed in functional and binding studies described in chapter 6, which confirmed expression levels and receptor functionality. As anticipated from the good performance in functional and binding assays, F-1 showed the highest affinity among the selection of fluorescent ligands (Table 5.1) with a good total to nonspecific signal ratio (Figure 5.3A and B). In contrast, the affinity of F-2 was 13-fold lower (Table 5.1). To determine the signal resulting from nonspecific binding of F-1 and F-2, synthesis intermediates LinkGLPG-3 and

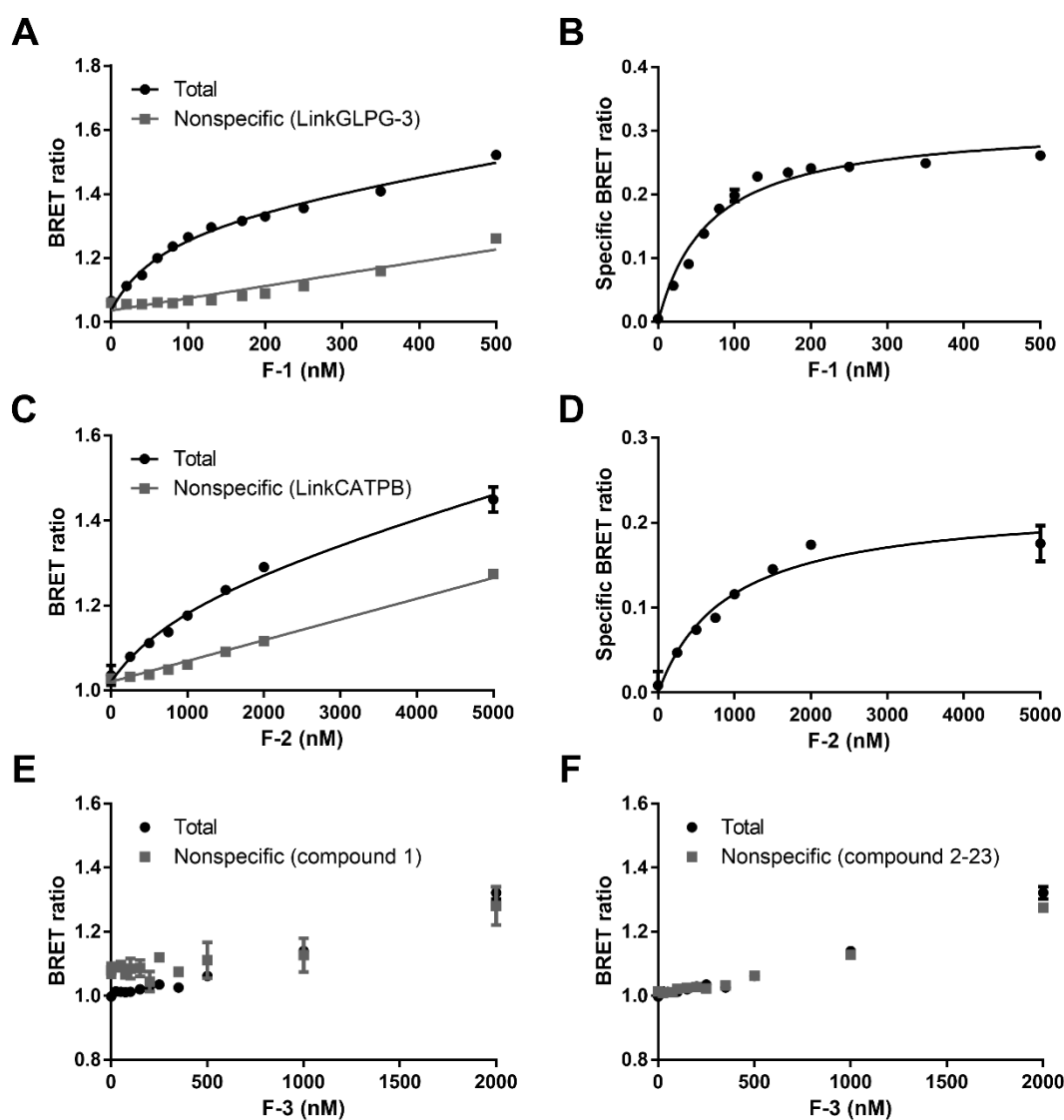


Figure 5.3 Fluorescent tracer F-1 shows highest affinity for hFFA2 in the BRET binding assay Binding of increasing concentrations of F-1 (A, B), F-2 (C, D) and F-3 (E, F) to membranes isolated from cells induced to express NLuc-hFFA2 is shown from representative experiments. Nonspecific binding of F-1 and F-2 was determined in presence of 50 μ M LinkGLPG-3 and 100 μ M LinkCATPB, respectively. The nonspecific signal was subtracted from the total signal to calculate the specific signal. To determine nonspecific binding of F-3, 100 μ M compound 1 (E) or compound 2-23 (F) were employed, but no specific signal could be detected.

LinkCATPB were employed to compete with respective fluorescent ligands for binding to the specific binding pocket. These compounds contain a *tert*-butyloxycarbonyl (BOC) group in place of the NBD fluorophore, which served as a protecting group of one of the linker amines during linker attachment. As these linker intermediates are identical to the fluorescent tracers apart from the attached fluorophore, they are likely to occupy the same binding site and can therefore be employed to determine the level of nonspecific binding of the tracers. For agonist-based fluorophore F-3 such a linker intermediate was not available, and it is difficult to predict the binding site of the tracer after fluorophore attachment. However, F-3 retained some agonist activity (**Figure 5.2B**) and homology modelling studies in chapter 4 suggested that orthosteric agonists need to adapt similar binding poses to engage Arg180^{5.39} and Arg255^{7.39} in a specific fashion to induce receptor activation. Therefore, synthetic agonists compound 1 (**Figure 5.3E**) and compound 2-23 (**Figure 5.3F**) were employed for quantification of the nonspecific signal. However, no specific signal representing F-3 binding was detected at concentrations of up to 2 μM , which suggested that the affinity of F-3 was indeed significantly lower than that of F-1 or F-2.

The results in the IP1 accumulation, [³H]-GLPG0974 competition and BRET binding assay demonstrated that F-1 had the best properties among fluorescent ligands tested. This compound showed the highest affinity and seemed to associate with the orthosteric site, unlike F-2, which appears to be allosteric. As the primary aim of this work was to generate an orthosteric probe, F-1 was employed in further investigations. However, more detailed characterisation of F-2 may facilitate development of a fluorescent probe for an allosteric binding site of FFA2, which could also be of value.

5.2.2 Real-time tracking of F-1 association and dissociation

The ability to track the binding kinetics of fluorescent ligands in real-time is one key advantage of fluorescent over radioactive ligand binding assays. Filtration-based kinetic binding assays that employ a radioligand are time-consuming and work-intensive because they need to be performed in a time-staggered manner. In contrast, light emission of the BRET donor and acceptor can be monitored in real-time using an appropriate plate reader. To measure dissociation of F-1 an “infinite dilution” approach was employed, which was achieved by

centrifugation of membranes expressing NLuc-hFFA2 with pre-associated F-1, aspiration of supernatant containing free fluorescent ligand and addition of binding buffer to dilute the membrane pellet by at least 100-fold. Measurement of the resulting reduction in the specific BRET ratio allowed determination of the K_{off} of F-1 (**Figure 5.4A**), which was $0.0237 \pm 0.0016 \text{ min}^{-1}$. The K_{on} of F-1 was determined by monitoring association of four concentrations of F-1 in parallel (**Figure 5.4B**), which resulted in an estimated association rate of $368,000 \pm 29,300 \text{ M}^{-1} \text{ min}^{-1}$. In agreement with the law of mass action, the association half-time increased with ligand concentration. Using the kinetic rate constants determined for F-1 in **figure 5.4**, the affinity of the fluorescent ligand was calculated by dividing the K_{off} by the K_{on} , yielding a K_{d} of $67.7 \pm 5.9 \text{ nM}$, which is close to the affinity determined in saturation binding (**Table 5.1**).

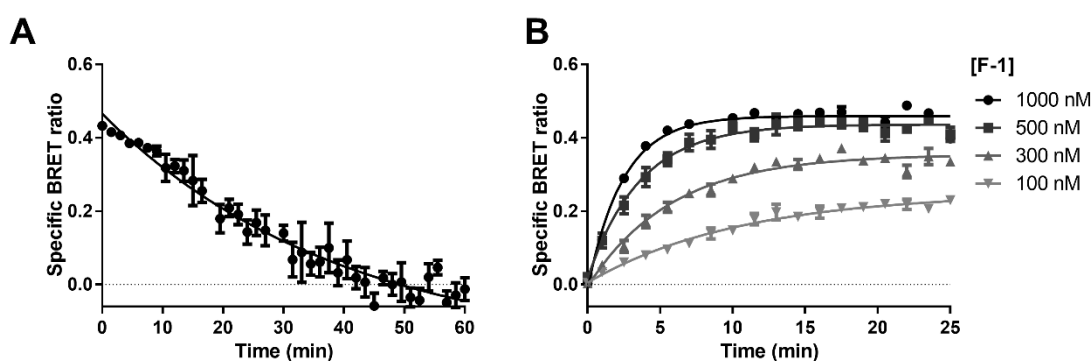


Figure 5.4 BRET binding assay can be employed to monitor F-1 binding kinetics in real-time. Dissociation of 100 nM F-1 from NLuc-hFFA2 was induced by preventing rebinding using an “infinite dilution” approach after 2 h pre-association of F-1 and was monitored over time (**A**). Association of varying concentrations of F-1 to NLuc-hFFA2 is shown (**B**). Nonspecific binding was determined in presence of 50 μM LinkGLPG-3 and subtracted from the total signal to obtain the specific signal. Data from representative experiments are shown.

5.2.3 Assessment of hFFA2 antagonist binding and kinetics using fluorescent ligand F-1

As the BRET binding assay was, in part, developed with the aim to establish a novel compound screening system, the suitability of F-1 for competition binding assays was assessed using a selection of hFFA2 antagonists: GLPG0974 (**Figure 5.5A**), CATPB (**Figure 5.5B**) and MeCATPB (**Figure 5.5C**). All three ligands were able to fully outcompete F-1 and with increasing concentrations of F-1 a rightward shift of the competition curve could be observed (**Figure 5.5**), while the K_{i} values determined from competition binding curves with different

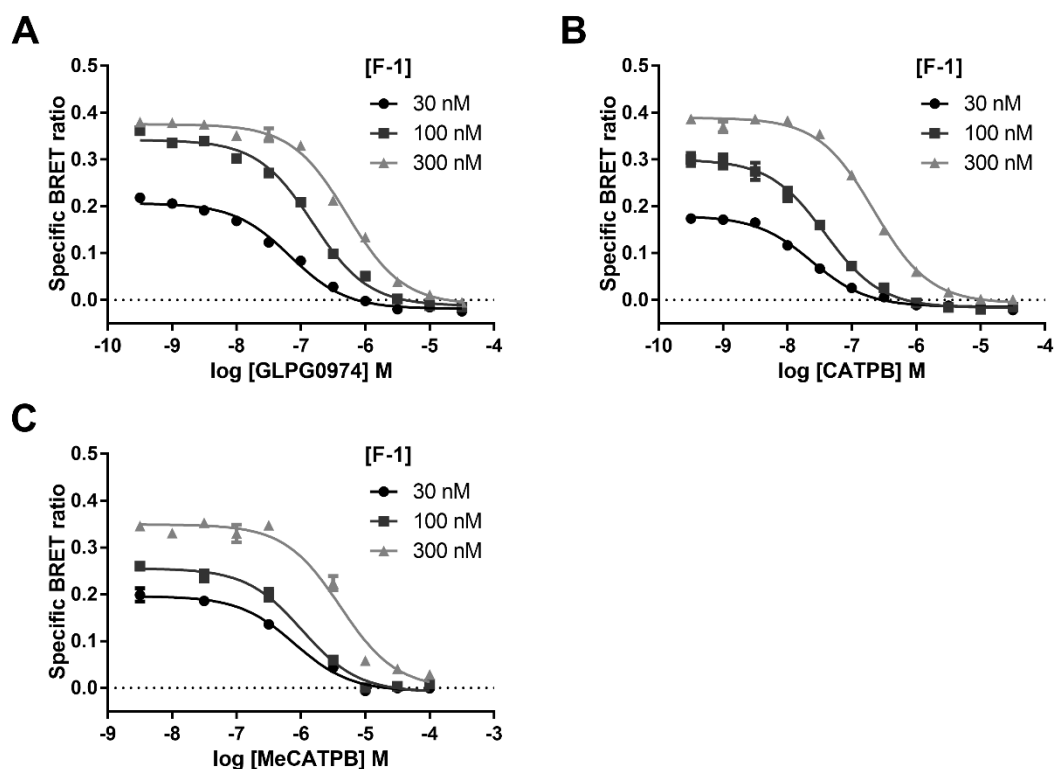


Figure 5.5 F-1 competition binding assay can be employed to determine unlabelled hFFA2 antagonist affinity The ability of increasing concentrations of GLPG0974 (A), CATPB (B) and MeCATPB (C) to compete with varying concentrations of F-1 for binding to NLuc-hFFA2 is shown from representative experiments. Nonspecific binding was determined in presence of 50 μ M LinkGLPG-3 and subtracted from the total signal to obtain the specific signal.

concentrations of F-1 were consistent. Taken together, these observations suggest a competitive relationship between competing and fluorescent ligand. In agreement with previous investigations of antagonist analogues (see section 4.2.3), replacement of the CATPB carboxylate with a methyl ester resulted in a 26-fold decrease in affinity (Table 5.2). Therefore, the F-1 competition binding assay was indeed capable of detecting similar trends as the radioligand competition binding assay. However, the estimated affinity of GLPG0974 was lower than previously determined in [3 H]-GLPG0974 competition binding assays, where the K_i of GLPG0974 was estimated at 13 nM (see chapter 4), while binding assays utilising F-1 yielded a K_i of approximately 70 nM (Table 5.2).

Table 5.2 Affinities of hFFA2 antagonists determined in F-1 competition binding assay

Compound	GLPG0974	CATPB	MeCATPB
pK _i	7.16 \pm 0.03	7.84 \pm 0.02	6.42 \pm 0.03***

* Comparison of MeCATPB pK_i values with CATPB by unpaired *t* test with significant differences denoted as P = *** \leq 0.001

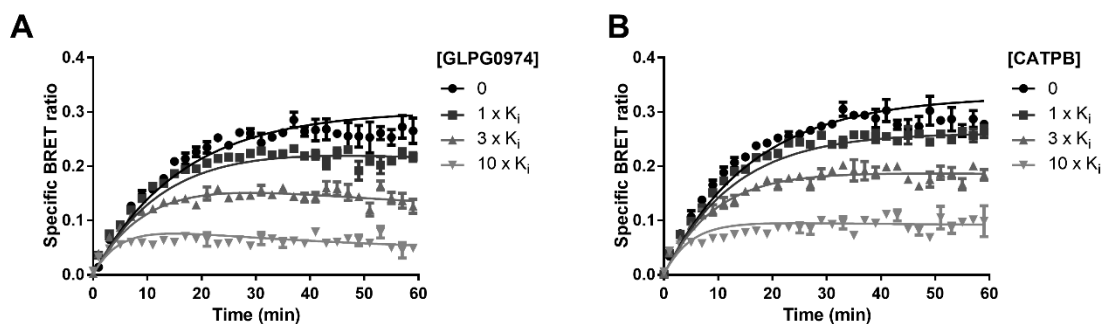


Figure 5.6 Use of F-1 competitive kinetic binding assay to determine kinetic parameters of hFFA2 antagonists The association of 100 nM F-1 to NLuc-hFFA2 was monitored in the presence or absence of GLPG0974 (**A**) and CATPB (**B**). A competitive kinetic binding model (Dowling and Charlton, 2006) was used to fit shown data to estimate the kinetic parameters of unlabelled competing ligands and resulting analysis is shown in table 5.3. Respective K_i values of antagonists are shown in table 5.2. Nonspecific binding was determined in the presence of 50 μ M LinkGLPG-3 and subtracted from the total signal to obtain the specific signal. Data from representative experiments are shown.

Assessment of GLPG0974 and CATPB binding kinetics in radioligand binding assays revealed that GLPG0974 has a significantly slower kinetic profile than CATPB (see section 4.2.6). To examine whether an equivalent competitive kinetic binding assay can be established using F-1, the effect of increasing concentrations of GLPG0974 (**Figure 5.6A**) and CATPB (**Figure 5.6B**) on the association rate of F-1 was monitored. Indeed, application of a competitive kinetic binding model allowed the estimation of association and dissociation rates of GLPG0974 and CATPB (**Table 5.3**). As observed in the radioligand-based competition kinetic binding assay, CATPB showed a significantly faster association and dissociation rate than GLPG0974 by 5-fold and 2-fold, respectively. Resulting K_d values calculated using the estimated rate constants (**Table 5.3**) correlated well with affinities determined in the equilibrium competition binding assay (**Table 5.2**).

Table 5.3 Kinetics of FFA2 antagonists determined in F-1 competitive kinetic binding assay

Parameter	GLPG0974	CATPB
K_{off} (min^{-1})	0.0099 ± 0.0014	$0.0205 \pm 0.0010^{**}$
K_{on} ($\text{M}^{-1} \text{min}^{-1}$)	$211,000 \pm 4,780$	$1,083,000 \pm 59,800^{***}$
K_d^a (nM)	46.9 ± 6.7	18.9 ± 1.4

^a Determined by dividing the K_{off} by the K_{on} value of at least three independent experiments

* Analysis of K_{off} and K_{on} values by unpaired t test with significant differences denoted as $P = ** \leq 0.01$ and $P = *** \leq 0.001$

5.2.4 FFA2 agonists and allosteric ligands cannot outcompete fluorescent ligand F-1 binding

While the tested hFFA2 antagonists behaved in a competitive fashion with F-1, which allowed determination of unlabelled ligand affinity and binding kinetics, this does not seem to be the case for FFA2 agonists. Increasing concentrations of C3 and compound 1 were unable to fully outcompete F-1 (**Figure 5.7A**), which suggested that F-1 did not bind to the same site as these FFA2 agonists. Perhaps this observation was not fully unexpected, as the NBD fluorophore and linker were attached at the carboxylate moiety, which is thought to represent the main point of interaction with the orthosteric binding site. However, the ability of hFFA2 antagonists to fully outcompete F-1 binding suggested that the binding site of F-1 should, at least partially, overlap with that of orthosteric hFFA2 antagonists. To examine whether the binding site of F-1 coincides with that of other allosteric FFA2 ligands, the effect of increasing concentrations of 4-CMTB and AZ1729 on the binding of F-1 was assessed (**Figure 5.7B**). Neither 4-CMTB nor AZ1729 affected binding of F-1, indicating that the F-1 binding site is distinct from that of other allosteric ligands. However, cooperativity between allosteric ligand and F-1 binding cannot be ruled out based on these results, as the F-1 concentration employed may be too high to detect low levels of cooperativity.

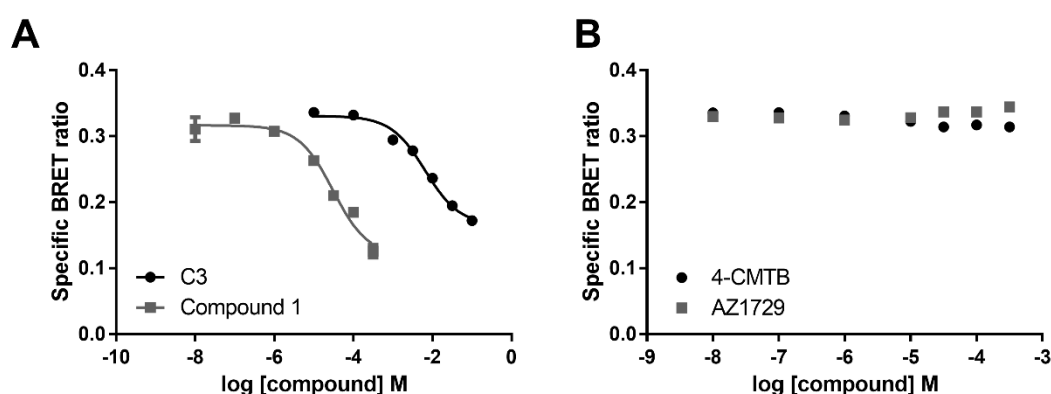


Figure 5.7 FFA2 agonists are unable to fully outcompete F-1 The ability of increasing concentrations of C3 and compound 1 (**A**), and 4-CMTB and AZ1729 (**B**) to compete with 100 nM F-1 for binding to NLuc-hFFA2 is shown from representative experiments. Nonspecific binding was determined in presence of 50 μ M LinkGLPG-3 and subtracted from the total signal to obtain the specific signal.

5.2.5 Fluorescent ligand F-1 can be used to assess binding to R180A-R255A hFFA2

The inability of FFA2 agonists C3 and compound 1 to fully outcompete F-1 at NLuc-hFFA2 suggested that the mode of F-1 binding to hFFA2 might be distinct to that of orthosteric ligands. To examine the binding site of F-1 in more detail, saturation binding assays were performed at alanine replacement mutants of key orthosteric binding site residues. F-1 affinity was increased significantly at single orthosteric arginine mutants R180A (**Figure 5.8A**) and R255A (**Figure 5.8B**) by 5.2- and 6.6-fold, respectively. This result was in agreement with the observation that other antagonist analogues with modifications at the carboxylate moiety, such as methyl ester analogues, showed an increased affinity at R180A and R255A hFFA2 (see section 4.2.3). Interestingly, F-1

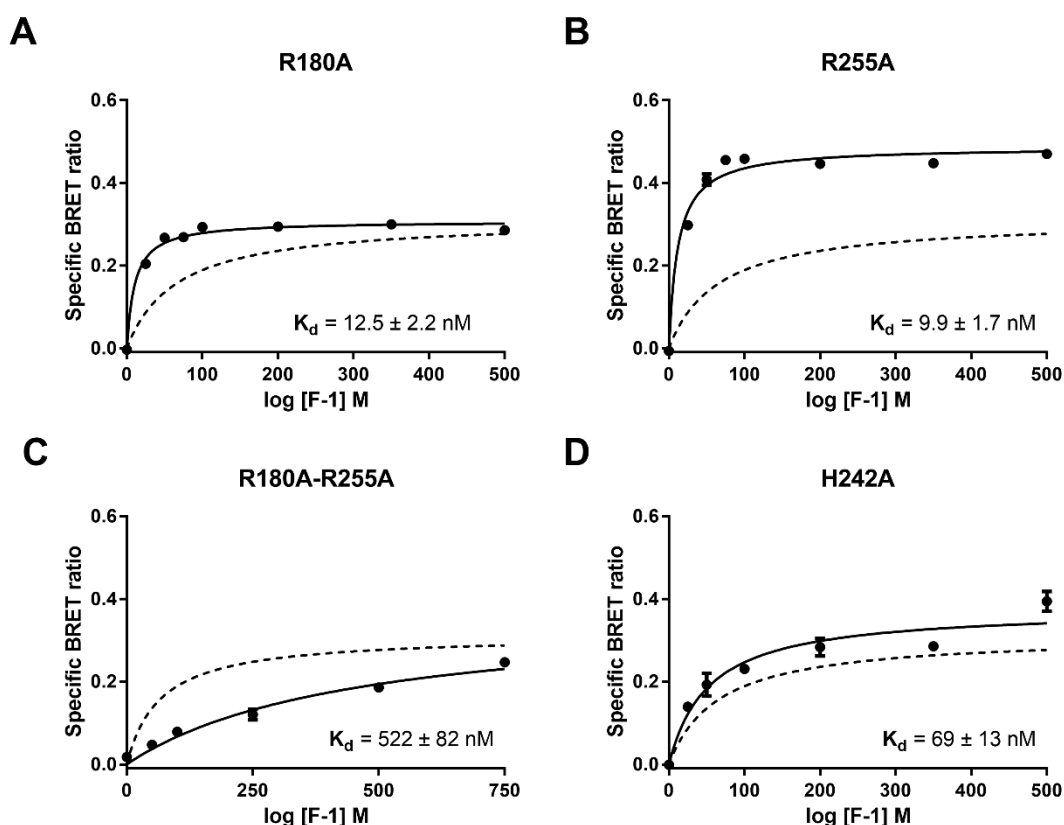


Figure 5.8 Binding characteristics of F-1 to orthosteric binding site mutants of hFFA2

Binding of F-1 to membranes isolated from Flp-In™ T-REx™ 293 cells induced to express mutant forms of NLuc-hFFA2 with alanine replacement of Arg180^{5.39} (**A**), Arg255^{7.35} (**B**) Arg180^{5.39} and Arg255^{7.35} (**C**) or His242^{6.55} (**D**) was assessed and is shown from representative experiments. Nonspecific binding was determined in presence of 50 μ M (**A, B, D**) or 100 μ M (**C**) LinkGLPG-3 and subtracted from the total signal to obtain the specific signal. K_d values shown are means pooled from independent experiments ($n \geq 3$) that were performed in triplicate. For comparison, saturation binding of F-1 to wild type FFA2 is included (*broken line*) with original data shown in figure 5.3.

retained the ability to bind the dual mutant R180A-R255A hFFA2 with a relatively modest 8-fold loss in affinity (**Figure 5.8C**). Alanine replacement of His242^{6.55}, which is a residue demonstrated to be important for agonist but not antagonist binding (see section 4.2.2), did not significantly affect F-1 affinity, suggesting that F-1 does not interact with this residue.

As the radioligand [³H]-GLPG0974 did not display specific binding at the R180A-R255A mutant of hFFA2 (see section 4.2.1), the ability of F-1 to bind to R180A-R255A hFFA2 provided the unique opportunity to assess whether other hFFA2 antagonists are also able to bind to this hFFA2 mutant. Neither GLPG0974 nor CATPB were able to compete with F-1 for binding to R180A-R255A hFFA2 (**Figure 5.9A**), confirming the hypothesis stated in chapter 4, which suggested that orthosteric antagonists do require at least one arginine residue to interact with

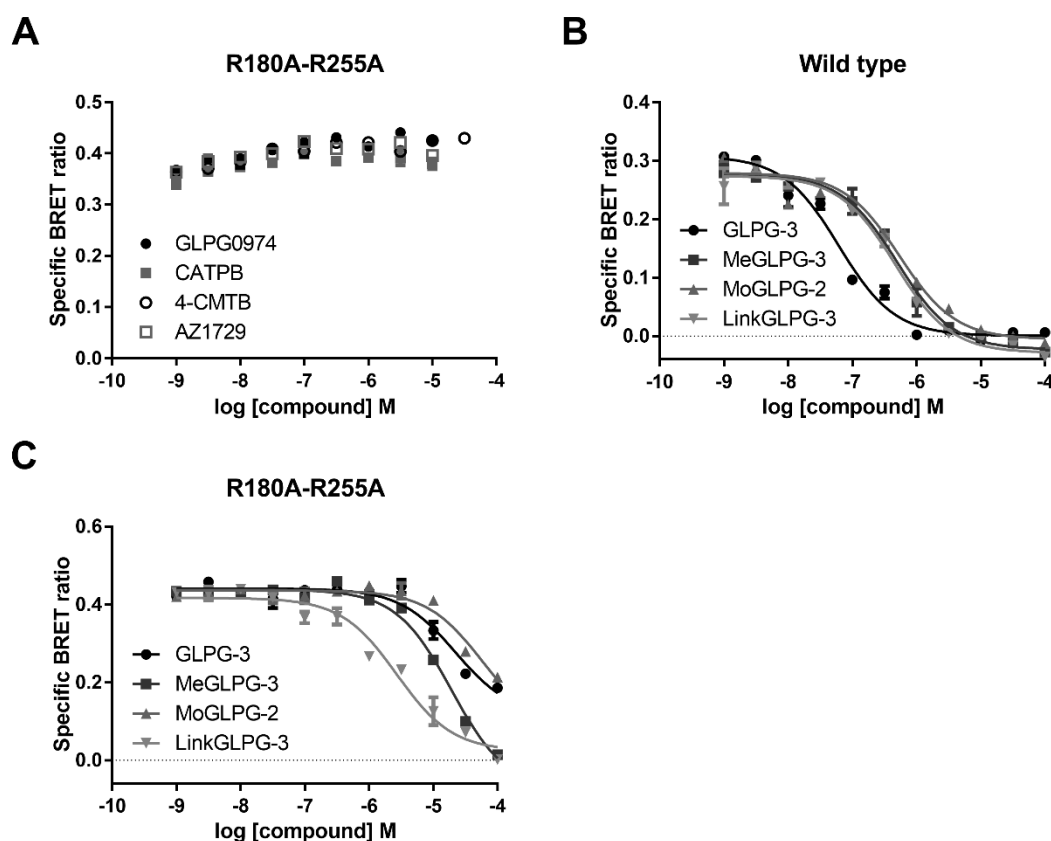
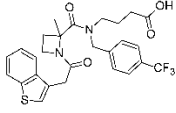
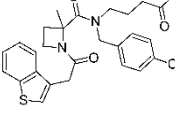
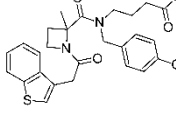
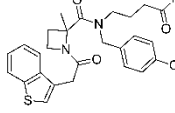


Figure 5.9 Selected hFFA2 antagonists are able to compete with F-1 for binding to R180A-R255A hFFA2 The ability of increasing concentrations of hFFA2 antagonists GLPG0974 and CATPB, and the allosteric hFFA2 ligands 4-CMTB and AZ1729 to compete with 500 nM F-1 for binding to R180A-R255A NLuc-hFFA2 is shown (**A**). The effect of increasing concentrations of GLPG-3, MeGLPG-3, MoGLPG-2 and LinkGLPG-3 on 100 nM (**B**) and 500 nM (**C**) F-1 binding to wild type (**B**) and R180A-R255A (**C**) NLuc-hFFA2 is shown. Nonspecific binding was determined in presence of 100 μ M (**A, C**) or 50 μ M (**B**) LinkGLPG-3 and subtracted from the total signal to obtain the specific signal. Data from representative experiments are shown.

hFFA2 (see section 4.2.1). Although allosteric ligands 4-CMTB and AZ1729 are able to activate R180A-R255A hFFA2, their binding site did not seem to overlap with that of F-1 as increasing concentrations of neither allosteric ligand were unable to compete with the fluorescent probe (**Figure 5.9A**). To examine the structural determinants that allow F-1 to interact with R180A-R255A hFFA2, a selection of different antagonist analogues with different carboxylate modifications were tested at wild type and R180A-R255A hFFA2: Carboxylate-containing parent compound GLPG-3, methyl ester analogue MeGLPG-3, structurally related morpholine-containing compound MoGLPG-2 and synthesis intermediate LinkGLPG-3. At wild type hFFA2, all antagonist analogues were able to fully outcompete F-1 (**Figure 5.9B**) and replacement of the carboxylate moiety resulted in an approximately 10-fold reduction in affinity of all tested analogues (**Table 5.4**). However, the estimated affinity of compounds without carboxylates was not significantly different, suggesting that the size of the modification did not play an important role. At R180A-R255A hFFA2, Link-GLPG-3 showed the highest affinity (**Figure 5.9C**), however, compared to wild type hFFA2, a 5.5-fold reduction in affinity could be observed (**Table 5.4**). In addition to LinkGLPG-3, MeGLPG-3 was also able to fully outcompete F-1 at R180A-R255A hFFA2 (**Figure 5.9C**), but the affinity of MeGLPG-3 was affected more by the dual arginine mutation than that of LinkGLPG-3 with a 46-fold decrease in affinity compared to wild type hFFA2 (**Table 5.4**). Carboxylate-containing GLPG-3 was unable to fully outcompete F-1 at concentrations of up to 100 μM , however, in contrast to GLPG0974 and CATPB, it appeared to have some affinity for R180A-R255A hFFA2 as 100 μM of GLPG-3 were able to induce approximately

Table 5.4 Affinities of hFFA2 antagonists for wild type versus R180A-R255A hFFA2

Receptor	 GLPG-3	 MeGLPG-3	 MoGLPG-2	 LinkGLPG-3
Wild type	7.09 \pm 0.16	6.10 \pm 0.10***	6.13 \pm 0.09***	6.20 \pm 0.11***
R180A-R255A	< 4.00	4.44 \pm 0.11\$\$\$	< 4.00	5.50 \pm 0.03\$\$\$

* Comparison of pK_i values at wild type hFFA2 one-way ANOVA followed by Dunnett's test with the pK_i of GLPG-3 as a reference with significant differences denoted as $P = *** \leq 0.001$

§ Comparison of pK_i values of MeGLPG-3 and LinkGLPG-3 at wild type and R180A-R255A hFFA2 by unpaired t test with significant differences denoted as $P = $$$ \leq 0.001$

50% displacement of F-1 (**Figure 5.9C**). Interestingly, MoGLPG-2 behaved in a similar manner as GLPG-3, suggesting that the morpholine modification of GLPG-2 did not improve its ability to bind to R180A-R255A hFFA2.

5.3 Discussion

5.3.1 GLPG0974 analogue GLPG-3 provides a good backbone for NBD fluorophore attachment

The most common strategy followed when designing fluorescent probes based on small molecules is to attach the fluorophore to a known pharmacophore using an appropriate linker (Stoddart et al., 2015b). The choice of linker and fluorophore can affect a multitude of properties of the resulting fluorescent ligand such as pharmacological behaviour, binding affinity and solubility (Baker et al., 2010, Vernall et al., 2013). Although fluorescent ligands are often designed with a rationale in mind, much of the development process comes down to trial-and-error. Unlike radioligands, each newly synthesised fluorescent probe must be considered as a separate pharmacological entity distinct from its parent compound and needs to be characterised in detail prior to further application. This important consideration was exemplified by results described in this chapter that demonstrated the distinct effects of fluorophore attachment on the pharmacology of different FFA2 pharmacophores.

To generate the antagonist-based fluorescent probes F-1 and F-2, the NBD fluorophore was attached via linkage to the carboxylate moiety, as this was previously shown to be dispensable for high-affinity binding of hFFA2 antagonists (see section 4.2.3). The parent molecules used to generate F-1 and F-2 were GLPG0974 analogue GLPG-3 and CATPB, respectively. Interestingly, although in ligand docking poses the carboxylate of GLPG0974 and CATPB adopted relatively similar conformations (see section 4.2.4), the attachment of NBD had different effects on the pharmacology of the respective fluorescent probes. F-1 retained the ability to inhibit the hFFA2 response to C3 with a relatively high pIC₅₀ and showed good affinity for hFFA2 in [³H]-GLPG0974 competition and BRET binding assays. In contrast, the inhibitory action and binding affinity of F-2 was detrimentally affected. Furthermore, F-2 also showed behaviour typical of allosteric ligands in the [³H]-GLPG0974 competition binding assay, as increasing

concentrations of F-2 were unable to fully outcompete the radioligand. These observations suggest that F-1 and F-2 have distinct modes of binding, although their chemistry was based on parent molecules that are thought to interact in a similar way with the receptor, which highlights that it is indeed difficult to predict the behaviour of a fluorescent probe based on its parent compound. While the affinity of F-1 and F-2 for hFFA2 was in the high nM range, specific binding of agonist-based fluorophore F-3 could not be detected at concentrations of up to 2 μM in the BRET binding assay. The [^3H]-GLPG0974 competition binding assay suggested an estimated K_d of greater than 30 μM . Therefore, the point of fluorophore attachment in F-3 has likely affected binding affinity to an extent which makes it difficult to work with this fluorescent tracer and perhaps other points of attachment should be explored for generation of a fluorescent agonist ligand.

Examination of F-1, F-2 and F-3 pharmacology highlights that it can be difficult to predict how fluorophore and linker attachment to a small molecule will change the pharmacology of the resulting fluorescent tracer. This was also reflected in the development of fluorescent ligands for other GPCRs (Vernall et al., 2014). In the case of the CB₂ cannabinoid receptor, a conjugable analogue of the CB₂-selective inverse agonist SR144528 was generated by synthesising an analogue with a primary amino group that allowed attachment of a linker arm (Bai et al., 2008). Following conjugation of a near-infrared dye resulted in a fluorescent tracer suitable for fluorescence imaging. However, exploration of other linker attachment points in SR144528 resulted in loss of ligand binding to the receptor (Sexton et al., 2011). These studies exemplify that the point of linker and fluorophore attachment needs to be structurally tolerated and selection of an appropriate point of modification is largely a process of trial-and-error without additional structural information. A more detailed investigation of fluorescent ligands for the A₁ adenosine receptor revealed that not only the attachment point itself is of crucial importance, but that the resulting fluorophore affinity is also highly dependent on the combination of fluorophore and linker employed (Baker et al., 2010). Although the most common strategy for development of fluorescent tracer is the conjugation of a known pharmacophore to a fluorophore using a linker, alternatively the fluorophore can also be incorporated as part of the pharmacophore, which is possible with

smaller fluorophores such as NBD. Although this approach was not successful in the case of the agonist-based F-3 fluorescent tracer described here, an isatin acylhydrazone-based CB₂ antagonist was able to tolerate incorporation of NBD as part of its pharmacophore and, despite a slightly reduced affinity, specific binding of the resulting fluorescent probe to T-cells could be visualised with fluorescent confocal microscopy (Petrov et al., 2011).

5.3.2 BRET binding assay utilising fluorescent ligand F-1 can be employed to screen hFFA2 antagonists

From a drug discovery perspective, fluorescent ligands play an important role in the development of high-throughput screening formats (Janzen, 2014). Among the selection of synthesised fluorescent tracers, F-1 displayed the highest binding affinity, a good specific to nonspecific binding ratio and did initially not show allosteric behaviour. Therefore, F-1 was selected for further investigation and its suitability for screening of FFA2 ligands was assessed. In BRET-based F-1 competition binding assays a similar trend as in [³H]-GLPG0974 competition binding assays could be observed when comparing the affinities of a representative carboxylate/methyl ester hFFA2 antagonist pair (CATPB/MeCATPB). However, increasing concentrations of FFA2 agonists C3 and compound 1 were unable to fully displace F-1 from hFFA2, which suggests that F-1 binding is negatively modulated in an allosteric fashion by FFA2 agonists, which will be discussed in more detail in the following section.

Drug residence time is an increasingly important property to consider in drug development, as discussed in detail in chapter 4, and can be a deciding factor for therapeutic success (Guo et al., 2014). However, accurate monitoring of ligand binding kinetics using radioligand binding assays can be challenging. One of the most important advantages of fluorescent tracers is the possibility to monitor ligand binding kinetics in real-time, in particular as the competitive kinetic binding assay allows estimation of kinetic parameters of unlabelled ligands by assessing their effect on probe association (Dowling and Charlton, 2006). Therefore, it was examined whether F-1 could be utilised in a BRET binding assay to determine the binding kinetics of hFFA2 antagonists. The qualitative differences in binding kinetics of GLPG0974 and CATPB that were observed in the radioligand-based assay (see section 4.2.6) were indeed mirrored

in the competitive kinetic binding assay using F-1. However, the estimated association and dissociation values were different, which may have been in part due to the increased temperature at which the assay was performed. Conceptually, the rate constants should increase with higher temperatures, but surprisingly this was not the case here. The association rates of GLPG0974 and CATPB were actually reduced rather than increased. Therefore, the F-1 competitive kinetic binding assay could perhaps be useful to identify qualitative trends in binding kinetics, but to quantify rate constants the radioligand-based assay would be more appropriate. One limitation of the BRET binding assay is the depletion of the NLuc substrate employed in kinetic assays. With decreasing substrate concentration the data quality decreases, therefore the measurement error increases at later time points. Optimisation of substrate concentration and selection of a substrate that is more stable over time could improve data quality and potentially contribute to more accurate quantitative measurements.

5.3.3 Fluorescent tracer F-1 does not behave as an orthosteric FFA2 ligand

The first observation suggesting that F-1 may not be an orthosteric ligand was the partial competition with orthosteric FFA2 agonists in the competition binding assay, i.e. F-1 was able to occupy the receptor in the presence of SCFA C3 and synthetic agonist compound 1, albeit with reduced affinity. Such behaviour is typical for allosteric ligands, as partial competition in binding assays can be attributed to the negative cooperative effect of competing ligand binding on radioactive or fluorescent probe affinity (Gregory et al., 2007). Further support for an allosteric binding mode of F-1 was provided by its ability to bind to the dual mutant R180A-R255A hFFA2. Although binding of antagonists to hFFA2 was shown to be less dependent on the interaction between ligand carboxylate and the orthosteric arginine pair, binding of [³H]-GLPG0974 required at least one arginine to be present for a high-affinity interaction (see section 4.1.1). Furthermore, alanine replacement of single arginine residues had a modest negative effect on [³H]-GLPG0974 binding affinity. In contrast, the affinity of F-1 for R180A and R255A hFFA2 was significantly increased. In the case of H242A hFFA2, F-1 binding affinity was unchanged compared to wild type hFFA2, while this mutation increased the binding affinity of [³H]-GLPG0974. Taken together,

these results suggest that the key determinants of F-1 binding may differ compared to orthosteric antagonist GLPG0974.

How could F-1 be interacting with the hFFA2 binding pocket? This question is difficult to answer definitively without further site-directed mutagenesis and ligand docking studies. Competition binding studies with F-1 suggest that the binding sites of F-1 and orthosteric antagonists overlap, while orthosteric agonists exert an allosteric effect on F-1 binding and do therefore not bind to the same site. Previous [³H]-GLPG0974 binding studies and homology modelling suggested that the primary overlap of FFA2 agonist and antagonist binding sites is centred at the ionic interaction between the ligand carboxylate and the orthosteric Arg180^{5.39} and Arg255^{7.35} pair (see chapter 4). Furthermore, one hypothesis to explain the positive cooperative effect of agonists on [³H]-GLPG0974 dissociation implied that orthosteric agonists and antagonists bind to distinct sites in the receptor that both incorporate the orthosteric arginine pair, suggesting that orthosteric antagonists primarily interact with a secondary binding site (see chapter 4). As the core structure of F-1 is based on a GLPG0974 analogue, it may occupy such a secondary antagonist binding pocket, which lies outside of the defined orthosteric binding site and contains the additional residue contacts that are required for high-affinity binding of orthosteric antagonists (**Figure 5.10**). Linking of a fluorophore to the carboxylate moiety may force this region to adopt a different conformation compared to GLPG0974 to accommodate for its increased size, such that the interaction with the orthosteric arginines is lost (**Figure 5.10**). Thereby, C3 and compound 1 would be able to bind simultaneously with F-1 and exert the allosteric modulation observed in competition binding assays. Such a mode of F-1 binding would also serve as an explanation as to why other allosteric FFA2 ligands such as 4-CMTB and AZ1729 did not compete with F-1 binding to hFFA2 or indeed R180A-R255A hFFA2, as the allosteric binding pocket of F-1 is a component of the secondary binding site of orthosteric antagonists. The presence of several allosteric binding sites in FFA2 is not necessarily unexpected, as free fatty acid receptor FFA1 is also thought to contain multiple allosteric binding sites (Milligan et al., 2017). A recent crystal structure of FFA1 revealed an allosteric binding site outside of the transmembrane helices to which allosteric agonist AP8 binds to exert its positive modulatory effects

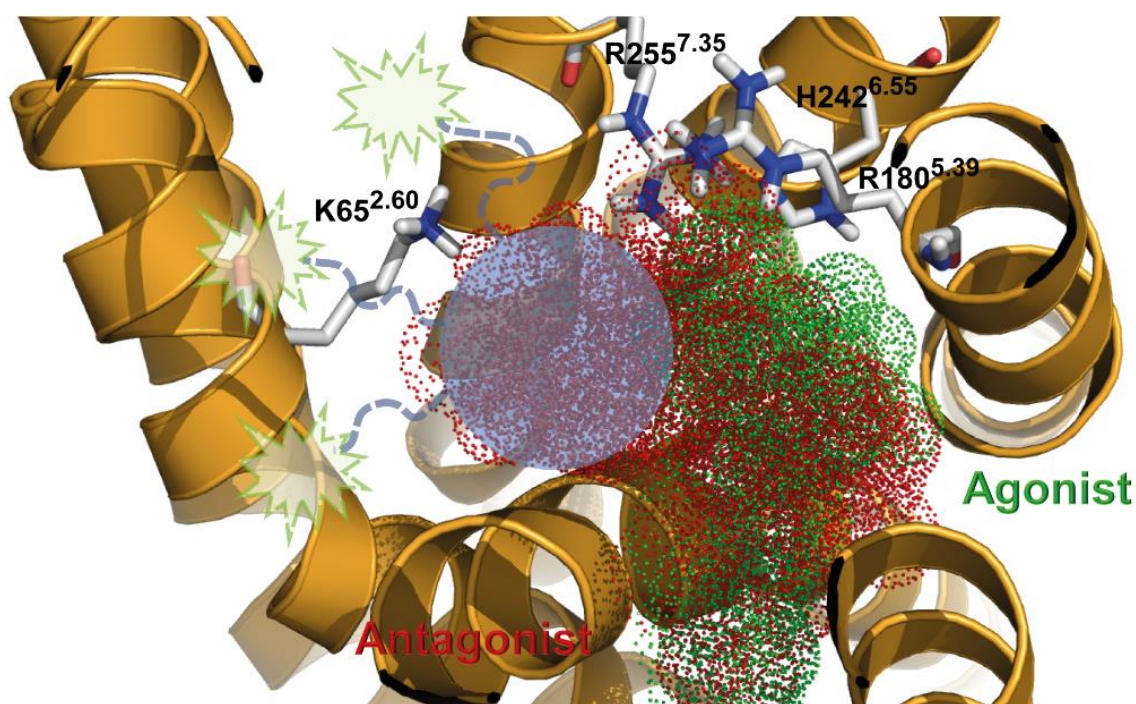


Figure 5.10 Potential F-1 binding site in relation to FFA2 agonists and antagonists A hFFA2 homology model constructed using a FFA1 crystal structure as a template is shown (see section 4.2.4). Area occupied by agonists C3 and compound 1 (*green*) and antagonists GLPG0974 and CATPB (*red*) is illustrated. The binding site of the F-1 pharmacophore that was based on a GLPG0974 analogue likely overlaps with that of FFA2 antagonists in the area highlighted in blue, while the linker (*blue line*) and fluorophore (*green*) adopt an unknown conformation outside of the orthosteric Arg-His-Arg triad.

(Lu et al., 2017). FFA1 is not the only GPCR with an extra-helical binding site; crystal structures of the glucagon (Jazayeri et al., 2016) and PAR2 (Cheng et al., 2017) receptors in complex with allosteric antagonists revealed that allosteric ligands can interfere with active-state conformational helical rearrangements by binding outside of the transmembrane helical bundle. These studies highlight that areas apart from the ligand-accessible surface area need to be considered as potential allosteric binding sites, which can make it difficult to define the mode of allosteric ligand binding without structural information.

5.3.4 Certain hFFA2 antagonists retain the ability to bind to R180A-R255A hFFA2

Although the ability of fluorescent probe F-1 to interact with R180A-R255A hFFA2 complicates its pharmacological behaviour and indicates that F-1 is indeed not an orthosteric ligand, it provided an opportunity to examine whether other antagonists are able to bind to R180A-R255A hFFA2. Interestingly, distinct analogues of GLPG0974 have different affinities for the dual arginine mutant.

While GLPG0974 was unable to compete with F-1 for binding to R180A-R255A hFFA2 at concentrations of up to 30 μM , its analogue GLPG-3 was able to compete with F-1 at concentrations of over 3 μM . Replacement of the GLPG-3 carboxylate with a methyl ester further increased the capacity of the ligand to bind to R180A-R255A hFFA2. It would be interesting to test a larger set of hFFA2 antagonist analogues at R180A-R255A hFFA2, as it might provide information on the structural modifications that resulted in the switch from the orthosteric antagonist GLPG0974 to allosteric ligand F-1. To some extent the allosteric nature of F-1 ties in with the cooperative effect of agonists observed on [^3H]-GLPG0974 dissociation. Perhaps the observations in this chapter provide support for the hypothesis that strong negative cooperativity between agonist and GLPG0974 binding masks the allosteric nature of GLPG0974. However, the lack of GLPG0974 binding to R180A-R255A supports an orthosteric mode of binding. The pharmacology of hFFA2 antagonists clearly appears to be complex and more detailed studies are necessary to fully understand their mode of binding, in particular outside of the orthosteric binding site.

5.4 Conclusions

Fluorescent ligands have become important tools for investigation of GPCRs and their ligands (Stoddart et al., 2015b). By taking advantage of previously obtained information on the structural requirements of hFFA2 antagonists, the fluorescent probe F-1 was identified. F-1 was utilised to develop a proximity-based BRET binding assay that monitors the resonance energy transfer between the NBD fluorophore linked to F-1 and NLuc fused to the N terminus of hFFA2 by following a strategy previously successfully applied for FFA1 (Christiansen et al., 2016). Although F-1 can be employed to determine unlabelled antagonist affinity and binding kinetics, a closer investigation of its binding site revealed that F-1 is likely not an orthosteric probe. This exemplifies that even though the initial characterisation of F-1 binding and function suggested orthosteric behaviour, this did not turn out to be the case. Closer assessment of the pharmacology and binding site of F-1 would definitely be necessary, if it should be employed for FFA2 ligand screening. Although the complex pharmacology of F-1 complicates the interpretations of competition binding assays, it is not guaranteed that other fluorescent tracers for FFA2 will not also show such effects. Furthermore, F-1 could also serve as a useful tool for other applications. The NBD fluorophore was

in part selected due to its compatibility with NLuc for BRET binding assays, however other fluorophores can be more suitable for detection of direct fluorescent ligand binding. Attachment of a different fluorophore could therefore expand its range of application to e.g. study FFA2 expression in endogenous systems. In conclusion, work presented in this chapter only represents the beginning of the development of a fluorescent ligand tool kit for FFA2 and although further studies are necessary to understand the detailed pharmacology of F-1, it serves as a first step into the desired direction.

6 Investigating the role of Lys65 in FFA2 signalling and ligand binding

6.1 Introduction

Since its deorphanisation, the SCFA receptor FFA2 has attracted attention as a potential drug target due to the nature of its ligands, which place it at the interface of gut microbiome activity and human health (Rowland et al., 2017, Sun et al., 2017). SCFAs are produced by the gut microbiome as a fermentation product of non-digestible carbohydrates that are present in dietary fibre. Therefore, dietary habits can influence gut microbiota composition and SCFA production by adjusting the level of fibre consumed (Sweeney and Morton, 2013). However, defining the physiological role and function of FFA2 has proved more difficult than anticipated. The co-expression of FFA2 with the closely related SCFA receptor FFA3 in tissues of interest such as the gastrointestinal tract (Nohr et al., 2013, Karaki et al., 2006) has complicated the dissection of FFA2 versus FFA3 contribution to SCFA-mediated effects. To address this issue, significant effort has been invested over the last decade to develop specific tool compounds for SCFA receptors (Schmidt et al., 2011, Hudson et al., 2013a, Hudson et al., 2014, Brown et al., 2015, Park et al., 2016), but with mixed success. The majority of the work presented in previous chapters of this thesis has focussed on development of novel tool compounds and techniques to expand the toolkit for FFA2 research, as well as the definition of ligand structure-activity relationships and agonist versus antagonist binding sites to serve as a guide for future drug development. However, the premise of the work described here was to solve some of the pressing issues that are limiting progress in FFA2 research by utilising the tools developed in previous chapters.

The role of hFFA2 in augmenting neutrophil chemotaxis in response to SCFA treatment suggests that treatment with antagonists could reduce inflammation by inhibiting recruitment of immune cells to chronic sites of infection, for example, in inflammatory bowel disease (Vinolo et al., 2011). With this potential application in mind the antagonist GLPG0974 was developed by the clinical-stage biotechnology company Galapagos (Pizzonero et al., 2014). Characterisation of GLPG0974 in human blood demonstrated that GLPG0974 was able to block migration of neutrophils induced by C2 and reduced expression of CD11b on

neutrophils, which is an activation marker for neutrophil migration and served as a means of confirming FFA2 engagement by GLPG0974 (Pizzonero et al., 2014). These results showed promise for GLPG0974 as a potential therapeutic. Traditionally the next step in the drug development process would include pre-clinical studies in animals, usually rodents, to confirm the therapeutic potential of GLPG0974 in disease models of interest. However, one important limitation did not allow such progression: GLPG0974, and indeed all other known antagonists of FFA2 (Hudson et al., 2012b, Park et al., 2016, Milligan et al., 2017), are species selective for the human orthologue of FFA2 and inactive at rodent forms of FFA2 (Pizzonero et al., 2014). GLPG0974 was also inactive at other more rarely employed animal model orthologues such as rabbits and canines (Beetens, 2013), therefore Galapagos decided to move on directly to first-in-man clinical trials in ulcerative colitis patients. In these studies GLPG0974 showed a good safety profile, but treatment over four weeks did not result in improvement of ulcerative colitis symptoms, although target engagement by GLPG0974 and reduction in neutrophil migration could be confirmed (Vermeire et al., 2015). This highlights that further research on FFA2 is necessary to confirm its drug target potential and develop rational targeting strategies. Potentially the lack of GLPG0974 efficacy in the ulcerative colitis trial could have been anticipated if an animal model had been available for more detailed proof-of-concept studies. However, animal studies do not only allow validation of the therapeutic benefit of antagonist treatment, but they also represent an important means of confirming that effects observed in response to agonist dosing are specific to the targeted receptor. Considering the problems that arise from the lack of antagonists for rodent forms of FFA2, why have no cross-species antagonists been identified yet? Perhaps, the distinct pharmacology of human versus murine FFA2 prohibits this and it would be necessary to screen specifically for antagonists active at rodent orthologues to identify novel ligands (see chapter 3). Most importantly, the molecular basis of antagonist species selectivity, which might allow rational development of a rodent FFA2 antagonist, is not understood. One clear alternative to developing cross-species antagonists is the generation of a humanized mouse model that expresses the human orthologue of FFA2. Such a strategy was successfully applied previously to develop human glucagon-like peptide-1 (GLP-1) receptor knock-in mice (Jun et al., 2014). Although humanised mouse models are

undoubtedly a useful means of circumventing issues arising from species-specific receptor pharmacology, generation of knock-in mice is a costly and time-consuming process that is not available to all research groups. Furthermore, depending on the disease of interest, knock-in animals need to be crossed with specific mouse models of human disease to assess the therapeutic potential of the receptor, which is also time-consuming and work-intensive. Therefore, dissection of the molecular basis for the selectivity of antagonists for the human versus rodent orthologues of FFA2 remains important and could contribute to the development of cross-species antagonists.

A hFFA2 homology model constructed to assess agonist versus antagonist binding sites (see chapter 4) was employed herein to identify residues that might define antagonist species selectivity. This investigation resulted in the identification of a single lysine residue in TM2 that was predicted to interact with both GLPG0974 and CATPB. Most importantly, rodent orthologues of FFA2 have an arginine residue in the equivalent position, which might affect antagonist binding. To explore whether species variation in this position indeed contributes to the species-selective pharmacology of FFA2 antagonists, a selection of point mutations was generated to explore their effect on antagonist function and binding, and further homology modelling was performed to rationalise resulting observations.

In the process of investigating the role of the identified lysine residue in the species selectivity of antagonists, the effect of different alterations on agonist action was also assessed. Interestingly, the positive charge at this position was critical for agonist-induced coupling of hFFA2 to $G_{q/11}$, but not for coupling to $G_{i/o}$, while the affinity of agonists for the receptor was only modestly affected. FFA2 has previously demonstrated a relatively promiscuous signalling profile, as it could couple to multiple G protein subtypes, including $G_{i/o}$, $G_{q/11}$ and $G_{12/13}$ (Brown et al., 2003). This may be relevant in some physiological systems, where $G_{i/o}$ versus $G_{q/11}$ signalling can promote opposing actions such as the regulation of insulin secretion in pancreatic β cells, which is enhanced by activation of $G_{q/11}$ (Sassmann et al., 2010) and suppressed by $G_{i/o}$ (Berger et al., 2015). Moreover, the recent identification of the allosteric agonist AZ1729, which is able to activate $G_{i/o}$ but not $G_{q/11}$ through FFA2, demonstrated that FFA2 is capable of

biased signalling (Bolognini et al., 2016a). Therefore, examination of the molecular mechanisms underlying the promiscuous G protein coupling of FFA2 would be highly interesting, in particular in context of the identified lysine residue, as it only seemed to play a role in FFA2 coupling to selective G protein subtypes. The role of this residue in hFFA2 coupling to different G proteins was explored here by utilising a variety of assays that reflect $G_{i/o}$ and $G_{q/11}$ signalling. In addition, coupling of hFFA2 to $G_{12/13}$ was also assessed by employing the recently developed TGF α shedding assay (Inoue et al., 2012) and a selection of genome-edited cell lines that lack expression of specific G α subtypes. Thereby, work presented in this chapter encompasses numerous aspects of FFA2 structure and function, and provides valuable information that can be employed to validate FFA2 as a potential drug target.

6.2 Results

6.2.1 Assessment of the structural basis for the selectivity of FFA2 antagonists for the human versus mouse orthologue

One limitation that has affected progress in understanding the physiological role of FFA2 is the species selectivity of antagonists for the human orthologue (see section 1.1.1). Multiple studies have demonstrated species-specific differences in FFA2 activity between human and rodent orthologues, including the distinct rank order of endogenous SCFA potencies and changes in constitutive activity levels (Hudson et al., 2012b), as well as differing signalling responses to the biased allosteric ligand AZ1729 (Bolognini et al., 2016a). Indeed, C3 was able to induce accumulation of IP1 in cells induced to express hFFA2 or mFFA2 (**Figure 6.1A**). However, a 65-fold difference in C3 potency could be observed between the two orthologues with an estimated pEC_{50} of 4.36 ± 0.12 at hFFA2 and a pEC_{50} of 2.54 ± 0.11 at mFFA2. Although C3 has previously been shown to be selective for human over murine FFA2, the potency of C3 at hFFA2 versus mFFA2 was only improved by 3-fold in a [^{35}S]-GTP γ S binding assay (Hudson et al., 2012b). Therefore, the substantial species-specific potency differences observed here might relate to distinct levels of receptor reserve. Increasing concentrations of the antagonists GLPG0974 (**Figure 6.1B**) and CATPB (**Figure 6.1C**) were able to inhibit the response of hFFA2 to an EC_{80} concentration of C3 but had no effect at mFFA2. Interestingly, the fluorescent tracer F-1, which previously behaved as

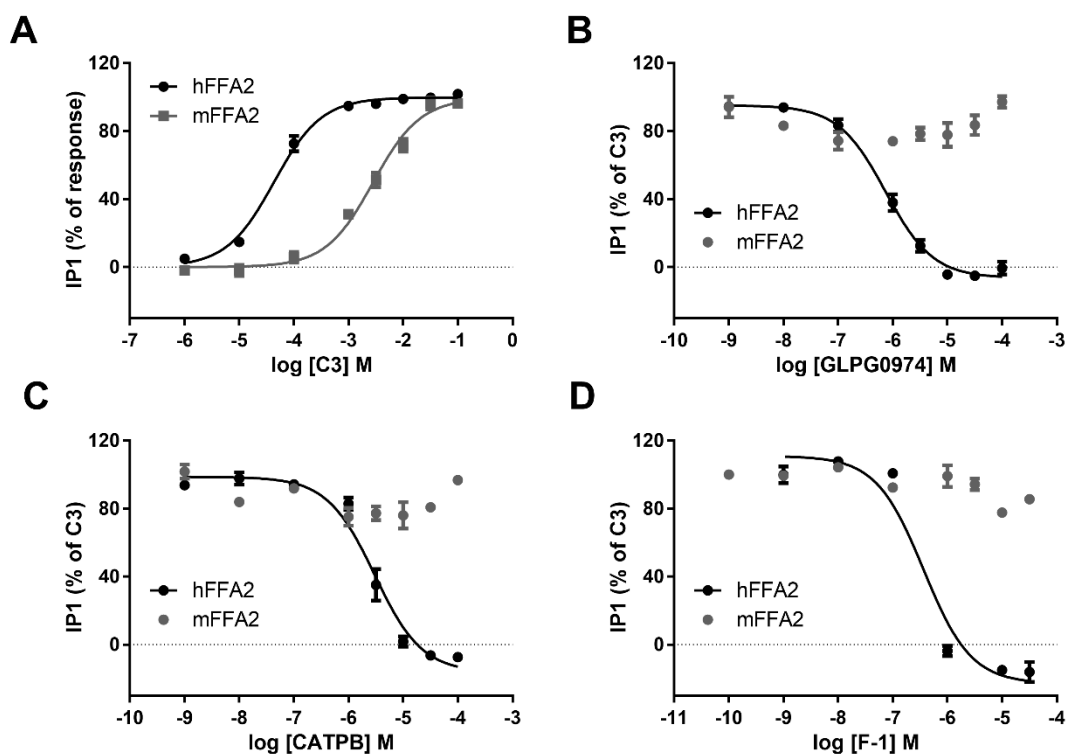


Figure 6.1 FFA2 antagonists display species selectivity for the human versus mouse orthologue The ability of varying concentrations of C3 to induce accumulation of IP1 in Flp-In™ T-REx™ 293 cells induced to express hFFA2- or mFFA2-eYFP is shown (A). Increasing concentrations of GLPG0974 (B), CATPB (C) and F-1 (D) were able to inhibit the response of hFFA2 to 3 mM C3, but not the response of mFFA2 to 10 mM C3. All data are means pooled from independent experiments ($n \geq 3$) that were performed in duplicate.

an allosteric ligand and potentially has a distinct binding site from orthosteric antagonists GLPG0974 and CATPB (see section 5.3.3), was also not active at the rodent orthologue (Figure 6.1D). While F-1 is not likely to interact with the orthosteric arginine pair (see section 5.2.5) and contains a NBD fluorophore and linker in place of a carboxylate moiety, the remaining structure of F-1 is based on GLPG0974 analogue GLPG-3. Therefore, an interaction outside of the orthosteric site might be responsible for the lack of antagonist action at mFFA2.

To identify additional points of antagonist interactions apart from the orthosteric Arg180-His242-Arg255 triad, the docking poses of GLPG0974 and CATPB to a hFFA2 homology model (see section 4.2.4) were explored in more detail. Two main residues outside of the orthosteric binding pocket were predicted to be important for positioning antagonists in the hFFA2 binding pocket, Lys65^{2.60} and Phe89^{3.28} (Figure 6.2). Lys65^{2.60} forms a hydrogen bonding interaction with the amide in the central region of GLPG0974 and CATPB and is positioned by two glutamic acid residues, Glu68^{2.63} and Glu166^{ECL2} (Figure 6.2).

Phe89^{3.28} interacts with the aromatic functional groups of GLPG0974 and CATPB by forming a π -stacking interaction (**Figure 6.2**). While Phe89^{3.28} is conserved between human and rodent FFA2, the residue at position 2.60 differs between the orthologues with an arginine residue in place of lysine in rodent forms of FFA2.

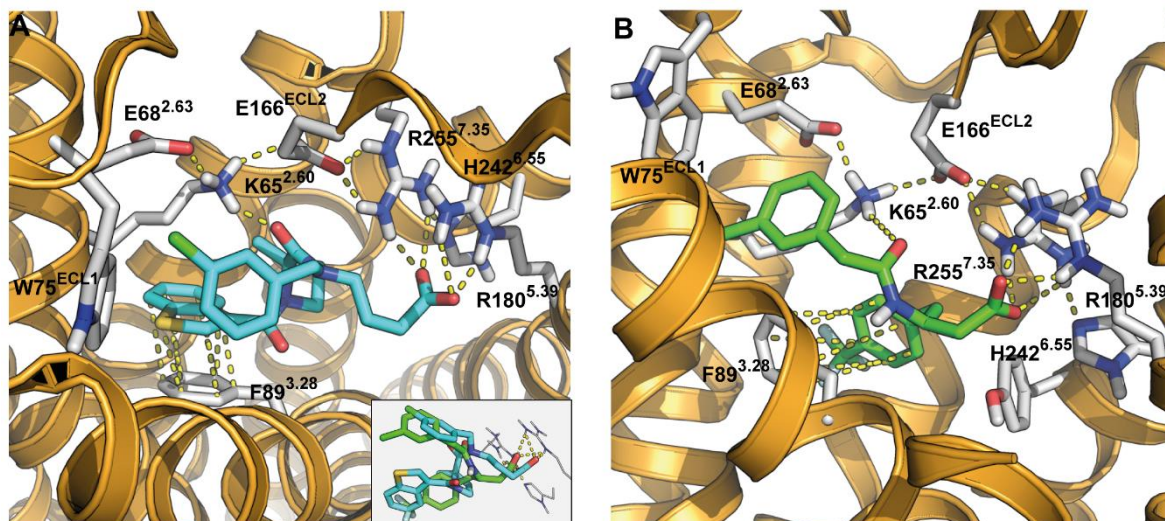


Figure 6.2 Lys65 plays a role in anchoring antagonists in the hFFA2 binding pocket Docking of GLPG0974 (**A**) and CATPB (**B**) into a homology model of hFFA2 is illustrated. While the carboxylate moiety of GLPG0974 and CATPB is anchored by interaction with Arg180^{5.39} and Arg255^{7.35}, Lys65^{2.60} interacts with the central portion of the compounds and positions them in the hFFA2 binding pocket. Furthermore, Phe89^{3.28} forms an aromatic interaction with GLPG0974 and CATPB. The inset in **A** highlights that GLPG0974 (cyan) and CATPB (green) adopt overlapping poses within the binding pocket despite their structural differences.

6.2.2 Identity of residue 65 in human versus mouse FFA2 defines species selectivity of antagonists

To examine whether the species variation in residues at position 2.60 is indeed responsible for selectivity of antagonists for human FFA2, the effect of different alterations of Lys65^{2.60} on antagonist action was examined. The Lys65^{2.60} mutants assessed include K65R, which is equivalent to the identity of this residue in murine FFA2; K65A, to assess the importance of a positive charge at position 2.60; and K65E, which reverses the charge in this position. Prior to investigating the effect of respective mutations on antagonist action, the ability of the agonists C3 and compound 1 to stimulate accumulation of IP1 at Lys65^{2.60} mutants of hFFA2 was assessed to determine appropriate EC₈₀ concentrations to employ for antagonist inhibition assays. Increasing concentrations of C3 (**Figure 6.3A**) and compound 1 (**Figure 6.3B**) were able to induce IP1 accumulation via K65R hFFA2 with a minor reduction in potency by approximately 2-fold compared to

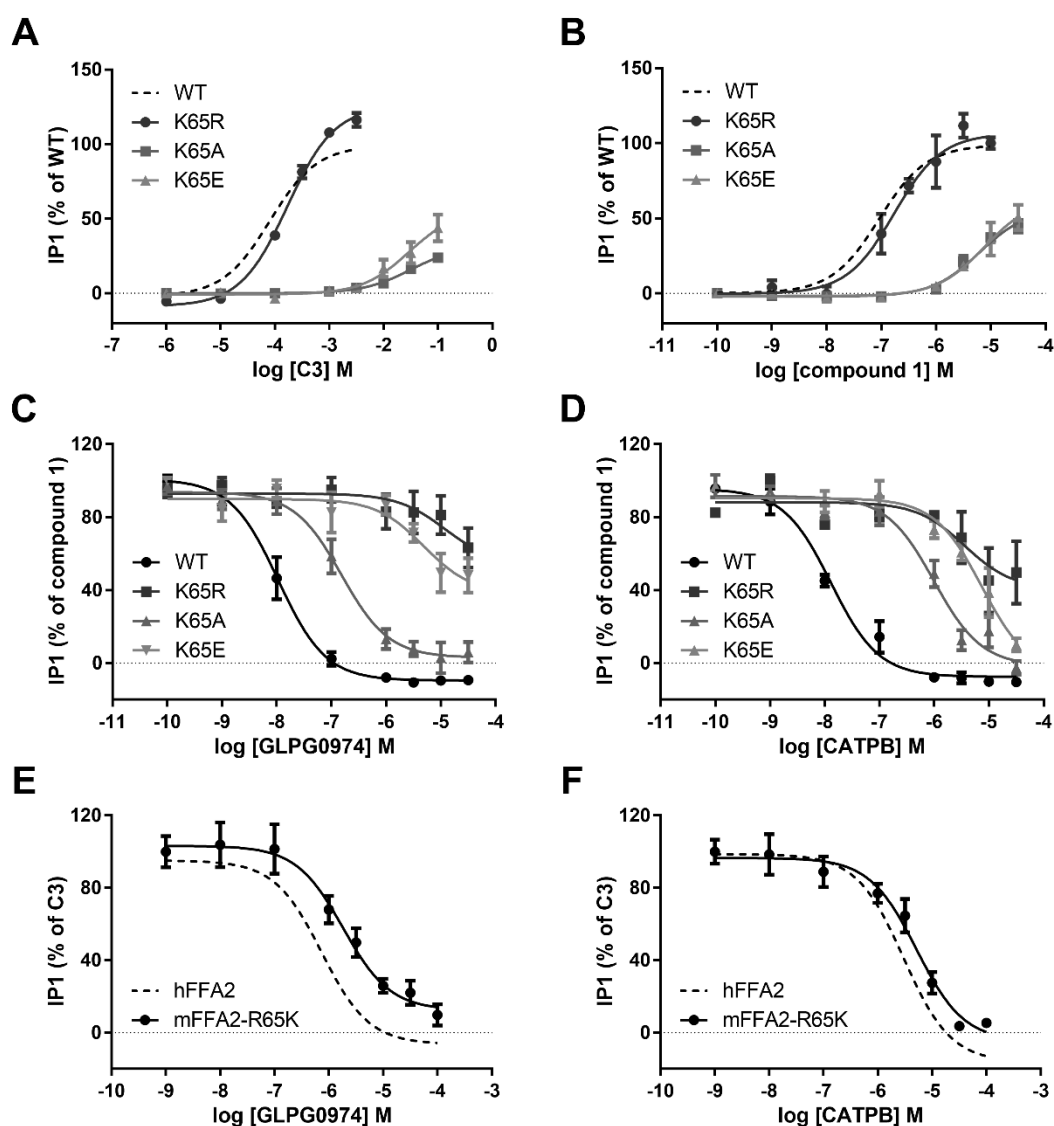


Figure 6.3 Species selectivity of antagonists for human FFA2 is defined by the identity of residue 65 in FFA2 The ability of increasing concentrations of C3 (A) and compound 1 (B) to induce production of IP1 in Flp-In™ T-REx™ 293 cells induced to express the specified variants of hFFA2 is shown. The capacity of varying concentrations of GLPG0974 (C) and CATPB (D) to inhibit IP1 production induced by respective EC₈₀ concentrations of compound 1 is illustrated. The ability of GLPG0974 (E) and CATPB (F) to inhibit C3-mediated IP1 production at specified forms of mFFA2 is shown. All data are means pooled from independent experiments (n ≥ 3) that were performed in duplicate.

wild type hFFA2 (Table 6.1). Interestingly, although Lys65^{2.60} is not in close proximity to the core orthosteric binding pocket (Figure 6.2), charge-altering Lys65 mutations K65A and K65E had a detrimental effect on the potency of C3 (Figure 6.3A) and compound 1 (Figure 6.3B) with a reduction in potency of at least 30-fold (Table 6.1). As compound 1 potency was affected by K65A and K65E mutations to a lesser extent than C3 (Table 6.1), the capacity of GLPG0974 (Figure 6.3C) and CATPB (Figure 6.3D) to inhibit the IP1 response of those mutant forms of hFFA2 to an approximate EC₈₀ concentration of compound 1 was

Table 6.1 Alterations of Lys65 in hFFA2 affect both agonist potency to generate IP1 and the ability of antagonists to inhibit this response

Compound		WT	K65R	K65A	K65E
Agonist (pEC ₅₀)	C3	4.06 ± 0.08	3.71 ± 0.05*	< 1.5	< 1.5
	Compound 1	6.98 ± 0.06	6.70 ± 0.07*	< 5.5	< 5.5
Antagonist (pIC ₅₀)	GLPG0974	7.92 ± 0.19	< 4.5	7.36 ± 0.17 [§]	< 4.5
	CATPB	7.72 ± 0.14	< 4.5	6.36 ± 0.19 ^{\$\$\$}	< 5.0

* Comparison of pEC₅₀ values at WT and K65R hFFA2 by unpaired *t* test with significant differences denoted as P = * ≤ 0.05

§ Comparison of pIC₅₀ values at WT and K65A hFFA2 by unpaired *t* test with significant differences denoted as P = [§] ≤ 0.05 and P = ^{\$\$\$} ≤ 0.001

examined. As predicted by docking poses in the homology model (**Figure 6.2**), the IC₅₀ of GLPG0974 and CATPB was significantly affected by 3.9- and 23-fold, respectively, at K65A hFFA2 (**Table 6.1**). This observation suggested that the interaction of antagonists with Lys65^{2.60} contributes to high-affinity binding, in particular in the case of CATPB. Interestingly, the K65R and K65E mutations also had a detrimental effect on antagonist action (**Figure 6.3C and D**) with an affinity loss of at least 500-fold (**Table 6.1**). As the inhibitory actions of GLPG0974 and CATPB were affected to such a substantial degree by the K65R mutation, which represents the rodent residue in position 2.60, the potential of the reverse mutation R65K in mFFA2 to rescue antagonist binding and function was assessed. Indeed, GLPG0974 (**Figure 6.3E**) and CATPB (**Figure 6.3F**) gained the ability to inhibit the response of R65K mFFA2 to an EC₈₀ concentration of C3 in an IP1 accumulation assay. The IC₅₀ of CATPB at R65K mFFA2 (5.42 ± 0.10) was only 2.9-fold lower than that at hFFA2 (5.88 ± 0.17), while there was a larger difference between the IC₅₀ of GLPG0974 at R65K mFFA2 (5.51 ± 0.12) and hFFA2 (6.14 ± 0.09) of 4.3-fold. These results could relate to the fact that antagonist action of CATPB was affected to a greater extent by the K65A mutation than GLPG0974 (**Table 6.1**). This might suggest that Lys65^{2.60} plays a more important role for CATPB binding and that GLPG0974 forms additional contacts with residues that are unique to the human orthologue of FFA2.

To confirm whether the observed effect of Lys65^{2.60} alterations on antagonist action are due to differences in antagonist affinity, [³H]-GLPG0974 equilibrium binding assays were performed in membranes containing the receptor of interest (**Figure 6.4**). No specific binding of [³H]-GLPG0974 to K65R hFFA2 could be detected at concentrations of the radioligand that were practical to employ (**Figure 6.4B**), while the affinity of [³H]-GLPG0974 for K65A hFFA2 (**Figure 6.4C**)

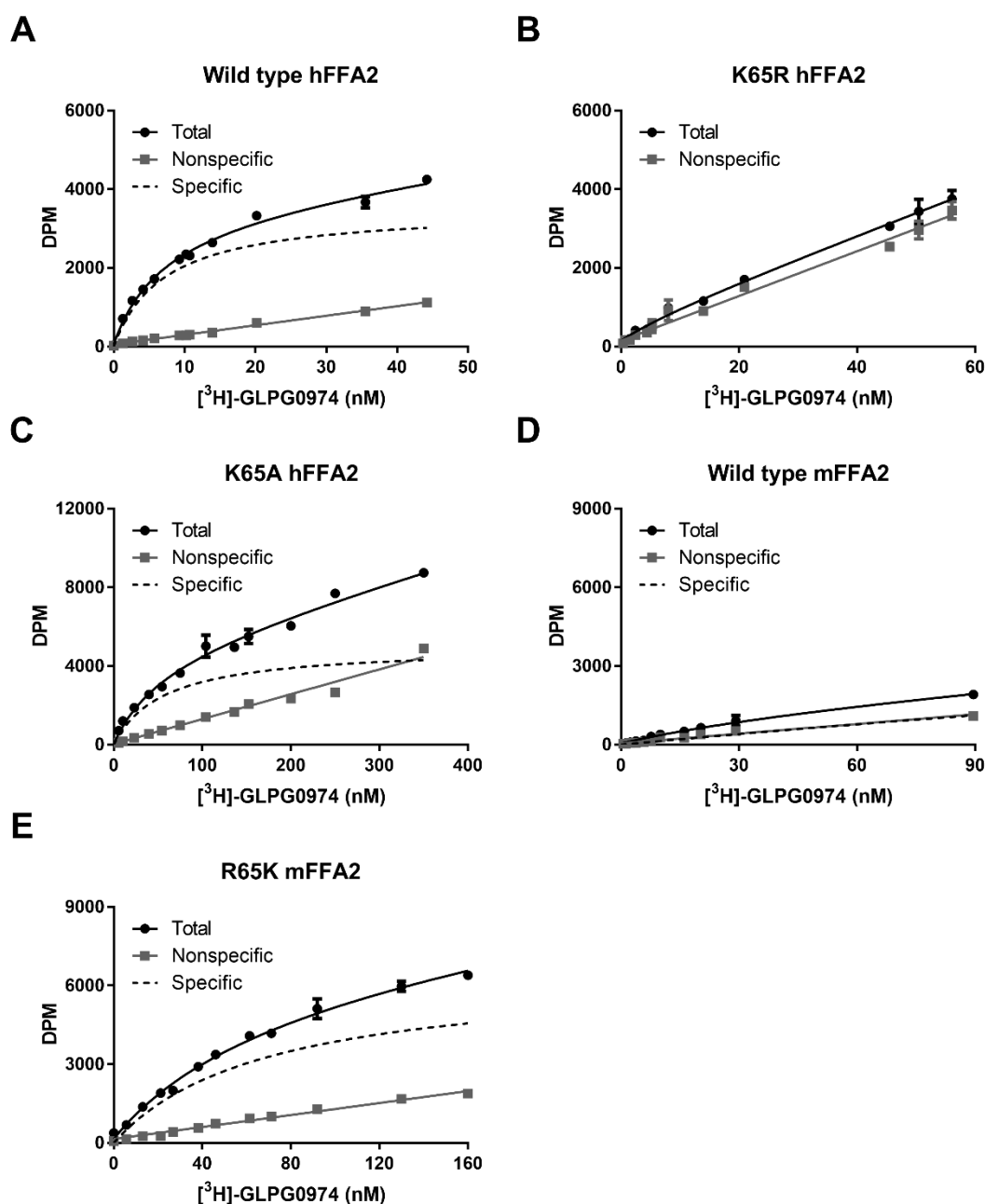


Figure 6.4 Binding of $[^3\text{H}]\text{-GLPG0974}$ to various forms of human and mouse FFA2 confirms the importance of residue 65 for antagonist binding affinity Binding of increasing concentrations of $[^3\text{H}]\text{-GLPG0974}$ to membranes isolated from Flp-In™ T-REx™ cells induced to express wild type hFFA2 (A), K65R hFFA2 (B), K65A hFFA2 (C), wild type mFFA2 (D) or R65K mFFA2 (E) is shown from representative experiments performed in duplicate. Nonspecific binding was determined in presence of 10 μM CATPB and subtracted from total binding to calculate levels of specific binding.

was reduced by some 10-fold compared to wild type hFFA2 (Table 6.2). At mFFA2 only a minor level of specific binding of $[^3\text{H}]\text{-GLPG0974}$ could be detected that did not approach saturation over the range of concentrations employed (Figure 6.4D), while the binding affinity of the radioligand for R65K mFFA2 was greatly increased and estimated to be in the region of 50 nM (Table 6.2). Taken

Table 6.2 Effect of Lys65 alterations in hFFA2 on the binding affinity of radioligand [³H]-GLPG0974 and fluorescent tracer F-1

Compound	hFFA2 (nM)			mFFA2 (nM)	
	WT	K65R	K65A	WT	R65K
[³ H]-GLPG0974	7.30 ± 0.36	> 1000	67.3 ± 8.6**	> 1000	51.5 ± 10.6*
F-1	66.5 ± 7.8	> 5000	> 10,000		954 ± 236 [§]

* Comparison of K_d values at WT and mutant hFFA2 by one-way ANOVA followed by Dunnett's test with WT hFFA2 as a reference with significant differences denoted as $P = * \leq 0.05$ and $P = ** \leq 0.01$

[§] Comparison of K_d values at WT hFFA2 and R65K mFFA2 by unpaired t test with significant differences denoted as $P = ^{\$} \leq 0.05$

together, these results indicate that Lys65^{2.60} is indeed a defining residue for the species selectivity of orthosteric FFA2 antagonists for the human orthologue, whose replacement by Arg65^{2.60} in rodent FFA2 is responsible for the loss of antagonist affinity.

While GLPG0974 and CATPB represent orthosteric examples of FFA2 antagonists, fluorescent tracer F-1 clearly shows more complex pharmacology (see chapter 5). However, despite the non-competitive relationship between F-1 and orthosteric agonists that indicated a distinct, allosteric mode of F-1 binding, the fluorescent tracer was also unable to inhibit the response of mFFA2 to C3 (**Figure 6.1D**). To examine whether the binding affinity of F-1 was also affected by Lys65^{2.60} mutations similarly to orthosteric antagonists, BRET binding assays in membranes containing the receptor of interest were utilised. Interestingly, while an F-1 saturation binding curve could be obtained for wild type hFFA2 (**Figure 6.5A**), no specific binding of F-1 to K65R (**Figure 6.5B**) nor K65A (**Figure 6.5C**) hFFA2 could be detected at concentrations of up to 500 nM. In contrast, F-1 was able to bind to R65K mFFA2, albeit with 15-fold reduction in affinity compared to wild type hFFA2 (**Table 6.2**). These observations demonstrate that Lys65^{2.60} is essential for F-1 binding to hFFA2 and while F-1 is able to bind to the 'humanising' mutant R65K mFFA2, the reduced affinity compared to wild type hFFA2 suggests that additional residues form the basis of the species selectivity of F-1.

Can the gain of antagonist binding to R65K mFFA2 be rationalised structurally? To explore how arginine versus lysine at position 2.60 impacts the nature of the ligand binding pocket, homology models of wild type and R65K mFFA2 were generated. Interestingly, investigation of the wild type mFFA2 binding pocket

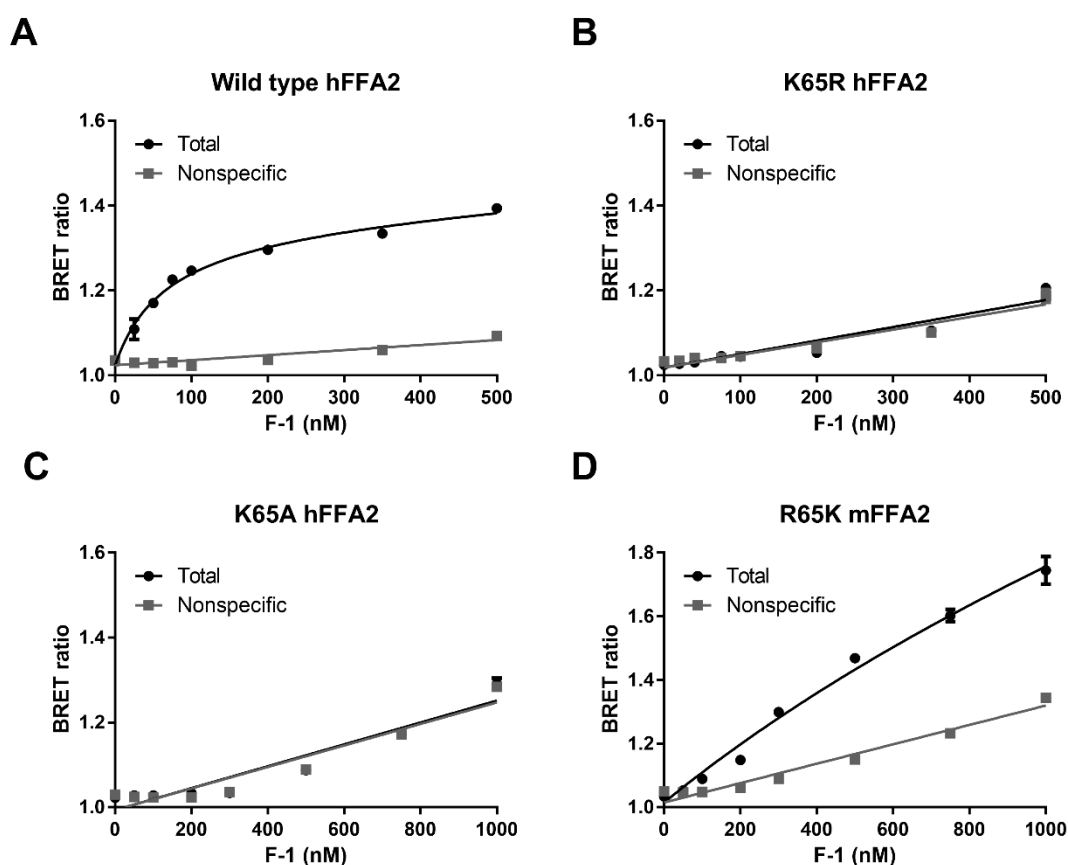


Figure 6.5 Binding of fluorescent tracer F-1 to hFFA2 is dependent on Lys65 Binding of increasing concentrations of F-1 to membranes isolated from Flp-In™ T-REx™ cells induced to express NLuc-tagged forms of wild type hFFA2 (A), K65R hFFA2 (B), K65A hFFA2 (C) and R65K mFFA2 (D) is shown from representative experiments performed in duplicate. Table 6.2 contains the K_d values derived from the illustrated data. The nonspecific BRET signal was determined in the presence of 50 μ M LinkGLPG-3.

revealed that Arg65^{2.60} was predicted to be sequestered by an ionic interaction with Glu68^{2.63} (Figure 6.6A inset). This likely results in a rearrangement of the ligand-accessible pocket of mFFA2 and does not provide a point of interaction for antagonists. Docking of CATPB into R65K mFFA2 suggested that CATPB adopts a similar binding pose as in wild type hFFA2 with the altered Lys65^{2.60} forming an interaction with the central amide (Figure 6.6A). In contrast, GLPG0974 favours a binding pose distinct to that in wild type hFFA2 and the mutated Lys65^{2.60} anchors the ligand through interaction with its aromatic chlorobenzene group (Figure 6.6B). These predicted docking poses correlate well with the observation that inhibition of the C3 response by CATPB was restored to a greater extent by the R65K alteration in mFFA2 compared to GLPG0974. Therefore, it is likely that GLPG0974 binding has additional species-specific binding determinants.

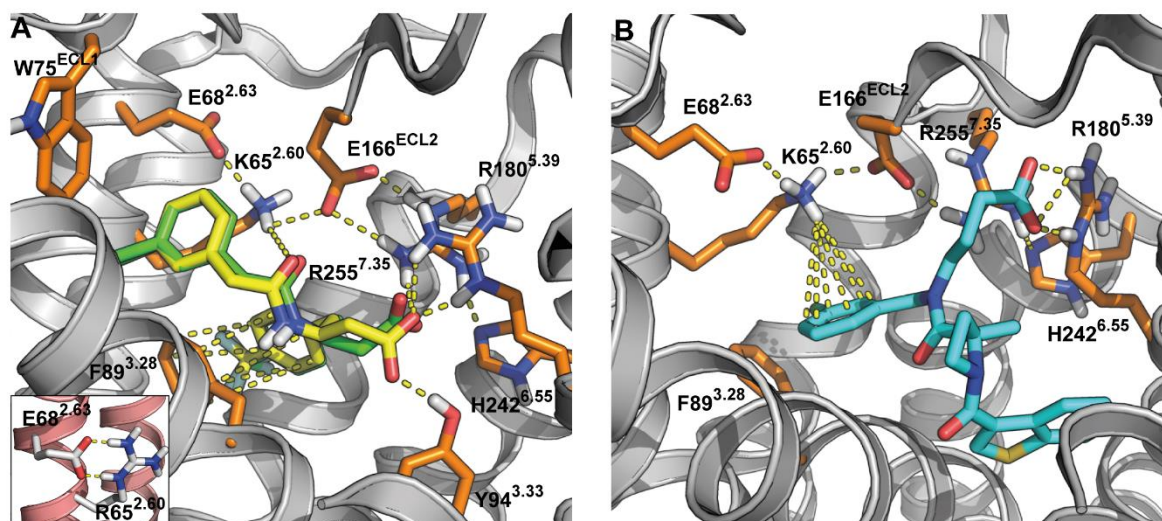


Figure 6.6 Predicted binding poses of antagonists in R65K mFFA2 Docking of CATPB (**A**) and GLPG0974 (**B**) into a homology model of mFFA2 containing the humanising R65K mutation. The predicted binding pose of CATPB to hFFA2 (green) is overlaid with the low energy docking pose obtained for CATPB binding to R65K mFFA2 (yellow) (**A**). The inset in **A** illustrates the position of Arg65^{2.60} in wild type mFFA2, which is fixed through an ionic interaction with Glu68^{2.63}. Although the binding position of GLPG0974 to R65K mFFA2 differs compared to hFFA2 (Figure 6.2), K65^{2.60} is important for positioning the chlorobenzene moiety of GLPG0974 (**B**).

6.2.3 Charge-altering Lys65 mutations in hFFA2 affect G_{q/11}- but not G_{i/o}-mediated responses to agonists

Although Lys65^{2.60} is not a component of the core orthosteric binding pocket, charge-modifying alterations of this residue had a detrimental effect on the ability of C3 (Figure 6.3A) and compound 1 (Figure 6.3B) to activate hFFA2. To examine whether this observed loss in potency was due to a loss of agonist binding, [³H]-GLPG0974 competition binding assays at K65A hFFA2 were performed. Interestingly, C3 (Figure 6.7A) and compound 1 (Figure 6.7B) were

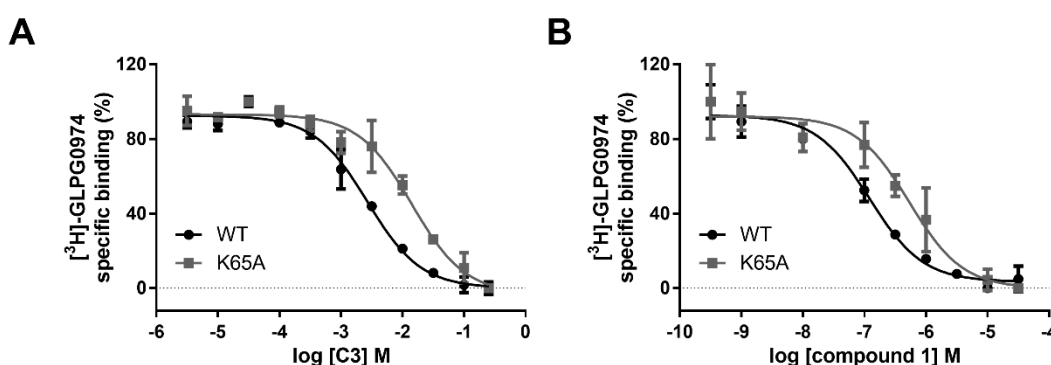


Figure 6.7 FFA2 agonists are able to bind to K65A hFFA2 with modest loss in affinity The ability of increasing concentrations of C3 (**A**) and compound 1 (**B**) to compete with approximate K_d concentrations of [³H]-GLPG0974 to bind to membranes isolated from Flp-In™ T-REx™ cells induced to express wild type or K65A hFFA2 is shown from representative experiments performed in duplicate.

able to fully outcompete the radioligand at K65A hFFA2 with a modest effect on their estimated affinity. The K_i of C3 at K65A hFFA2 (2.12 ± 0.10) was reduced by 4.1-fold compared to wild type hFFA2 (2.73 ± 0.08), while in the case of compound 1 the effect was more pronounced with a 5.4-fold reduction in K_i at K65A hFFA2 (6.29 ± 0.18) compared to wild type hFFA2 (7.02 ± 0.09). Analysis of pK_i values at wild type versus K65A hFFA2 with an unpaired t test yielded a P value of less than 0.05, confirming statistical significance of the observed differences in affinity. Therefore, although the affinity of C3 and compound 1 for K65A was modestly reduced, both agonists retained the ability to bind to this mutant of hFFA2. Conceptually, this suggests that the detrimental impact of the K65A alteration on the potency of agonists in the IP1 accumulation assay could not be explained by a loss of agonist binding. It is more likely that charge-altering alterations of Lys65^{2.60} affected the ability of agonists to induce specific G protein coupling.

While IP1 accumulation is induced by activation of $G_{q/11}$ G proteins, the ability of hFFA2 to couple to $G_{i/o}$ G proteins is also well established (Brown et al., 2003, Schmidt et al., 2011, Hudson et al., 2012b). Therefore, the effect of different Lys65^{2.60} alterations on the ability of C3 and compound 1 to promote activation of $G_{i/o}$ -mediated signalling was examined. Interestingly, C3 (**Figure 6.8A**) and compound 1 (**Figure 6.8B**) were able to induce a concentration-dependent inhibition of cAMP production at hFFA2 with all tested alterations of Lys65^{2.60}, including K65A and K65E. While the potencies of compound 1 at wild type, K65R, K65A and K65E hFFA2 were not significantly different, C3 displayed a minor 3.0- and 5.0-fold reduction in potency at K65R and K65A hFFA2, respectively (**Table 6.3**). These observations were mirrored in the [³⁵S]-GTP γ S binding assay, which also primarily detects coupling of GPCRs to $G_{i/o}$ G proteins (Milligan, 2003). C3 retained the ability to induce [³⁵S]-GTP γ S binding through K65R, K65A and K65E hFFA2 (**Figure 6.8C**), with minor, but significant, reduction in potency at all three mutant forms compared to wild type hFFA2 (**Table 6.3**). This was also the case for compound 1, which produced a concentration-dependent response in the [³⁵S]-GTP γ S binding assay at all tested alterations of Lys65^{2.60}, with a significant reduction in potency at K65A (6.0-fold) and K65E (3.0-fold) (**Table 6.3**). The minor loss in agonist potency observed at K65A hFFA2 correlates well with the reduction in affinity demonstrated in radioligand competition assays.

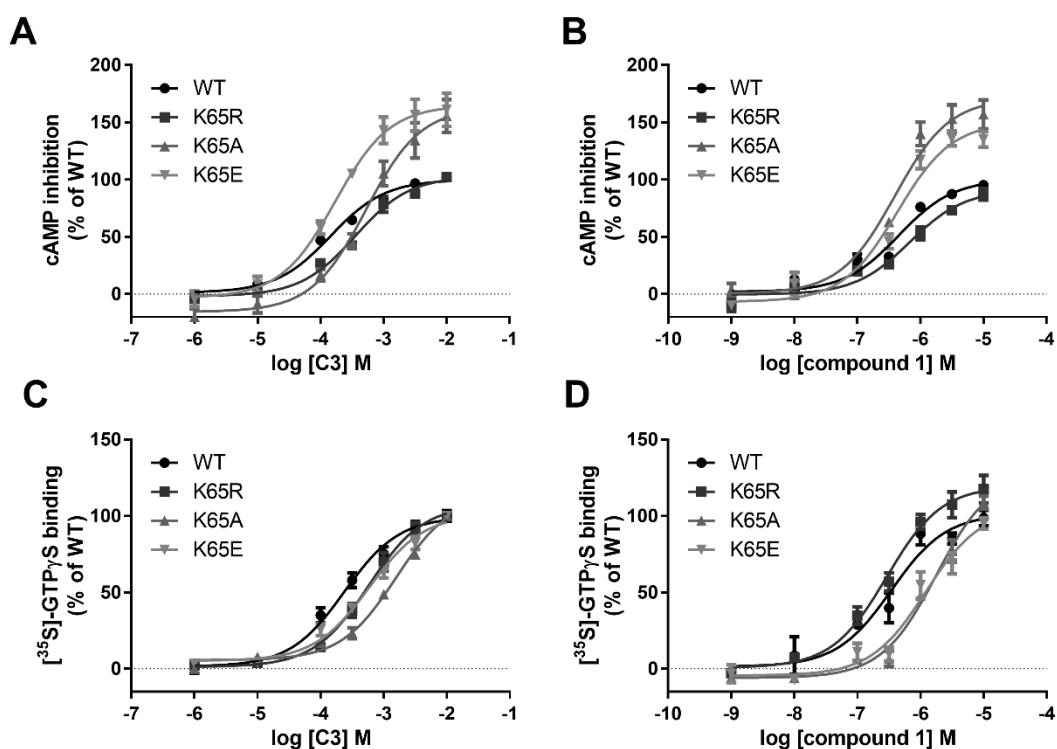


Figure 6.8 Activation of $G_{i/o}$ G proteins by FFA2 agonists is only modestly affected by charge-altering mutations of Lys65 The ability of C3 (**A, C**) and compound 1 (**B, D**) to inhibit forskolin-stimulated production of cAMP in Flp-In™ T-REx™ 293 cells induced to express mutant forms of hFFA2 (**A, B**) or to induce binding of [³⁵S]-GTPγS in membranes isolated from respective cell lines (**C, D**). All data are means pooled from independent experiments ($n \geq 3$) that were performed in triplicate.

Therefore, the impact of charge-altering Lys65²⁻⁶⁰ mutations on hFFA2 agonist potency seems to depend on the subtype of G protein whose coupling is being assessed. This would suggest that Lys65²⁻⁶⁰ has an important role in translating agonist binding to coupling of hFFA2 to $G_{q/11}$, but not $G_{i/o}$ G proteins.

Table 6.3 Alterations of Lys65 in hFFA2 have modest effects on agonist potency in $G_{i/o}$ -coupled assays

Assay	Compound	WT	K65R	K65A	K65E
cAMP	C3	3.90 ± 0.09	3.42 ± 0.06**	3.20 ± 0.1***	3.79 ± 0.08
	Compound 1	6.37 ± 0.06	6.18 ± 0.08	6.54 ± 0.10	6.47 ± 0.13
	AZ1729	6.35 ± 0.13	6.47 ± 0.15	6.42 ± 0.03	6.45 ± 0.15
GTPγS	C3	3.59 ± 0.08	3.29 ± 0.08*	2.83 ± 0.06***	3.21 ± 0.05**
	Compound 1	6.46 ± 0.04	6.52 ± 0.06	5.68 ± 0.08***	5.98 ± 0.07***
	AZ1729	6.97 ± 0.02	6.79 ± 0.07	6.94 ± 0.14	6.79 ± 0.12
Expression (% of WT)		100 ± 1	187 ± 3	96 ± 1	97 ± 1

* Comparison of pEC₅₀ values of one compound at different forms of hFFA2 by one-way ANOVA followed by Dunnett's test with WT hFFA2 as a reference with significant differences denoted as P = * ≤ 0.05, P = ** ≤ 0.01 and P = *** ≤ 0.001

6.2.4 Alterations of Lys65 do not affect response of hFFA2 to $G_{i/o}$ -biased allosteric ligand AZ1729

The distinct effect of charge-altering Lys65^{2.60} mutations on $G_{q/11}$ versus $G_{i/o}$ coupling of hFFA2 suggests that this residue may regulate coupling to different G protein subtypes in a biased fashion. Therefore, K65A and K65E hFFA2 may represent a biased form of the receptor that retains the ability to transduce signals via $G_{i/o}$ G proteins, but couples more poorly to $G_{q/11}$ G proteins. To test this hypothesis the recently identified allosteric ligand AZ1729 was employed, which previously showed a biased signalling profile as it was able to promote $G_{i/o}$ - but not $G_{q/11}$ -mediated hFFA2 signalling (Bolognini et al., 2016a). Indeed, AZ1729 was able to promote $G_{i/o}$ -coupled [³⁵S]-GTP γ S binding and inhibition of cAMP production in a concentration-dependent fashion, while a $G_{q/11}$ -coupled IP1 accumulation response to increasing concentrations of AZ1729 could not be detected (Figure 6.9A). Lys65^{2.60} mutations K65R, K65A and K65E did not result in a gain of AZ1729 ability to induce IP1 accumulation (Figure 6.9B) and the

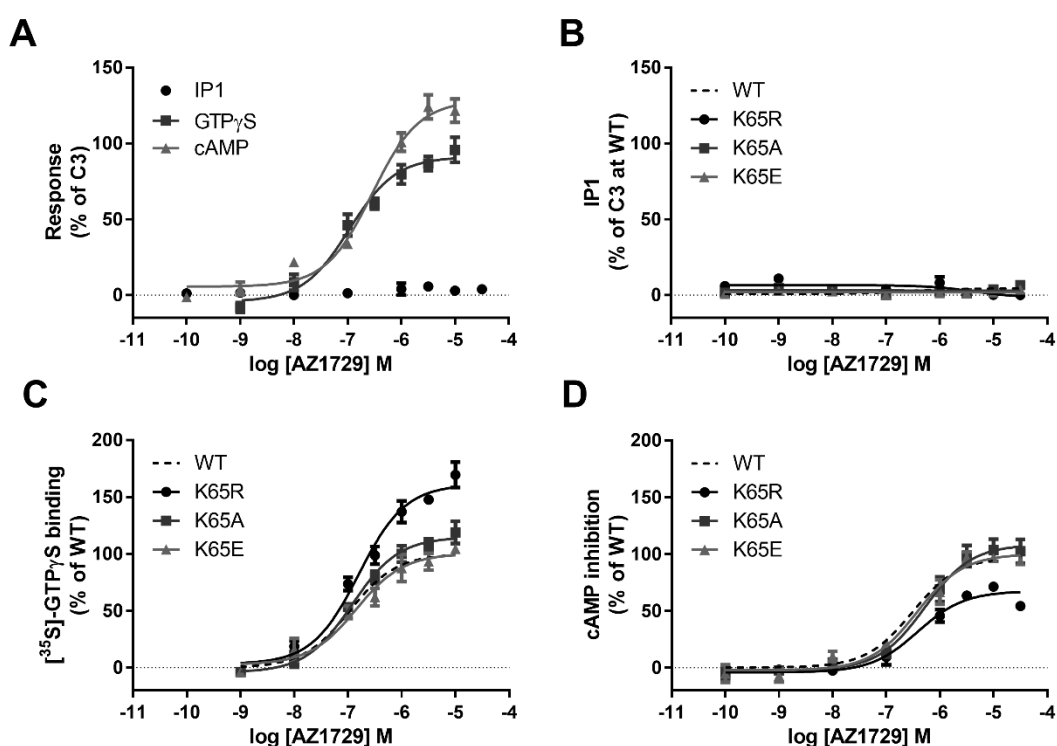


Figure 6.9 Signalling of the allosteric ligand AZ1729 is unaffected by mutation of Lys65 in hFFA2 The ability of increasing concentrations of AZ1729 to inhibit cAMP levels stimulated by forskolin, promote binding of [³⁵S]-GTP γ S and induce production of IP1 in Flp-InTM T-RExTM 293 cells induced to express wild type hFFA2 is illustrated (A). The effect of Lys65 alterations on the response to AZ1729 in IP1 accumulation (B), [³⁵S]-GTP γ S binding (C) and cAMP inhibition (D) assays is shown. All data are means pooled from independent experiments (n \geq 3) that were performed in duplicate (B) or triplicate (C, D).

potency of AZ1729 in the [³⁵S]-GTPγS binding (**Figure 6.9C**) and cAMP inhibition (**Figure 6.9D**) assay was not significantly affected (**Table 6.3**). These results confirm that Lys65^{2,60} alterations do indeed not intrinsically affect coupling of hFFA2 to G_{i/o} G proteins.

6.2.5 A TGFα shedding assay can be employed to assess impact of Lys65 mutations on signalling of hFFA2 via G_{q/11} and G_{12/13}

To examine the role of Lys65^{2,60} in selective G protein coupling in more detail, a recently developed cell-based assay was employed, which detects shedding of TGFα into the cell medium (Inoue et al., 2012). The TGFα shedding assay required co-transfection of AP-tagged TGFα and the receptor of interest into HEK293 cells. Following compound treatment, the conditioned medium was separated from the cells and the percentage of AP-TGFα released into the medium was quantified by measuring the conversion of the AP substrate p-nitrophenyl phosphate into p-nitrophenol, which absorbs light at 405 nm. Shedding of TGFα occurs in response to activation of G_{q/11} and G_{12/13} G proteins and as coupling of hFFA2 to G_{q/11} and G_{12/13} could be detected in a yeast-based chimeric G protein assay (Brown et al., 2003), this should be a suitable assay to detect hFFA2 activation. Indeed, increasing concentrations of C3 were able to induce shedding of TGFα (**Figure 6.10A**) with a 10-fold increase in potency (**Table 6.4**) compared to the IP1 accumulation assay (**Table 6.1**). To dissect the contribution of G_{q/11} and G_{12/13} to the TGFα shedding response of hFFA2, genome-edited HEK293 cell lines were employed. These cells were engineered to either lack expression of Gα_q and Gα₁₁ (ΔG_{q/11}) or of Gα₁₂ and Gα₁₃ (ΔG_{12/13}), such that the respective remaining G protein subtypes are responsible for inducing the observed TGFα shedding response: G_{12/13} in ΔG_{q/11} cells (Schrage et al., 2015, Alvarez-Curto et al., 2016), and G_{q/11} in ΔG_{12/13} cells (O'Hayre et al., 2016). In agreement with hFFA2 coupling to both G_{q/11} and G_{12/13} G proteins, C3 was able to induce a concentration-dependent TGFα shedding response via hFFA2 in each of ΔG_{q/11} and ΔG_{12/13} cells (**Figure 6.10A**), albeit with minor reduction in potency by approximately 3.5-fold in comparison with parental HEK293 cells (**Table 6.4**). In cells with deletion of all four G protein subtypes Gα_q, Gα₁₁, Gα₁₂ and Gα₁₃ (ΔG_{q/11/12/13} or ΔΔ) (Devost et al., 2017) increasing concentrations of C3 did not induce TGFα shedding (**Figure 6.10A**), confirming that shedding of TGFα lies downstream of activation of G_{q/11} and G_{12/13} only (Inoue et al., 2012).

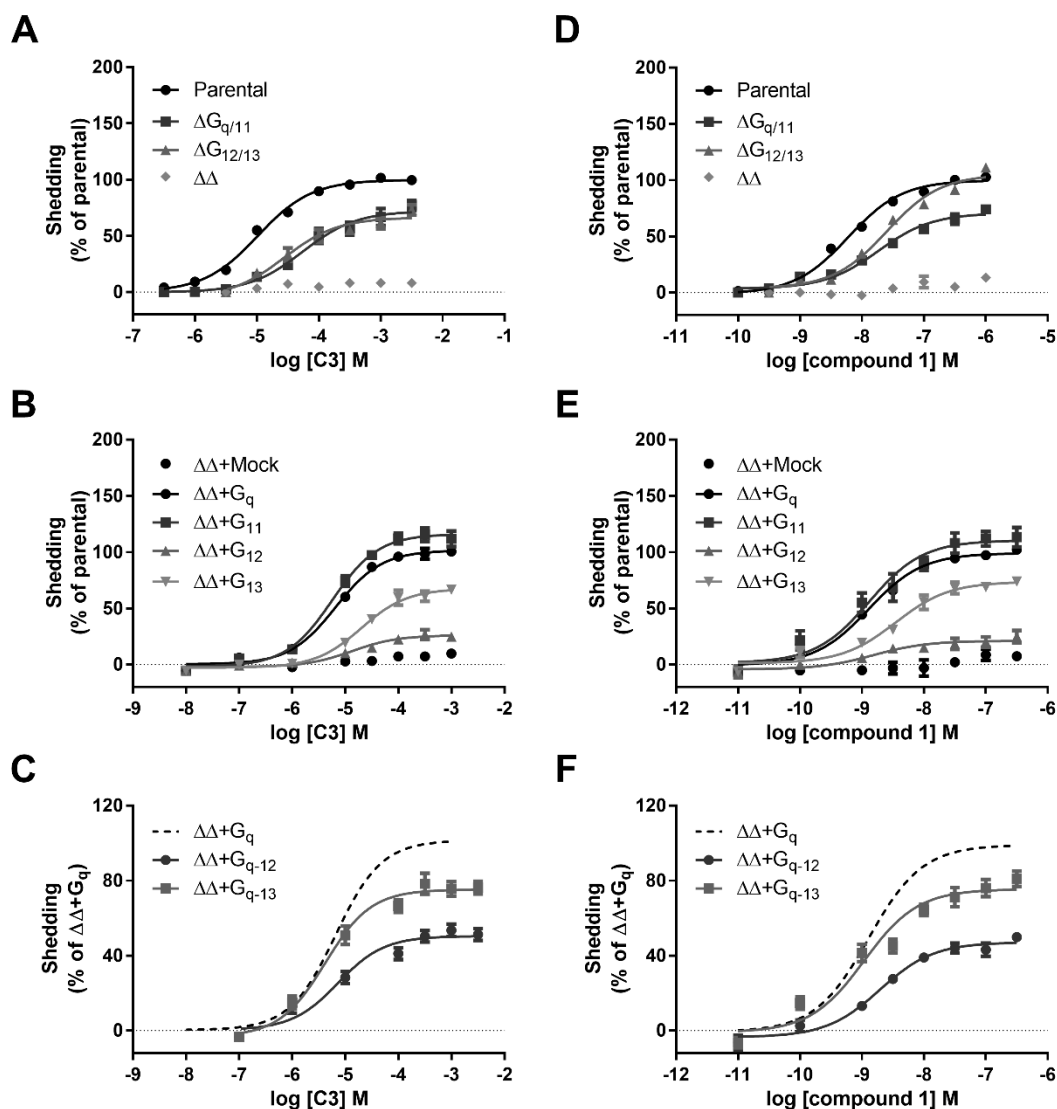


Figure 6.10 FFA2 agonists C3 and compound 1 induce a TGF α shedding response through G $\alpha_{q/11}$ and G $\alpha_{12/13}$ Increasing concentrations of C3 (A) or compound 1 (D) are able to promote shedding of TGF α in parental HEK293 cells and those genome-edited to lack expression of G $\alpha_{q/11}$ ($\Delta G_{q/11}$), G $\alpha_{12/13}$ ($\Delta G_{12/13}$) or G $\alpha_{q/11/12/13}$ ($\Delta\Delta$), which were transfected with hFFA2. Reintroduction of G α_q , G α_{11} , G α_{12} and G α_{13} into $\Delta\Delta$ cells resulted in rescue of TGF α shedding via hFFA2 by C3 (B) and compound 1 (E). Introduction of chimeric G α_{q-12} and G α_{q-13} into $\Delta\Delta$ cells resulted in an increased TGF α shedding response to C3 (C) and compound 1 (F) compared to reintroduction of native G α_{12} and G α_{13} . All data are means pooled from independent experiments ($n \geq 3$) that were performed in triplicate.

To assess the contribution of single G protein subtypes to the TGF α shedding response, native G protein subunits G α_q , G α_{11} , G α_{12} and G α_{13} were reintroduced into the $\Delta G_{q/11/12/13}$ cells background. C3 was able to promote shedding of TGF α via hFFA2 when each of the four G protein subtypes were reintroduced into the cells (Figure 6.10B). However, the level of TGF α shedding induced by activation of different G protein subtypes was different, with the signal produced by G α_q and G α_{11} being substantially greater than the signal observed upon reintroduction of G α_{12} and, to a lesser extent, G α_{13} . This observation may reflect

weak coupling of hFFA2 to $G\alpha_{13}$ and, in particular, $G\alpha_{12}$ compared to $G\alpha_q$ and $G\alpha_{11}$, but it could also result from poor coupling efficiency of $G\alpha_{12}$ and $G\alpha_{13}$ to the downstream mechanisms that lead to TGF α shedding. To understand which of these hypotheses was true, chimeric G proteins were utilised that were composed of a $G\alpha_q$ backbone with substitution of its six C-terminal residues with the corresponding sequence from $G\alpha_{12}$ or $G\alpha_{13}$, as this region represents the part of the C-terminal $\alpha 5$ helix that is a defining factor for G protein selection (Milligan and Kostenis, 2006). Upon introduction of $G\alpha_{q-12}$ and $G\alpha_{q-13}$ chimeric G proteins instead of full-length $G\alpha_{12}$ and $G\alpha_{13}$, the TGF α shedding response induced by C3 was substantially increased (**Figure 6.10C**). This result suggests that the efficiency of $G\alpha_{12}$, and to some extent also $G\alpha_{13}$, to promote TGF α shedding is indeed relatively poor compared to $G\alpha_q$ and $G\alpha_{11}$, but that hFFA2 is able to couple effectively to both $G\alpha_{12}$ and $G\alpha_{13}$. When employing synthetic agonist compound 1 instead of C3 in the assay formats described above, equivalent results were obtained. As for C3, increasing concentrations of compound 1 were able to promote a TGF α shedding response (**Figure 6.10D**) with potency that was 10-fold higher (**Table 6.4**) than in the IP1 assay (**Table 6.1**). In studies utilising full-length (**Figure 6.10E**) and chimeric (**Figure 6.10F**) G proteins, a similar contribution of each G protein to the TGF α shedding response was observed. This suggests that, at least in this assay system, C3 and compound 1 produce similar hFFA2 signalling profiles.

Table 6.4 Effect of Lys65 mutations on FFA2 agonist potency in the TGF α shedding assay

Cells	Compound	WT	K65R	K65A	K65E
Parental	C3	4.93 \pm 0.04	4.68 \pm 0.09	2.23 \pm 0.13***	2.79 \pm 0.07***
	Compound 1	8.12 \pm 0.08	8.14 \pm 0.03	6.88 \pm 0.04***	6.88 \pm 0.04***
$\Delta G_{q/11}$	C3	4.40 \pm 0.07\$\$\$	3.98 \pm 0.04*	2.67 \pm 0.17***	2.39 \pm 0.07***
	Compound 1	7.84 \pm 0.08\$	7.51 \pm 0.10	6.02 \pm 0.11***	5.94 \pm 0.08***
$\Delta G_{12/13}$	C3	4.38 \pm 0.10\$\$\$	4.11 \pm 0.09	2.14 \pm 0.08***	2.52 \pm 0.05***
	Compound 1	7.49 \pm 0.08\$\$\$	7.33 \pm 0.11	6.23 \pm 0.11***	6.16 \pm 0.13***

\$ Comparison of pEC₅₀ values of one compound at different forms of hFFA2 by one-way ANOVA followed by Dunnett's test with WT hFFA2 () or parental cells (\$) as a reference with significant differences denoted as P = *\$ \leq 0.05, P = **\$\$ \leq 0.01 and P = ***\$\$\$ \leq 0.001

As the TGF α shedding assay allows dissection of $G_{q/11}$ and $G_{12/13}$ signalling when employed in combination with appropriate genome-edited cell lines, the assay system was utilised to assess whether charge-modifying alterations of Lys65^{2,60} had a similar impact on hFFA2 coupling to $G_{12/13}$ as they do $G_{q/11}$. Indeed, the

ability of C3 (**Figure 6.11A**) and compound 1 (**Figure 6.11B**) to induce a TGF α shedding response in parental HEK293 cells was severely impaired by K65A and K65E mutations, while at K65R hFFA2 only a very limited effect on agonist potency was detected (**Table 6.4**). A similar impact of the various Lys65^{2.60} mutations could be observed in $\Delta G_{q/11}$ (**Figures 6.11C and D**) and $\Delta G_{12/13}$ (**Figures 6.11E and F**) cell backgrounds. This suggests that not only hFFA2 coupling to G_{q/11} G proteins is affected by charge-altering Lys65^{2.60} mutations, but also coupling to G_{12/13} G proteins. To confirm that the TGF α shedding responses detected indeed represented coupling of hFFA2 to G_{q/11} and/or G_{12/13}, equivalent experiments were performed in $\Delta G_{q/11/12/13}$ cells and as anticipated increasing concentrations of C3 (**Figure 6.11G**) and compound 1 (**Figure 6.11H**) did not change basal levels of TGF α shedding.

The higher potency of C3 and compound 1 in the TGF α shedding compared to the IP1 accumulation assay allowed effective quantification of agonist potencies at K65A and K65E hFFA2 (**Table 6.5**). By comparing agonist potency values at the various mutant forms of the receptor in G_{i/o}- versus G_{q/11}- and G_{12/13}-coupled assays, the degree of bias imbued by charge-altering mutations of Lys65^{2.60} could be calculated (**Table 6.5**). Three common approaches exist that can be utilised to assess signalling bias (Rajagopal et al., 2011): Equimolar comparison (Gregory et al., 2010), equiactive comparison (Ehlert, 2008) and the operational model (Evans et al., 2011). Equimolar comparison involves plotting of concentration-response curves of a selected ligand in two different assay systems against one another and comparison of the curve shape to a reference agonist can provide information on whether it shows biased signalling behaviour (Gregory et al., 2010). However, this method is more visual than quantitative, and it is less suitable for separating system bias (Rajagopal et al., 2011), therefore this method was not employed here. Instead agonist potencies were analysed by equiactive comparison (see section 2.7.4), which traditionally involves the comparison of the potency and efficacy of the potentially biased ligand in different assay systems to a reference compound (Ehlert, 2008). However, in this case the intrinsic activity of agonists at Lys65^{2.60} mutants of hFFA2 was compared to their effect at the wild type receptor, which served as a reference. Applying this analysis to C3 concentration response curves suggested that hFFA2 function was biased between 41- and 60-fold by K65A and K65E mutations to

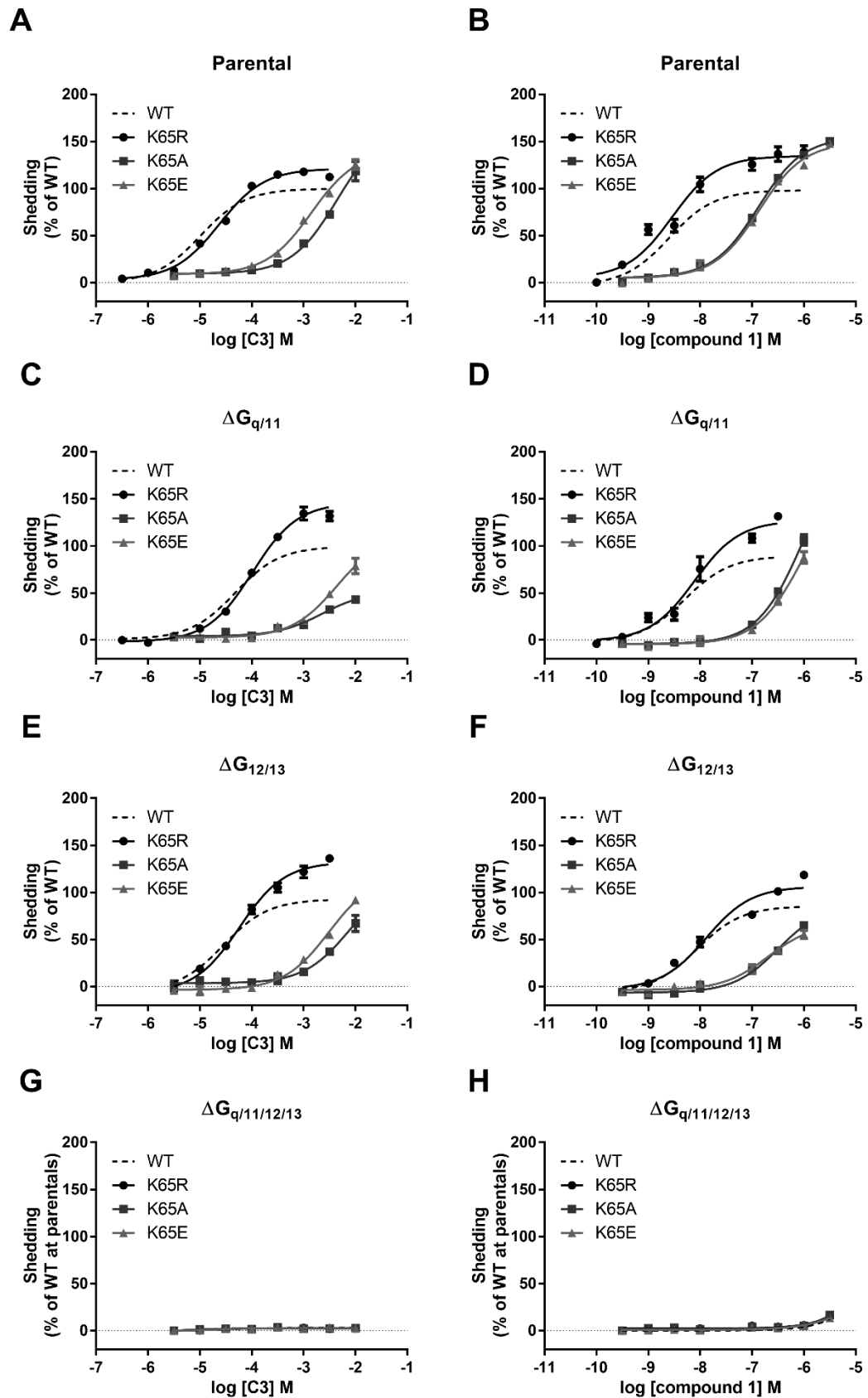


Figure 6.11 Charge-modifying mutations of Lys65 have a detrimental effect on hFFA2 response to agonists in $G_{q/11}$ - and $G_{12/13}$ -coupled TGF α shedding assays The effect of different Lys65 alterations on the response of hFFA2 to C3 (A, C, E, G) or compound 1 (B, D, F, H) in parental HEK293 cells (A, B) or those genome-edited to lack $G\alpha_{q/11}$ (C, D), $G\alpha_{12/13}$ (E, F) or $G\alpha_{q/11/12/13}$ (G, H) is illustrated. All data are means pooled from independent experiments ($n \geq 3$) that were performed in triplicate.

Table 6.5 Agonist bias factor calculation for Lys65 mutants of hFFA2

Pathway 1	Pathway 2	Agonist	β factor (compared to WT)		
			K65R	K65A	K65E
cAMP	TGF α shedding	C3	-0.30	2.00	2.10
		Compound 1	-0.39	1.44	1.33
GTP γ S	TGF α shedding	C3	-0.10	1.78	1.62
		Compound 1	-0.03	0.36	0.59

favour $G_{i/o}$ -mediated signalling when utilising data from the [35 S]-GTP γ S binding assay, or between 100- and 125-fold when comparing TGF α shedding with the cAMP inhibition assay (Table 6.5). Equivalent results could be obtained when performing calculations based on compound 1, however the quantified bias towards $G_{i/o}$ -coupled pathways was less extensive as it was estimated to be 21- to 27-fold when employing values from the cAMP inhibition assay (Table 6.5). Although conceptually the operational model might yield a better estimate of bias (Rajagopal et al., 2011), affinity measures of FFA2 agonists at all forms of FFA2 were not available due to the loss of antagonist binding to K65R and K65E hFFA2, prohibiting the use of sigma comparison (Brust et al., 2015). In contrast, the transduction coefficient model derives ligand dissociation constants directly from concentration responses (Kenakin et al., 2012). However, when agonist concentration response curves yield slopes that approach unity, results from equiactive comparison and transduction coefficient calculation become nearly identical (Kenakin and Christopoulos, 2013). In the case of this study, agonist concentration response curves were fit using a three-parameter model that constrains the slope of the sigmoidal curve to unity, therefore equiactive comparison was selected for signalling bias quantification.

6.2.6 Use of chimeric G proteins to examine the diverse effect of charge-altering Lys65 mutations on hFFA2 signalling

Chimeric G proteins with a $G\alpha_q$ backbone and a six-residue substitution at the C terminus were employed in the previous section to demonstrate that hFFA2 indeed couples efficiently to $G_{12/13}$ and that reduced agonist responses upon reintroduction of full-length $G\alpha_{12}$ and $G\alpha_{13}$ were likely due to the poor coupling of these $G\alpha$ subtypes to mechanisms that result in shedding of TGF α (Figures 6.10C and F). To examine whether this strategy could also be utilised to detect coupling of hFFA2 to G proteins that do not naturally promote TGF α shedding, $G\alpha_{q-i}$ and $G\alpha_{q-o}$ chimeras were co-transfected into $\Delta G_{q/11/12/13}$ cells with AP-TGF α

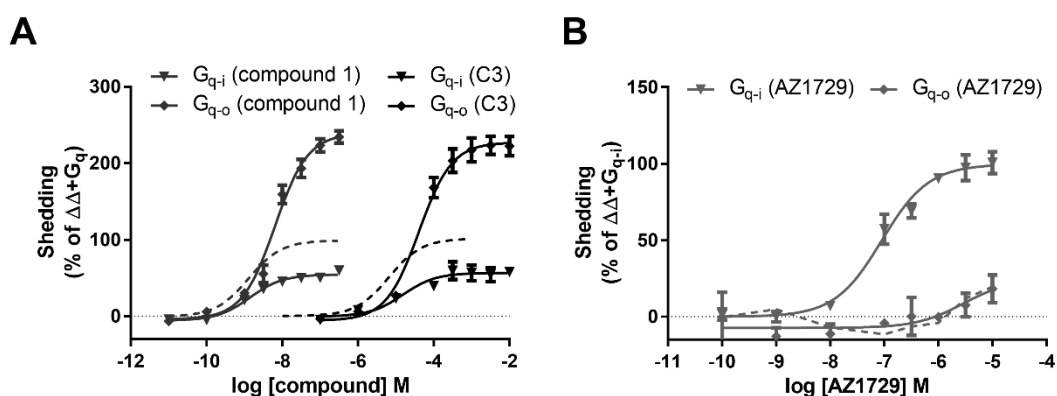


Figure 6.12 Introduction of chimeric $G_{\alpha_{q-i}}$ and $G_{\alpha_{q-o}}$ allows detection of hFFA2-mediated $G_{i/o}$ signalling in TGF α shedding assay The ability of increasing concentrations of C3 and compound 1 (**A**) or AZ1729 (**B**) to promote shedding of TGF α in cells genome-edited to lack $G_{\alpha_{q/11/12/13}}$ when transfected with chimeric $G_{\alpha_{q-i}}$ and $G_{\alpha_{q-o}}$ G proteins is illustrated. The agonist response in cells transfected with full-length G_{α_q} from figure 6.10 is shown for comparison (---). All data are means pooled from independent experiments ($n \geq 3$) that were performed in triplicate.

and hFFA2. Now, increasing concentrations of C3 and compound 1 were able to promote TGF α shedding via hFFA2 activation of the $G_{\alpha_{q-i}}$ and $G_{\alpha_{q-o}}$ chimeras (**Figure 6.12A**). However, agonist potency at hFFA2 in $G_{\alpha_{q-i}}$ - and $G_{\alpha_{q-o}}$ -transfected cells was reduced compared to that in those transfected with full-length G_{α_q} (**Table 6.6**). Interestingly, the maximal response to agonists upon $G_{\alpha_{q-o}}$ reintroduction was doubled compared to G_{α_q} , which may reflect improved coupling of hFFA2 to this G protein subtype.

The allosteric ligand AZ1729 displayed a biased signalling profile in previous studies, as it was able to promote activation of $G_{i/o}$ but not $G_{q/11}$ signalling pathways (Bolognini et al., 2016a). To examine whether this signalling bias could be detected by the TGF α shedding assay when utilising chimeric G proteins, the response of $\Delta G_{q/11/12/13}$ cells transfected with hFFA2 and G_{α_q} , $G_{\alpha_{q-i}}$ or $G_{\alpha_{q-o}}$ to increasing concentrations of AZ1729 was assessed (**Figure 6.12B**). In agreement with the lack of AZ1729 action in $G_{q/11}$ -coupled assays, AZ1729 was unable to produce a response upon reintroduction of G_{α_q} . In contrast, a concentration-dependent response to AZ1729 could be detected in $G_{\alpha_{q-i}}$ -transfected cells with a pEC_{50} of 7.01 ± 0.16 , similar to the potency of AZ1729 measured in the [35 S]-GTP γ S binding assay (**Table 6.3**). Interestingly, reintroduction of $G_{\alpha_{q-o}}$ did not result in a gain of AZ1729 agonism (**Figure 6.12B**), which may suggest that AZ1729 is biased towards activation of G_i specifically, rather than the entire $G_{i/o}$

Table 6.6 FFA2 agonists display increased potency at charge-altering mutations of Lys65 when $G\alpha_{q-i}$ versus $G\alpha_q$ or $G\alpha_{q-o}$ is reintroduced into cells with a $\Delta G_{q/11/12/13}$ background

Transfection	Compound	WT	K65R	K65A	K65E
$G\alpha_q$	C3	5.21 ± 0.03	4.90 ± 0.14	2.61 ± 0.06	2.90 ± 0.04
	Compound 1	8.83 ± 0.03	8.76 ± 0.09	6.66 ± 0.14	6.91 ± 0.02
$G\alpha_{q-i}$	C3	5.18 ± 0.06	4.79 ± 0.06	3.21 ± 0.02***	3.38 ± 0.10*
	Compound 1	7.89 ± 0.04***	8.81 ± 0.09	7.49 ± 0.04**	7.44 ± 0.03***
$G\alpha_{q-o}$	C3	4.37 ± 0.04***	3.52 ± 0.02***	< 2	< 2
	Compound 1	8.22 ± 0.12***	7.84 ± 0.07***	< 6	< 6

* Comparison of C3 or compound 1 pEC₅₀ values at different G protein transfections by one-way ANOVA followed by Dunnett's test with G_q transfection as a reference with significant differences denoted as P = * ≤ 0.05, P = ** ≤ 0.01 and P = *** ≤ 0.001

subfamily. Regardless, the ability of AZ1729 to promote TGF α shedding in $\Delta G_{q/11/12/13}$ cells transfected with $G\alpha_{q-i}$ confirmed that this experimental setup could be utilised to detect G_i signalling.

As results discussed in previous sections suggested that charge-altering alterations of Lys65^{2,60} can generate a hFFA2 receptor that displays signalling bias towards $G_{i/o}$ -coupled pathways, the effect of $G_{i/o}$ chimera reintroduction on the agonist response at Lys65^{2,60} mutants of hFFA2 was assessed (Figure 6.13). At K65R hFFA2, C3 behaved in a similar fashion as at wild type FFA2 (Figure 6.13A) with the highest potency observed upon $G\alpha_q$ reintroduction (Table 6.6). Interestingly, the potency loss with $G\alpha_{q-o}$ compared to $G\alpha_q$, which was observed at wild type hFFA2, was enhanced at K65R hFFA2 with a 24-fold loss compared to 6.9-fold at wild type hFFA2. At K65A (Figure 6.13B) and K65E (Figure 6.13C) hFFA2, the reintroduction of the G protein chimeras had a substantially different effect. In agreement with the hypothesis that K65A and K65E hFFA2 display improved coupling to $G_{i/o}$ G proteins, transfection of $G\alpha_{q-i}$ did result in an improved response to C3 with potency increased by 4.0- and 3.0-fold at K65A and K65E hFFA2, respectively, compared to transfection of $G\alpha_q$ (Table 6.6). Surprisingly, in $G\alpha_{q-o}$ -transfected cells increasing concentrations of C3 failed to promote shedding of TGF α (Figures 6.13B and C). This may suggest that, charge-altering Lys65^{2,60} mutations bias hFFA2 towards coupling to G_i specifically. Equivalent experiments performed with compound 1 led to a similar conclusion with K65R hFFA2 behaving in a comparable fashion to wild type receptor (Figure 6.13D), while at K65A (Figure 6.13E) and K65E (Figure 6.13F) hFFA2 reintroduction of $G\alpha_{q-i}$, but not $G\alpha_{q-o}$, resulted in an improved response to compound 1 compared to $G\alpha_q$ transfection.

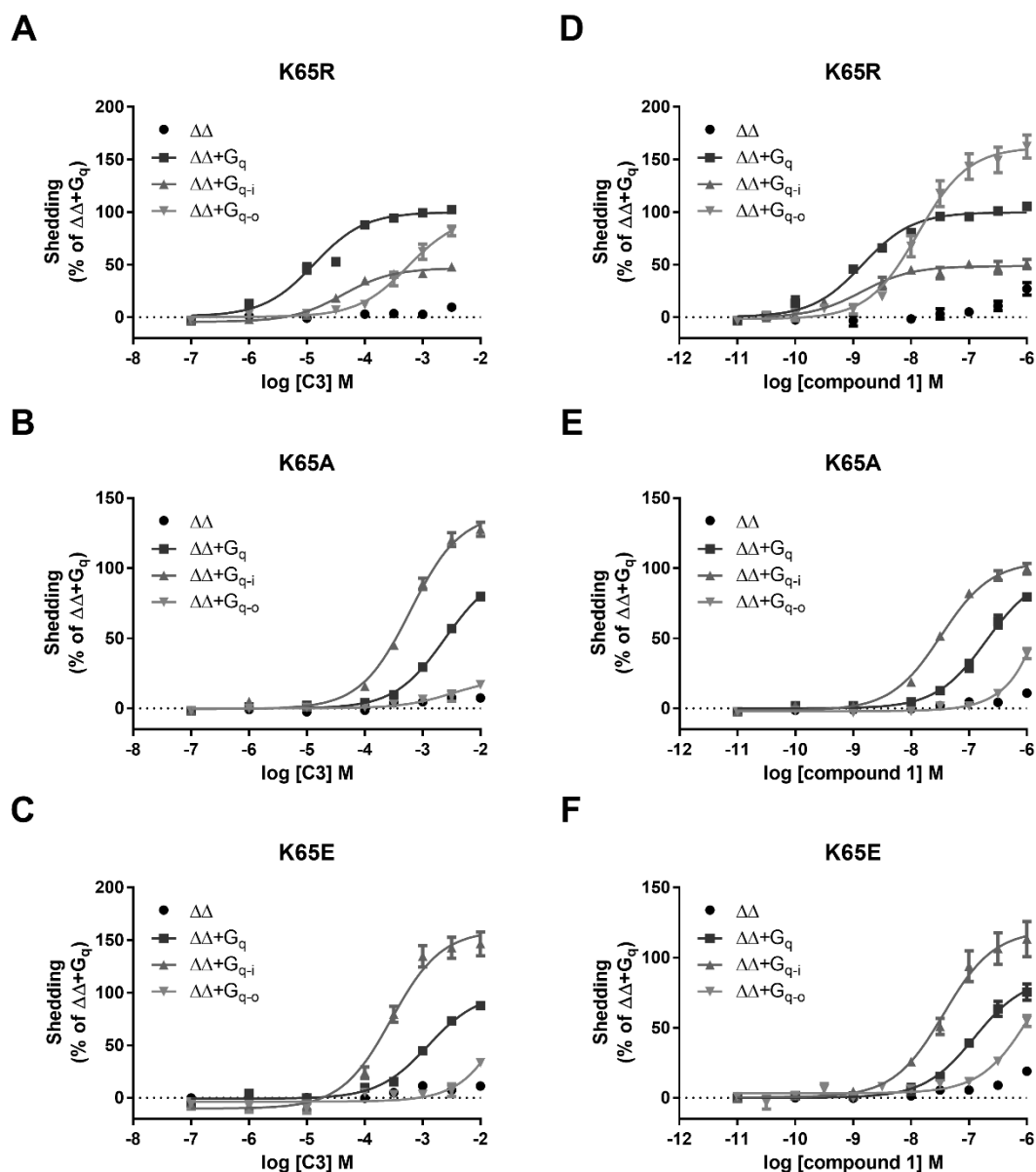


Figure 6.13 Charge-modifying Lys65 mutants of hFFA2 show enhanced TGF α shedding response to agonists upon introduction of chimeric G α_{q-i} but not G α_{q-o} The ability of varying concentrations of C3 (A, B, C) and compound 1 (D, E, F) to induce shedding of TGF α in cells transfected with K65R (A, D), K65A (B, E) and K65E (C, F) hFFA2 is shown. The HEK293 cell line employed was genome-edited to lack G $\alpha_{11/12/13}$ and respective G α subunits were reintroduced prior to performing the experiment. All data are means pooled from independent experiments ($n \geq 3$) that were performed in triplicate.

6.2.7 Allosteric modulation of hFFA2 response to C3 by AZ1729 may differ between G $\alpha_{q/11}$ - and G $\alpha_{12/13}$ -mediated signals

Previous characterisation of AZ1729 revealed that in addition to displaying biased agonism, its ability to modulate the response of hFFA2 to C3 was also dependent on the coupled G protein subtype examined (Bolognini et al., 2016a). While AZ1729 acted as a positive allosteric modulator of C3 potency in G $\alpha_{i/o}$ -coupled assays, it had a negative modulatory effect on C3 efficacy when G $\alpha_{q/11}$ -

mediated responses were assessed. However, due to the lack of an appropriate assay system, it was not examined if and how AZ1729 may modulate $G_{12/13}$ -mediated hFFA2 responses to C3. Therefore, the effect of increasing AZ1729 concentrations on the C3 concentration response curve was assessed in the TGF α shedding assay employing parental and the genome-edited cell lines $\Delta G_{q/11}$ and $\Delta G_{12/13}$ (Figure 6.14). Visual inspection of the effect of AZ1729 allosteric modulation of the C3 concentration response in parental cells showed AZ1729 to behave simply as a negative allosteric modulator of C3 efficacy (Figure 6.14A), as observed in other $G_{q/11}$ -coupled assays (Bolognini et al., 2016a). However, increasing concentrations of AZ1729 resulted in an increased basal signal, which may indicate low levels of intrinsic agonism (Figure 6.14A). Furthermore, with increasing AZ1729 concentration the potency of C3 displayed a small increase (Figure 6.14A) that was reflected by an increase in pEC₅₀ values (Table 6.7).

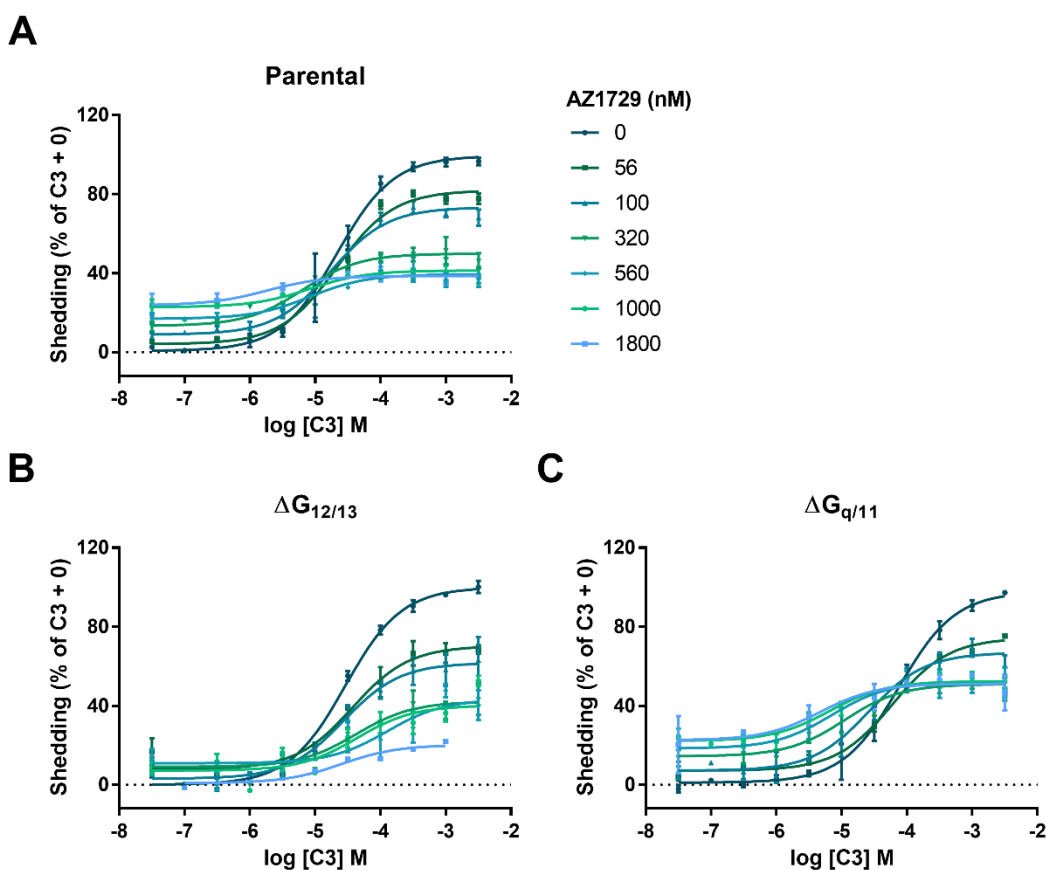


Figure 6.14 Differences in AZ1729 allosteric modulation of $G_{q/11}$ - and $G_{12/13}$ -mediated hFFA2 response to C3 in TGF α shedding assay The effect of varying AZ1729 concentrations (A) on the ability of C3 to induce shedding of TGF α via hFFA2 in HEK293 cells with parental background (A) or genome-edited to lack $G_{12/13}$ (B) or $G_{q/11}$ (C) is illustrated. All data are means pooled from independent experiments ($n \geq 3$) that were performed in triplicate.

Table 6.7 Effect of AZ1729 on the potency of C3 in the TGF α shedding assay in different cell backgrounds

AZ1729 (nM)	Cells ^a		
	Parental	$\Delta G_{q/11}$	$\Delta G_{12/13}$
0	4.67 \pm 0.06	4.12 \pm 0.09	4.54 \pm 0.04
56	4.67 \pm 0.08	4.22 \pm 0.05	4.43 \pm 0.15
100	4.76 \pm 0.09	4.58 \pm 0.13	4.56 \pm 0.16
320	5.19 \pm 0.18	4.96 \pm 0.21	4.37 \pm 0.23
560	5.08 \pm 0.33	5.15 \pm 0.33	3.89 \pm 0.40
1000	5.08 \pm 0.24	5.19 \pm 0.18	4.36 \pm 0.26
1800	5.74 \pm 0.43	5.33 \pm 0.42	4.60 \pm 0.22

^a Data shown as pEC₅₀ values of C3 with respective concentrations of AZ1729 co-added

These observations differ from results obtained in other G_{q/11}-dependent assay systems, however the TGF α shedding assay incorporates signals from both G_{q/11} and G_{12/13} activation. To dissect how G_{q/11} and G_{12/13} coupling might contribute to the allosteric effect observed, equivalent experiments were performed in genome-edited $\Delta G_{q/11}$ and $\Delta G_{12/13}$ cells. In $\Delta G_{12/13}$ cells, in which the TGF α shedding signal is exclusively mediated by activation of G_{q/11}, AZ1729 behaved as in other G_{q/11}-mediated assay systems (**Figure 6.14B**). Increasing concentrations of AZ1729 resulted in reductions of the maximal C3 response with no alteration in potency (**Table 6.7**). In contrast, in $\Delta G_{q/11}$ cells, where TGF α shedding occurs exclusively through G_{12/13} activation, equivalent concentrations of AZ1729 resulted in a smaller reduction in the maximal C3 response (**Figure 6.14C**) and a leftward shift of C3 potency with increasing AZ1729 concentration was observed (**Table 6.7**). These results suggest that AZ1729 may not only show biased allosteric modulation of the C3 response between G_{i/o}- and G_{q/11}-mediated signalling, but AZ1729 potentially also displays a different allosteric mechanism in G_{12/13}-coupled assays.

6.2.8 Loss of positive charge at position 65 also affects β -arrestin recruitment by FFA2

The investigation of the role of Lys65^{2.60} in FFA2 signalling has focussed primarily on the altered coupling to different G protein subtypes compared to the wild type receptor. If charge-altering mutations of Lys65^{2.60} indeed change the capacity of FFA2 to couple to specific G protein subtypes, this suggests that the active conformation of such mutant forms of FFA2 will differ to the wild type receptor and likely be most prominent in the intracellular portion of the

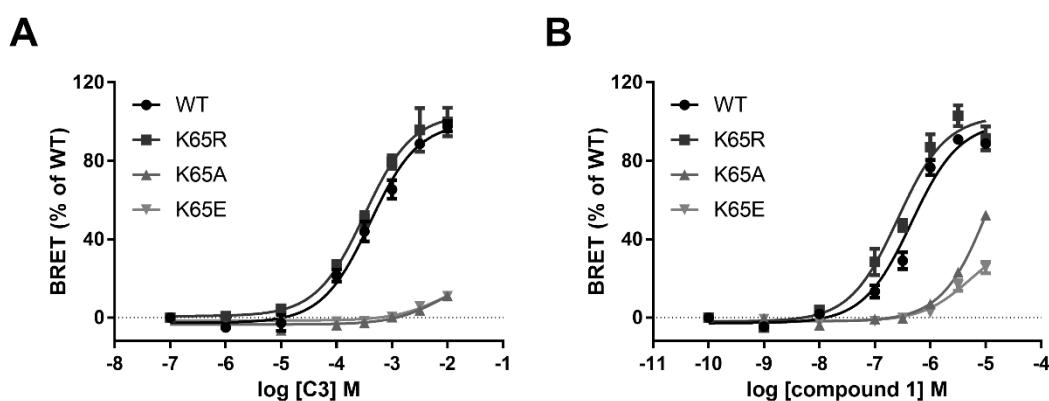


Figure 6.15 Recruitment of β -arrestin in response to FFA2 agonists is affected by charge-altering mutations of Lys65 The ability of C3 (A) and compound 1 (B) to induce recruitment of β -arrestin 2 in HEK293T cells transiently transfected with RLuc- β -arrestin 2 and either wild type, K65R, K65A or K65E hFFA2 is shown. Results were normalised to the maximal agonist response at the wild type receptor. All data are means pooled from independent experiments ($n \geq 3$) that were performed in triplicate.

receptor that mediates the interaction with G proteins. However, FFA2 is also able to interact with β -arrestin 2, whose recruitment may also be affected by such conformational rearrangements. To investigate this hypothesis, the impact of Lys65^{2,60} mutations on β -arrestin 2 recruitment was assessed. Interestingly, as in the case of $G_{q/11}$ -coupled signalling assays, charge-altering mutations K65A and K65E affected the response of FFA2 to both C3 (Figure 6.15A) and compound 1 (Figure 6.15B). In contrast, at the positive charge-retaining mutant K65R hFFA2 both agonists displayed the same potency as at the wild type receptor (Table 6.8). Unfortunately, the lack of a saturable response at the charge-altering mutants did not permit calculation of potency values, therefore bias factors could not be generated to compare coupling of mutants of interest to G_i G proteins versus β -arrestin. However, the loss of FFA2 agonist response in this assay supports the hypothesis that the loss of the positive charge in position 65 may lead to an intracellular conformational rearrangement that does not only affect recruitment of specific G proteins, but also other signalling partners such as β -arrestin.

Table 6.8 Effect of Lys65 mutations on FFA2 agonist potency in the BRET-based β -arrestin recruitment assay

Compound	WT	K65R	K65A	K65E
C3 ^a	3.40 ± 0.07	3.51 ± 0.05	< 2	< 2
Compound 1 ^a	6.34 ± 0.04	6.56 ± 0.05	< 5	< 5

^a Data shown as pEC₅₀ values

6.3 Discussion

6.3.1 Lys65 defines a secondary binding site that is unique to the human orthologue of FFA2

Differences in pharmacological properties and ligand efficiency at species orthologues of GPCRs do not always present an issue for research progress and in some cases, such as SCFA receptor FFA2, it makes sense from an evolutionary perspective that species orthologues display distinct behaviour. Invariably the composition of the gut microbiome will differ between humans and rodents, and the role that SCFAs play in respective species may differ depending on distinct requirements of metabolic regulation (Nguyen et al., 2015). This hypothesis would provide an explanation for the various differences observed between human and murine FFA2, including different rank orders of SCFA potency and constitutive activity levels (Hudson et al., 2012b). Although the impact of species-specific FFA2 pharmacology on its function in humans versus rodents is not fully understood, it is very important to consider when drawing conclusions from studies in animal models. The validation of FFA2 as a therapeutic target using animal models is complicated further by the lack of FFA2 antagonist action at the rodent orthologues. As an alternative means of assessing the impact of FFA2 inactivity, transgenic knock-out mouse lines that do not express FFA2 have been employed to help define physiological roles of FFA2 (Psichas et al., 2015, Kimura et al., 2013, Maslowski et al., 2009). However, in at least one study knock-out of FFA3 altered expression levels of FFA2 (Zaibi et al., 2010), which complicated interpretation of resulting observations. Using an antagonist to confirm receptor-specific effects would be less costly than transgenic animal development and avoid limitations of knock-out animal models. Therefore, development of an antagonist active at mFFA2 would contribute to furthering FFA2 research and understanding the molecular basis for antagonist species selectivity could represent the first step in such efforts.

Previous assessment of antagonist binding to hFFA2 included examination of the binding pocket using functional and binding studies, and construction of a hFFA2 homology model to computationally predict antagonist binding poses (see chapters 3 and 4). These studies revealed that the carboxylate moiety of the most widely employed antagonists CATPB and GLPG0974 was anchored by the

orthosteric arginines Arg180^{5,39} and Arg255^{7,35}. However, each antagonist class preferred different arginine residues, CATPB interacting preferentially with Arg255^{7,35} and GLPG0974 with Arg180^{5,39}, and interaction with a single arginine residue was sufficient for high-affinity binding (see chapter 4). Furthermore, replacement of the carboxylate moiety with a methyl ester or morpholine had only a modest effect on antagonist action and affinity (see chapters 3 and 4). This implied that CATPB and GLPG0974 likely form additional important contacts with hFFA2, which define high-affinity binding and may be responsible for the species selectivity of these antagonists. However, initial alignment of human and rodent orthologues of FFA2 did not reveal residues that could be responsible for antagonist species selectivity, as the core ligand binding pockets of these orthologues mostly contain residues with similar properties (Figure 6.16).

Therefore, docking poses of GLPG0974 and CATPB in the hFFA2 homology model were explored in detail for residues that may form an interaction with both antagonists and where the equivalent residue in rodent FFA2 might limit antagonist binding. This assessment led to the identification of a lysine residue at the top of TM2, which participated in a hydrogen bond with the central amide moiety in GLPG0974 and CATPB. Lys65^{2,60} is conserved across the majority of FFA2 orthologues, however rodent FFA2 contains an arginine in this position

	TM2	ECL1	TM3	ICL2		
Human	LLL P F K I I E	AASNFRWYLPKVV	CALTSFGF	YSSIYCSTWLLAGIS	IERYLGVAFFVQYKL 119	
Chimpanzee	LLL P F K I I E	AASNFRWYLPKVV	CALTSFGF	YSSIYCSTWLLAGIS	IERYLGVAFFVQYKL 119	
Sumatran orangutan	LLL P F K I I E	AASNFRWYLPKVV	CALTSFGF	YSSIYCSTWLLAGIS	IERYLGVAFFVQYKL 119	
Cat	LLL P F K M V E	AAYNFRWYLP	ELLCALTGFGF	YSSIYCSTWLLAGIS	IERYLGVAFFVQYKL 118	
Dog	LLL P F K M V E	AAADFQWYLP	ELLCALTGFGF	YSSIYCSTWLLAGIS	IERYLGVAFFVQYKL 118	
Pig	LLL P L K I T E	AASNFRWYLP	GIVCALMGFGF	YSSIYCSTWLLAGIS	IERYLGVAFFVQYKL 119	
Horse	LLL P F K I I E	AASDFHWYLP	EVVCAIVGFGF	YSSIYCSTWLLAAIS	IERYLGVAFFVQYKL 113	
Bovine	LLL P F K I I E	AASDFRWELSN	LACALMGFGF	YGSICYSTLLLAGIS	VERYLGVAFFVQYKL 118	
African elephant	LLL P F K I I E	AAQGLQWYLP	VVLCALTGFGF	YSSIYCSTWLLAGIS	IERYLGVAFFVQYKL 116	
Sheep	LLL P F K I I E	AAASDFLWYLP	ELSLACALMGFGF	YSSIYCSTWLLAGIS	IERYLGVAFFLQYKL 119	
Rabbit	LLL P F K I V E	AASNFRWYLP	QVVCALTGFGF	YSSIYCSTWLLAGIS	MERYLGVAFFVQYKL 119	
Squirrel	LLL P F K I I E	AAASDFHWYLP	QIVCALTGFGF	YSSIYCSTWLLAGIS	IERYLGVAFFVQYKL 119	
Guinea pig	LLL P F R I I E	AASNFRWYLP	QIVCALTGFGF	YSCICYSTWLLAGIS	IERYLGVAFFVQYKL 119	
Hamster	LLL P F R I V E	AASNFRWYLP	KIVCALTGFGF	YSSIYCSTWLLAGIS	MERYLGVAFFVQYKL 119	
Mouse	LLL P F R I V E	AASNFRWYLP	KIVCALTGFGF	YSSIYCSTWLLAGIS	MERYLGVAFFVQYKL 119	
Rat	LLL P F R I V E	AASNFRWYLP	KIVCALTGFGF	YSSIYCSTWLLAGIS	IERYLGVAFFVQYKL 119	
Kangaroo rat	LLL P F K M A E	AAWGFAPL	PRALCAPTAF	YSSIYCSTGLLAAIS	VERYLGVAFFVRYKL 118	
American alligator	L F L P F K M A E	AAAADMNW	PLPGFLCALTN	YSSIIYSTFLLTAVS	VERYLGVAFFVQYKL 117	
King cobra	I F L P F K M A E	VAMAFTW	PLPFLFCPLAN	FFYSSIIYISTLFL	MGVSIERYLCIAPVKHKL 115	
Western clawed frog	M F L P F K M D E	AASNMMW	RLPQFLCPLTG	FYSSIIYISTLFL	TAVSVERYLGVAHP	IKYKL 118
Channel catfish	L F L P L R I K E	A-ANMKWT	LSSEFLCPLSG	FYFSTIHNSTLL	LTAISVERYLGVAFF	PIKYKL 118
	2.60	2.63		3.28		

Figure 6.16 Sequence alignment of FFA2 orthologues with focus on residue 65 Alignments of the primary amino acid sequence of various orthologues of FFA2 were performed with the human residues as the reference sequence using Clustal Omega (Sievers et al., 2011) and residues 60 to 119 are shown. Presence of lysine (yellow) or arginine (green) in position 65^{2,60} is highlighted in colour. Glu68^{2,63}, which forms an ionic interaction with Arg65^{2,60} in the mFFA2 homology model (Figure 6.6), is fully conserved and Phe89^{3,28}, which appears to be important for anchoring antagonists in the hFFA2 binding pocket (Figure 6.2), is mostly conserved apart from in kangaroo rat, western clawed frog and channel catfish.

(**Figure 6.16**). This variation has previously not attracted much attention as arginine and lysine are considered similar amino acids due to their fixed positive charge, but a homology model of mFFA2 revealed that Arg65^{2.60} is likely to form an ionic bond with Glu68^{2.63}. This interaction could result in a structural rearrangement of the binding pocket and may thereby affect antagonist binding.

To examine the importance of Lys65^{2.60} for antagonist binding in more detail, mutant forms of hFFA2 were generated with different alterations of Lys65^{2.60}, specifically to arginine, alanine and glutamic acid. Interestingly, CATPB and GLPG0974 lost the ability to inhibit the response of K65R and K65E hFFA2 to C3 and displayed a reduction in potency at K65A hFFA2. Furthermore, [³H]-GLPG0974 binding assays demonstrated that the observed lack of inhibition of agonist function was caused by a reduction in antagonist affinity. Therefore, the employed homology model was indeed able to accurately predict an important interaction of antagonists with hFFA2. Most importantly, the alteration of Lys65^{2.60} to arginine, which reflects the identity of the equivalent residue at mFFA2, had a detrimental effect on antagonist binding. To assess whether species variation in position 2.60 could be responsible for antagonist selectivity, a form of mFFA2 containing the ‘humanising’ R65K mutation was generated and utilised in functional and binding studies. In agreement with the proposed hypothesis, CATPB and GLPG0974 gained the ability to inhibit the response to C3 at R65K mFFA2 and [³H]-GLPG0974 was able to bind with high affinity to R65K mFFA2. Interestingly, affinity of CATPB was almost fully restored to hFFA2 levels by the R65K alteration of mFFA2, while the pIC₅₀ and binding affinity of GLPG0974 remained reduced at R65K mFFA2 compared to wild type hFFA2. Furthermore, docking of antagonists into R65K mFFA2 suggested that CATPB adopts a similar binding pose in R65K mFFA2 as in hFFA2 with an interaction between the modified Lys65^{2.60} and the CATPB amide moiety. In contrast, GLPG0974 adopted a low-energy pose that differed substantially from that in hFFA2. This suggests that there may be differences in the defining factors of CATPB and GLPG0974 species selectivity and additional human orthologue-specific residues are likely important for GLPG0974 binding. Perhaps this divergence is not entirely unexpected, as previous investigations also suggested distinct modes of CATPB and GLPG0974 binding, such as their preference to interact with different orthosteric arginine residues and the difference in

binding kinetics (see chapter 4). Furthermore, GLPG0974 has also been reported to be inactive at rabbit and canine orthologues of FFA2 (Beetens, 2013). Both contain a lysine at position 2.60 (**Figure 6.15**), suggesting that further studies may be necessary to fully understand the species selective behaviour of GLPG0974.

Interestingly, Lys65^{2.60} was essential for binding of the fluorescent tracer F-1 to hFFA2. Previous characterisation of F-1 revealed that it is likely an allosteric ligand, whose allosteric binding site overlaps in part with that of orthosteric antagonists (see chapter 5). The lack of F-1 binding to K65R and K65A hFFA2 suggests that Lys65^{2.60} lies within the area of overlap between F-1 and orthosteric antagonist binding sites. F-1 shares part of its structure with the GLPG0974 analogue GLPG-3, which also contains a central amide moiety, therefore F-1 might interact in a similar fashion with Lys65^{2.60} as CATPB and GLPG0974. However, further work would be required to confirm this hypothesis. Interestingly, a role of Lys65^{2.60} in defining an allosteric binding site of hFFA2 was suggested previously in a study designed to define the binding mode of the allosteric agonist 4-CMTB (Grundmann et al., 2016). It was proposed that 4-CMTB binds in a sequential fashion to hFFA2 by initially occupying the orthosteric binding pocket for a short period of time and then transitioning to an allosteric binding site from which it exerts its allosteric modulation of the C3 response. To support this hypothesis, two mutants of hFFA2 were studied: R255A, to prohibit binding to the orthosteric site; and K65R, to disrupt allosteric binding of 4-CMTB (Grundmann et al., 2016). However, 4-CMTB was unable to compete with F-1 binding to hFFA2, which makes it unlikely that 4-CMTB interacts directly with Lys65^{2.60}. Homology models described here suggest that the K65R alteration in hFFA2 may result in Arg65^{2.60} forming an ionic interaction with Glu68^{2.63}. Conformational changes that could occur in response to this ionic bond being formed may indirectly result in a disruption of the allosteric 4-CMTB binding site. Assessment of the structural changes that occur upon mutation of Lys65^{2.60} to arginine in hFFA2 could therefore provide additional information on the binding sites of 4-CMTB.

6.3.2 Generation of a biased form of hFFA2 by modifying the positive charge of the residue in position 2.60

GPCRs are often defined by their ability to transduce signals through activation of specific G protein subtypes within the G_s , $G_{i/o}$, $G_{q/11}$ or $G_{12/13}$ families. However, several GPCRs have the capacity to activate more than one family of G proteins and this can have important implications for their physiological role. FFA2 represents one such example, as it is well established that it is able to couple to G proteins of the $G_{i/o}$ and $G_{q/11}$ families, and responses mediated by these G proteins are routinely assessed in assay systems that measure changes in secondary messengers such as cAMP or IP1 (see chapter 3). Coupling of hFFA2 to $G_{12/13}$ G proteins was also demonstrated in a study that employed chimeric G proteins in a yeast-based assay to identify G protein subtypes that interact with hFFA2 (Brown et al., 2003), however this avenue of FFA2 signalling has not been explored further since. This is likely due to the fact that assay systems that allow straightforward detection of $G_{12/13}$ activation were not readily available. However, recent development of the TGF α shedding assay has changed this situation, as it can be employed to detect signalling through $G_{q/11}$ and $G_{12/13}$. Combination of the TGF α shedding assay with a set of recently developed genome-edited cell lines that lack specific G protein subtypes, such as G_{α_q} and $G_{\alpha_{11}}$ (Alvarez-Curto et al., 2016), allows specific detection of the $G_{12/13}$ -mediated response of hFFA2. Prior to generation of these cell lines, bacterial toxins such as PTX were employed to dissect contributions of specific G proteins to downstream signals or small molecule inhibitors of $G_{q/11}$ (Schrage et al., 2015). However, treatment with toxins such as PTX also affects other cellular processes such as activation of tyrosine kinases (Mangmool and Kurose, 2011). Therefore genome-edited cell lines represent a complimentary approach to dissecting contribution of G protein subtypes to signalling responses, in particular for G proteins that cannot be blocked by known toxins such as $G_{12/13}$.

The recent identification of the allosteric agonist AZ1729, which is able to activate $G_{i/o}$ but not $G_{q/11}$ through FFA2, demonstrated that the signalling pathways induced by FFA2 activation differ depending on the cell type (Bolognini et al., 2016a). Treatment of primary mouse adipocytes with AZ1729 resulted in inhibition of lipolysis and migration of isolated human neutrophils was enhanced in the presence of AZ1729, suggesting that these processes are mediated by $G_{i/o}$

G proteins (Bolognini et al., 2016a). In contrast, murine colonic crypts, which have been shown to release GLP-1 in response to FFA2 activation by SCFAs (Tolhurst et al., 2012), did not respond to AZ1729 treatment, and in concert with G protein inhibitor studies confirmed that GLP-1 release is mediated through a G_q -coupled mechanism. Therefore, the contribution of $G_{q/11}$ versus $G_{i/o}$ signalling to FFA2 function in different tissues is relevant to its physiological role. Although a biased ligand such as AZ1729 is undoubtedly of great use to dissect FFA2 signalling, the underlying mechanism that defines its biased behaviour has not been explored. Understanding how promiscuous GPCRs couple to multiple G proteins and the means by which biased ligands can promote specific downstream signalling is important to expand our knowledge of the relationship between GPCR structure and function, but, as discussed above, can also have important therapeutic implications.

Here, the importance of Lys65^{2.60} in regulating hFFA2 signalling through a range of different G proteins was examined in detail by utilising a selection of assay systems, including conventional measures of second messenger regulation generated by $G_{i/o}$ and $G_{q/11}$ activation and the TGF α shedding assay to detect $G_{q/11}$ and $G_{12/13}$ -mediated responses. During the assessment of antagonist action at different Lys65^{2.60} mutants of hFFA2, a detrimental effect of charge-modifying alterations on agonist responses in the $G_{q/11}$ -coupled IP1 accumulation assay was observed. However, despite this, in [³H]-GLPG0974 competition binding assays agonists retained ability to compete with the radioligand for binding to K65A hFFA2. These observations provided the first indication that Lys65^{2.60} alterations may only contribute in a minor fashion to agonist binding affinity and Lys65^{2.60} may instead play a role in hFFA2 coupling to G proteins. Interestingly, the detrimental effect of charge-altering Lys65^{2.60} mutations K65A and K65E was exclusive to $G_{q/11}$ - and $G_{12/13}$ -coupled responses. In assays that detect activation of $G_{i/o}$ G proteins mutation of Lys65^{2.60} had at most a minor effect on responses to agonists. Taken together, this suggested that signalling of K65A and K65E hFFA2 is biased towards activation of $G_{i/o}$ compared to $G_{q/11}$ and $G_{12/13}$ and calculation of the bias factor β confirmed that K65A and K65E indeed show a level of signalling bias compared to wild type hFFA2 that could be quantified.

To explore the $G_{i/o}$ bias induced by charge-altering mutations of Lys65^{2.60}, a genome-edited cell line lacking expression of each of $G\alpha_q$, $G\alpha_{11}$, $G\alpha_{12}$ and $G\alpha_{13}$ (Devost et al., 2017) was employed in the TGF α shedding assay. In these cells FFA2 agonists did not produce a TGF α shedding response as they do not express the G proteins that mediate this response, but upon co-transfection of $G\alpha$ subunits the TGF α shedding response mediated specifically by the reintroduced G protein can be detected. Such assessment of the contribution of $G\alpha_q$, $G\alpha_{11}$, $G\alpha_{12}$ and $G\alpha_{13}$ to TGF α shedding in response to FFA2 agonists revealed that while all G protein subunits couple to hFFA2, they have different capacities to promote shedding of TGF α . Therefore, chimeric $G\alpha$ proteins with a backbone based on $G\alpha_q$ and substitution of the six C-terminal amino acids with the $G\alpha$ protein of interest were utilised to compare FFA2 coupling to different G proteins. Furthermore, the use of such chimeric $G\alpha$ proteins also allowed the use of the TGF α shedding assay to detect coupling of FFA2 to $G_{i/o}$ G proteins, which do not naturally promote shedding of TGF α . In agreement with the signalling bias induced by charge-altering Lys65^{2.60} mutations, K65A and K65E hFFA2 displayed an improved TGF α shedding response when the $G\alpha_{q-i}$ chimera was reintroduced. In contrast, reintroduction of $G\alpha_{q-o}$ resulted in a reduced response compared to co-transfection of $G\alpha_q$. This may suggest that charge-modifying Lys65^{2.60} alterations do not only bias hFFA2 signalling toward coupling to the $G_{i/o}$ family but result in the receptor specifically favouring interaction with $G\alpha_i$ and not $G\alpha_o$. HEK293 cells that were employed throughout the work presented do not express $G\alpha_o$ (Atwood et al., 2011). Therefore, the bias factor β that was calculated to assess the degree of bias displayed by K65A and K65E hFFA2 for signalling through cAMP inhibition and [³⁵S]-GTP γ S binding assays rather than the TGF α shedding assay, actually compares exclusively G_i coupling with $G_{q/11}$ and $G_{12/13}$ activation. Although selection between G proteins within one subfamily is not common, there are other examples of GPCRs that display such a signalling profile. While the dopamine D₂ receptor is able to activate multiple G proteins within the $G_{i/o}$ subfamily, the dopamine D₃ receptor has been shown to selectively couple to $G\alpha_o$ with the third intracellular loop of the D₂ receptor playing a role in defining the promiscuity of its G protein coupling profile (Lane et al., 2008). G protein coupling bias has also been observed within the $G_{12/13}$ subfamily in the case of chemokine receptors CCR5 and CCR2, where chemokines promoted activation of $G\alpha_{12}$, but not $G\alpha_{13}$ (Corbisier et al., 2015), and the

orphan GPCR GPR35 was shown to selectively couple to $G\alpha_{13}$, but not $G\alpha_{12}$, in response to synthetic ligand zaprinast and endogenous tryptophan metabolite kynurenic acid (Jenkins et al., 2011). These studies indicate that it is certainly possible for GPCRs to select between $G\alpha$ proteins within a single subfamily family. However, additional studies on K65A and K65E hFFA2 would certainly be required to confirm G protein bias within the $G_{i/o}$ family. Nowadays there are well-established approaches that can be employed to monitor interactions between GPCRs and specific G protein subunits (Gales et al., 2005), and applying such techniques to investigate Lys65^{2.60} could yield interesting results.

Even though GPCR signalling bias based on the selection between different G protein subtypes has been the focus of this chapter and has been described previously in other studies (Bolognini et al., 2016a; Goupil et al., 2010), signalling bias between G protein-dependent and β -arrestin-mediated pathways is also an established concept with therapeutic relevance (Oh et al., 2010; Carr et al., 2016; Ranjan et al., 2017). FFA4 is a prominent example within the FFA receptor family for which it has been demonstrated that therapeutically beneficial anti-inflammatory effects are mediated by β -arrestin-dependent signalling (Oh et al., 2010). Although the structural basis for the preferred interaction between GPCRs and G proteins versus β -arrestins is not fully understood, there are some factors that are known to regulate β -arrestin recruitment, such as the phosphorylation state and nature of the C-terminal tail. Different patterns of phosphorylation and presence of negatively charged residues in the C-terminal tail of FFA4 have been shown to define the interaction of the receptor with β -arrestin 3 (Butcher et al., 2014). The ability of charge-altering mutations in position 65 to affect the recruitment of β -arrestin in addition to coupling to $G_{q/11}$ and $G_{12/13}$ G proteins, suggests that the conformational rearrangements imposed on the active form of the receptor by K65A and K65E mutations occur in a region that affects interaction with both signalling partners. This would support observations from other studies that have suggested that the site of β -arrestin interaction with GPCRs overlaps with that of the $\alpha 5$ helix of G proteins, which lies within the crevice formed by the rearrangement of TM3, TM5 and TM7 upon receptor activation (Szczepek et al., 2014, Kang et al., 2015).

6.3.3 Complex allosterism of biased FFA2 ligand AZ1729

GPCR ligands that display signalling bias have recently attracted much attention and in particular the selective activation of G proteins or β -arrestins has been demonstrated to result in different downstream effects (Whalen et al., 2011). However, in the context of promiscuous receptors such as FFA2, a ligand that displays bias between different G protein subtypes would be of great use to dissect the contribution of respective G proteins to FFA2 signalling and respective physiological outputs. Indeed, the identification of allosteric ligand AZ1729, which acted as an agonist in $G_{i/o}$ - but not $G_{q/11}$ -coupled assays, helped to confirm which FFA2-mediated physiological effects resulted from activation of $G_{i/o}$ or $G_{q/11}$ (Bolognini et al., 2016a). This biased signalling behaviour of AZ1729 was also useful in the study described here, as it was utilised to confirm that charge-altering Lys65^{2.60} mutations do not intrinsically affect $G_{i/o}$ -coupled signalling by hFFA2. Interestingly, when chimeric G proteins $G\alpha_{q-i}$ and $G\alpha_{q-o}$ were reintroduced into $\Delta G_{q/11/12/13}$ cells to detect $G_{i/o}$ activation in the TGF α shedding assay, AZ1729 was only able to produce a shedding response in cells transfected with $G\alpha_{q-i}$ and not $G\alpha_{q-o}$. As in discussed in the case of K65A and K65E hFFA2, selection between coupling to G_i versus G_o would certainly be an interesting hypothesis to investigate further. However, more detailed assessment of hFFA2 coupling to different G protein subtypes will be necessary to confirm these observations.

While AZ1729 activation of $G_{i/o}$ and $G_{q/11}$ has previously been well characterised (Bolognini et al., 2016a), there was little information on the effect of AZ1729 in $G_{12/13}$ -mediated pathways. Therefore, the TGF α shedding assay was employed to examine the allosteric modulation of C3 by AZ1729 in a $G_{12/13}$ -coupled assay system. In a previous study AZ1729 also displayed biased behaviour in its ability to modulate the response of hFFA2 to C3, in acting as a positive allosteric modulator of C3 potency in $G_{i/o}$ -coupled assays and a negative allosteric modulator of C3 efficacy in $G_{q/11}$ -coupled assays. When assessing the effect of AZ1729 on the ability of C3 to induce a shedding response in $\Delta G_{12/13}$ cells, in which this response is mediated exclusively by $G_{q/11}$, a similar effect could be observed with a concentration-dependent reduction in the maximal response to C3. In contrast, in parental cells and $\Delta G_{q/11}$ cells, in which the TGF α shedding response is induced exclusively by $G_{12/13}$, a different pattern emerged. While a

concentration-dependent reduction in the C3 efficacy could still be observed in response to AZ1729, a leftward shift of the C3 concentration-response could also be detected. This would suggest that in $G_{12/13}$ -coupled systems AZ1729 acts simultaneously as a negative allosteric modulator of C3 efficacy and a positive allosteric modulator of C3 affinity. Although such allosteric behaviour is unusual, it was observed previously in negative allosteric modulators of the cannabinoid CB1 receptor (Price et al., 2005) and a compound series developed for FFA3 (Hudson et al., 2014). Selected analogues within the investigated FFA3 compound series also had the capacity to reduce the maximal C3 response while producing a leftward shift of the C3 concentration response curve in [35 S]-GTP γ S binding assays. While the complex allosteric modulation of C3 responses by AZ1729 is certainly of pharmacological interest, the comparably minor increase in C3 potency induced by AZ1729 in $G_{12/13}$ -coupled assays is not likely to translate into a strong effect in physiological systems and it would be challenging to differentiate between $G_{q/11}$ - and $G_{12/13}$ -mediated responses as AZ1729 has a negative modulatory effect on C3 efficacy in both.

6.4 Conclusions

Although the work described in this chapter was originally designed to uncover the molecular mechanisms underlying the species selectivity of FFA2 antagonists, it expanded into a study that assessed a range of different aspects of FFA2 function. Initially, close investigation of a hFFA2 homology model facilitated the identification of Lys65^{2.60} as a residue that defines species selectivity of FFA2 antagonists for the human versus murine orthologue. The interaction between the central amide moiety present in GLPG0974 and CATPB with Lys65^{2.60} contributed significantly to high-affinity binding and the replacement of lysine with arginine at position 2.60, as in rodent forms of FFA2, resulted in loss of antagonist binding. Moreover, introduction of the ‘humanising’ R65K mutation in mFFA2 led to a gain of antagonist function with the inhibitory action of CATPB comparable to that at wild type hFFA2. Using this information, a homology model of R65K mFFA2 was constructed to understand how the R65K mutation might alter the receptor binding pocket to allow for ligand binding. Conceptually, taking experimental observations and computational ligand docking into account, it should now be possible to rationally design an antagonist that binds to both human and rodent FFA2 with high affinity. However, the

replacement of lysine with arginine at position 2.60 in mFFA2 may result in major conformational rearrangements, if Arg65^{2.60} indeed forms an ionic bond with Glu68^{2.63}, which may inherently change the nature of the ligand-accessible binding site. Molecular dynamics simulations could contribute to defining the structural changes that occur when such an ionic lock is formed and this may provide some guidance for the design of an antagonist active at rodent forms of FFA2. Should design of an antagonist for rodent forms of FFA2 not be possible, the use of transgenic animals represents an alternative approach. Introduction of the R65K alteration in mFFA2 should theoretically not disrupt endogenous signalling, as long as a positive charge at position 2.60 is retained, and would allow specific inhibition by available antagonists. It would be interesting to perform parallel studies in mice expressing R65K mFFA2 versus humanised mice expressing hFFA2 to assess whether the differences in pharmacology observed between species translate into distinct physiological function.

Interestingly, Lys65^{2.60} also plays a role in selectively regulating activation of G proteins by hFFA2. A positive charge at position 2.60 was required for hFFA2 coupling to G_{q/11} and G_{12/13}, but not G_i G proteins. There is a growing interest in understanding the molecular mechanisms behind GPCRs coupling to multiple G proteins. Novel structural and informatics approaches have been employed to dissect promiscuous GPCR coupling, including studies that use specific “mini-G proteins” in crystallography to detect G protein subtype-specific structural changes in active-state receptors (Carpenter and Tate, 2016) or investigations that utilise an informatics approach to identify residues across the family of Class A GPCRs responsible for conducting activation pathways (Venkatakrisnan et al., 2016). However, in many cases the focus lies on residue networks near the intracellular surface mediating potential interactions with coupled G proteins or along the transmembrane domains guiding rearrangements resulting in an active-state conformation upon ligand engagement. In contrast, here a residue near the extracellular portion of the receptor was identified, whose positive charge is essential for maintaining promiscuous G protein coupling of the receptor and alteration resulted in G protein coupling of hFFA2 being biased towards the G_i subtype within the G_{i/o} family. The fact that the positive charge at position 2.60 is conserved among species orthologues, suggests that it is essential for endogenous FFA2 function. Taken together, this provides an

interesting basis for the selection of GPCR coupling between G protein subtypes. The generation of a model animal that expresses a G_i-biased form of FFA2, by replacing lysine or arginine at position 2.60 with alanine or glutamic acid, could be an interesting approach to explore the contribution of respective G protein signalling to the physiological function of FFA2. However, in future studies that employ these biased FFA2 mutants as a tool it will be important to consider that β -arrestin recruitment was also affected by charge-altering mutations.

Additional avenues of investigation should be explored to assess whether receptor internalisation and desensitisation is affected by the impaired recruitment of β -arrestin. It may also be of interest to assess if mutation of Lys65^{2.60} affects β -arrestin recruitment directly by altering the affinity of β -arrestin for the altered active conformation of FFA2 or whether K65A and K65E mutations exert an indirect effect by e.g. altering phosphorylation of the C-terminal tail of FFA2 that would result in reduced β -arrestin recruitment.

7 Final discussion

The GPCR family represents the largest group of transmembrane receptors in the human genome (Fredriksson et al., 2003) and includes some of the most successfully utilised therapeutic targets, with a third of all approved small-molecule drugs targeting GPCRs (Santos et al., 2017). The success of GPCRs as drug targets is undoubtedly linked to their ability to sense an extraordinary range of extracellular stimuli and translate environmental changes into a cellular response by inducing an appropriate signalling cascade (Lagerstrom and Schiöth, 2008). Therefore, GPCR research is often conducted with future drug discovery in mind. The orphanisation of SCFA receptors generated much excitement due to their ability to respond to by-products of gut microbiome activity. The contribution of the gut microbiota to human health is well-established, in particular its involvement in the pathogenesis of inflammatory bowel disease (Zhang et al., 2017), and modulation of SCFA receptor signalling may represent a novel approach to therapeutically targeting the gut microbiome (Husted et al., 2017). Studies investigating the physiological role of SCFA receptors have confirmed their involvement in a range of gut microbiome-related processes including the ability of SCFAs to modulate gut hormone release (Tolhurst et al., 2012), insulin secretion (Priyadarshini et al., 2015) and immune cell recruitment (Maslowski et al., 2009). Despite the potential involvement of SCFA receptors in the pathogenesis of diseases with a great need for novel therapeutics, SCFA receptors remain far from fully validated as drug targets. The co-expression of SCFA receptors FFA2 and FFA3 in tissues of interest such as the gastrointestinal tract (Nohr et al., 2013) and pancreatic β cells (Priyadarshini et al., 2015), makes it difficult to dissect contributions of the respective receptors to the physiological effects of SCFAs. Therefore, development of specific tool compounds for FFA2 and FFA3 is crucial for understanding their physiological role. While the only available tool compounds for FFA3 display complex allosteric behaviour (Hudson et al., 2014), a larger selection of orthosteric agonists (Hudson et al., 2013a, Forbes et al., 2015), orthosteric antagonists (Hudson et al., 2012b, Pizzonero et al., 2014) and allosteric ligands (Smith et al., 2011, Bolognini et al., 2016a) have been developed and characterised in the last decade to investigate FFA2. However, pharmacological variations in species orthologues have limited the application of such tool compounds (Hudson et al.,

2013b). Human and rodent orthologues of FFA2 display distinct properties including different rank orders of SCFA potencies, variation in constitutive activity and, perhaps most importantly, there is a lack of FFA2 antagonists active at rodent orthologues (Hudson et al., 2012b, Pizzonero et al., 2014).

The work described in this thesis has focussed on investigating the pharmacology of FFA2 with the aim of providing a guide for the design of future tool compounds and potential therapeutics. In contrast to endogenous small-molecule GPCR ligands that contain multiple functional groups and occupy a large portion of the ligand-accessible binding pocket, SCFA are small molecules that essentially only interact with the orthosteric Arg-His-Arg triad (Stoddart et al., 2008). Therefore, synthetic ligands for FFA2 invariably have to interact with additional regions of the binding pocket to achieve high-affinity binding, which may contribute to the complex pharmacology of FFA2 antagonists. Functional and binding studies employed throughout all chapters confirmed the main defining factor for agonist versus antagonist action at hFFA2: Interaction between the ligand carboxylate moiety and the orthosteric arginines Arg180^{5.39} and Arg255^{7.35}. These interactions are required for FFA2 agonist binding, as alanine replacement of either arginine residue (see chapter 4) or modification of the agonist carboxylate (Schmidt et al., 2011, Hudson et al., 2013a) resulted in loss of agonist binding and action, and may therefore confer the first step in the conformational changes required for an active-state receptor. A comparison of inactive and active state crystal structures across the GPCR family revealed that while activation-dependent structural changes at the extracellular face are usually highly receptor-specific, rearrangements that occur at the intracellular side upon receptor activation are in part conserved within the *Rhodopsin* family (Venkatakrisnan et al., 2016). Interestingly, the orthosteric arginine pair is conserved between free fatty acid receptors FFA1 (Sum et al., 2007), FFA2 and FFA3 (Stoddart et al., 2008), which may suggest that these receptors share a mechanism of receptor activation by agonist engagement of these residues, perhaps due to the fact that they arose by gene duplication given that FFA1, FFA2 and FFA3 are tandemly located on chromosome 19. However, the coupling of FFA2 and FFA3 to G proteins differs, with FFA2 signalling through multiple G protein subtypes including G_{q/11}, G_{12/13} and G_{i/o}, while FFA3 only couples to G_{i/o} G proteins (Brown et al., 2003). Therefore, part of the activation network that

translates agonist binding to G protein coupling likely differs between FFA2 and FFA3. However, investigation of the role of Lys65^{2.60} in hFFA2 coupling to G protein subtypes revealed that it selectively regulates coupling of hFFA2 to G_i , but not $G_{q/11}$ or $G_{12/13}$, while leaving agonist binding mostly unaffected (see chapter 6). Interestingly, $G_{i/o}$ -coupled FFA3, and indeed FFA1, both contain a positively charged residue at position 2.60 and it may be interesting to explore whether G protein coupling at these free fatty acid receptors is also affected by charge-altering mutations of the equivalent residue.

In contrast to agonists, FFA2 antagonist action does not rely to the same extent on the interaction between ligand carboxylate and the orthosteric arginine pair. While the interaction certainly contributes to anchoring antagonists in the binding pocket, it is not essential. Analogues of the representative FFA2 antagonists GLPG0974 and CATPB with modifications at the carboxylate moiety retained their ability to bind to and inhibit agonist responses at hFFA2 and only required one arginine residue for high-affinity binding (see chapters 3 and 4). Regardless, assessed antagonists were competitive with FFA2 agonists and behaved as orthosteric ligands. Furthermore, high-affinity binding of the radioligand [³H]-GLPG0974 was lost upon mutation of both arginine residues to alanine (see chapter 4), confirming that at least one orthosteric arginine residue is required for antagonist binding. This structure-activity information was utilised to develop the fluorescent tracer F-1, which was generated by linking a NBD fluorophore to the carboxylate moiety of the GLPG0974 analogue GLPG-3 (see chapter 5). Using fluorescent tracer F-1, a BRET binding assay utilising a Nanoluciferase-tagged form of FFA2 was successfully developed that allowed determination of unlabelled antagonist binding affinity and kinetics. However, in contrast to its parent molecule, F-1 was non-competitive with FFA2 agonists and behaved like to an allosteric ligand, while antagonists retained the ability to fully outcompete F-1 binding to hFFA2. Examination of the F-1 binding site by measuring its affinity at key orthosteric binding site mutants revealed that F-1 retains the ability to bind the dual R180A-R255A mutant of hFFA2, albeit with reduced affinity. Interestingly, assessment of GLPG0974 analogues with modifications of the carboxylate region in F-1 competition binding assays demonstrated that analogues of the same parent compound with larger modifications showed increased affinity at R180A-R255A hFFA2. However,

neither GLPG0974 nor CATPB were able to compete with F-1 for binding to the dual arginine mutant of hFFA2, confirming that interaction with at least one orthosteric arginine residue is required for binding of the parent compounds of the two most commonly employed orthosteric hFFA2 antagonist series.

Taken together, these observations suggest that orthosteric FFA2 antagonists are most likely bitopic ligands that interact with the orthosteric site comprised of Arg180^{5.39} and Arg255^{7.35} with their carboxylate moiety. The remaining part of the orthosteric antagonist molecule occupies a secondary binding site, which is shared with allosteric fluorescent tracer F-1, resulting in a competitive relationship between orthosteric antagonists and F-1 in BRET binding assays. The replacement of the F-1 carboxylate region with a linker and fluorophore NBD resulted in the loss of orthosteric interactions, thereby making F-1 an allosteric ligand. This hypothesis was supported by identification of Lys65^{2.60}, a residue that defines the species selectivity of antagonists for the human versus rodent orthologues of FFA2 (see chapter 6). Molecular modelling suggested that GLPG0974 and CATPB form an interaction with Lys65^{2.60}, which is lost in rodent forms of FFA2 due to an alteration of Lys65^{2.60} to Arg65^{2.60}, which is likely sequestered in an interaction with Glu68^{2.63}. Thereby the mFFA2 binding site may be restructured in a fashion that prohibits antagonist binding. The role of Lys65^{2.60} in defining the species selectivity of antagonists was confirmed by generating a 'humanised' R65K mFFA2 mutant at which FFA2 antagonists gained binding affinity and function. Docking of CATPB and GLPG0974 into a R65K mFFA2 homology model suggested that CATPB adopts a binding pose similar to that in hFFA2. However, this was not the case for GLPG0974 and there are likely additional species-specific residue contacts that define GLPG0974 binding to hFFA2. Interestingly, Lys65^{2.60} was not only important for activity of orthosteric antagonists GLPG0974 and CATPB, but also essential for binding of F-1. This suggests that Lys65^{2.60} lies within the secondary antagonist binding site shared between orthosteric antagonists and the allosteric fluorescent tracer. Therefore, extensive modifications of the antagonist carboxylate moiety may facilitate a switch from an orthosteric to an allosteric mode of binding.

The studies presented in this thesis have not only provided information on how agonists and antagonists bind to FFA2 and why antagonists display species

selectivity for the human orthologue of FFA2 (see chapter 6), but also contributed to understanding the mechanisms underlying FFA2 activation (see chapter 4) and G protein coupling (see chapter 6). Considering the conclusions described above, which directions may be of interest to explore further? From a basic research perspective, to further the understanding of GPCR structure and function, FFA2 is an interesting receptor to explore due to its promiscuous G protein coupling profile. Identification of Lys65^{2.60} as a residue at the extracellular portion of the receptor that may selectively regulate G protein coupling may facilitate examination of the molecular basis of biased signalling. Recent studies aiming to understand the mechanism of G protein coupling to GPCRs have explored the role of hydrogen bond networks, mediated by water molecules within the neurokinin-1 receptor, in defining biased G protein and β -arrestin coupling (Valentin-Hansen et al., 2015) and attempted to define the G protein subtype-specific interactions between GPCRs and $G\alpha_q$ versus $G\alpha_s$ proteins (Semack et al., 2016). Molecular dynamics simulations and more detailed investigations of the neighbourhood of Lys65^{2.60} may be of interest to define the role of Lys65^{2.60} in the activation pathway that contributes to $G_{q/11}$ and $G_{12/13}$, but not G_i coupling, of hFFA2. Although the loss of β -arrestin recruitment at charge-altering mutants of Lys65^{2.60} adds a further layer of complexity to the importance of this residue for FFA2 signalling, molecular dynamics simulations of respective mutants may shine some light on the structural determinants that G protein and β -arrestin coupling have in common. Comparison of results from such studies to equivalent investigations at FFA3 may also help to understand the distinct signalling profile of these two SCFA receptors.

In addition to providing an opportunity to explore the mechanism of GPCR coupling to G proteins, findings discussed above can also be applied in translational studies to validate the potential of FFA2 as a therapeutic target. The broad expression profile of FFA2 and its ability to couple to multiple G protein subfamilies has made dissection of its physiological roles difficult and in some cases, studies have yielded contradictory results (Milligan et al., 2017). One prominent example is the effect of SCFAs on glucose-stimulated insulin secretion in the pancreas, in which independent studies observed activation (Priyadarshini et al., 2015) and inhibition (Tang et al., 2015) of insulin secretion in response to SCFA treatment. These observations may relate to the opposing

effects of $G_{q/11}$ (Sassmann et al., 2010) versus $G_{i/o}$ (Berger et al., 2015) activation on glucose-stimulated insulin secretion, however, the G protein coupling of FFA2 in pancreatic β cells remains undefined (Milligan et al., 2017). The identification of the charge-altering mutations at position 2.60 that biased FFA2 signalling towards G_i G proteins (see chapter 6) may represent a convenient means of exploring the contribution of FFA2 signalling through $G_{q/11}$ versus $G_{i/o}$ to biological outcomes. Generation of a rodent model expressing K65A or K65E hFFA2 could allow assessment of the impact of FFA2 signalling exclusively through G_i on physiological processes. Furthermore, in combination with FFA2-specific tool compounds, important questions could be addressed, such as whether FFA2 is capable of inhibiting insulin secretion by activating G_i signalling in pancreatic β cells. To initially assess whether such a strategy is feasible, the genome of an immortalised cell line of interest, such as the pancreatic β cell line MIN-6 (Ishihara et al., 1993), could be edited using CRISPR/Cas9 (Tschaharganeh et al., 2016) to knock-in a G_i -biased form of FFA2. Such a rodent model could then be utilised to examine how responses to SCFAs and tool compounds compare to cells expressing the wild-type receptor.

While the complex signalling profile of FFA2 complicates the understanding of its physiological roles, the species-specific differences between human and rodent orthologues raise more fundamental questions regarding the usefulness of animal models. In addition to the selectivity of FFA2 antagonists for the human form of FFA2, assessment of the structure-activity relationship of a novel agonist series at human and murine FFA2 also revealed species differences (see chapter 3). Therefore, optimising compounds at hFFA2 in heterologous expression systems with the aim of developing a potential therapeutic and performing pre-clinical testing in rodent models does not seem to be a suitable strategy for FFA2. Transgenic animal models may be an alternative, as generation of a rodent model that expresses the human form of FFA2 would circumvent issues arising from species-specific pharmacology. However, it is also crucial to address whether differences in human versus murine FFA2 pharmacology translate into distinct physiological function. There are also general concerns regarding the reliance on mouse models for gut microbiota-related research, as variations in experimental conditions can affect microbiome composition and activity (Nguyen et al., 2015). Therefore, establishing a controlled experimental setup and being

aware of the limitations of animal models when translating results from mouse models to humans is highly recommended for future research on FFA2. In addition, a recent investigation of the GPCR repertoire expressed in human versus murine islets demonstrated differences in expression levels of the adenosine A₃ and galanin receptors (Amisten et al., 2017), hence species-specific expression profiles in certain tissues should also be considered. Apart from such general considerations, the known pharmacological differences in endogenous FFA2 pharmacology in mice versus humans are comparably minor, with distinct rank orders of SCFA potency and differences in constitutive activity (Hudson et al., 2012b). The best approach is likely to compare results obtained from studies in animal models to those performed using isolated human tissue or cells, such as immune cells isolated from whole blood (Pizzonero et al., 2014, Bolognini et al., 2016a). The activation or inhibition of FFA2 will likely have an effect across multiple tissues involved in metabolic regulation, therefore observing the systemic impact of tool compounds in models of disease may be necessary to confirm whether targeting of FFA2 indeed provides a therapeutic benefit.

References

- Ahmadian, M., Suh, J. M., Hah, N., Liddle, C., Atkins, A. R., Downes, M. and Evans, R. M. (2013) 'PPARgamma signaling and metabolism: the good, the bad and the future', *Nat Med*, 19(5), pp. 557-66.
- Akanji, A. O., Humphreys, S., Thursfield, V. and Hockaday, T. D. (1989) 'The relationship of plasma acetate with glucose and other blood intermediary metabolites in non-diabetic and diabetic subjects', *Clin Chim Acta*, 185(1), pp. 25-34.
- Alvarez-Curto, E., Inoue, A., Jenkins, L., Raihan, S. Z., Prihandoko, R., Tobin, A. B. and Milligan, G. (2016) 'Targeted Elimination of G Proteins and Arrestins Defines Their Specific Contributions to Both Intensity and Duration of G Protein-coupled Receptor Signaling', *J Biol Chem*, 291(53), pp. 27147-59.
- Aminoshariae, A. and Khan, A. (2015) 'Acetaminophen: old drug, new issues', *J Endod*, 41(5), pp. 588-93.
- Amisten, S., Atanes, P., Hawkes, R., Ruz-Maldonado, I., Liu, B., Parandeh, F., Zhao, M., Huang, G. C., Salehi, A. and Persaud, S. J. (2017) 'A comparative analysis of human and mouse islet G-protein coupled receptor expression', *Sci Rep*, 7, pp. 46600.
- Ang, Z. and Ding, J. L. (2016) 'GPR41 and GPR43 in Obesity and Inflammation - Protective or Causative?', *Front Immunol*, 7, pp. 28.
- Ang, Z., Xiong, D., Wu, M. and Ding, J. L. (2017) 'FFAR2-FFAR3 receptor heteromerization modulates short-chain fatty acid sensing', *FASEB J*, 32(1), pp. 289-303.
- Antony, J., Kellershohn, K., Mohr-Andra, M., Kebig, A., Prilla, S., Muth, M., Heller, E., Disingrini, T., Dallanocce, C., Bertoni, S., Schrobang, J., Trankle, C., Kostenis, E., Christopoulos, A., Holtje, H. D., Barocelli, E., De Amici, M., Holzgrabe, U. and Mohr, K. (2009) 'Dualsteric GPCR targeting: a novel route to binding and signaling pathway selectivity', *FASEB J*, 23(2), pp. 442-50.
- Arora, A. and Scholar, E. M. (2005) 'Role of tyrosine kinase inhibitors in cancer therapy', *J Pharmacol Exp Ther*, 315(3), pp. 971-9.
- Atwood, B. K., Lopez, J., Wager-Miller, J., Mackie, K. and Straiker, A. (2011) 'Expression of G protein-coupled receptors and related proteins in HEK293, AtT20, BV2, and N18 cell lines as revealed by microarray analysis', *BMC Genomics*, 12, pp. 14.
- Bai, M., Sexton, M., Stella, N. and Bornhop, D. J. (2008) 'MBC94, a conjugable ligand for cannabinoid CB 2 receptor imaging', *Bioconjug Chem*, 19(5), pp. 988-92.

- Baker, J. G., Hall, I. P. and Hill, S. J. (2003) 'Agonist and inverse agonist actions of beta-blockers at the human beta 2-adrenoceptor provide evidence for agonist-directed signaling', *Mol Pharmacol*, 64(6), pp. 1357-69.
- Baker, J. G., Middleton, R., Adams, L., May, L. T., Briddon, S. J., Kellam, B. and Hill, S. J. (2010) 'Influence of fluorophore and linker composition on the pharmacology of fluorescent adenosine A1 receptor ligands', *Br J Pharmacol*, 159(4), pp. 772-86.
- Ballesteros, J. A. and Weinstein, H. (1995) 'Integrated methods for the construction of three-dimensional models and computational probing of structure-function relations in G protein-coupled receptors', *Methods in Neurosciences*, 25, pp. 366-428.
- Banks, J. L., Beard, H. S., Cao, Y., Cho, A. E., Damm, W., Farid, R., Felts, A. K., Halgren, T. A., Mainz, D. T., Maple, J. R., Murphy, R., Philipp, D. M., Repasky, M. P., Zhang, L. Y., Berne, B. J., Friesner, R. A., Gallicchio, E. and Levy, R. M. (2005) 'Integrated Modeling Program, Applied Chemical Theory (IMPACT)', *J Comput Chem*, 26(16), pp. 1752-80.
- Barbas, C. F., 3rd, Burton, D. R., Scott, J. K. and Silverman, G. J. (2007) 'Quantitation of DNA and RNA', *CSH Protoc*, doi:10.1101/pdb.ip47.
- Bazarsuren, A., Grauschopf, U., Wozny, M., Reusch, D., Hoffmann, E., Schaefer, W., Panzner, S. and Rudolph, R. (2002) 'In vitro folding, functional characterization, and disulfide pattern of the extracellular domain of human GLP-1 receptor', *Biophys Chem*, 96(2-3), pp. 305-18.
- Beetens, J. 'GLPG0974, a selective FFA2 antagonist'. *Fatty acid activation of G protein-coupled receptors: Basic and clinical perspectives (ASPET meeting)*, Boston, 2013.
- Berger, M., Scheel, D. W., Macias, H., Miyatsuka, T., Kim, H., Hoang, P., Ku, G. M., Honig, G., Liou, A., Tang, Y., Regard, J. B., Sharifnia, P., Yu, L., Wang, J., Coughlin, S. R., Conklin, B. R., Deneris, E. S., Tecott, L. H. and German, M. S. (2015) 'Galphan/o-coupled receptor signaling restricts pancreatic beta-cell expansion', *Proc Natl Acad Sci U S A*, 112(9), pp. 2888-93.
- Bergsdorf, C., Kropp-Goerkis, C., Kaehler, I., Ketscher, L., Boemer, U., Parczyk, K. and Bader, B. (2008) 'A one-day, dispense-only IP-One HTRF assay for high-throughput screening of Galphaq protein-coupled receptors: towards cells as reagents', *Assay Drug Dev Technol*, 6(1), pp. 39-53.
- Berridge, M. J. (1993) 'Inositol trisphosphate and calcium signalling', *Nature*, 361(6410), pp. 315-25.
- Bertram, L. and Tanzi, R. E. (2008) 'Thirty years of Alzheimer's disease genetics: the implications of systematic meta-analyses', *Nat Rev Neurosci*, 9(10), pp. 768-78.

- Bjursell, M., Admyre, T., Goransson, M., Marley, A. E., Smith, D. M., Oscarsson, J. and Bohlooly, Y. M. (2011) 'Improved glucose control and reduced body fat mass in free fatty acid receptor 2-deficient mice fed a high-fat diet', *Am J Physiol Endocrinol Metab.*, 300(1), pp. E211-20.
- Bolognini, D., Moss, C., Nilsson, K., Petersson, A., Donnelly, I., Sergeev, E., König, G., Kostenis, E., Kurowska-Stolarska, M., Miller, A., Dekker, N., Tobin, A. and Milligan, G. (2016a) 'A Novel Allosteric Activator of Free Fatty Acid 2 Receptor Displays Unique Gi-functional Bias', *J Biol Chem*, 291(36), pp. 18915-31.
- Bolognini, D., Tobin, A. B., Milligan, G. and Moss, C. E. (2016b) 'The Pharmacology and Function of Receptors for Short-Chain Fatty Acids', *Mol Pharmacol*, 89(3), pp. 388-98.
- Borders, C. L., Jr., Broadwater, J. A., Bekeny, P. A., Salmon, J. E., Lee, A. S., Eldridge, A. M. and Pett, V. B. (1994) 'A structural role for arginine in proteins: multiple hydrogen bonds to backbone carbonyl oxygens', *Protein Sci*, 3(4), pp. 541-8.
- Bradley, S. J., Bourgognon, J. M., Sanger, H. E., Verity, N., Mogg, A. J., White, D. J., Butcher, A. J., Moreno, J. A., Molloy, C., Macedo-Hatch, T., Edwards, J. M., Wess, J., Pawlak, R., Read, D. J., Sexton, P. M., Broad, L. M., Steinert, J. R., Mallucci, G. R., Christopoulos, A., Felder, C. C. and Tobin, A. B. (2017) 'M1 muscarinic allosteric modulators slow prion neurodegeneration and restore memory loss', *J Clin Invest*, 127(2), pp. 487-499.
- Brantis, C. E., Ooms, F. and Bernard, J. (2011) 'Novel amino acid derivatives and their use as gpr43 receptor modulators', *International Patent*, Application WO2011/092284.
- Briscoe, C. P., Tadayyon, M., Andrews, J. L., Benson, W. G., Chambers, J. K., Eilert, M. M., Ellis, C., Elshourbagy, N. A., Goetz, A. S., Minnick, D. T., Murdock, P. R., Sauls, H. R., Jr., Shabon, U., Spinage, L. D., Strum, J. C., Szekeres, P. G., Tan, K. B., Way, J. M., Ignar, D. M., Wilson, S. and Muir, A. I. (2003) 'The orphan G protein-coupled receptor GPR40 is activated by medium and long chain fatty acids', *J Biol Chem*, 278(13), pp. 11303-11.
- Brooks, L., Viardot, A., Tsakmaki, A., Stolarczyk, E., Howard, J. K., Cani, P. D., Everard, A., Sleeth, M. L., Psichas, A., Anastasovskaj, J., Bell, J. D., Bell-Anderson, K., Mackay, C. R., Ghatei, M. A., Bloom, S. R., Frost, G. and Bewick, G. A. (2017) 'Fermentable carbohydrate stimulates FFAR2-dependent colonic PYY cell expansion to increase satiety', *Mol Metab*, 6(1), pp. 48-60.

- Brown, A. J., Goldsworthy, S. M., Barnes, A. A., Eilert, M. M., Tcheang, L., Daniels, D., Muir, A. I., Wigglesworth, M. J., Kinghorn, I., Fraser, N. J., Pike, N. B., Strum, J. C., Steplewski, K. M., Murdock, P. R., Holder, J. C., Marshall, F. H., Szekeres, P. G., Wilson, S., Ignar, D. M., Foord, S. M., Wise, A. and Dowell, S. J. (2003) 'The Orphan G protein-coupled receptors GPR41 and GPR43 are activated by propionate and other short chain carboxylic acids', *J Biol Chem*, 278(13), pp. 11312-9.
- Brown, A. J., Tsoulou, C., Ward, E., Gower, E., Bhudia, N., Chowdhury, F., Dean, T. W., Faucher, N., Gangar, A. and Dowell, S. J. (2015) 'Pharmacological properties of acid N-thiazolylamide FFA2 agonists', *Pharmacol Res Perspect*, 3(3), pp. E00141.
- Brust, T. F., Hayes, M. P., Roman, D. L., Burris, K. D. and Watts, V. J. (2015) 'Bias analyses of preclinical and clinical D2 dopamine ligands: studies with immediate and complex signaling pathways', *J Pharmacol Exp Ther*, 352(3), pp. 480-93.
- Busse, D., Kudella, P., Gruning, N. M., Gisselmann, G., Stander, S., Luger, T., Jacobsen, F., Steinstrasser, L., Paus, R., Gkogkolou, P., Bohm, M., Hatt, H. and Benecke, H. (2014) 'A synthetic sandalwood odorant induces wound-healing processes in human keratinocytes via the olfactory receptor OR2AT4', *J Invest Dermatol*, 134(11), pp. 2823-32.
- Butcher, A. J., Hudson, B. D., Shimpukade, B., Alvarez-Curto, E., Prihandoko, R., Ulven, T., Milligan G. and Tobin A. B. (2014) 'Concomitant action of structural elements and receptor phosphorylation determines arrestin-3 interaction with the free fatty acid receptor FFA4', *J Biol Chem*, 289(26), pp. 18451-65.
- Bylund, D. B. and Toews, M. L. (1993) 'Radioligand binding methods: practical guide and tips', *Am J Physiol*, 265(5 Pt 1), pp. L421-9.
- Cahill, T. J., 3rd, Thomsen, A. R., Tarrasch, J. T., Plouffe, B., Nguyen, A. H., Yang, F., Huang, L. Y., Kahsai, A. W., Bassoni, D. L., Gavino, B. J., Lamerdin, J. E., Triest, S., Shukla, A. K., Berger, B., Little, J. t., Antar, A., Blanc, A., Qu, C. X., Chen, X., Kawakami, K., Inoue, A., Aoki, J., Steyaert, J., Sun, J. P., Bouvier, M., Skiniotis, G. and Lefkowitz, R. J. (2017) 'Distinct conformations of GPCR-beta-arrestin complexes mediate desensitization, signaling, and endocytosis', *Proc Natl Acad Sci U S A*, 114(10), pp. 2562-7.
- Carr, R., Schilling, J., Song, J., Carter, R. L., Du, Y., Yoo, S. M., Traynham, C. J., Koch, W. J., Cheung, J. Y., Tilley, D. G. and Benovic, J. L. (2016) 'B-arrestin-biased signaling through the B2-adrenergic receptor promotes cardiomyocyte contraction', *Proc Natl Acad Sci U S A*, 113(28), pp. E4107-16.
- Carpenter, B. and Tate, C. G. (2016) 'Engineering a minimal G protein to facilitate crystallisation of G protein-coupled receptors in their active conformation', *Protein Eng Des Sel*, 29(12), pp. 583-94.

- Casarosa, P., Bouyssou, T., Germeyer, S., Schnapp, A., Gantner, F. and Pieper, M. (2009) 'Preclinical evaluation of long-acting muscarinic antagonists: comparison of tiotropium and investigational drugs', *J Pharmacol Exp Ther*, 330(2), pp. 660-8.
- Chan, W. Y., McKinzie, D. L., Bose, S., Mitchell, S. N., Witkin, J. M., Thompson, R. C., Christopoulos, A., Lazareno, S., Birdsall, N. J., Bymaster, F. P. and Felder, C. C. (2008) 'Allosteric modulation of the muscarinic M4 receptor as an approach to treating schizophrenia', *Proc Natl Acad Sci U S A*, 105(31), pp. 10978-83.
- Chandrashekar, J., Mueller, K. L., Hoon, M. A., Adler, E., Feng, L., Guo, W., Zuker, C. S. and Ryba, N. J. (2000) 'T2Rs function as bitter taste receptors', *Cell*, 100(6), pp. 703-11.
- Charlton, S. J. and Vauquelin, G. (2010) 'Elusive equilibrium: the challenge of interpreting receptor pharmacology using calcium assays', *Br J Pharmacol*, 161(6), pp. 1250-65.
- Cheng, R. K. Y., Fiez-Vandal, C., Schlenker, O., Edman, K., Aggeler, B., Brown, D. G., Brown, G. A., Cooke, R. M., Dumelin, C. E., Dore, A. S., Geschwindner, S., Grebner, C., Hermansson, N. O., Jazayeri, A., Johansson, P., Leong, L., Prihandoko, R., Rappas, M., Soutter, H., Snijder, A., Sundstrom, L., Tehan, B., Thornton, P., Troast, D., Wiggin, G., Zhukov, A., Marshall, F. H. and Dekker, N. (2017) 'Structural insight into allosteric modulation of protease-activated receptor 2', *Nature*, 545(7652), pp. 112-5.
- Choe, H. W., Kim, Y. J., Park, J. H., Morizumi, T., Pai, E. F., Krauss, N., Hofmann, K. P., Scheerer, P. and Ernst, O. P. (2011) 'Crystal structure of metarhodopsin II', *Nature*, 471(7340), pp. 651-5.
- Christiansen, E., Hudson, B. D., Hansen, A. H., Milligan, G. and Ulven, T. (2016) 'Development and Characterization of a Potent Free Fatty Acid Receptor 1 (FFA1) Fluorescent Tracer', *J Med Chem*, 59(10), pp. 4849-58.
- Christiansen, E., Watterson, K. R., Stocker, C. J., Sokol, E., Jenkins, L., Simon, K., Grundmann, M., Petersen, R. K., Wargent, E. T., Hudson, B. D., Kostenis, E., Ejsing, C. S., Cawthorne, M. A., Milligan, G. and Ulven, T. (2015) 'Activity of dietary fatty acids on FFA1 and FFA4 and characterisation of pinolenic acid as a dual FFA1/FFA4 agonist with potential effect against metabolic diseases', *Br J Nutr*, 113(11), pp. 1677-88.
- Christopoulos, A. and Kenakin, T. (2002) 'G protein-coupled receptor allosterism and complexing', *Pharmacol Rev*, 54(2), pp. 323-74.
- Colquhoun, D. (2007) 'Why the Schild method is better than Schild realised', *Trends Pharmacol Sci*, 28(12), pp. 608-14.
- Congreve, M., Langmead, C. and Marshall, F. H. (2011) 'The use of GPCR structures in drug design', *Adv Pharmacol*, 62, pp. 1-36.

- Conte, C., Ebeling, M., Marcuz, A., Nef, P. and Andres-Barquin, P. J. (2002) 'Identification and characterization of human taste receptor genes belonging to the TAS2R family', *Cytogenet Genome Res*, 98(1), pp. 45-53.
- Cook, S. I. and Sellin, J. H. (1998) 'Review article: short chain fatty acids in health and disease', *Aliment Pharmacol Ther*, 12(6), pp. 499-507.
- Cooper, A., Singh, S., Hook, S., Tyndall, J. D. A. and Vernall, A. J. (2017) 'Chemical Tools for Studying Lipid-Binding Class A G Protein-Coupled Receptors', *Pharmacol Rev*, 69(3), pp. 316-53.
- Corbisier, J., Gales, C., Huszagh, A., Parmentier, M. and Springael, J. Y. (2015) 'Biased signaling at chemokine receptors', *J Biol Chem*, 290(15), pp. 9542-54.
- Costanzi, S. (2013) 'Modeling G protein-coupled receptors and their interactions with ligands', *Curr Opin Struct Biol*, 23(2), pp. 185-90.
- Cummings, J. H., Pomare, E. W., Branch, W. J., Naylor, C. P. and Macfarlane, G. T. (1987) 'Short chain fatty acids in human large intestine, portal, hepatic and venous blood', *Gut*, 28(10), pp. 1221-7.
- Daaka, Y., Luttrell, L. M., Ahn, S., Della Rocca, G. J., Ferguson, S. S., Caron, M. G. and Lefkowitz, R. J. (1998) 'Essential role for G protein-coupled receptor endocytosis in the activation of mitogen-activated protein kinase', *J Biol Chem*, 273(2), pp. 685-8.
- Daly, C. J., Ross, R. A., Whyte, J., Henstridge, C. M., Irving, A. J. and McGrath, J. C. (2010) 'Fluorescent ligand binding reveals heterogeneous distribution of adrenoceptors and 'cannabinoid-like' receptors in small arteries', *Br J Pharmacol*, 159(4), pp. 787-96.
- Dann, C. E., Hsieh, J. C., Rattner, A., Sharma, D., Nathans, J. and Leahy, D. J. (2001) 'Insights into Wnt binding and signalling from the structures of two Frizzled cysteine-rich domains', *Nature*, 412(6842), pp. 86-90.
- Darzi, J., Frost, G. S. and Robertson, M. D. (2011) 'Do SCFA have a role in appetite regulation?', *Proc Nutr Soc.*, 70(1), pp. 119-28.
- DeLapp, N. W. (2004) 'The antibody-capture [(35)S]GTPgammaS scintillation proximity assay: a powerful emerging technique for analysis of GPCR pharmacology', *Trends Pharmacol Sci*, 25(8), pp. 400-1.
- den Besten, G., van Eunen, K., Groen, A. K., Venema, K., Reijngoud, D. J. and Bakker, B. M. (2013) 'The role of short-chain fatty acids in the interplay between diet, gut microbiota, and host energy metabolism', *J Lipid Res*, 54(9), pp. 2325-40.
- Devost, D., Sleno, R., Petrin, D., Zhang, A., Shinjo, Y., Okde, R., Aoki, J., Inoue, A. and Hebert, T. E. (2017) 'Conformational Profiling of the AT1 Angiotensin II Receptor Reflects Biased Agonism, G Protein Coupling, and Cellular Context', *J Biol Chem*, 292(13), pp. 5443-56.

- DeWire, S. M., Ahn, S., Lefkowitz, R. J. and Shenoy, S. K. (2007) 'Beta-arrestins and cell signaling', *Annu Rev Physiol*, 69, pp. 483-510.
- Dewulf, E. M., Ge, Q., Bindels, L. B., Sohet, F. M., Cani, P. D., Brichard, S. M. and Delzenne, N. M. (2013) 'Evaluation of the relationship between GPR43 and adiposity in human', *Nutr Metab (Lond)*, 10(1), pp. 11.
- DiMasi, J. A., Grabowski, H. G. and Hansen, R. W. (2016) 'Innovation in the pharmaceutical industry: New estimates of R&D costs', *J Health Econ*, 47, pp. 20-33.
- Dowling, M. R. and Charlton, S. J. (2006) 'Quantifying the association and dissociation rates of unlabelled antagonists at the muscarinic M3 receptor', *Br J Pharmacol*, 148(7), pp. 927-37.
- Dragic, T., Trkola, A., Thompson, D. A., Cormier, E. G., Kajumo, F. A., Maxwell, E., Lin, S. W., Ying, W., Smith, S. O., Sakmar, T. P. and Moore, J. P. (2000) 'A binding pocket for a small molecule inhibitor of HIV-1 entry within the transmembrane helices of CCR5', *Proc Natl Acad Sci U S A*, 97(10), pp. 5639-44.
- Dror, R. O., Arlow, D. H., Maragakis, P., Mildorf, T. J., Pan, A. C., Xu, H., Borhani, D. W. and Shaw, D. E. (2011) 'Activation mechanism of the beta2-adrenergic receptor', *Proc Natl Acad Sci U S A*, 108(46), pp. 18684-9.
- Dror, R. O., Mildorf, T. J., Hilger, D., Manglik, A., Borhani, D. W., Arlow, D. H., Philippsen, A., Villanueva, N., Yang, Z., Lerch, M. T., Hubbell, W. L., Kobilka, B. K., Sunahara, R. K. and Shaw, D. E. (2015) 'SIGNAL TRANSDUCTION. Structural basis for nucleotide exchange in heterotrimeric G proteins', *Science*, 348(6241), pp. 1361-5.
- Eder, J., Sedrani, R. and Wiesmann, C. (2014) 'The discovery of first-in-class drugs: origins and evolution', *Nat Rev Drug Discov*, 13(8), pp. 577-87.
- Ehlert, F. J. (2008) 'On the analysis of ligand-directed signaling at G protein-coupled receptors', *Naunyn Schmiedebergs Arch Pharmacol*, 377(4-6), pp. 549-77.
- Engelstoft, M. S., Park, W. M., Sakata, I., Kristensen, L. V., Husted, A. S., Osborne-Lawrence, S., Piper, P. K., Walker, A. K., Pedersen, M. H., Nohr, M. K., Pan, J., Sinz, C. J., Carrington, P. E., Akiyama, T. E., Jones, R. M., Tang, C., Ahmed, K., Offermanns, S., Egerod, K. L., Zigman, J. M. and Schwartz, T. W. (2013) 'Seven transmembrane G protein-coupled receptor repertoire of gastric ghrelin cells', *Mol Metab*, 2(4), pp. 376-92.
- Erlanson, D. A., Fesik, S. W., Hubbard, R. E., Jahnke, W. and Jhoti, H. (2016) 'Twenty years on: the impact of fragments on drug discovery', *Nat Rev Drug Discov*, 15(9), pp. 605-19.
- Evans, B. A., Broxton, N., Merlin, J., Sato, M., Hutchinson, D. S., Christopoulos, A. and Summers, R. J. (2011) 'Quantification of functional selectivity at the human alpha(1A)-adrenoceptor', *Mol Pharmacol*, 79(2), pp. 298-307.

- Ferreira, S. G., Goncalves, F. Q., Marques, J. M., Tome, A. R., Rodrigues, R. J., Nunes-Correia, I., Ledent, C., Harkany, T., Venance, L., Cunha, R. A. and Kofalvi, A. (2015) 'Presynaptic adenosine A2A receptors dampen cannabinoid CB1 receptor-mediated inhibition of corticostriatal glutamatergic transmission', *Br J Pharmacol*, 172(4), pp. 1074-86.
- Fleischer, J., Bumbalo, R., Bautze, V., Strotmann, J. and Breer, H. (2015) 'Expression of odorant receptor Olfr78 in enteroendocrine cells of the colon', *Cell Tissue Res*, 361(3), pp. 697-710.
- Foord, S. M., Bonner, T. I., Neubig, R. R., Rosser, E. M., Pin, J. P., Davenport, A. P., Spedding, M. and Harmar, A. J. (2005) 'International Union of Pharmacology. XLVI. G protein-coupled receptor list', *Pharmacol Rev*, 57(2), pp. 279-88.
- Forbes, S., Stafford, S., Coope, G., Heffron, H., Real, K., Newman, R., Davenport, R., Barnes, M., Grosse, J. and Cox, H. (2015) 'Selective FFA2 Agonism Appears to Act via Intestinal PYY to Reduce Transit and Food Intake but Does Not Improve Glucose Tolerance in Mouse Models', *Diabetes*, 64(11), pp. 3763-71.
- Fredriksson, R., Lagerstrom, M. C., Lundin, L. G. and Schiöth, H. B. (2003) 'The G-protein-coupled receptors in the human genome form five main families. Phylogenetic analysis, paralogon groups, and fingerprints', *Mol Pharmacol*, 63(6), pp. 1256-72.
- Fukumoto, S., Tatewaki, M., Yamada, T., Fujimiya, M., Mantyh, C., Voss, M., Eubanks, S., Harris, M., Pappas, T. N. and Takahashi, T. (2003) 'Short-chain fatty acids stimulate colonic transit via intraluminal 5-HT release in rats', *Am J Physiol Regul Integr Comp Physiol*, 284(5), pp. R1269-76.
- Gales, C., Rebois, R. V., Hogue, M., Trieu, P., Breit, A., Hebert, T. E. and Bouvier, M. (2005) 'Real-time monitoring of receptor and G-protein interactions in living cells', *Nat Methods*, 2(3), pp. 177-84.
- Ge, H., Li, X., Weiszmann, J., Wang, P., Baribault, H., Chen, J. L., Tian, H. and Li, Y. (2008) 'Activation of G protein-coupled receptor 43 in adipocytes leads to inhibition of lipolysis and suppression of plasma free fatty acids', *Endocrinology*, 149(9), pp. 4519-26.
- Gershengorn, M. C., Geras-Raaka, E., Varma, A. and Clark-Lewis, I. (1998) 'Chemokines activate Kaposi's sarcoma-associated herpesvirus G protein-coupled receptor in mammalian cells in culture', *J Clin Invest*, 102(8), pp. 1469-72.
- Gherbi, K., May, L. T., Baker, J. G., Briddon, S. J. and Hill, S. J. (2015) 'Negative cooperativity across beta1-adrenoceptor homodimers provides insights into the nature of the secondary low-affinity CGP 12177 beta1-adrenoceptor binding conformation', *FASEB J*, 29(7), pp. 2859-71.

- Gomez-Lechon, M. J., Castell, J. V. and Donato, M. T. (2010) 'The use of hepatocytes to investigate drug toxicity', *Methods Mol Biol*, 640, pp. 389-415.
- Goodman, O. B., Jr., Krupnick, J. G., Santini, F., Gurevich, V. V., Penn, R. B., Gagnon, A. W., Keen, J. H. and Benovic, J. L. (1996) 'Beta-arrestin acts as a clathrin adaptor in endocytosis of the beta2-adrenergic receptor', *Nature*, 383(6599), pp. 447-50.
- Goupil, E., Tassy, D., Bourguet, C., Quiniou, C., Wisehart, V., Petrin, D., Le Guill, C., Devost, D., Zingg, H. H., Bouvier, M., Saragovi, H. U., Chemtob, S., Lubell, W. D., Claing, A., Hebert, T. E. and Laporte, S. A. (2010) 'A novel biased allosteric compound inhibitor of parturition selectively impedes the prostaglandin F2alpha-mediated Rho/ROCK signaling pathway', *J Biol Chem*, 285(33), pp. 25624-36.
- Gouy, M., Guindon, S. and Gascuel, O. (2010) 'SeaView version 4: A multiplatform graphical user interface for sequence alignment and phylogenetic tree building', *Mol Biol Evol*, 27(2), pp. 221-4.
- Graff, E. C., Fang, H., Wanders, D. and Judd, R. L. (2016) 'Anti-inflammatory effects of the hydroxycarboxylic acid receptor 2', *Metabolism*, 65(2), pp. 102-13.
- Gregory, K. J., Hall, N. E., Tobin, A. B., Sexton, P. M. and Christopoulos, A. (2010) 'Identification of orthosteric and allosteric site mutations in M2 muscarinic acetylcholine receptors that contribute to ligand-selective signaling bias', *J Biol Chem*, 285(10), pp. 7459-74.
- Gregory, K. J., Sexton, P. M. and Christopoulos, A. (2007) 'Allosteric modulation of muscarinic acetylcholine receptors', *Curr Neuropharmacol*, 5(3), pp. 157-67.
- Griffin, C. A., Kafadar, K. A. and Pavlath, G. K. (2009) 'MOR23 promotes muscle regeneration and regulates cell adhesion and migration', *Dev Cell*, 17(5), pp. 649-61.
- Grundmann, M., Tikhonova, I. G., Hudson, B. D., Smith, N. J., Mohr, K., Ulven, T., Milligan, G., Kenakin, T. and Kostenis, E. (2016) 'A Molecular Mechanism for Sequential Activation of a G Protein-Coupled Receptor', *Cell Chem Biol*, 23(3), pp. 392-403.
- Guo, D., Heitman, L. H. and AP, I. J. (2017) 'Kinetic Aspects of the Interaction between Ligand and G Protein-Coupled Receptor: The Case of the Adenosine Receptors', *Chem Rev*, 117(1), pp. 38-66.
- Guo, D., Hillger, J. M., AP, I. J. and Heitman, L. H. (2014) 'Drug-target residence time--a case for G protein-coupled receptors', *Med Res Rev*, 34(4), pp. 856-92.
- Guo, D., Mulder-Krieger, T., AP, I. J. and Heitman, L. H. (2012) 'Functional efficacy of adenosine A(2)A receptor agonists is positively correlated to their receptor residence time', *Br J Pharmacol*, 166(6), pp. 1846-59.

- Hall, M. P., Unch, J., Binkowski, B. F., Valley, M. P., Butler, B. L., Wood, M. G., Otto, P., Zimmerman, K., Vidugiris, G., Machleidt, T., Robers, M. B., Benink, H. A., Eggers, C. T., Slater, M. R., Meisenheimer, P. L., Klaubert, D. H., Fan, F., Encell, L. P. and Wood, K. V. (2012) 'Engineered luciferase reporter from a deep sea shrimp utilizing a novel imidazopyrazinone substrate', *ACS Chem Biol*, 7(11), pp. 1848-57.
- Han, J. H., Kim, I. S., Jung, S. H., Lee, S. G., Son, H. Y. and Myung, C. S. (2014) 'The effects of propionate and valerate on insulin responsiveness for glucose uptake in 3T3-L1 adipocytes and C2C12 myotubes via G protein-coupled receptor 41', *PLoS One*, 9(4), pp. E95268.
- Hewavitharana, T. and Wedegaertner, P. B. (2012) 'Non-canonical signaling and localizations of heterotrimeric G proteins', *Cell Signal*, 24(1), pp. 25-34.
- Hirasawa, A., Tsumaya, K., Awaji, T., Katsuma, S., Adachi, T., Yamada, M., Sugimoto, Y., Miyazaki, S. and Tsujimoto, G. (2005) 'Free fatty acids regulate gut incretin glucagon-like peptide-1 secretion through GPR120', *Nat Med*, 11(1), pp. 90-4.
- Hoffmann, C., Castro, M., Rinken, A., Leurs, R., Hill, S. J. and Vischer, H. F. (2015) 'Ligand Residence Time at G-protein-Coupled Receptors-Why We Should Take Our Time To Study It', *Mol Pharmacol*, 88(3), pp. 552-60.
- Hong, Y. H., Nishimura, Y., Hishikawa, D., Tsuzuki, H., Miyahara, H., Gotoh, C., Choi, K. C., Feng, D. D., Chen, C., Lee, H. G., Katoh, K., Roh, S. G. and Sasaki, S. (2005) 'Acetate and propionate short chain fatty acids stimulate adipogenesis via GPCR43', *Endocrinology*, 146(12), pp. 5092-9.
- Hothersall, J. D., Brown, A. J., Dale, I. and Rawlins, P. (2016) 'Can residence time offer a useful strategy to target agonist drugs for sustained GPCR responses?', *Drug Discov Today*, 21(1), pp. 90-96.
- Hoveyda, H., Brantis, C. E., Dutheil, G., Zoute, L., Schils, D. and Bernard, J. (2010) 'Compounds, pharmaceutical composition and methods for use in treating metabolic disorders', *International Patent*, Application WO 2010/066682.
- Hoveyda, H., Brantis, C. E., Dutheil, G., Zoute, L., Schils, D. and Fraser, G. (2011) 'Compounds, pharmaceutical composition and methods for use in treating gastrointestinal disorders', *International Patent*, Application WO 2011/076732 A1.
- Huang, W., Manglik, A., Venkatakrishnan, A. J., Laeremans, T., Feinberg, E. N., Sanborn, A. L., Kato, H. E., Livingston, K. E., Thorsen, T. S., Kling, R. C., Granier, S., Gmeiner, P., Husbands, S. M., Traynor, J. R., Weis, W. I., Steyaert, J., Dror, R. O. and Kobilka, B. K. (2015) 'Structural insights into micro-opioid receptor activation', *Nature*, 524(7565), pp. 315-21.
- Hubbard, T. A., Brown, A. J., Bell, I. A. and Cockroft, S. L. (2016) 'The Limit of Intramolecular H-Bonding', *J Am Chem Soc*, 138(46), pp. 15114-7.

- Hudson, B. D., Christiansen, E., Murdoch, H., Jenkins, L., Hansen, A. H., Madsen, O., Ulven, T. and Milligan, G. (2014) 'Complex pharmacology of novel allosteric free fatty acid 3 receptor ligands', *Mol Pharmacol*, 86(2), pp. 200-10.
- Hudson, B. D., Christiansen, E., Tikhonova, I. G., Grundmann, M., Kostenis, E., Adams, D. R., Ulven, T. and Milligan, G. (2012a) 'Chemically engineering ligand selectivity at the free fatty acid receptor 2 based on pharmacological variation between species orthologs', *FASEB J*, 26(12), pp. 4951-65.
- Hudson, B. D., Due-Hansen, M. E., Christiansen, E., Hansen, A. M., Mackenzie, A. E., Murdoch, H., Pandey, S. K., Ward, R. J., Marquez, R., Tikhonova, I. G., Ulven, T. and Milligan, G. (2013a) 'Defining the molecular basis for the first potent and selective orthosteric agonists of the FFA2 free fatty acid receptor', *J Biol Chem*, 288(24), pp. 17296-312.
- Hudson, B. D., Murdoch, H. and Milligan, G. (2013b) 'Minireview: The effects of species ortholog and SNP variation on receptors for free fatty acids', *Mol Endocrinol*, 27(8), pp. 1177-87.
- Hudson, B. D., Smith, N. J. and Milligan, G. (2011) 'Experimental challenges to targeting poorly characterized GPCRs: uncovering the therapeutic potential for free fatty acid receptors', *Adv Pharmacol*, 62, pp.175-218.
- Hudson, B. D., Tikhonova, I. G., Pandey, S. K., Ulven, T. and Milligan, G. (2012b) 'Extracellular ionic locks determine variation in constitutive activity and ligand potency between species orthologs of the free fatty acid receptors FFA2 and FFA3', *J Biol Chem*, 287(49), pp. 41195-209.
- Hughes, J. P., Rees, S., Kalindjian, S. B. and Philpott, K. L. (2011) 'Principles of early drug discovery', *Br J Pharmacol*, 162(6), pp. 1239-49.
- Hulme, E. C. and Birdsall, N. J. (1992) *Receptor-Ligand Interactions: A Practical Approach*. Oxford University Press, Oxford, UK: IRL Press, p. 63-176.
- Hulme, E. C. and Trevethick, M. A. (2010) 'Ligand binding assays at equilibrium: validation and interpretation', *Br J Pharmacol*, 161(6), pp. 1219-37.
- Husted, A. S., Trauelsen, M., Rudenko, O., Hjorth, S. A. and Schwartz, T. W. (2017) 'GPCR-Mediated Signaling of Metabolites', *Cell Metab*, 25(4), pp. 777-96.
- Inoue, A., Ishiguro, J., Kitamura, H., Arima, N., Okutani, M., Shuto, A., Higashiyama, S., Ohwada, T., Arai, H., Makide, K. and Aoki, J. (2012) 'TGF α shedding assay: an accurate and versatile method for detecting GPCR activation', *Nat Methods*, 9(10), pp. 1021-9.
- Isberg, V., Mordalski, S., Munk, C., Rataj, K., Harpsoe, K., Hauser, A. S., Vroling, B., Bojarski, A. J., Vriend, G. and Gloriam, D. E. (2016) 'GPCRdb: an information system for G protein-coupled receptors', *Nucleic Acids Res*, 44(D1), pp. D356-64.

- Ishihara, H., Asano, T., Tsukuda, K., Katagiri, H., Inukai, K., Anai, M., Kikuchi, M., Yazaki, Y., Miyazaki, J. I. and Oka, Y. (1993) 'Pancreatic beta cell line MIN6 exhibits characteristics of glucose metabolism and glucose-stimulated insulin secretion similar to those of normal islets', *Diabetologia*, 36(11), pp. 1139-45.
- Itoh, Y., Kawamata, Y., Harada, M., Kobayashi, M., Fujii, R., Fukusumi, S., Ogi, K., Hosoya, M., Tanaka, Y., Uejima, H., Tanaka, H., Maruyama, M., Satoh, R., Okubo, S., Kizawa, H., Komatsu, H., Matsumura, F., Noguchi, Y., Shinohara, T., Hinuma, S., Fujisawa, Y. and Fujino, M. (2003) 'Free fatty acids regulate insulin secretion from pancreatic beta cells through GPR40', *Nature*, 422(6928), pp. 173-6.
- Janzen, W. P. (2014) 'Screening technologies for small molecule discovery: the state of the art', *Chem Biol*, 21(9), pp. 1162-70.
- Jazayeri, A., Dore, A. S., Lamb, D., Krishnamurthy, H., Southall, S. M., Baig, A. H., Bortolato, A., Koglin, M., Robertson, N. J., Errey, J. C., Andrews, S. P., Teobald, I., Brown, A. J., Cooke, R. M., Weir, M. and Marshall, F. H. (2016) 'Extra-helical binding site of a glucagon receptor antagonist', *Nature*, 533(7602), pp. 274-7.
- Jenkins, L., Alvarez-Curto, E., Campbell, K., de Munnik, S., Canals, M., Schlyer, S. and Milligan, G. (2011) 'Agonist activation of the G protein-coupled receptor GPR35 involves transmembrane domain III and is transduced via Galpha(1)(3) and beta-arrestin-2', *Br J Pharmacol*, 162(3), pp. 733-48.
- Jia, W., Li, H., Zhao, L. and Nicholson, J. K. (2008) 'Gut microbiota: a potential new territory for drug targeting', *Nat Rev Drug Discov*, 7(2), pp. 123-9.
- Jun, L. S., Showalter, A. D., Ali, N., Dai, F., Ma, W., Coskun, T., Ficorilli, J. V., Wheeler, M. B., Michael, M. D. and Sloop, K. W. (2014) 'A novel humanized GLP-1 receptor model enables both affinity purification and Cre-LoxP deletion of the receptor', *PLoS One*, 9(4), pp. e93746.
- Kang, Y., Zhou, X. E., Gao, X., He, Y., Liu, W., Ishchenko, A., Barty, A., White, T. A., Yefanov, O., Han, G. W., Xu, Q., de Waal, P. W., Ke, J., Tan, M. H., Zhang, C., Moeller, A., West, G. M., Pascal, B. D., Van Eps, N., Caro, L. N., Vishnivetskiy, S. A., Lee, R. J., Suino-Powell, K. M., Gu, X., Pal, K., Ma, J., Zhi, X., Boutet, S., Williams, G. J., Messerschmidt, M., Gati, C., Zatsopin, N. A., Wang, D., James, D., Basu, S., Roy-Chowdhury, S., Conrad, C. E., Coe, J., Liu, H., Lisova, S., Kupitz, C., Grotjohann, I., Fromme, R., Jiang, Y., Tan, M., Yang, H., Li, J., Wang, M., Zheng, Z., Li, D., Howe, N., Zhao, Y., Standfuss, J., Diederichs, K., Dong, Y., Potter, C. S., Carragher, B., Caffrey, M., Jiang, H., Chapman, H. N., Spence, J. C., Fromme, P., Weierstall, U., Ernst, O. P., Katritch, V., Gurevich, V. V., Griffin, P. R., Hubbell, W. L., Stevens, R. C., Cherezov, V., Melcher, K. and Xu, H. E. (2015) 'Crystal structure of rhodopsin bound to arrestin by femtosecond X-ray laser', *Nature*, 523(7562), pp. 561-7.

- Karaki, S., Mitsui, R., Hayashi, H., Kato, I., Sugiya, H., Iwanaga, T., Furness, J. B. and Kuwahara, A. (2006) 'Short-chain fatty acid receptor, GPR43, is expressed by enteroendocrine cells and mucosal mast cells in rat intestine', *Cell Tissue Res.*, 324(3), pp. 353-60.
- Kenakin, T. (2001) 'Inverse, protean, and ligand-selective agonism: matters of receptor conformation', *FASEB J*, 15(3), pp. 598-611.
- Kenakin, T. (2002) 'Efficacy at G-protein-coupled receptors', *Nat Rev Drug Discov*, 1(2), pp. 103-10.
- Kenakin, T. and Christopoulos, A. (2013) 'Signalling bias in new drug discovery: detection, quantification and therapeutic impact', *Nat Rev Drug Discov*, 12(3), pp. 205-16.
- Kenakin, T. and Miller, L. J. (2010) 'Seven transmembrane receptors as shapeshifting proteins: the impact of allosteric modulation and functional selectivity on new drug discovery', *Pharmacol Rev*, 62(2), pp. 265-304.
- Kenakin, T., Watson, C., Muniz-Medina, V., Christopoulos, A. and Novick, S. (2012) 'A simple method for quantifying functional selectivity and agonist bias', *ACS Chem Neurosci*, 3(3), pp. 193-203.
- Kim, M. H., Kang, S. G., Park, J. H., Yanagisawa, M. and Kim, C. H. (2013) 'Short-chain fatty acids activate GPR41 and GPR43 on intestinal epithelial cells to promote inflammatory responses in mice', *Gastroenterology*, 145(2), pp. 396-406.
- Kimura, I., Inoue, D., Maeda, T., Hara, T., Ichimura, A., Miyauchi, S., Kobayashi, M., Hirasawa, A. and Tsujimoto, G. (2011) 'Short-chain fatty acids and ketones directly regulate sympathetic nervous system via G protein-coupled receptor 41 (GPR41)', *Proc Natl Acad Sci U S A*, 108(19), pp. 8030-5.
- Kimura, I., Ozawa, K., Inoue, D., Imamura, T., Kimura, K., Maeda, T., Terasawa, K., Kashihara, D., Hirano, K., Tani, T., Takahashi, T., Miyauchi, S., Shioi, G., Inoue, H. and Tsujimoto, G. (2013) 'The gut microbiota suppresses insulin-mediated fat accumulation via the short-chain fatty acid receptor GPR43', *Nat Commun*, 4, pp. 1829.
- Klein Herenbrink, C., Sykes, D. A., Donthamsetti, P., Canals, M., Coudrat, T., Shonberg, J., Scammells, P. J., Capuano, B., Sexton, P. M., Charlton, S. J., Javitch, J. A., Christopoulos, A. and Lane, J. R. (2016) 'The role of kinetic context in apparent biased agonism at GPCRs', *Nat Commun*, 7, pp. 10842.
- Kocan, M., Dalrymple, M. B., Seeber, R. M., Feldman, B. J. and Pflieger, K. D. (2010) 'Enhanced BRET Technology for the Monitoring of Agonist-Induced and Agonist-Independent Interactions between GPCRs and beta-Arrestins', *Front Endocrinol (Lausanne)*, 1, pp. 12.
- Kolakowski, L. F., Jr. (1994) 'GCRDb: a G-protein-coupled receptor database', *Receptors Channels*, 2(1), pp. 1-7.

- Koole, C., Wootten, D., Simms, J., Valant, C., Sridhar, R., Woodman, O. L., Miller, L. J., Summers, R. J., Christopoulos, A. and Sexton, P. M. (2010) 'Allosteric ligands of the glucagon-like peptide 1 receptor (GLP-1R) differentially modulate endogenous and exogenous peptide responses in a pathway-selective manner: implications for drug screening', *Mol Pharmacol*, 78(3), pp. 456-65.
- Kotarsky, K., Nilsson, N. E., Olde, B. and Owman, C. (2003) 'Progress in methodology. Improved reporter gene assays used to identify ligands acting on orphan seven-transmembrane receptors', *Pharmacol Toxicol*, 93(6), pp. 249-58.
- Kotz, J. 'Translational Notes: Phenotypic screening, take two'. *Keystone Symposium: Addressing the Challenges of Drug Discovery*, Lake Tahoe: Science-Business eXchange, 2012.
- Kruse, A. C., Ring, A. M., Manglik, A., Hu, J., Hu, K., Eitel, K., Hubner, H., Pardon, E., Valant, C., Sexton, P. M., Christopoulos, A., Felder, C. C., Gmeiner, P., Steyaert, J., Weis, W. I., Garcia, K. C., Wess, J. and Kobilka, B. K. (2013) 'Activation and allosteric modulation of a muscarinic acetylcholine receptor', *Nature*, 504(7478), pp. 101-6.
- Kufareva, I., Rueda, M., Katritch, V., Stevens, R. C. and Abagyan, R. (2011) 'Status of GPCR modeling and docking as reflected by community-wide GPCR Dock 2010 assessment', *Structure*, 19(8), pp. 1108-26.
- Kumar, V., Moritz, A. E., Keck, T. M., Bonifazi, A., Ellenberger, M. P., Sibley, C. D., Free, R. B., Shi, L., Lane, J. R., Sibley, D. R. and Newman, A. H. (2017) 'Synthesis and Pharmacological Characterization of Novel trans-Cyclopropylmethyl-Linked Bivalent Ligands That Exhibit Selectivity and Allosteric Pharmacology at the Dopamine D3 Receptor (D3R)', *J Med Chem*, 60(4), pp. 1478-94.
- Kunishima, N., Shimada, Y., Tsuji, Y., Sato, T., Yamamoto, M., Kumasaka, T., Nakanishi, S., Jingami, H. and Morikawa, K. (2000) 'Structural basis of glutamate recognition by a dimeric metabotropic glutamate receptor', *Nature*, 407(6807), pp. 971-7.
- Lagerstrom, M. C. and Schioth, H. B. (2008) 'Structural diversity of G protein-coupled receptors and significance for drug discovery', *Nat Rev Drug Discov*, 7(4), pp. 339-57.
- Lambright, D. G., Sondek, J., Bohm, A., Skiba, N. P., Hamm, H. E. and Sigler, P. B. (1996) 'The 2.0 Å crystal structure of a heterotrimeric G protein', *Nature*, 379(6563), pp. 311-9.
- Lane, J. R., Donthamsetti, P., Shonberg, J., Draper-Joyce, C. J., Dentry, S., Michino, M., Shi, L., Lopez, L., Scammells, P. J., Capuano, B., Sexton, P. M., Javitch, J. A. and Christopoulos, A. (2014) 'A new mechanism of allostery in a G protein-coupled receptor dimer', *Nat Chem Biol*, 10(9), pp. 745-52.

- Lane, J. R., Powney, B., Wise, A., Rees, S. and Milligan, G. (2008) 'G protein coupling and ligand selectivity of the D2L and D3 dopamine receptors', *J Pharmacol Exp Ther*, 325(1), pp. 319-30.
- Langlois, X., Megens, A., Lavreysen, H., Atack, J., Cik, M., te Riele, P., Peeters, L., Wouters, R., Vermeire, J., Hendrickx, H., Macdonald, G. and De Bruyn, M. (2012) 'Pharmacology of JNJ-37822681, a specific and fast-dissociating D2 antagonist for the treatment of schizophrenia', *J Pharmacol Exp Ther*, 342(1), pp. 91-105.
- Latorraca, N. R., Venkatakrishnan, A. J. and Dror, R. O. (2017) 'GPCR Dynamics: Structures in Motion', *Chem Rev*, 117(1), pp. 139-55.
- Lazareno, S. and Birdsall, N. J. (1993) 'Estimation of competitive antagonist affinity from functional inhibition curves using the Gaddum, Schild and Cheng-Prusoff equations', *Br J Pharmacol*, 109(4), pp. 1110-9.
- Le Poul, E., Loison, C., Struyf, S., Springael, J. Y., Lannoy, V., Decobecq, M. E., Brezillon, S., Dupriez, V., Vassart, G., Van Damme, J., Parmentier, M. and Detheux, M. (2003) 'Functional characterization of human receptors for short chain fatty acids and their role in polymorphonuclear cell activation', *J Biol Chem*, 278(28), pp. 25481-9.
- Lebon, G., Warne, T. and Tate, C. G. (2012) 'Agonist-bound structures of G protein-coupled receptors', *Curr Opin Struct Biol*, 22(4), pp. 482-90.
- Lee, T., Schwandner, R., Swaminath, G., Weiszmann, J., Cardozo, M., Greenberg, J., Jaeckel, P., Ge, H., Wang, Y., Jiao, X., Liu, J., Kayser, F., Tian, H. and Li, Y. (2008) 'Identification and functional characterization of allosteric agonists for the G protein-coupled receptor FFA2', *Mol Pharmacol*, 74(6), pp. 1599-609.
- Lee, H. M., Giguere P. M. and Roth B. L. (2014) 'DREADDs: novel tools for drug discovery and development', *Drug Discov Today*, 19(4), pp. 469-7374.
- Lefkowitz, R. J. and Shenoy, S. K. (2005) 'Transduction of receptor signals by beta-arrestins', *Science*, 308(5721), pp. 512-7.
- Leonard, J. N., Chu, Z. L., Bruce, M. A. and Boatman, P. D. (2016) 'GPR41 and modulators thereof for the treatment of insulin-related disorders' *International Patent*, Application WO 2006/052566.
- Leopoldo, M., Lacivita, E., Berardi, F. and Perrone, R. (2009) 'Developments in fluorescent probes for receptor research', *Drug Discov Today*, 14(13-14), pp. 706-12.
- Leppik, R. A., Lazareno, S., Mynett, A. and Birdsall, N. J. (1998) 'Characterization of the allosteric interactions between antagonists and amiloride analogues at the human alpha2A-adrenergic receptor', *Mol Pharmacol*, 53(5), pp. 916-25.

- Leroy, D., Missotten, M., Waltzinger, C., Martin, T. and Scheer, A. (2007) 'G protein-coupled receptor-mediated ERK1/2 phosphorylation: towards a generic sensor of GPCR activation', *J Recept Signal Transduct Res*, 27(1), pp. 83-97.
- Lew, M. J. (2012) 'Bad statistical practice in pharmacology (and other basic biomedical disciplines): you probably don't know P.', *Br J Pharmacol*, 166(5), pp. 1559-67.
- Liang, Y. L., Khoshouei, M., Radjainia, M., Zhang, Y., Glukhova, A., Tarrasch, J., Thal, D. M., Furness, S. G. B., Christopoulos, G., Coudrat, T., Danev, R., Baumeister, W., Miller, L. J., Christopoulos, A., Kobilka, B. K., Wootten, D., Skiniotis, G. and Sexton, P. M. (2017) 'Phase-plate cryo-EM structure of a class B GPCR-G-protein complex', *Nature*, 546(7656), pp. 118-23.
- Lin, S. and Struve, W. S. (1991) 'Time-resolved fluorescence of nitrobenzoxadiazole-aminohexanoic acid: effect of intermolecular hydrogen-bonding on non-radiative decay', *Photochem Photobiol*, 54(3), pp. 361-5.
- Lipinski, C. A., Lombardo, F., Dominy, B. W. and Feeney, P. J. (2001) 'Experimental and computational approaches to estimate solubility and permeability in drug discovery and development settings', *Adv Drug Deliv Rev*, 46(1-3), pp. 3-26.
- Lohse, M. J., Benovic, J. L., Codina, J., Caron, M. G. and Lefkowitz, R. J. (1990) 'beta-Arrestin: a protein that regulates beta-adrenergic receptor function', *Science*, 248(4962), pp. 1547-50.
- Lohse, M. J. and Hoffmann, C. (2014) 'Arrestin interactions with G protein-coupled receptors', *Handb Exp Pharmacol*, 219, pp. 15-56.
- Lu, J., Byrne, N., Wang, J., Bricogne, G., Brown, F. K., Chobanian, H. R., Colletti, S. L., Di Salvo, J., Thomas-Fowlkes, B., Guo, Y., Hall, D. L., Hadix, J., Hastings, N. B., Hermes, J. D., Ho, T., Howard, A. D., Josien, H., Kornienko, M., Lumb, K. J., Miller, M. W., Patel, S. B., Pio, B., Plummer, C. W., Sherborne, B. S., Sheth, P., Souza, S., Tummala, S., Vornrhein, C., Webb, M., Allen, S. J., Johnston, J. M., Weinglass, A. B., Sharma, S. and Soisson, S. M. (2017) 'Structural basis for the cooperative allosteric activation of the free fatty acid receptor GPR40', *Nat Struct Mol Biol*, 24(7), pp. 570-7.
- Ma, Z., Du, L. and Li, M. (2014) 'Toward fluorescent probes for G-protein-coupled receptors (GPCRs)', *J Med Chem*, 57(20), pp. 8187-203.
- Magnani, F., Serrano-Vega, M. J., Shibata, Y., Abdul-Hussein, S., Lebon, G., Miller-Gallacher, J., Singhal, A., Strega, A., Thomas, J. A. and Tate, C. G. (2016) 'A mutagenesis and screening strategy to generate optimally thermostabilized membrane proteins for structural studies', *Nat Protoc*, 11(8), pp. 1554-71.

- Manglik, A., Kim, T. H., Masureel, M., Altenbach, C., Yang, Z., Hilger, D., Lerch, M. T., Kobilka, T. S., Thian, F. S., Hubbell, W. L., Prosser, R. S. and Kobilka, B. K. (2015) 'Structural Insights into the Dynamic Process of beta2-Adrenergic Receptor Signaling', *Cell*, 161(5), pp. 1101-11.
- Mangmool, S. and Kurose, H. (2011) 'G(i/o) protein-dependent and -independent actions of Pertussis Toxin (PTX)', *Toxins (Basel)*, 3(7), pp. 884-99.
- Mann, D., Teuber, C., Tennigkeit, S. A., Schroter, G., Gerwert, K. and Kotting, C. (2016) 'Mechanism of the intrinsic arginine finger in heterotrimeric G proteins', *Proc Natl Acad Sci U S A*, 113(50), pp. E8041-50.
- Maslowski, K. M., Vieira, A. T., Ng, A., Kranich, J., Sierro, F., Yu, D., Schilter, H. C., Rolph, M. S., Mackay, F., Artis, D., Xavier, R. J., Teixeira, M. M. and Mackay, C. R. (2009) 'Regulation of inflammatory responses by gut microbiota and chemoattractant receptor GPR43', *Nature*, 461(7268), pp. 1282-6.
- Masui, R., Sasaki, M., Funaki, Y., Ogasawara, N., Mizuno, M., Iida, A., Izawa, S., Kondo, Y., Ito, Y., Tamura, Y., Yanamoto, K., Noda, H., Tanabe, A., Okaniwa, N., Yamaguchi, Y., Iwamoto, T. and Kasugai, K. (2013) 'G protein-coupled receptor 43 moderates gut inflammation through cytokine regulation from mononuclear cells', *Inflamm Bowel Dis*, 19(13), pp. 2848-56.
- May, L. T., Bridge, L. J., Stoddart, L. A., Briddon, S. J. and Hill, S. J. (2011) 'Allosteric interactions across native adenosine-A3 receptor homodimers: quantification using single-cell ligand-binding kinetics', *FASEB J*, 25(10), pp. 3465-76.
- May, L. T., Self, T. J., Briddon, S. J. and Hill, S. J. (2010) 'The effect of allosteric modulators on the kinetics of agonist-G protein-coupled receptor interactions in single living cells', *Mol Pharmacol*, 78(3), pp. 511-23.
- McHugh, M. L. (2011) 'Multiple comparison analysis testing in ANOVA', *Biochem Med*, 21(3), pp. 203-9.
- Milligan, G. (2003) 'Principles: extending the utility of [35S]GTP gamma S binding assays', *Trends Pharmacol Sci*, 24(2), pp. 87-90.
- Milligan, G. and Kostenis, E. (2006) 'Heterotrimeric G-proteins: a short history', *Br J Pharmacol*, 147, pp. S46-55.
- Milligan, G., Shimpukade, B., Ulven, T. and Hudson, B. D. (2017) 'Complex Pharmacology of Free Fatty Acid Receptors', *Chem Rev*, 117(1), pp. 67-110.
- Nakajima, A., Nakatani, A., Hasegawa, S., Irie, J., Ozawa, K., Tsujimoto, G., Suganami, T., Itoh, H. and Kimura, I. (2017) 'The short chain fatty acid receptor GPR43 regulates inflammatory signals in adipose tissue M2-type macrophages', *PLoS One*, 12(7), pp. E0179696.

- Nguyen, T. L., Vieira-Silva, S., Liston, A. and Raes, J. (2015) 'How informative is the mouse for human gut microbiota research?', *Dis Model Mech*, 8(1), pp. 1-16.
- Nilsson, N. E., Kotarsky, K., Owman, C. and Olde, B. (2003) 'Identification of a free fatty acid receptor, FFA2R, expressed on leukocytes and activated by short-chain fatty acids', *Biochem Biophys Res Commun.*, 303(4), pp. 1047-52.
- Nobles, K. N., Xiao, K., Ahn, S., Shukla, A. K., Lam, C. M., Rajagopal, S., Strachan, R. T., Huang, T. Y., Bressler, E. A., Hara, M. R., Shenoy, S. K., Gygi, S. P. and Lefkowitz, R. J. (2011) 'Distinct phosphorylation sites on the beta(2)-adrenergic receptor establish a barcode that encodes differential functions of beta-arrestin', *Sci Signal*, 4(185), pp. ra51.
- Nohr, M. K., Egerod, K. L., Christiansen, S. H., Gille, A., Offermanns, S., Schwartz, T. W. and Moller, M. (2015) 'Expression of the short chain fatty acid receptor GPR41/FFAR3 in autonomic and somatic sensory ganglia', *Neuroscience*, 290, pp. 126-37.
- Nohr, M. K., Pedersen, M. H., Gille, A., Egerod, K. L., Engelstoft, M. S., Husted, A. S., Sichlau, R. M., Grunddal, K. V., Poulsen, S. S., Han, S., Jones, R. M., Offermanns, S. and Schwartz, T. W. (2013) 'GPR41/FFAR3 and GPR43/FFAR2 as cosensors for short-chain fatty acids in enteroendocrine cells vs FFAR3 in enteric neurons and FFAR2 in enteric leukocytes', *Endocrinology*, 154(10), pp. 3552-64.
- Norskov-Lauritsen, L., Thomsen, A. R. and Brauner-Osborne, H. (2014) 'G protein-coupled receptor signaling analysis using homogenous time-resolved Forster resonance energy transfer (HTRF®) technology', *Int J Mol Sci*, 15(2), pp. 2554-72.
- O'Hayre, M., Inoue, A., Kufareva, I., Wang, Z., Mikelis, C. M., Drummond, R. A., Avino, S., Finkel, K., Kalim, K. W., DiPasquale, G., Guo, F., Aoki, J., Zheng, Y., Lionakis, M. S., Molinolo, A. A. and Gutkind, J. S. (2016) 'Inactivating mutations in GNA13 and RHOA in Burkitt's lymphoma and diffuse large B-cell lymphoma: a tumor suppressor function for the Galpha13/RhoA axis in B cells', *Oncogene*, 35(29), pp. 3771-80.
- Oakley, R. H., Hudson, C. C., Sjaastad, M. D. and Loomis, C. R. (2006) 'The ligand-independent translocation assay: an enabling technology for screening orphan G protein-coupled receptors by arrestin recruitment', *Methods Enzymol*, 414, pp. 50-63.
- Offermanns, S., Colletti, S. L., Lovenberg, T. W., Semple, G., Wise, A. and AP, I. J. (2011) 'International Union of Basic and Clinical Pharmacology. LXXXII: Nomenclature and Classification of Hydroxy-carboxylic Acid Receptors (GPR81, GPR109A, and GPR109B)', *Pharmacol Rev*, 63(2), pp. 269-90.

- Oh, D. Y., Talukdar, S., Bae, E. J., Imamura, T., Morinaga, H., Fan, W., Li, P., Lu, W. J., Watkins, S. M. and Olefsky, J. M. (2010) 'GPR120 is an omega-3 fatty acid receptor mediating potent anti-inflammatory and insulin-sensitizing effects', *Cell*, 142(5), pp. 687-98.
- Olsson, M. H., Sondergaard, C. R., Rostkowski, M. and Jensen, J. H. (2011) 'PROPKA3: Consistent Treatment of Internal and Surface Residues in Empirical pKa Predictions', *J Chem Theory Comput*, 7(2), pp. 525-37.
- Oswald, C., Rappas, M., Kean, J., Dore, A. S., Errey, J. C., Bennett, K., Deflorian, F., Christopher, J. A., Jazayeri, A., Mason, J. S., Congreve, M., Cooke, R. M. and Marshall, F. H. (2016) 'Intracellular allosteric antagonism of the CCR9 receptor', *Nature*, 540(7633), pp. 462-5.
- Pardon, E., Laeremans, T., Triest, S., Rasmussen, S. G., Wohlkonig, A., Ruf, A., Muyltermans, S., Hol, W. G., Kobilka, B. K. and Steyaert, J. (2014) 'A general protocol for the generation of Nanobodies for structural biology', *Nat Protoc*, 9(3), pp. 674-93.
- Park, B. O., Kim, S. H., Kong, G. Y., Kim, D. H., Kwon, M. S., Lee, S. U., Kim, M. O., Cho, S., Lee, S., Lee, H. J., Han, S. B., Kwak, Y. S., Lee, S. B. and Kim, S. (2016) 'Selective novel inverse agonists for human GPR43 augment GLP-1 secretion', *Eur J Pharmacol*, 771, pp. 1-9.
- Park, S. H., Das, B. B., Casagrande, F., Tian, Y., Nothnagel, H. J., Chu, M., Kiefer, H., Maier, K., De Angelis, A. A., Marassi, F. M. and Opella, S. J. (2012) 'Structure of the chemokine receptor CXCR1 in phospholipid bilayers', *Nature*, 491(7426), pp. 779-83.
- Petrov, R. R., Ferrini, M. E., Jaffar, Z., Thompson, C. M., Roberts, K. and Diaz, P. (2011) 'Design and evaluation of a novel fluorescent CB2 ligand as probe for receptor visualization in immune cells', *Bioorg Med Chem Lett*, 21(19), pp. 5859-62.
- Pizzonero, M., Dupont, S., Babel, M., Beaumont, S., Bienvenu, N., Blaque, R., Cherel, L., Christophe, T., Crescenzi, B., De Lemos, E., Delerive, P., Deprez, P., De Vos, S., Djata, F., Fletcher, S., Kopiejewski, S., L'Ebraly, C., Lefrancois, J. M., Lavazais, S., Manioc, M., Nelles, L., Oste, L., Polancec, D., Quenehen, V., Soulas, F., Triballeau, N., van der Aar, E. M., Vandeghinste, N., Wakselman, E., Brys, R. and Saniere, L. (2014) 'Discovery and optimization of an azetidone chemical series as a free fatty acid receptor 2 (FFA2) antagonist: from hit to clinic', *J Med Chem*, 57(23), pp. 10044-57.
- Pluznick, J. L., Protzko, R. J., Gevorgyan, H., Peterlin, Z., Sipos, A., Han, J., Brunet, I., Wan, L. X., Rey, F., Wang, T., Firestein, S. J., Yanagisawa, M., Gordon, J. I., Eichmann, A., Peti-Peterdi, J. and Caplan, M. J. (2013) 'Olfactory receptor responding to gut microbiota-derived signals plays a role in renin secretion and blood pressure regulation', *Proc Natl Acad Sci U S A*, 110(11), pp. 4410-5.

- Pluznick, J. L., Zou, D. J., Zhang, X., Yan, Q., Rodriguez-Gil, D. J., Eisner, C., Wells, E., Greer, C. A., Wang, T., Firestein, S., Schnermann, J. and Caplan, M. J. (2009) 'Functional expression of the olfactory signaling system in the kidney', *Proc Natl Acad Sci U S A*, 106(6), pp. 2059-64.
- Pommier, Y., Johnson, A. A. and Marchand, C. (2005) 'Integrase inhibitors to treat HIV/AIDS', *Nat Rev Drug Discov*, 4(3), pp. 236-48.
- Price, M. R., Baillie, G. L., Thomas, A., Stevenson, L. A., Easson, M., Goodwin, R., McLean, A., McIntosh, L., Goodwin, G., Walker, G., Westwood, P., Marrs, J., Thomson, F., Cowley, P., Christopoulos, A., Pertwee, R. G. and Ross, R. A. (2005) 'Allosteric modulation of the cannabinoid CB1 receptor', *Mol Pharmacol*, 68(5), pp. 1484-95.
- Priyadarshini, M., Villa, S. R., Fuller, M., Wicksteed, B., Mackay, C. R., Alquier, T., Poitout, V., Mancebo, H., Mirmira, R. G., Gilchrist, A. and Layden, B. T. (2015) 'An Acetate-Specific GPCR, FFAR2, Regulates Insulin Secretion', *Mol Endocrinol*, 29(7), pp. 1055-66.
- Pronin, A. N., Tang, H., Connor, J. and Keung, W. (2004) 'Identification of ligands for two human bitter T2R receptors', *Chem Senses*, 29(7), pp. 583-93.
- Psichas, A., Sleeth, M. L., Murphy, K. G., Brooks, L., Bewick, G. A., Hanyaloglu, A. C., Ghatei, M. A., Bloom, S. R. and Frost, G. (2015) 'The short chain fatty acid propionate stimulates GLP-1 and PYY secretion via free fatty acid receptor 2 in rodents', *Int J Obes (Lond)*, 39(3), pp. 424-9.
- Puhl, H. L., 3rd, Won, Y. J., Lu, V. B. and Ikeda, S. R. (2015) 'Human GPR42 is a transcribed multisite variant that exhibits copy number polymorphism and is functional when heterologously expressed', *Sci Rep*, 5, pp. 12880.
- Rajagopal, S., Ahn, S., Rominger, D. H., Gowen-MacDonald, W., Lam, C. M., Dewire, S. M., Violin, J. D. and Lefkowitz, R. J. (2011) 'Quantifying ligand bias at seven-transmembrane receptors', *Mol Pharmacol*, 80(3), pp. 367-77.
- Ranjan, R., Dwivedi, H., Baidya, M., Kumar, M. and Shukla, A. K. (2017) 'Novel Structural Insights into GPCR-B-Arrestin Interaction and Signaling', *Trends Cell Biol*, 27(11), pp. 851-62.
- Rask-Andersen, M., Almen, M. S. and Schioth, H. B. (2011) 'Trends in the exploitation of novel drug targets', *Nat Rev Drug Discov*, 10(8), pp. 579-90.
- Rasmussen, S. G., DeVree, B. T., Zou, Y., Kruse, A. C., Chung, K. Y., Kobilka, T. S., Thian, F. S., Chae, P. S., Pardon, E., Calinski, D., Mathiesen, J. M., Shah, S. T., Lyons, J. A., Caffrey, M., Gellman, S. H., Steyaert, J., Skinotitis, G., Weis, W. I., Sunahara, R. K. and Kobilka, B. K. (2011) 'Crystal structure of the beta2 adrenergic receptor-Gs protein complex', *Nature*, 477(7366), pp. 549-55.
- Raybould, H. E. (2012) 'Gut microbiota, epithelial function and derangements in obesity', *J Physiol*, 590(3), pp. 441-6.

- Rosenbaum, D. M., Cherezov, V., Hanson, M. A., Rasmussen, S. G., Thian, F. S., Kobilka, T. S., Choi, H. J., Yao, X. J., Weis, W. I., Stevens, R. C. and Kobilka, B. K. (2007) 'GPCR engineering yields high-resolution structural insights into beta2-adrenergic receptor function', *Science*, 318(5854), pp. 1266-73.
- Rosenkilde, M. M. and Schwartz, T. W. (2000) 'Potency of ligands correlates with affinity measured against agonist and inverse agonists but not against neutral ligand in constitutively active chemokine receptor', *Mol Pharmacol*, 57(3), pp. 602-9.
- Roses, A. D. (2008) 'Pharmacogenetics in drug discovery and development: a translational perspective', *Nat Rev Drug Discov*, 7(10), pp. 807-17.
- Ross, E. M. (2014) 'G Protein-coupled receptors: Multi-turnover GDP/GTP exchange catalysis on heterotrimeric G proteins', *Cell Logist*, 4, pp. E29391.
- Rovati, G. E., Capra, V. and Neubig, R. R. (2007) 'The highly conserved DRY motif of class A G protein-coupled receptors: beyond the ground state', *Mol Pharmacol*, 71(4), pp. 959-64.
- Rowland, I., Gibson, G., Heinken, A., Scott, K., Swann, J., Thiele, I. and Tuohy, K. (2017) 'Gut microbiota functions: metabolism of nutrients and other food components', *Eur J Nutr*, 57(1), pp. 1-24.
- Samuel, B. S., Shaito, A., Motoike, T., Rey, F. E., Backhed, F., Manchester, J. K., Hammer, R. E., Williams, S. C., Crowley, J., Yanagisawa, M. and Gordon, J. I. (2008) 'Effects of the gut microbiota on host adiposity are modulated by the short-chain fatty-acid binding G protein-coupled receptor, Gpr41', *Proc Natl Acad Sci U S A*, 105(43), pp. 16767-72.
- Santos, G. A., Duarte, D. A., Parreiras, E. S. L. T., Teixeira, F. R., Silva-Rocha, R., Oliveira, E. B., Bouvier, M. and Costa-Neto, C. M. (2015) 'Comparative analyses of downstream signal transduction targets modulated after activation of the AT1 receptor by two beta-arrestin-biased agonists', *Front Pharmacol*, 6, pp. 131.
- Santos, R., Ursu, O., Gaulton, A., Bento, A. P., Donadi, R. S., Bologa, C. G., Karlsson, A., Al-Lazikani, B., Hersey, A., Oprea, T. I. and Overington, J. P. (2017) 'A comprehensive map of molecular drug targets', *Nat Rev Drug Discov*, 16(1), pp. 19-34.
- Sassmann, A., Gier, B., Grone, H. J., Drews, G., Offermanns, S. and Wettschureck, N. (2010) 'The Gq/G11-mediated signaling pathway is critical for autocrine potentiation of insulin secretion in mice', *J Clin Invest*, 120(6), pp. 2184-93.
- Sawzdargo, M., George, S. R., Nguyen, T., Xu, S., Kolakowski, L. F. and O'Dowd, B. F. (1997) 'A cluster of four novel human G protein-coupled receptor genes occurring in close proximity to CD22 gene on chromosome 19q13.1', *Biochem Biophys Res Commun*, 239(2), pp. 543-7.

- Schiele, F., Ayaz, P. and Fernandez-Montalvan, A. (2015) 'A universal homogeneous assay for high-throughput determination of binding kinetics', *Anal Biochem*, 468, pp. 42-9.
- Schmidt, J., Smith, N. J., Christiansen, E., Tikhonova, I. G., Grundmann, M., Hudson, B. D., Ward, R. J., Drewke, C., Milligan, G., Kostenis, E. and Ulven, T. (2011) 'Selective orthosteric free fatty acid receptor 2 (FFA2) agonists: identification of the structural and chemical requirements for selective activation of FFA2 versus FFA3', *J Biol Chem*, 286(12), pp. 10628-40.
- Schmidt, M. E., Kent, J. M., Daly, E., Janssens, L., Van Osselaer, N., Husken, G., Anghelescu, I. G. and Van Nueten, L. (2012) 'A double-blind, randomized, placebo-controlled study with JNJ-37822681, a novel, highly selective, fast dissociating D(2) receptor antagonist in the treatment of acute exacerbation of schizophrenia', *Eur Neuropsychopharmacol*, 22(10), pp. 721-33.
- Schrage, R., Schmitz, A. L., Gaffal, E., Annala, S., Kehraus, S., Wenzel, D., Bullesbach, K. M., Bald, T., Inoue, A., Shinjo, Y., Galandrin, S., Shridhar, N., Hesse, M., Grundmann, M., Merten, N., Charpentier, T. H., Martz, M., Butcher, A. J., Slodczyk, T., Armando, S., Effern, M., Namkung, Y., Jenkins, L., Horn, V., Stossel, A., Dargatz, H., Tietze, D., Imhof, D., Gales, C., Drewke, C., Muller, C. E., Holzel, M., Milligan, G., Tobin, A. B., Gomeza, J., Dohlman, H. G., Sondek, J., Harden, T. K., Bouvier, M., Laporte, S. A., Aoki, J., Fleischmann, B. K., Mohr, K., Konig, G. M., Tuting, T. and Kostenis, E. (2015) 'The experimental power of FR900359 to study Gq-regulated biological processes', *Nat Commun*, 6, pp. 10156.
- Semack, A., Sandhu, M., Malik, R. U., Vaidehi, N. and Sivaramakrishnan, S. (2016) 'Structural Elements in the Galphas and Galphaq C Termini That Mediate Selective G Protein-coupled Receptor (GPCR) Signaling', *J Biol Chem*, 291(34), pp. 17929-40.
- Sexton, M., Woodruff, G., Horne, E. A., Lin, Y. H., Muccioli, G. G., Bai, M., Stern, E., Bornhop, D. J. and Stella, N. (2011) 'NIR-mbc94, a fluorescent ligand that binds to endogenous CB(2) receptors and is amenable to high-throughput screening', *Chem Biol*, 18(5), pp. 563-8.
- Sharif, N. A., Davis, T. L. and Williams, G. W. (1999) '[³H]AL-5848 ([³H]9beta-(+)-Fluprostenol). Carboxylic acid of travoprost (AL-6221), a novel FP prostaglandin to study the pharmacology and autoradiographic localization of the FP receptor', *J Pharm Pharmacol*, 51(6), pp. 685-94.
- Shimazu, T., Hirschey, M. D., Newman, J., He, W., Shirakawa, K., Le Moan, N., Grueter, C. A., Lim, H., Saunders, L. R., Stevens, R. D., Newgard, C. B., Farese, R. V., Jr., de Cabo, R., Ulrich, S., Akassoglou, K. and Verdin, E. (2013) 'Suppression of oxidative stress by beta-hydroxybutyrate, an endogenous histone deacetylase inhibitor', *Science*, 339(6116), pp. 211-4.

- Shukla, A. K., Westfield, G. H., Xiao, K., Reis, R. I., Huang, L. Y., Tripathi-Shukla, P., Qian, J., Li, S., Blanc, A., Oleskie, A. N., Dosey, A. M., Su, M., Liang, C. R., Gu, L. L., Shan, J. M., Chen, X., Hanna, R., Choi, M., Yao, X. J., Klink, B. U., Kahsai, A. W., Sidhu, S. S., Koide, S., Penczek, P. A., Kossiakoff, A. A., Woods, V. L., Jr., Kobilka, B. K., Skiniotis, G. and Lefkowitz, R. J. (2014) 'Visualization of arrestin recruitment by a G-protein-coupled receptor', *Nature*, 512(7513), pp. 218-22.
- Sievers, F., Wilm, A., Dineen, D., Gibson, T. J., Karplus, K., Li, W., Lopez, R., McWilliam, H., Remmert, M., Soding, J., Thompson, J. D. and Higgins, D. G. (2011) 'Fast, scalable generation of high-quality protein multiple sequence alignments using Clustal Omega', *Mol Syst Biol*, 7, pp. 539.
- Sina, C., Gavrilova, O., Forster, M., Till, A., Derer, S., Hildebrand, F., Raabe, B., Chalaris, A., Scheller, J., Rehmann, A., Franke, A., Ott, S., Hasler, R., Nikolaus, S., Folsch, U. R., Rose-John, S., Jiang, H. P., Li, J., Schreiber, S. and Rosenstiel, P. (2009) 'G protein-coupled receptor 43 is essential for neutrophil recruitment during intestinal inflammation', *J Immunol*, 183(11), pp. 7514-22.
- Sklar, L. A., Edwards, B. S., Graves, S. W., Nolan, J. P. and Prossnitz, E. R. (2002) 'Flow cytometric analysis of ligand-receptor interactions and molecular assemblies', *Annu Rev Biophys Biomol Struct*, 31, pp. 97-119.
- Smith, N. J., Ward, R. J., Stoddart, L. A., Hudson, B. D., Kostenis, E., Ulven, T., Morris, J. C., Trankle, C., Tikhonova, I. G., Adams, D. R. and Milligan, G. (2011) 'Extracellular loop 2 of the free fatty acid receptor 2 mediates allosterism of a phenylacetamide ago-allosteric modulator', *Mol Pharmacol*, 80(1), pp. 163-73.
- Smith, P. M., Howitt, M. R., Panikov, N., Michaud, M., Gallini, C. A., Bohlooly, Y. M., Glickman, J. N. and Garrett, W. S. (2013) 'The microbial metabolites, short-chain fatty acids, regulate colonic Treg cell homeostasis', *Science*, 341(6145), pp. 569-73.
- Southern, C., Cook, J. M., Neetoo-Isseljee, Z., Taylor, D. L., Kettleborough, C. A., Merritt, A., Bassoni, D. L., Raab, W. J., Quinn, E., Wehrman, T. S., Davenport, A. P., Brown, A. J., Green, A., Wigglesworth, M. J. and Rees, S. (2013) 'Screening beta-arrestin recruitment for the identification of natural ligands for orphan G-protein-coupled receptors', *J Biomol Screen*, 18(5), pp. 599-609.
- Srivastava, A., Yano, J., Hirozane, Y., Kefala, G., Gruswitz, F., Snell, G., Lane, W., Ivetac, A., Aertgeerts, K., Nguyen, J., Jennings, A. and Okada, K. (2014) 'High-resolution structure of the human GPR40 receptor bound to allosteric agonist TAK-875', *Nature*, 513(7516), pp. 124-7.
- Stables, J., Mattheakis, L. C., Chang, R. and Rees, S. (2000) 'Recombinant aequorin as reporter of changes in intracellular calcium in mammalian cells', *Methods Enzymol*, 327, pp. 456-71.

- Stoddart, L. A., Johnstone, E. K. M., Wheal, A. J., Goulding, J., Robers, M. B., Machleidt, T., Wood, K. V., Hill, S. J. and Pflieger, K. D. G. (2015a) 'Application of BRET to monitor ligand binding to GPCRs', *Nat Methods*, 12(7), pp. 661-3.
- Stoddart, L. A., Kilpatrick, L. E., Briddon, S. J. and Hill, S. J. (2015b) 'Probing the pharmacology of G protein-coupled receptors with fluorescent ligands', *Neuropharmacology*, 98, pp. 48-57.
- Stoddart, L. A., Smith, N. J., Jenkins, L., Brown, A. J. and Milligan, G. (2008) 'Conserved polar residues in transmembrane domains V, VI, and VII of free fatty acid receptor 2 and free fatty acid receptor 3 are required for the binding and function of short chain fatty acids', *J Biol Chem*, 283(47), pp. 32913-24.
- Sum, C. S., Tikhonova, I. G., Neumann, S., Engel, S., Raaka, B. M., Costanzi, S. and Gershengorn, M. C. (2007) 'Identification of residues important for agonist recognition and activation in GPR40', *J Biol Chem*, 282(40), pp. 29248-55.
- Sun, M., Wu, W., Liu, Z. and Cong, Y. (2017) 'Microbiota metabolite short chain fatty acids, GPCR, and inflammatory bowel diseases', *J Gastroenterol*, 52(1), pp. 1-8.
- Suzuki, M., Takaishi, S., Nagasaki, M., Onozawa, Y., Iino, I., Maeda, H., Komai, T. and Oda, T. (2013) 'Medium-chain fatty acid-sensing receptor, GPR84, is a proinflammatory receptor', *J Biol Chem*, 288(15), pp. 10684-91.
- Sweeney, T. E. and Morton, J. M. (2013) 'The human gut microbiome: a review of the effect of obesity and surgically induced weight loss', *JAMA Surg*, 148(6), pp. 563-9.
- Sweetnam, P. M., Caldwell, L., Lancaster, J., Bauer, C., Jr., McMillan, B., Kinnier, W. J. and Price, C. H. (1993) 'The role of receptor binding in drug discovery', *J Nat Prod*, 56(4), pp. 441-55.
- Swinney, D. C. (2013) 'Phenotypic vs. target-based drug discovery for first-in-class medicines', *Clin Pharmacol Ther*, 93(4), pp. 299-301.
- Szcepek, M., Beyriere, F., Hofmann, K. P., Elgeti, M., Kazmin, R., Rose, A., Bartl, F. J., von Stetten, D., Heck, M., Sommer, M. E., Hildebrand, P. W. and Scheerer, P. (2014) 'Crystal structure of a common GPCR-binding interface for G protein and arrestin', *Nat Commun*, 5, pp. 4801.
- Taggart, A. K., Kero, J., Gan, X., Cai, T. Q., Cheng, K., Ippolito, M., Ren, N., Kaplan, R., Wu, K., Wu, T. J., Jin, L., Liaw, C., Chen, R., Richman, J., Connolly, D., Offermanns, S., Wright, S. D. and Waters, M. G. (2005) '(D)-beta-Hydroxybutyrate inhibits adipocyte lipolysis via the nicotinic acid receptor PUMA-G', *J Biol Chem*, 280(29), pp. 26649-52.

- Tang, C., Ahmed, K., Gille, A., Lu, S., Grone, H. J., Tunaru, S. and Offermanns, S. (2015) 'Loss of FFA2 and FFA3 increases insulin secretion and improves glucose tolerance in type 2 diabetes', *Nat Med*, 21(2), pp. 173-7.
- Thomsen, W., Frazer, J. and Unett, D. (2005) 'Functional assays for screening GPCR targets', *Curr Opin Biotechnol*, 16(6), pp. 655-65.
- Tikhonova, I. G. and Poerio, E. (2015) 'Free fatty acid receptors: structural models and elucidation of ligand binding interactions', *BMC Struct Biol*, 15, pp. 16.
- Tobin, A. B., Butcher, A. J. and Kong, K. C. (2008) 'Location, location, location...site-specific GPCR phosphorylation offers a mechanism for cell-type-specific signalling', *Trends Pharmacol Sci*, 29(8), pp. 413-20.
- Tolhurst, G., Heffron, H., Lam, Y. S., Parker, H. E., Habib, A. M., Diakogiannaki, E., Cameron, J., Grosse, J., Reimann, F. and Gribble, F. M. (2012) 'Short-chain fatty acids stimulate glucagon-like peptide-1 secretion via the G-protein-coupled receptor FFAR2', *Diabetes*, 61(2), pp. 364-71.
- Trompette, A., Gollwitzer, E. S., Yadava, K., Sichelstiel, A. K., Sprenger, N., Ngom-Bru, C., Blanchard, C., Junt, T., Nicod, L. P., Harris, N. L. and Marsland, B. J. (2014) 'Gut microbiota metabolism of dietary fiber influences allergic airway disease and hematopoiesis', *Nat Med*, 20(2), pp. 159-66.
- Tschaharganeh, D. F., Lowe, S. W., Garippa, R. J. and Livshits, G. (2016) 'Using CRISPR/Cas to study gene function and model disease in vivo', *FEBS J*, 283(17), pp. 3194-203.
- Turcatti, G., Vogel, H. and Chollet, A. (1995) 'Probing the binding domain of the NK2 receptor with fluorescent ligands: evidence that heptapeptide agonists and antagonists bind differently', *Biochemistry*, 34(12), pp. 3972-80.
- Urizar, E., Claeysen, S., Deupi, X., Govaerts, C., Costagliola, S., Vassart, G. and Pardo, L. (2005) 'An activation switch in the rhodopsin family of G protein-coupled receptors: the thyrotropin receptor', *J Biol Chem*, 280(17), pp. 17135-41.
- Valant, C., Gregory, K. J., Hall, N. E., Scammells, P. J., Lew, M. J., Sexton, P. M. and Christopoulos, A. (2008) 'A novel mechanism of G protein-coupled receptor functional selectivity. Muscarinic partial agonist McN-A-343 as a bitopic orthosteric/allosteric ligand', *J Biol Chem*, 283(43), pp. 29312-21.
- Valant, C., Robert Lane, J., Sexton, P. M. and Christopoulos, A. (2012) 'The best of both worlds? Bitopic orthosteric/allosteric ligands of g protein-coupled receptors', *Annu Rev Pharmacol Toxicol*, 52, pp. 153-78.
- Valentin-Hansen, L., Frimurer, T. M., Mokrosinski, J., Holliday, N. D. and Schwartz, T. W. (2015) 'Biased Gs versus Gq proteins and beta-arrestin signaling in the NK1 receptor determined by interactions in the water hydrogen bond network', *J Biol Chem*, 290(40), pp. 24495-508.

- Vallance, P. (2016) 'Industry-Academic Relationship in a New Era of Drug Discovery', *J Clin Oncol*, 34(29), pp. 3570-5.
- Valler, M. J. and Green, D. (2000) 'Diversity screening versus focussed screening in drug discovery', *Drug Discov Today*, 5(7), pp. 286-93.
- Vauquelin, G., Van Liefde, I., Birzbier, B. B. and Vanderheyden, P. M. (2002) 'New insights in insurmountable antagonism', *Fundam Clin Pharmacol*, 16(4), pp. 263-72.
- Venkatakrishnan, A. J., Deupi, X., Lebon, G., Heydenreich, F. M., Flock, T., Miljus, T., Balaji, S., Bouvier, M., Veprintsev, D. B., Tate, C. G., Schertler, G. F. and Babu, M. M. (2016) 'Diverse activation pathways in class A GPCRs converge near the G-protein-coupling region', *Nature*, 536(7617), pp. 484-7.
- Vermeire, S., Kojecký, V., Knoflíček, V., Reinisch, W., Van Kaem, T., Namour, F., Beetens, J. and Vanhoutte, F. (2015) 'DOP030 GLPG0974, an FFA2 antagonist, in ulcerative colitis: efficacy and safety in a multicenter proof-of-concept study', *J Crohns Colitis*, 9, pp. S36.
- Vernall, A. J., Hill, S. J. and Kellam, B. (2014) 'The evolving small-molecule fluorescent-conjugate toolbox for Class A GPCRs', *Br J Pharmacol*, 171(5), pp. 1073-84.
- Vernall, A. J., Stoddart, L. A., Briddon, S. J., Ng, H. W., Laughton, C. A., Doughty, S. W., Hill, S. J. and Kellam, B. (2013) 'Conversion of a non-selective adenosine receptor antagonist into A3-selective high affinity fluorescent probes using peptide-based linkers', *Org Biomol Chem*, 11(34), pp. 5673-82.
- Vieira, A. T., Macia, L., Galvao, I., Martins, F. S., Canesso, M. C., Amaral, F. A., Garcia, C. C., Maslowski, K. M., De Leon, E., Shim, D., Nicoli, J. R., Harper, J. L., Teixeira, M. M. and Mackay, C. R. (2015) 'A Role for Gut Microbiota and the Metabolite-Sensing Receptor GPR43 in a Murine Model of Gout', *Arthritis Rheumatol*, 67(6), pp. 1646-56.
- Vinolo, M. A., Ferguson, G. J., Kulkarni, S., Damoulakis, G., Anderson, K., Bohlooly, Y. M., Stephens, L., Hawkins, P. T. and Curi, R. (2011) 'SCFAs induce mouse neutrophil chemotaxis through the GPR43 receptor', *PLoS One*, 6(6), pp. E21205.
- Vu, T. K., Hung, D. T., Wheaton, V. I. and Coughlin, S. R. (1991) 'Molecular cloning of a functional thrombin receptor reveals a novel proteolytic mechanism of receptor activation', *Cell*, 64(6), pp. 1057-68.
- Wang, D. D. and Hu, F. B. (2017) 'Dietary Fat and Risk of Cardiovascular Disease: Recent Controversies and Advances', *Annu Rev Nutr*, 37, pp. 423-46.
- Wang, J., Wu, X., Simonavicius, N., Tian, H. and Ling, L. (2006) 'Medium-chain fatty acids as ligands for orphan G protein-coupled receptor GPR84', *J Biol Chem*, 281(45), pp. 34457-64.

- Wang, Y., Jiao, X., Kayser, F., Liu, J., Wang, Z., Wanska, M., Greenberg, J., Weizmann, J., Ge, H., Tian, H., Wong, S., Schwandner, R., Lee, T. and Li, Y. (2010) 'The first synthetic agonists of FFA2: Discovery and SAR of phenylacetamides as allosteric modulators', *Bioorg Med Chem Lett*, 20(2), pp. 493-8.
- Watson, C., Jenkinson, S., Kazmierski, W. and Kenakin, T. (2005) 'The CCR5 receptor-based mechanism of action of 873140, a potent allosteric noncompetitive HIV entry inhibitor', *Mol Pharmacol*, 67(4), pp. 1268-82.
- Wess, J. (1993) 'Mutational analysis of muscarinic acetylcholine receptors: structural basis of ligand/receptor/G protein interactions', *Life Sci*, 53(19), pp. 1447-63.
- Whalen, E. J., Rajagopal, S. and Lefkowitz, R. J. (2011) 'Therapeutic potential of beta-arrestin- and G protein-biased agonists', *Trends Mol Med*, 17(3), pp. 126-39.
- Wooten, D., Christopoulos, A. and Sexton, P. M. (2013) 'Emerging paradigms in GPCR allostery: implications for drug discovery', *Nat Rev Drug Discov*, 12(8), pp. 630-44.
- Xiong, Y., Miyamoto, N., Shibata, K., Valasek, M. A., Motoike, T., Kedzierski, R. M. and Yanagisawa, M. (2004) 'Short-chain fatty acids stimulate leptin production in adipocytes through the G protein-coupled receptor GPR41', *Proc Natl Acad Sci U S A*, 101(4), pp. 1045-50.
- Yang, Y., Adelstein, S. J. and Kassis, A. I. (2012) 'Target discovery from data mining approaches', *Drug Discov Today*, 17 Suppl, pp. S16-23.
- Yousefi, S., Cooper, P. R., Potter, S. L., Mueck, B. and Jarai, G. (2001) 'Cloning and expression analysis of a novel G-protein-coupled receptor selectively expressed on granulocytes', *J Leukoc Biol*, 69(6), pp. 1045-52.
- Zaibi, M. S., Stocker, C. J., O'Dowd, J., Davies, A., Bellahcene, M., Cawthorne, M. A., Brown, A. J., Smith, D. M. and Arch, J. R. (2010) 'Roles of GPR41 and GPR43 in leptin secretory responses of murine adipocytes to short chain fatty acids', *FEBS Lett*, 584(11), pp. 2381-6.
- Zhang, M., Sun, K., Wu, Y., Yang, Y., Tso, P. and Wu, Z. (2017) 'Interactions between Intestinal Microbiota and Host Immune Response in Inflammatory Bowel Disease', *Front Immunol*, 8, pp. 942.
- Zhang, R. and Xie, X. (2012) 'Tools for GPCR drug discovery', *Acta Pharmacol Sin*, 33(3), pp. 372-84.
- Zhao, X., Jones, A., Olson, K. R., Peng, K., Wehrman, T., Park, A., Mallari, R., Nebalasca, D., Young, S. W. and Xiao, S. H. (2008) 'A homogeneous enzyme fragment complementation-based beta-arrestin translocation assay for high-throughput screening of G-protein-coupled receptors', *J Biomol Screen*, 13(8), pp. 737-47.